APPLICATION OF THE MULTIPLE MODEL ADAPTIVE CONTROL METHOD TO THE CONTROL OF THE LATERAL DYNAMICS OF AN AIRCRAFT

by

Christopher S. Greene

B.S. University of Colorado
(1973)

SUBMITTED IN PARTIAL FULFILLMENT OF THE
REQUIREMENTS FOR THE DEGREE OF
MASTER OF SCIENCE
and
(Electrical Engineer)

at the

MASSACHUSETTS INSTITUTE OF TECHNOLOGY
June 1975

Signature of Author.....
Department of Electrical Engineering, May 23, 1975

Certified by.....
Thesis Supervisor

Accepted by..
Chairman, Departmental Committee on Graduate Students

APPLICATION OF THE MULTIPLE MODEL ADAPTIVE CONTROL METHOD TO THE CONTROL OF THE LATERAL DYNAMICS OF AN AIRCRAFT

by

Christopher S. Greene

Submitted to the Department of Electrical Engineering and Computer Science on May 23, 1975 in partial fullfillment of the requirements for the Degree of Master of Science and Electrical Engineer.

ABSTRACT

High performance aircraft, operating over a wide range of flight conditions, cannot be adequately stabilized by fixed gain controllers. This thesis investigates the application of one advanced technique called Multiple Model Adaptive Control (MMAC) to the stabilization of the lateral dynamics of the F-8 aircraft. The MMAC method requires the design of linear-quadratic-Gaussian (LQG) controllers at various flight conditions. Therefore, a regulator cost criterion which is automatically flight condition dependent and believed to give satisfactory response is developed. In addition, Kalman filters are designed and their acceptability for aircraft control discussed. The design and analysis of the filters and regulator cost function are given in detail. Simulations using both a linear and a nonlinear model are included which indicate that the method provides satisfactory response under most conditions. Some problems and their possible solutions are discussed.

THESIS SUPERVISOR: Alan S. Willsky

TITLE: Assistant Professor of Electrical Engineering

ACKNOWLEDGMENTS

Many people have aided in developing this thesis. Special thanks must go to my adviser, Alan S. Willsky for encouragement. Also, I must thank Michael Athans, who directed the larger research effort of which this thesis was a part, and Keh-Ping Dunn for his patience and assistance. Many people at Langley Research Center have also been of great help, especially in conducting the experiments with the nonlinear simulator. J. Elliot, R. Montgomery, J. Gera, and C. Woolley have all provided much needed guidance and assistance. Finally, I must thank all those who aided in the technical aspects of the preparation of this thesis. These include Art Giordani and Norman Darling for assistance in preparing the figures and Fifa Monserrate for typing the final version. Last, but not least, I must thank my wife for her patience and understanding through it all.

This research was carried out at the M.I.T. Electronic Systems Laboratory with partial support extended by NASA under Grant NSG-1018.

TABLE OF CONTENTS

Chapter 1	Introduction	6
1.1	Motivation and Problem Description	6
1.2	Organization of the Thesis	7
1.3	Notation	8
Chapter 2	Theory	9
Chapter 3	The Aircraft Model	14
3.1	The Basic Aircraft	14
3.2	Actuator Dynamics	16
3.3	Effects of Wind Turbulence	17
3.4	Discretization of Systems	20
Chapter 4	Design of LQG Controllers	22
4.1	The Regulator	22
4.2	Kalman Filters	28
4.3	Discussion of Individual Models	35
Chapter 5	Simulation Results-Linear Case	40
Chapter 6	Non-linear Case Simulations	46
Chapter 7	Conclusions and Comments	54
7.1	Assumptions and Approximations on the Model	54
7.2	Conclusions	55
7.3	Pilot Inputs	58
7.4	Suggestions for Future Research	58

CONT. OF TABLE OF CONTENTS

Appendix A 60

Appendix B 93

Appendix C 138

Appendix D 203

Appendix E 246

Bibliography 258

FIGURES

Figure 2.1 Structure of the MMAC Controller 12

Figure 3.1 State Variables 15

Figure 4.1 Closed-Loop Regulator Poles 26

Figure 4.2 Sensor Data 29

Figure 4.3 Kalman Filter Poles 33

Figure 4.4 Mismatch Stability Table 37

Chapter I - INTRODUCTION

1.1 Motivation and Problem Description

This thesis reports on research which has been directed at applying advanced concepts of modern control theory to the control of the lateral dynamics of the F-8 aircraft, a high performance jet fighter. The purpose of this work has not been to improve the performance of the F-8, which already has acceptable handling qualities, but instead to investigate the feasibility of applying an advanced control technique to aircraft in general. The approach chosen for investigation is the Multiple Model Adaptive Control (MMAC) method.

In the past, the design of aircraft control laws has been based largely on experience and usually has involved a fixed gain control system. The principle disadvantage of such an approach is that these gains must give satisfactory response at all flight conditions (i.e. altitudes, speeds, dynamic pressures, etc.). This clearly leads to a compromise in overall performance, as the dynamics of the airplane change greatly with flight condition. In fact, a set of gains which are "best" in some sense at one flight condition may lead to an unstable system when applied at another flight condition. Extensive simulation is therefore needed to ensure satisfactory response under all conditions.

Thus, what seems to be required is some type of adaptive control system that is capable of adjusting to changing flight conditions. Many types of adaptive control concepts are presently being proposed to deal with this problem [11,16]. The approach explored herein, called Multiple-Model Adaptive Control, has been suggested and explored by Lainiotis [3,17], Magill [13] and Willner [18].

1.2 Organization of the thesis

The theory underlying the MMAC method will be discussed in Chapter 2. That section is based largely on the thesis of Willner, and the reader will be referred to that source for all proofs. Chapter 3 describes in detail the model of the F-8 lateral dynamics used in this design. The linearized dynamics were obtained primarily from the report by Gera [9]. Chapter 4 develops the regulators and Kalman filters necessary to apply the MMAC method. It is believed that this is one of the first efforts involving the use of a Kalman filter in an aircraft control system, and thus the design procedure is included in detail. In addition, state regulators are not often employed in aircraft either, and thus the ideas used in arriving at the cost criterion are important. In fact, the methods used and insights gained in this study are seen as being of greater importance than the actual results of this test case. It is our hope that this study will yield some valuable insight into the use of advanced control concepts in the design of sophisticated aircraft control systems.

Chapters 5 and 6 present some of the results of simulations, first when the control system is applied to a linear model and then, in Chapter 6, when the same system is applied to a nonlinear model. A parallel effort to that described herein has been aimed at designing a control system for the longitudinal aircraft dynamics. Obviously, a considerable amount of overlap and therefore co-operation between the two efforts has occurred. Dunn [5-7] has reported on the longitudinal aspects of this problem. The simulations of Chapter 6 investigate, in addition to the non-linear effects, how the longitudinal system aids the lateral in system identification and therefore control

of the lateral system. Chapter 7 presents recommendations for future research. In addition some general thoughts are presented on the problems of applying modern control methods to aircraft control problems.

1.3 Notation

Equations and figures are consecutively numbered within a chapter with each new chapter starting over again with the number one. When referring to an equation or figure of another chapter, explicit reference to the appropriate chapter will be made i.e., "Chapter 3 Equation (3)".

All state variables are obviously functions of time. Such time dependence will be dropped from the notation for simplicity when no confusion can occur.

At various times it will be necessary to distinguish between a matrix of a continuous time system and the corresponding matrix in a discrete time system. The subscripts C and D will be used to denote the difference. A prime will be used to denote the transpose of a matrix.

Chapter 2 - THEORY

The goal of this section is to provide the theoretical justification for the use of the MMAC method. None of what follows is new, and the interested reader is referred to Willner's thesis [18] for proofs of the results quoted. Also, areas in which only intuition is presently available to justify the method are pointed out.

Consider the following problem. Only the discrete time case will be considered. Assume we have a black box known to contain one of N known linear stochastic systems

$$x(k+1) = A_i x(k) + B_i u(k) + \xi(k) \qquad i=1,2,\ldots,N \tag{1a}$$

with observations

$$z(k) = C_i x(k) + \eta(k) \qquad i=1,2,\ldots,N \tag{1b}$$

where $\xi(k)$ and $\eta(k)$ are white Gaussian vectors of known covariance. The task is then to find a feedback control $u(k)$ which minimizes

$$J(u) = E\left[\lim_{T\to\infty} \frac{1}{T} \sum_{k=0}^{k=T} x'(k)Qx(k) + u'(k)Ru(k)\right] \tag{2}$$

where $E[\cdot]$ is the expectation operator, Q is a given positive semi-definite matrix, and R is a given positive definite matrix.

Willner has attempted to solve this problem using dynamic programming but was unable to get a useful answer for the true optimum because the nonlinearities in the problem make it extremely difficult to solve the algorithm for anything but the single stage problem. However, he has found various bounds on performance, one of which forms the basis for the MMAC method.

It is well known that if, in the above problem, the system is known to be system j, then one can find a matrix G_j such that $u(k) = -G_j\hat{x}(k)$ is is the optimum control, where $\hat{x}(k)$ is the steady state Kalman filter (KF) estimate of the state for system j. This is the standard Linear-Quadratic-Gaussian (LQG) control problem [1]. It is then reasonable, as a solution to the original problem where the system is only known to be one of N systems, to use a control of the form

$$u(k) = -\sum_{j=1}^{N} P_j(k) G_j \hat{x}_j(k) \tag{3}$$

where $P_j(k)$ is the probability of system j being the true system conditioned on measurements up to time k, G_j is the LQG feedback gain for the j^{th} system and $\hat{x}_j$ is the LQG state estimate assuming the j^{th} system is the true one.

An equation for the probabilities will be given shortly. However, first a few comments on the properties of the proposed controller will be made. Willner has shown the following properties for this controller:

1) As time increases ($k\to\infty$) the control converges to the optimum (i.e. the $P_j(k)$ for the true model converges to 1).
2) The cost incurred by the controller is close to that of the "ideal" controller (the ideal has a priori knowledge of the true model which must be less than the cost incurred by the optimal, which does not have a priori knowledge).
3) The controller is in some respects a first order approximation to the optimal control and is, in fact, optimal for one step of the dynamic programming algorithm.

It remains to develop the equations used to calculate the probability P_j. It is well known [10,15] that, given that one uses the $j^{\underline{th}}$ filter on the $j^{\underline{th}}$ system (i.e. the matched case), the residuals of the KF are white and Gaussian (assuming all noise sources are white and Gaussian) with probability density given by

$$p_j(z(k)) = \left[(2\pi)^n|\Sigma_j|\right]^{1/2} \exp\left[-\frac{1}{2}(z-\hat{z}_j)'\Sigma_j^{-1}(z-\hat{z}_j)\right] \tag{4}$$

where

$z(k)$ is the observation vector

$\hat{z}_j$ is the predicted observation

and Σ_j is the error covariance of the residual for the jth Kalman filter.

Using Baye's rule, one can then derive the following expression for the probability of the $j^{\underline{th}}$ system being the one actually generating the observations at time k:

$$P_j(k) = \frac{p_j(k)P_j(k-1)}{\sum_{i=1}^{N} p_i(k)P_i(k-1)} \tag{5}$$

The structure of the resulting controller is shown in Figure 1.

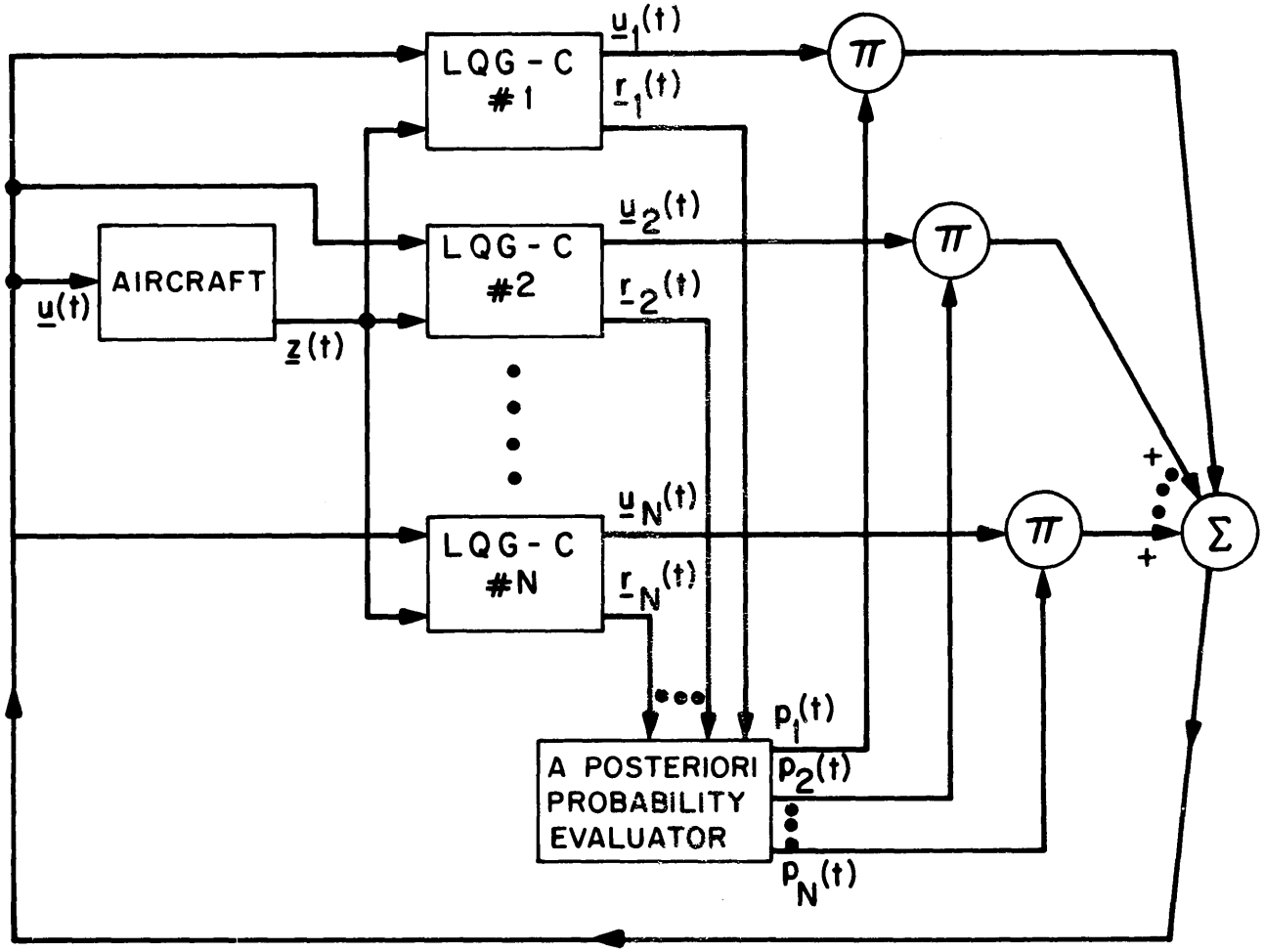

Figure 1 Structure of MMAC Controller

Although the above control scheme is reasonable, it is important to remember that, as applied to aircraft control, it is suboptimal in two ways. First of all, it is a suboptimal solution to the problem as presented above. Secondly, an aircraft actually operates over a continuum of flight conditions rather than the finite set of discrete flight conditions which the MMAC method requires to be postulated. There is presently no theoretical basis for determining the behavior of the MMAC controller if the true model is not among the set of hypothesized models. In fact, stability itself has not even been proved. Thus, much theoretical work remains, but it is hoped that the present empirical study will provide the insight needed to attack the more difficult theoretical issues.

Chapter 3 - THE AIRCRAFT MODEL

In this section the aircraft model used in this design will be discussed. This model will then form the basis for the design of both the regulators and Kalman filters (KFs) that are the necessary components of the MMAC method (see Chapter 4).

3.1 The Basic Aircraft

It is well known that the linearized equations of motion of an aircraft can be decoupled into the lateral and longitudinal equations [8]. When this is done, the usual choices of state variables for the lateral system are (see also Figure 1): roll rate (p), yaw rate (r), sideslip angle (β), and bank angle (ϕ) with aileron surface deflection (δ_a) and rudder surface deflection (δ_r) as control variables. The largest error due to linearization is from the resolution of the gravity vector into the lateral and longitudinal states. In the lateral case this involves terms of the form $\sin \phi \cos \theta$ (θ is pitch angle, a longitudinal variable), which are linearized to ϕ. This presents a problem, since for high performance fighter aircraft bank angle may be large as in, for example, a 360° roll and

$$\sin 360 \neq 2\pi.$$

The effects of this nonlinearity and several methods to overcome this problem will be discussed in Chapter 7.

Thus, the basic equations of motion for the lateral dynamics are given by the following:

State	Symbol	Units
Roll Rate	p	rad/sec
Yaw Rate	r	rad/sec
Sideslip angle	β	rad
Bank angle	ϕ	rad
Aileron Angle	δ_a	rad
Rudder Angle	δ_r	rad
Commanded Aileron Angle	δ_{ac}	rad
Commanded Rudder Angle	δ_{rc}	rad
Wind Turbulence	w	rad

Figure 3.1

Summary of the States of the Aircraft Model

$$\frac{d}{dt}\begin{bmatrix} p \\ r \\ \beta \\ \phi \end{bmatrix} = A_{lat}\begin{bmatrix} p \\ r \\ \beta \\ \phi \end{bmatrix} + B_{lat}\begin{bmatrix} \delta_a \\ \delta_r \end{bmatrix} \qquad (1)$$

where A_{lat} and B_{lat} are coefficient matrices from the linearized equations. A_{lat} and B_{lat} have been supplied for 16 flight conditions by two sources at NASA/Langley Research Center (LRC). The first source is a report by Gera [9] giving the coefficients of linearized dynamics derived from wind tunnel tests. The second source is a report by Woolley [19] in which he linearizes the mathematical equations used to simulate the F-8 on the LRC computer system. These reports give similar but not identical matrices, and this difference will be used later to aid in the modeling of plant uncertainty.

3.2 Actuator Dynamics

Each control surface is physically moved by an actuator which has been modeled as a unity gain first order lag with an appropriate time constant. (supplied by NASA engineers). Thus, the dynamics of the secondary actuators (much faster than the primary ones) and higher order nonlinear effects such as hysteresis have been ignored. Taking commanded aileron angle (δ_{ac}) and commanded rudder angle (δ_{rc}) as inputs to the actuators, the equations now become:

$$\frac{d}{dt}\begin{bmatrix} p \\ r \\ \beta \\ \phi \\ \delta_a \\ \delta_r \end{bmatrix} = \begin{bmatrix} A_{lat} & B_{lat} \\ (4x4) & (4x2) \\ 0\ 0\ 0\ 0 & -30\ \ 0 \\ 0\ 0\ 0\ 0 & 0\ \ -25 \end{bmatrix}\begin{bmatrix} p \\ r \\ \beta \\ \phi \\ \delta_a \\ \delta_r \end{bmatrix} + \begin{bmatrix} 0 & 0 \\ 0 & 0 \\ 0 & 0 \\ 0 & 0 \\ 30 & 0 \\ 0 & 25 \end{bmatrix}\begin{bmatrix} \delta_{ac} \\ \delta_{rc} \end{bmatrix} \qquad (2)$$

For the actual design, it was decided to use rate control. That is, the rate of change of the commanded control surface deflections ($\dot{\delta}_{ac}$ and $\dot{\delta}_{rc}$ respectively) were actually the control inputs. This was done for the following reasons:

1. $\dot{\delta}_{ac}(t)$ and $\dot{\delta}_{rc}(t)$ are good approximations to the aileron and rudder rates ($\dot{\delta}_a$ and $\dot{\delta}_r$ respectively) which are subject to saturation contraints of 140°/second and 70°/second respectively.
2. The use of rates as control variables introduces integrators into the control loop which help eliminate steady-state errors due to constant wind disturbances and modeling errors.

Including these integrators in equation (2) yields:

$$\frac{d}{dt}\begin{bmatrix} p \\ r \\ \beta \\ \phi \\ \delta_a \\ \delta_r \\ \delta_{ac} \\ \delta_{rc} \end{bmatrix} = \begin{bmatrix} A_{lat} & & B_{lat} & & \underline{0} \\ & & -30 & 0 & 30 & 0 \\ & & 0 & -25 & 0 & 25 \\ \underline{0} & & & & & \\ & & 0 & 0 & 0 & 0 \\ & & 0 & 0 & 0 & 0 \end{bmatrix} \begin{bmatrix} p \\ r \\ \beta \\ \phi \\ \delta_a \\ \delta_r \\ \delta_{ac} \\ \delta_{rc} \end{bmatrix} + \begin{bmatrix} 0 & 0 \\ 0 & 0 \\ 0 & 0 \\ 0 & 0 \\ & \\ 0 & 0 \\ 0 & 0 \\ 1 & 0 \\ 0 & 1 \end{bmatrix} \begin{bmatrix} \dot{\delta}_{ac} \\ \dot{\delta}_{rc} \end{bmatrix} \quad (3)$$

3.3 Effects of Wind Turbulence

The effect of wind turbulence on the lateral dynamics is modeled as a pure sideslip angle disturbance (i.e., a transverse gust), with no direct rolling component. The assumed power spectral density is given by

$$\Phi_g = \frac{\sigma^2}{\pi} \frac{L}{V_0} \left\{ \frac{4}{4 + \frac{L}{V_0} w^2} \right\} \tag{4}$$

where

$$L = \begin{cases} 2500 \text{ ft. when alt. } > 2500 \text{ ft.} \\ 200 \text{ ft. when alt. = sea level.} \end{cases}$$

V_0 = (Mach number) x (speed of sound.)

$$\sigma = \begin{cases} 6 \text{ ft./sec. normal} \\ 15 \text{ ft./sec. cumulus} \\ 30 \text{ ft./sec. thunderstorm} \end{cases}$$

w = radian frequency

This model for wind disturbance was provided by J. Elliot of LRC as a reasonable approximation to the von Karman spectrum.*

It is possible to show that this power spectral density can be realized by the following linear equation:

$$\frac{d}{dt} w(t) = \alpha w(t) + \frac{K}{V_0} \xi(t) \tag{5}$$

where

$$E[\xi(t)\xi(\tau)] = 1\delta(t-\tau) \tag{6}$$

ξ a white Gaussian noise

$$\alpha = 2\left(\frac{V_0}{L}\right) \tag{7}$$

---

* private communication - J. Elliot.

$$\frac{K}{V_0} = \frac{2\sigma}{\sqrt{\pi L V_0}} \tag{8}$$

Since this disturbance enters as a sideslip disturbance, its effects are exactly the same as the effects of sideslip. Thus, when this is included in (3) one gets:

$$\frac{dx(t)}{dt} = Ax(t) + Bu(t) + L\xi(t) \tag{9}$$

where $x'(t) = [p(t) \quad r(t) \quad \beta(t) \quad \phi(t) \quad \delta_a(t) \quad \delta_r(t) \quad \delta_{ac} \quad \delta_{rc} \quad w]$

$$A = \begin{bmatrix} A_{lat} & B_{lat} & \underline{0} & \begin{matrix} a_{13} \\ a_{23} \\ a_{33} \\ 0 \end{matrix} \\ & \begin{matrix} -30 & 0 & 30 & 0 & 0 \end{matrix} & \\ \begin{matrix} 0 \\ \\ \\ \\ \end{matrix} & \begin{matrix} 0 & -25 & 0 & 25 & 0 \\ 0 & 0 & 0 & 0 & 0 \\ 0 & 0 & 0 & 0 & 0 \\ 0 & 0 & 0 & 0 & -\alpha \end{matrix} & \end{bmatrix}$$

$$B = \begin{bmatrix} 0 & 0 \\ 0 & 0 \\ 0 & 0 \\ 0 & 0 \\ 0 & 0 \\ 0 & 0 \\ 1 & 0 \\ 0 & 1 \\ 0 & 0 \end{bmatrix} \qquad L = \begin{bmatrix} \underline{0} \\ \\ \frac{K}{V_0} \end{bmatrix}$$

$$u(t) = \frac{d}{dt} \begin{bmatrix} \delta_{ac}(t) \\ \delta_{rc}(t) \end{bmatrix}$$

It is the system described by (9) that will be used in the next chapter to design the individual LQG controllers. The matrices of (9) are listed in Appendix A for all flight conditions.

3.4 Discretization of Systems

Since the ultimate design will be implemented with a digital flight computer, the entire design must, at least eventually, be based on discrete time system equations. Techniques have been developed and computer programs written [12,19] to allow a linear continuous time problem to be transformed into an equivalent linear discrete time problem. The systems are equivalent in the sense that, if $x_C(t)$ is the state of the continuous system, $x_D(k)$ the state of the discrete time system and if the input is piecewise-constant and changes only immediately preceeding a sampling time, then $x_C(kT) = x_D(k)$, where T is the sampling or discretization period.

It is well known (see [12]) that the following equations hold: (subscripts C and D refer to continuous and discrete time dynamics respectively)

$$A_D = \exp\ [A_C T] \tag{10}$$

$$B_D = \int_0^T \exp[A_C \tau] d\tau] B \tag{11}$$

If $\underset{\sim}{\square}_C$ is the continuous time plant noise covariance then, in discrete time, the plant noise covariance becomes:

$$\underset{\sim}{\square}_D = \int_0^t [\exp[A_C \tau]]\ [\underset{\sim}{\square}_C][\exp[A_C' \tau]] d\tau. \tag{12}$$

The observation equation will be discussed and discretized in Chapter 4.

Under these conditions, it is also possible to transform a continuous time cost function of the form

$$J_C(u) = \int_0^\infty [x'(t)\ Q_C\ x(t) + u'(t)\ R_C u(t)]dt \tag{13}$$

into an equivalent discrete time cost function of the form

$$J_D(u) = \sum_{k=0}^{\infty} [x'(k)\ Q_D\ x(k) + x'(k)\ M_D\ u(k) + u'(k)\ R_D\ u(k)] \tag{14}$$

where

$$Q_D = \int_0^T \exp[A_C'\ \tau]\ Q_C\ \exp[A_C\ \tau]d\tau \tag{15}$$

$$M_D = \int_0^T [\exp[A_C'\ \tau]\ Q_C \int_0^{T_1} \exp[A_C\ \tau_1]d\tau_1\ B_C]d\tau\ T_1\varepsilon(0,T) \tag{16}$$

and

$$R_D = R_C T + \int_0^T B_C' \int_0^{T_1} \exp[A_C'\ \tau_1]d\tau_1\ Q_C \int_0^{T_1} \exp[A_C\ \tau_1]d\tau_1\ B_C]d\tau\ T_1\varepsilon(0,T). \tag{17}$$

One could now in principle apply the usual discrete time optimal regulator and filter theory to the discrete time model just developed. In the next chapter we will describe how this methodology has been applied to the F-8 control problem. For various numerical reasons, we have slightly modified the design from that which one would obtain by straightforward application of the methodology developed in Chapter 2 and in [12]. Our solution, however, is quite close to this design in both spirit and performance.

Chapter 4 - DESIGN OF THE LQG CONTROLLERS

In Chapter 2 the theory of the MMAC method has been discussed. It is clear that in order to apply this method it is necessary to design LQG controllers for the various flight conditions. In the current chapter we undertake the task of designing controllers for fifteen flight conditions ranging over the entire flight envelope for a clean, cruise type of aircraft configuration. This task is believed to be of some interest in its own right, as it represents one of the first thorough investigations of the use of LQG theory in aircraft control design.

4.1 The Regulator

Designing a regulator which would provide good aircraft response and not require "tuning" at each flight condition proved to be a fairly difficult problem, and many variations were tried. As is well known [2], the regulator problem consists of finding a constant matrix G such that the control law $u = -Gx$ minimizes a particular cost criterion. The standard form of this cost function (in continuous time) is

$$J(u) = \int_0^\infty [x'(t)Qx(t) + u'(t)Ru(t)]dt . \qquad (1)$$

The solution for G for a linear system with cost (1) is well known [1]. Thus the problem becomes to choose the Q and R matrices (possibly flight condition dependent) which will give "satisfactory" aircraft performance. What constitutes satisfactory performance is still a much discussed issue, and we have chosen one of many possible criteria.

The basic philosophy for determining Q and R was first to determine those quantities considered important in aircraft performance and then to

weight these quantities in the cost function by the inverse of the "maximum allowable or tolerable". After discussions with NASA engineers it was decided that the most important quantity appeared to be lateral acceleration. For the control penalty (recall that the rate of surface deflection is controlled) the rate saturation value was used, modified by a factor of two-thirds for the ailerons to reflect a greater willingness of the pilot to saturate the rudder rate than the aileron rate.

This leads to a cost of the form

$$J(\underline{u}) = \int_0^\infty \left[\left(\frac{a_y(t)}{a_{y_{max}}} \right)^2 + \left(\frac{\dot{\delta}_{ac}(t)}{\frac{2}{3}\dot{\delta}_{a_{max}}} \right)^2 + \left(\frac{\dot{\delta}_{rc}(t)}{\dot{\delta}_{r_{max}}} \right)^2 \right] dt \ . \qquad (2)$$

For $a_{y_{max}}$, a value of .25 g's was decided upon, while $\dot{\delta}_{a_{max}}$ and $\dot{\delta}_{r_{max}}$ were given by hardware limitations. Since lateral acceleration (in g's) can be written as

$$a_y(t) = \frac{V_0}{g} \left[\dot{\beta} + r - p\alpha_0 \right] - \sin\phi\cos\theta$$

(α_0 is the trimmed angle of attack, a longitudinal state), (2) can now be rewritten (after substitution for $\dot{\beta}$ and linearization of $\sin\phi\cos\theta$ to ϕ) in the form of (1). Note that θ is the pitch angle, a longitudinal variable.

Thus Q and R become:

$$Q = k\begin{bmatrix} (a_{31}-\alpha_0)^2 & (a_{31}-\alpha_0)(a_{32}+1) & (a_{31}-\alpha_0)a_{33} & (a_{31}-\alpha_0)(a_{34}-\frac{1}{k}) \\ (a_{31}-\alpha_0)(a_{32}+1) & (a_{32}+1)^2 & (a_{32}+1)a_{33} & (a_{32}+1)(a_{34}-\frac{1}{k}) \\ (a_{31}-\alpha_0)a_{33} & (a_{32}+1)a_{33} & a_{33}^2 & (a_{34}-\frac{1}{k})a_{33} \\ (a_{31}-\alpha_0)(a_{34}-\frac{1}{k}) & (a_{32}+1)(a_{34}-\frac{1}{k}) & (a_{34}-\frac{1}{k})a_{33} & (a_{34}-\frac{1}{k})^2 \\ 0 & 0 & 0 & 0 \\ (a_{31}-\alpha_0)a_{36} & (a_{32}+1)a_{36} & a_{33}\ a_{36} & (a_{34}-\frac{1}{k})a_{36} \end{bmatrix}$$

$$\begin{matrix} 0 \\ 0 \\ 0 \end{matrix} \quad \begin{matrix} 0 \\ 0 \\ 0 \end{matrix} \quad \begin{matrix} 0 \\ 0 \\ 0 \end{matrix} \quad \begin{matrix} 0 \\ 0 \\ 0 \end{matrix}$$

$$\begin{matrix} (a_{31}-\alpha_0)a_{36} \\ (a_{32}+1)a_{36} \\ a_{33}\ a_{36} \\ (a_{34}-\frac{1}{k})a_{36} \end{matrix}$$

$$\begin{bmatrix} 0 & 0 & 0 & 0 \\ 0 & 0 & 0 & 0 \\ 0 & 0 & 0 & 0 \\ 0 & 0 & 0 & 0 \\ 0 & 0 & 0 & 0 \\ 0 & 0 & 0 & 0 \\ 0 & 0 & 0 & 0 \\ 0 & 0 & 0 & 0 \\ 0 & 0 & 0 & 0 \end{bmatrix}$$

where $k = \left[\frac{V_0}{g}\right]^2$ and a_{ij} is the $ij^{\underline{th}}$ element of the A matrix of Equation 9, Chapter 3.

$$R = \begin{bmatrix} .378 & 0 \\ 0 & .671 \end{bmatrix}$$

It should be noted that, while R is flight condition independent, Q is implicitly flight condition dependent because of its dependence on the A matrix.

A set of FORTRAN programs [14] is available at MIT to solve the Riccati equation for the regulator problem. After obtaining the associated feedback matrices (G) and running a few responses, it was decided that they were not satisfactory. The principal reasons were too slow a sideslip response and too fast a bank angle response. For an ideal system bank angle is neutrally stable.) This problem was remedied by the addition of penalities on sideslip angle and roll rate. This remedy is also justified by pilot response considerations, as sideslip angle and roll rate are quantities deemed important by the pilot from a response point of view. The value of this added penalty was determined by trial and error. The values finally settled upon were 10% of the corresponding state penalty due to lateral acceleration alone. That is, the 1^{st} and 3^{rd} (p and β) diagonal terms of the state weighting matrix (Q) due to the lateral acceleration penalty were multiplied by 1.100. This cost function then adequately reflected handling qualities while not requiring "tuning" for each flight condition.

This modified cost function was then used in the FORTRAN programs to calculate feedback matrices for all flight conditions. Appendix B includes the gains, as well as the associated closed loop poles. The complex closed loop poles are plotted in Figure 1. Due to numerical problems, it was not

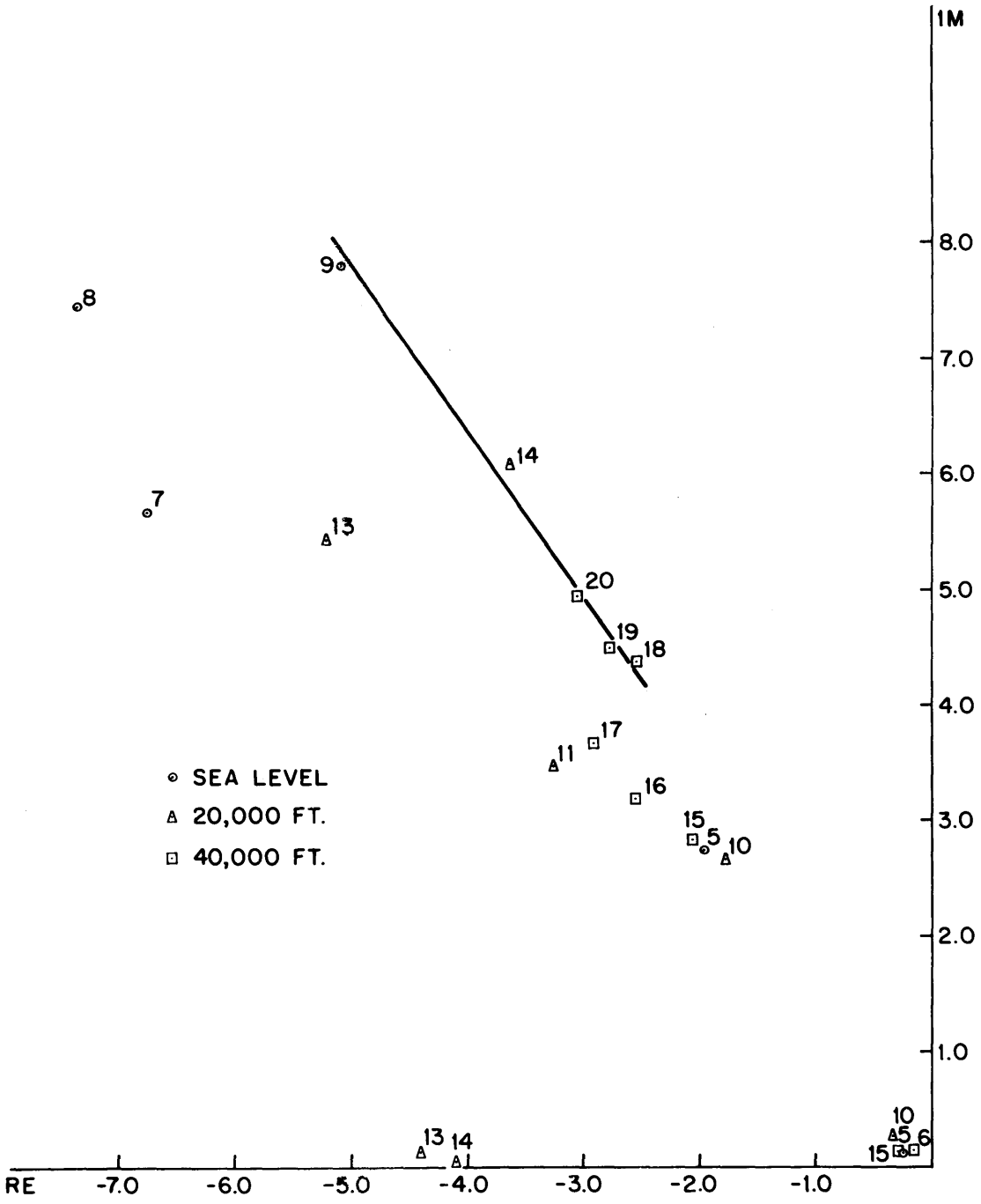

Figure 1 Poles of Regulators

possible to solve the Riccati equation for FCs 6 or 12. It is interesting to note that the poles come close to lying on a constant damping ratio line. The fit is even better in the longitudinal case [5-7]. The exact reason for this is unclear, but it is conjectured that it is a result of the dependence of the cost function on the system dynamics through lateral acceleration.

Since the above gains are for the continuous time system and since the design will be implemented on a digital computer, it next became necessary to find the equivalent discrete time gains for a sampling frequency of 8 Hz.* As stated in Chapter 3, one can reformulate the original problem as an equivalent discrete time problem and then solve the resulting discrete time problem. This was attempted, but numerical problems developed in solving the Riccati equation. Therefore, the following method was used. Let the subscripts D and C represent the discrete and continuous time matricies respectively.

Then $ACL_C = A_C - B_C G_C$.

Using the equations of [12] one finds that

$$ACL_D = \exp\{[ACL_C]T\}.$$

But we also know that

$$ACL_D = A_D - B_D G_D,$$

and we solve for G_D from the equation

---

*The 8Hz figure was chosen as a compromise between computer requirements and accuracy, and also to be compatible with LRC's nonlinear digital simulation which operates at 32 Hz.

$$G_D = -(B_D'B_D)^{-1} B_D' [ACL_D - A_D].$$

It should be noted that the value of G_D obtained need not be the same as the optimal gain for the discrete time LQG problem. However, the fast sampling rate together with the simulation results we have obtained justify our approximate method. Appendix B includes the discrete time gains and resulting eigenvalues.

4.2 Kalman Filters

The second element to be designed for each LQG controller was the Kalman filter. The design will first be given in continuous time and finally in discrete time. Questions as to what sensors are available on the F-8 arose. The final set of sensors is shown in Figure 2. Note that neither bank angle nor sideslip angle is measured directly, because of the existance of large, hard to model transients and nonlinearities in the currently available bank and sideslip indicators. For example, the bank angle measurement is unreliable beyond approximately 70°, and turbulence can cause the sideslip vane to "flip" around 360° in some flight attitudes. Thus it was decided not to incorporate these measurements into the initial design.

Measurement noise figures (see Figure 2), along with sensor bandwidths, were provided by NASA/Langley engineers. The noise figures are based on the static accuracies of the devices as no "in service" noise data is presently available. The sensor bandwidths are large compared to the plant dynamics and so are not included in the continuous time case.

Plant uncertainty is seen to come from three sources. The first source is due to a model of wind turbulence. This turbulence was discussed in

Sensor	Symbol	RMS Error	Bandwidth (HZ)
Lateral acceleration	Z_{a_y}	.04 g's	20
Roll rate	Z_p	2 deg/sec	2
Yaw rate	Z_r	.5 deg/sec	2
Sideslip angle*	Z_β	.3 deg	1
Bank angle*	Z_ϕ	.2 deg	30
Aileron angle	Z_{δ_a}	.1 deg	30
Rudder angle	Z_{δ_r}	.1 deg	30

* Not used in the design. See text.

Figure 4.2

Sensor Data for the F-8 Aircraft

Chapter 3. The second source of uncertainty is actuator noise in the aileron and rudder systems. The figures used were estimates provided by NASA engineers. The final source is some fictitious white noise added to represent modeling errors and to help open the bandwidth of the Kalman filter. The value used is based on the difference between two sets of data provided by NASA (see Chapter 3). The first was data derived from wind-tunnel tests, while the second was based on a mathematical model. The noise covariance was calculated by multiplying the differences between the system A and B matrices by some typical state and control values and squaring the result. The typical values chosen were

$\rho = 36°/sec.$

$r = 9°/sec.$

$\beta = 9°$

$\phi = 18°$

$\delta_a = 3°$

$\delta_r = .6°$

$\delta_{ac} = \delta_a$

$\delta_{rc} = \delta_r$

$w = 0$

$\dot{\delta}_{ac} = 14°/sec.$

$\dot{\delta}_{rc} = 7°/sec$

This leads to the following set of equations for the filtering problem.

$$x^T(t) = [p\ r\ \beta\ \phi\ \delta_a\ \delta_r\ \delta_{ac}\ \delta_{rc}\ w_D]$$

(3)

$$\dot{x}(t) = \begin{bmatrix} A_{lat}^{(4,4)} & B_{lat}^{(4,2)} & \underline{0} & 3^{rd} \\ & & & \text{Column of} \\ & & & A_{lat} \\ & \begin{matrix} -30 & 0 \end{matrix} & \begin{matrix} 30 & 0 \end{matrix} & \\ \underline{0} & \begin{matrix} 0 & -25 \end{matrix} & \begin{matrix} 0 & 25 \end{matrix} & \underline{0} \\ \underline{0} & \underline{0} & \underline{0} & \begin{matrix} 0 \\ 0 \\ \alpha \end{matrix} \end{bmatrix} + \begin{bmatrix} \underline{0} \\ \\ \\ \begin{matrix} 1 & 0 \\ 0 & 1 \\ 0 & 0 \end{matrix} \end{bmatrix} \begin{bmatrix} u_a \\ u_r \end{bmatrix}$$

$$+ \underline{\xi}(t)$$

$$Z(t) = Cx(t) + \eta(t)$$

where

C is given in Appendix A

$E[\xi(t)]=0 \quad E[\eta(t)]=0$

$E[\xi(t)\eta(\tau)]=0$

$E[\xi(t)\xi(\tau)] = \tilde{\Theta}\ \delta(t-\tau)$

$E[\eta(t)\eta(\tau)] = \Theta\ \delta(t-\tau)$

$\tilde{\Theta}$ and Θ are as in Appendix A.

It should be recognized that the assumption has been made that all noises are white and Gaussian. This, of course, is only an approximation but one often made in this type of problem. This assumption is most needed in the development of the probability Equation (4) of Chapter 2.

One obstacle remained to solving the filtering problem. The system (3) is not completely controllable from the noise (although it is observable and "stabilizable from the noise"). This means that the Riccati equation

solution is only semidefinite and that the filter gain matrix has two zero rows. This is numerically undesirable as it leads to very poor convergence properties of the solution to the Riccati equation. However, since the two undisturbable states are completely known, they can be easily removed from the filter to give a system which can be solved using the routines at MIT [14] for the solution of the resulting Riccati equation to get covariances and filter gain matrices. These can be augmented by zeros to get the matrices which form the solution to the original filtering problem. The resulting gains, covariances, and filter eigenvalues are shown in Appendix C, and the poles plotted in Figure 3.

In many ways, these filters give disappointing results. The reason can be seen by noticing that the bank angle is only weakly observable. This is reflected in the filter by large error covariances and very slow eigenvalues. Some of the filters have 15 second time constants so that initial errors require 45 to 60 seconds to disappear, and modeling errors influence the result strongly. These errors become especially important when used in a feedback controller. Methods to overcome this problem are discussed in Chapter 7.

As with the control gains, the filter must be converted to a discrete time representation. Using the method of Levis [12], the open loop system, input, and plant noise matrices were converted to the equivalent discrete time matrices as described in the preceding chapter. The method for defining the discrete time measurement equation is as follows. We will assume that the observation matrix (C) is the same in both continuous and discrete time, i.e.,

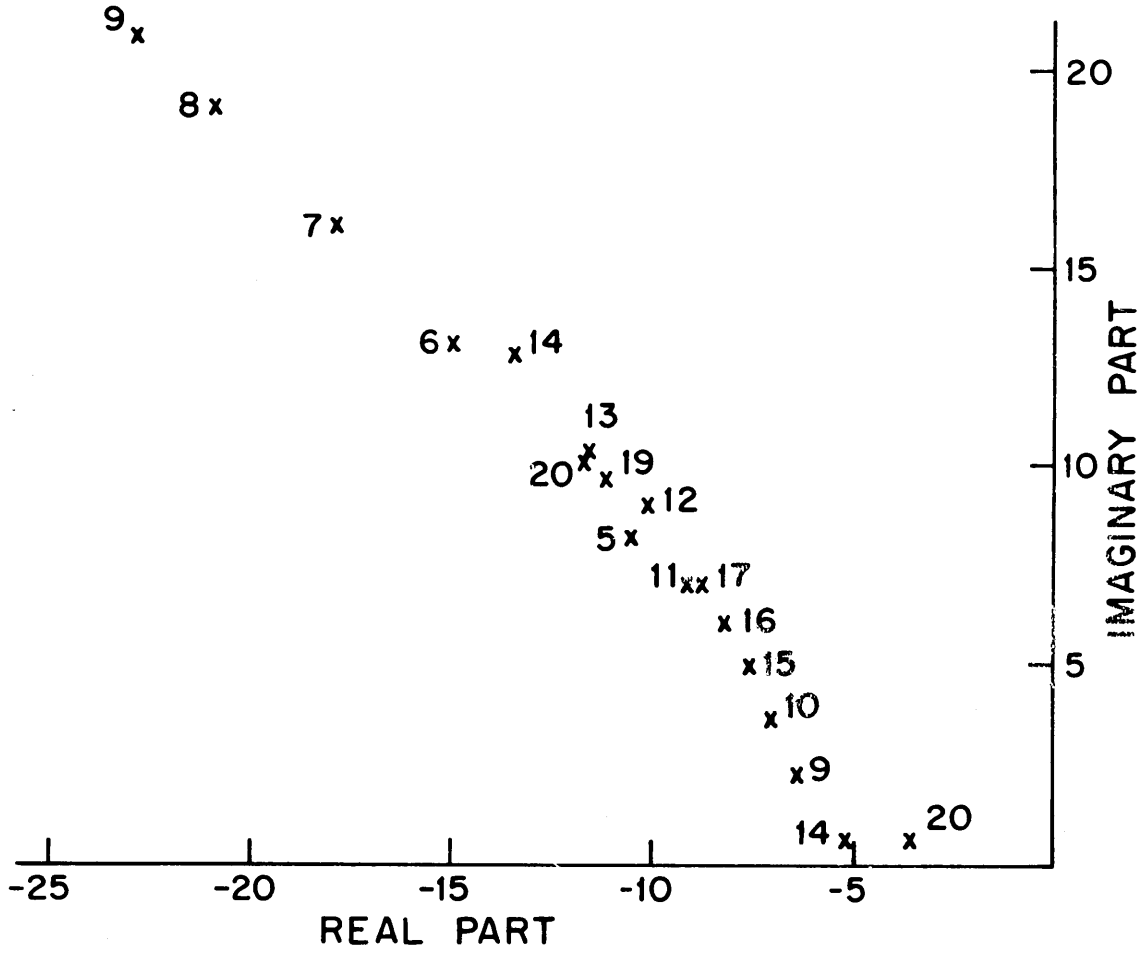

Figure 3(a) Complex Poles of KF's

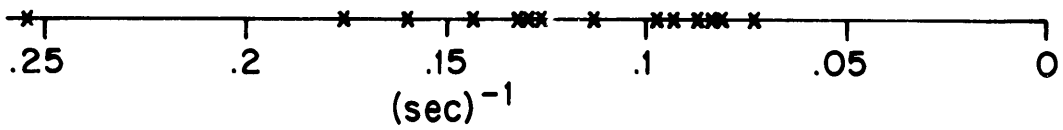

Figure 3(b) Dominant Poles of KF's

$$C_D = C_C$$

The equivalent discrete time observation noise covariance can then be calculated as follows. Correlation between sensors, which was not modeled in the continuous time case will be ignored and so the development given is for the scalar case. The scalar results then become the elements of the diagonal covariance matrix in the vector case. Let $\overline{\Theta}_C$ be the (scalar) continuous time observation noise covariance, and let b be the bandwidth of the sensor. Then the observation noise can be modeled as a Gauss-Markov random process [10]:

$$dx = -bx + bdw \qquad x(0) = x_0 \tag{14}$$

where w is a Wiener process with

$$E[dw_t dw_t] = \frac{2\overline{\Theta}_C}{b}\, dt \quad . \tag{15}$$

Sampling (14) we obtain

$$x(k+1) = b_D x(k) + w(k) \tag{16}$$

where $b_D = e^{-bT}$

$$E[w(i)w(j)] = \begin{cases} \overline{\Theta}_D & i=j \\ 0 & \text{otherwise} \end{cases} \tag{17}$$

and

$$\overline{\Theta}_D = \overline{\Theta}_C\, [1-\exp(-2bT)] \quad . \tag{18}$$

Using this result each of the sensor noise variances was converted to discrete time. When this was done, it was found that for the high sampling rate used

the resulting Θ_D matrix was not significantly different numerically from the continuous time Θ_C matrix. Therefore, to avoid lengthy calculations, the approximation of

$$\Theta_D \approx \Theta_C$$

was made. This approximation tends to increase the noise covariance which, it is thought, helps model the "dynamic" inaccuracies due to operating the sensors in a noisy environment. In any case, the errors introduced are small.

The resulting equations were then solved to obtain the Kalman filter for each flight condition using a discrete Riccati equation solution routine. The resulting covariances and gains are given in Appendix C.

4.3 Discussion of Individual Models

Some simulations were done using perfectly matched filter-gain combinations (i.e.,using the control for system i with system i). One very important point became evident at this stage. As the eigenvalues of Appendix C clearly show, all of the filters have at least one very slow pole (time constants of as much as 15 seconds). Physically this is because both bank angle and sideslip angle are nearly unobservable from the available rate measurements. This leads to serious problems of which more will be said throughout the remainder of this report.

The first effect of these slow poles is that, even with a perfect match between the plant and the filter-controller, the simulation results are somewhat disappointing. In most cases, there is an initial undesirable transient response if the initial filter estimates are not in close agreement with actual initial conditions. This is directly attributable to the

poor state estimates during the initial 45 to 60 seconds it takes for the estimates to converge to the true state. During this period the airplane's response will often leave any reasonable range of validity for the linear model (i.e., do a 360° roll). It is believed that this is due both to this slow pole and also to using a time-invariant filter when a time-varying one is really needed (to reflect greater initial uncertainties). Chapter 7 contains some recommendations for the solution of this problem.

Figure 4 gives the stability of the various closed-loop systems under mismatched conditions (i.e., system i with the LQG controller for system j). This table is interesting because of its implications for the MMAC control scheme. It is thought that the MMAC control system will not remain locked (have a probability near one for a long time) on a filter-controller which leads to an unstable system (although it may use an unstable combination for awhile). This remains unproven but does seem to be upheld in our limited sample.

To date it has not been possible to parameterize these instabilities in terms of physical variables such as dynamic pressure, airspeed, etc., although many of them are due to a simple pole believed to be a roll-mode type instability (no eigenvector calculations have been done).

Because of the inaccuracies mentioned above, a review of the KF design was undertaken. It was felt that the extra plant noise added to the roll rate equation in (3) was "unreasonably large". Thus, it was decided to reduce the variance by two orders of magnitude. This still made the roll rate variance the largest. This change did help to reduce the state

STABILITY SUMMARY TABLE

TRUE FC	CONTROLLER 5	6	7	8	10	11	12	13	14	15	16	17	18	19	20
5	*	*	*	*	*	U	*	*	*	U	U	U	U	U	U
6	*	*	*	*	*	*	*	*	*	*	*	*	*	*	*
7	U	*	*	*	U	U	*	*	*	U	U	U	U	*	*
8	U	*	*	*	U	U	*	U	U	U	U	U	U	U	*
10	U	*	*	*	*	U	*	*	*	U	U	U	U	U	U
11	*	*	*	*	*	*	*	*	*	*	U	U	U	U	U
12	*	*	*	*	*	*	*	*	*	*	*	*	*	*	*
13	U	*	*	*	U	*	*	*	*	U	U	U	U	*	*
14	*	*	U	U	*	*	*	*	*	*	*	*	*	*	*
15	U	*	*	*	*	U	*	*	*	*	U	U	U	U	U
16	U	*	*	*	*	*	*	*	*	*	*	U	U	U	U
17	U	*	*	*	*	*	*	*	*	*	*	*	U	U	U
18	*	*	U	U	*	*	*	*	*	*	*	*	*	*	*
19	*	*	U	U	*	*	*	U	*	*	*	*	*	*	*
20	U	*	U	U	*	*	*	U	*	*	U	U	U	*	*

U=UNSTABLE
*= STABLE

Figure 4 Mismatch Stability Table

estimation error covariances of bank angle and sideslip angle slightly but did little to aid convergence of the filter estimates.

Next, it was decided to investigate whether better results could be achieved if either a bank angle measurement or a sideslip angle measurement were made available. Three designs were investigated using different values for the bank angle sensor noise variance. One additional design employed a sideslip angle sensor. The first design included a very poor bank angle sensor (45° σ). This measurement was essentially ignored by the filter. The second design had a 15° σ bank angle measurement and resulted in some improvement (on the order of 5%) in both steady state error covariance and convergence rate. This was about the same improvement as when a 3° σ sideslip angle measurement was included in place of a bank angle measurement. The largest improvement cames when an accurate (1° σ) bank angle measurement was assumed. This resulted in a reduction in the convergence time-constant, which became approximately 1/2 second, with a similar reduction in steady state covariancesfor both bank angle and sideslip angle. Presently available sensors have static accuracies of .2 degrees RMS for bank angle and .3 degrees RMS for sideslip angle.

Both the filter with reduced plant noise and the filter with an accurate bank angle sensor were solved in discrete time, and the mismatch stability table for each was calculated. In both cases the table indicates that the system is almost universally mismatch unstable. It is believed that this is due to the very precise knowledge of both the plant and the observations resulting in a very narrow, fine tuned filter. In fact, in a number of cases, the system is slightly match unstable, probably due to round off

errors in the control gains (G) and filter gains (H) (only four significant figures were used on input for each of these matrices). This tradeoff in accuracy of estimation versus stability points out one large problem area for this, or any other, effort at applying modern control methods to aircraft. Identification and control appear to be conflicting goals in this type of design.

Because of these instabilities, it was decided to use the original filter design for the tests discussed in Chapters 5 and 6. Obviously, many other techniques could be used to design either the filters or the control gains, and much work remains in this important area.

In the next sections the results of simulations using this control scheme will be discussed.

Chapter 5 - SIMULATION RESULTS-LINEAR CASE

A variety of simulations have been done using both a linear model and a non-linear model of the F-8 aircraft. These models will be described shortly. None of these simulations are claimed to be valid tests of the design from an aircraft designers point of view but rather are attempts at discovering the characteristics of this type of design. Simulations using a linear simulator will be discussed in this chapter, and simulations using a non-linear simulator will be discussed in Chapter 6.

The first set of simulations were deterministic ones testing the regulator designed in Chapter 4 (full state feedback). The run shown is for a subsonic (Mach .6), middle altitude (20,000 ft.) flight condition. The longitudinal variables were ignored. This flight condition (FC 11 in Appendices A-C) has a dynamic pressure of 245 psf and is considered typical for this aircraft.* The simulation is shown in Appendix D, Figure 1. The initial condition for this run is a 2 degree sideslip angle (a "beta gust"). Also shown on the plots is the open loop response to the same initial conditions. The most important thing to note in this simulation is the lack of any oscillation in any state variables in the closed loop response. Also note the speed with which lateral acceleration and sideslip angle are reduced to near zero and held there.

In fact the response of the control system is to put the aircraft into a coordinated turn, i.e., a turn with zero lateral acceleration. Note that bank angle is very slow to return to zero. Simulations were also run for the original control law, which did not include the ten percent penalities on's

---

* Personal communication, J. Gera of LRC.

on roll rate or sideslip angle (see Chapter 4). The simulations presented in this paper differ from the ones without the 10% penalty principally in a slower bank angle response and a faster sideslip angle response than the results without the 10% penalty. In neither case do the control surface rates remain well within allowable limits. Simulations at other flight conditions and for other initial conditions have been run, and in all cases the results were similar to those shown in this sample run. In all cases tested the control system first places the aircraft into a coordinated turn within about one second and then slowly returns the plane to level flight.

The next phase of the simulation study was to include the KF and the actualsensors allowed in the feedback design. These simulations still assume that the true model is known a priori. The simulations, shown in Appendix D, Figures 2 and 3, are for a high altitude (40,000 ft), high speed (Mach 1.4) flight condition (FC 19 in Appendices A-C). This flight condition has a dynamic pressure of 537 psf. As before, the longitudinal dynamics were ignored. For each run, the initial condition was a 45 degree bank angle. In the first case, (Appendix D, Figure 2) the initial condition on the KF was zero while in the second, the KF was initialized with the true initial state (Appendix D, Figure 3). Both of the simulations include observation noise but do <u>not</u> include plant noise. (The KF was designed assuming both types of noise would be present).

The most important thing to note here is the difference in the bank angle response. When the true state is known by the KF, the bank angle slowly converges to zero. However, when the filter is initially in error, bank angle grows rapidly to approximately 150 degrees within 10 seconds. This obviously violates the assumptions of the linear model. The reason for

this poor response is the slow response of the KF, as described in Chapter 4. We recall that the large time constant of the KF was due to the near unobservability of the bank and sideslip angles. Thus, if there is a poor initial estimate, the KF yields poor overall transient response. However, when the initial estimate is good, the system behaves very much as it does in the pure deterministic case, i.e., sideslip angle remains close to zero as do the other variables. We note that the slow response in this case is an intrinsic characteristic of the LQG design philosophy when dealing with nearly unobservable, lightly damped states. More will be said on this in Chapter 7.

The final set of linear simulations attempted to investigate the properties of the MMAC method. This set of experiments had no noise introduced at all, primarily to allow better observation of the dynamical behavior of the closed-loop system. These simulations were conducted at the same flight condition as the previous set of experiments i.e. FC 19 in Appendices A-C. The set of models available in the MMAC controller were FC 8,14,18,19 and 20. Note that the true flight condition was included in the controller. The initial condition for the run was a sideslip angle of two degrees (a beta gust). All models were given equal a priori probabilities of being the correct model, and all of the KFs had the correct initial estimate.

The simulation is shown in Figure 4 of Appendix D. The correct model is initially chosen with high probability and then switches to another model after a few seconds. The states respond in very much the same manner as they did for the deterministic responses discussed earlier. Lateral acceleration is removed within about one second, while roll rate and sideslip angle are

reduced to zero almost as fast, i.e. the airplane is immediately put into a coordinated turn. It is believed that the probabilities tend to drift away from the true model after about five seconds as a result of a lack of information. With no noise perturbing the system, the states have settled to near zero after about five seconds. The state estimates from all stable filters have also gone to zero. Thus the residuals in all the stable filters approach zero. In this case the determinant in Equation (4), Chapter 2 tends to dominate the exponential term so that the probability converges to one for the system with the largest determinant for which the KF is mismatch stable. However, when the system is not perturbed, as in this case, no control function is needed. Thus, this does not hamper the system response. The last simulation of this section explores the response when the true flight condition is not included in the set of possible models, i.e. a mismatch case. The conditions for this run are identical to the ones for the previous simulation. That is, the plane is at 40,000 ft. with a speed of Mach 1.4. The only difference is that in this case the true model (FC 19) has not been included in the set of possible models. Flight Condition 17 (40,000 ft. altitude, Mach. 9) has been included instead. The most important point to note is that the responses of the critical variables are almost identical to the responses when FC 19 is included. Referring to the probabilities, the system chose to average the controls from two flight conditions at the same altitude and at neighboring speeds (Mach 1.2 and 1.6). As before, after the response has neared zero, the determinants start dominating the probabilities, and so the probability switches to FC 17.

Similar results were obtained with other initial conditions. However, the speed with which the determinant starts to dominate varies greatly. For

example, with a roll rate initial condition, the high determinant flight condition was favored much sooner. However, there is very little degradation in system's response.

With these relatively encouraging results, the final step is to test the method using a non-linear simulation of the F-8. This will be discussed in Chapter 6. A few comments appear to be in order at this point though. Other simulations with roll rate and bank angle initial conditions have been done, and these simulations display essentially the same behavior as that observed in the simulations we have just described. Based on all of these results, it is apparent that if the filters are not wrong initially, both the identification and control functions are performed satisfactorily. However, if the filters are initially grossly in error as to the true state, undesirable transients enter very strongly due to the very slow convergence of the estimates in the KFs. This has implications for the application of the method to an actual aircraft because the true initial state is never "perfectly" known. Unaccounted for modeling errors can also cause a similar type of condition. Thus, it is clear that one of the major steps in any following research must be to redesign the filters to improve convergence. Some further thoughts on this will be presented in Chapter 7.

One other problem that will need to be faced in future work is the dominating determinant. One could very reasonably hypothesize a case in which oscillations develop between a mismatched unstable but large determinant flight condition and the matched system. If the filter part of the mismatched system is stable, (that is the instability is in the control rather than the filter) then, when all disturbances converge to zero the probability of the unstable

system could increase due to the dominant determinant. This could then lead to an excitation of the system (due to the destabilizing control) which would again allow better system identification. Obviously the details of such an oscillation depend strongly on many factors including how much plant noise is actually present.

Thus, although the results presented in this chapter are encouraging, they also point to some of the problems involved in applying the MMAC method, in particular, and modern control theory, in general, to a real world problem.

Chapter 6 - NON-LINEAR CASE SIMULATIONS

In the previous chapter we have examined the performance of the control system when applied to a "linear aircraft". In this chapter, the same control system is applied to a non-linear model of the F-8.

After describing the simulator, we will discuss computer runs involving an implementation of the control system in which the controller is matched to the true flight condition. Following this, we will describe our results for the full MMAC method. The model used in the simulator is one developed by NASA/Langley Research Center and implemented on their CDC 6400. It is believed to be a relatively accurate model if operated within a fairly large region of validity (i.e. stalls are not modeled). The interested reader is referred to Woolley [19] for the details of the model. It should be noted that this nonlinear model yields linearized equations of motion with coefficients that are slightly different from those in the equations given by Gera [9] and used in the designs of Chapter 4.

This non-linear model, unlike the linear models discussed previously, does not ignore the coupling between the lateral and longitudinal systems. A control system for the longitudinal modes was designed in an effort parallel to this one, using precisely the same design logic [5-7]. Several of the simulations we will describe in this section involve the simultaneous use of the longitudinal and lateral MMAC systems.

In the first set of simulations, the closed loop response (Appendix E, Figure 2) is compared with the open loop response (Appendix E, Figure 1). There is no identification involved in the closed loop case, as the true FC is assumed to be known a priori with only the matched controller being used.

The aircraft is initially at FC 11, which has an altitude of 20,000 ft. and a Mach number of .6, and is given a two degree sideslip initial condition (a beta gust). The principle feature to note is the lack of oscillations in the controlled case. The controlled response looks very much like the response when a linear model is used as far as sideslip and lateral acceleration are concerned since they quickly decay to zero and remain there. However, bank angle wonders far too much and appears to be unstable. Nevertheless, the maneuver remains coordinated, i.e., lateral acceleration remains close to zero. The exact cause for this apparent unstable bank angle behavior is unknown, but it is somewhat consistant with the regulator's goal of neutral bank angle stability. This alone does not explain the results. A few other contributing factors appear to be:

1. The filters are initialized to zero. Thus there is a severe initial estimation error which, as seen in Chapter 5, can cause poor response.
2. The filters used have at least one very slow pole (time constants around 15 sec.) which can cause large estimation errors (primarily in bank angle).
3. The true model is nonlinear, especially in the way bank angle affects the other states. This error usually involves terms such as $\sin \phi$ or $\cos \phi$, the usual approximations of which are only accurate for small bank angles. This approximation of $\sin \phi \approx \phi$ is especially crucial in the lateral acceleration terms in both the regulator cost function and in the sensor equation. The former could cause the aircraft to "unwind" more than necessary (i.e. the controller does not recognize that 360 degrees is the same as 0 degrees), while the latter leads to meaningless estimations as ϕ approaches 180 degrees.

4. The true model includes coupling between the lateral and longitudinal states which has been ignored. These coupling terms become large with large bank angle (consider the case $\phi=90°$).

5. There is a slight mismatch due to the differences between the linearization of the simulator model and the linear model given by Gera [9].

The run described here is typical, and runs with other initial conditions and at other flight conditions have these same characteristics. It is thus obvious that a solution needs to be found to the unstable bank angle problem, but that the system does perform well as far as the other important states are concerned.

The remainder of the simulations presented in this report cover the true multiple model aspects of this problem. It should be evident that there are really two dependent but different problems of identification and control involved. The previously discussed "matched" simulation by-passed the identification problem. In many ways identification is the more difficult of the two problems and thus, as will be seen shortly it is the one which gives the largest problems.

The first set of simulation deal with the results when no wind turbulence is present to excite the system. The initial conditions are a two degree sideslip angle and a six degree angle of attack (a longitudinal variable).

The KFs are initialized at zero. These simulations are at FC 7 which is at sea level and Mach .7 with a dynamic pressure of 726 psf. The MMAC controller chosen consists of five different systems corresponding to five different flight conditions. The models used in the MMAC controller

are FC 5,7,8,13 and 14 (note that the actual model is included). All models were given a priori probability of being the true model.

The open loop response of Figure 3, Appendix E again shows considerable oscillatory behavior while the controlled system using just the lateral system (Figure 4, Appendix E) does not. However, it should be noted that the bank angle wanders more than in any other case ending up near 90 degrees. Also, unlike previous simulations, lateral acceleration is now affected. As far as the probabilities are concerned, the interesting points are the very rapid transitions and the immediate rejection of the "matched" model. After approximately one second the probabilities start oscillating between FC 5 and FC 13. Note that the filter-controller for FC 5 is unstable when applied to FC 7 (Figure 4, Chapter 4) and that there is a strong correlation between the time intervals when lateral acceleration appears to go unstable and when the controller for FC 5 is chosen. It was this run which led to the hypothesized "determinant dominance" effect discussed in the previous chapter.

When the combined lateral-longitudinal systems is used the results show some improvement over those with just the lateral controller (Appendix E, Figure 5). In this case the longitudinal system is available to aid the lateral system in identifying the model. The model is correctly identified during the critical first few seconds, and consequently lateral acceleration is quickly controlled. Both lateral acceleration and sideslip angle are held small with almost none of the oscillations seen in the open loop response. After the transients have died out, the probabilities again tend to drift toward a high determinant flight condition but <u>not</u> FC 5, the high

determinant, unstable FC. However, bank angle does drift and the probabilities start to show some instabilities when the bank angle nears 90 degrees.

The final set of simulations are also done at FC 7. The conditions of the simulations are identical to the previous set except that instead of any initial conditions on the system, a model of heavy turbulence (σ=15 ft/sec) is included. This is approximatly the intensity assumed in the design of Chapter 6. The filters are initialized to zero, and each model is given equal a priori probability. FC 5,7,8,13, and 14 are the available models. Figure 6, Appendix E shows the open loop response with the lateral system KF operating but with the feedback control disabled. Bank angle remains small (the system is open loop stable). The tendency to cycle between two high determinant models (FC 5 and 13) is present in this identification-only simulation.

The closed loop response with just the lateral system on is seen in Figure 7 of Appendix E. Bank angle is quite unstable, in this case reaching 90 degrees in approximately 6 seconds. Lateral acceleration shows about the same amount of deviation as in the open loop case and seems to have unstable tendencies while the probability of FC 5 is high. Note that FC 7 is never picked up. First, FC 5 is chosen and, at roughly the time that the instabilities become apparent, is replaced by FC 13 which, except for a very short change to FC 5, remains dominant until the bank angle nears 90 degrees.

Figure 8 of Appendix E contains the results when the combined lateral-longitudinal system is applied in this same high turbulence situation. Except for a very short period when FC 5 is used, the controller choses

FC 8 most of the time. The system appears to remain stable. Bank angle is still slightly unstable but much less so than in other runs. Also the intensity of both lateral acceleration and sideslip angle variations is reduced somewhat over the open loop response. The problems of poor identification seen in most of the simulations are believed to be in part related to the initial a priori probabilities given to the various models. In every case, each model was given equal a priori probability. Each filter was also given identical initial state estimates. Thus, for the initial few iterations of the KFs, the residuals of the KFs are nearly equal which again introduces the determinant dominance effect discussed in the previous chapter. To be perfectly correct in this case one would have to use time varying KFs which would introduce time varying error covariance matrices into the probability calculation. The assumption made in our design is that the time constants of these time varying matrices are sufficiently small compared to the relevent plant dynamics. It can be inferred from the slow poles of the KFs seen in Chapter 4 that this is probably a poor assumption, and some better approximation of the time-varying filter may be needed.

Simulations at other flight conditions and with other sets of available models tend to confirm the following observations.

1) If the system is correctly identified, the control system does a reasonably good job of controlling, except for a spiral mode type instability in bank angle which is present even when the true system is perfectly known.

2) This instability is not caused in any way by the MMAC method but is a result of a complex interaction of nonlinearities, slow filters, and the design of the regulators as discussed previously.

3) When there is no information (i.e. steady state is neared) the system tends to choose a high determinant flight condition over any other. The effects of this choice vary with the stability of the system.

4) Severe initial conditions aid identification by providing information as to the dynamics of the aircraft.

5) Nonlinearities associated with large bank angle ($\phi \rightarrow 90$) tend to complicate the identification problem in such a way that the wrong model is often chosen and the probabilities change more often than normally. This is in addition to, and possibly caused by, the problems of control due to the nonlinearities. (see comment 2 above).

6) The probabilities tend to be either zero or one with very little tendency for averaging.

7) Initial errors of estimation in the KFs affect the response of the system considerably. This is a direct result of the very slow dynamics of the KFs.

8) The initial probabilities assigned to the various models affect the response by slowing the identification of the correct model due to the determinant dominance problem.

9) The lateral control system appears to have a significant amount of trouble properly identifying the model. Alone, it has never been able to do so for any length of time. However, the addition of the longitudinal system aids greatly in the identification.

It should be noted that no runs have been done without the true model included in the MMAC controller. However, both the linear simulation results presented in the previous chapter and the fact that the lateral system never correctly identifies the model, even when it is included in the nonlinear simulation, indicate that the results would not be significantly different in this case.

Chapter 7 - CONCLUSIONS AND COMMENTS

This study is an attempt to apply modern control methods to the problem of controlling the lateral dynamics of a high performance aircraft. Previous chapters have presented the details of the particular design method chosen for this study. In the process many problems have been encountered, some of which have been solved but many of which have been left to future work. This process of discovering the pitfalls of practical design is seen as an important contribution of this research.

7.1 Assumptions and Approximations of the Model

At this point it is probably useful to review the various assumptions used in the design process. As with any first attempt at a practical design, the list appears formidable.

1) The model used has been linear. This assumption is particularly suspect at high bank angles.
2) All lateral-longitudinal coupling has been ignored.
3) All sensor outputs are assumed to be linear combinations of lateral states. This approximation is especially poor for the lateral acceleration sensor.
4) All sensors are assumed to be static devices and sensor noises are assumed to be white and Gaussian with no correlation between sensors. Only the static accuracy is used, thereby ignoring effects of a noisy environment such as vibration.
5) In designing the discrete time KFs, the sensor noise is not handled in a mathematically precise manner, thus slightly increasing the covariance used in the design.

7.2 Conclusions

In this study, which is one of the first in which LQG theory has been used in the design of an aircraft control system, we have attempted to give detailed descriptions of the design methods employed. The results indicate that the regulator cost function developed in Chapter 4 gives good results. However, by design, the bank angle is nearly neutrally stable and this, as was seen in the nonlinear simulation, causes problems. In addition, this neutrally stable bank angle is really only important modulo 360 degrees. A method is needed by which this fact can be taken into account to prevent "stupid" maneuvers such as unwinding 360 degrees after a full roll. One possible approach is to feedback sin ϕ instead of ϕ.

The major fault with the design proceedure is believed to be in the reliance of the LQG design on the Kalman filter to provide "optimal" state estimates. As seen in Chapters 4,5, and 6, the poor observability of the bank angle leads to a filter with a very slow time constant, which dominates the overall transient response. What appears to be needed is the inclusion of a bank angle sensor with some, possibly ad hoc, method for overcoming the poor performance of the sensor at bank angles near 90 degrees. If this is not possible than an approach similar to Breza [3] is needed in which a minimum-variance filter is developed subject to eigenvalue constraints. This would allow the designer to specify a maximum time constant for the filter with minimum degradation of the estimation variances. It is believed that with the accurate sensors presently available, the reduction in performance due to the increased estimation covariance would be small compared to the improved performance due to the faster filter response times.

The responses seen in Chapter 5 indicate that the MMAC method does perform satisfactorily when the simulation model is linear. The responses are very similar to the "ideal" deterministic responses given by the matched regulator alone. This is true whether the true model is included in the controller or not. However, identification is not always perfect. When less noise is included in the simulation than that assumed in the design step, there is a tendency for the highest determinant model to dominate the response. A large initial condition does help the identification, but, after the transient has passed, the determinant dominance reappears. It should be noted that it is important to have a very small initial estimation error. Violation of this condition can, because of the very slow poles of the KFs, lead to very poor response.

These linear simulations also indicate that the longitudinal control system can greatly aid the lateral system in correctly identifying the model. It is conjectured that the lateral system does <u>not</u> significantly aid the longitudinal system in identification. At present, however, this remains an unresolved issue.

Chapter 6 indicates that nonlinearities tend to hurt the response greatly. Both the identification and control functions give results which are significantly different from those observed in the linear case. The most significant nonlinearities appear to be of the form $\sin \phi$ in the expression for lateral acceleration, which is linearized to $\sin \phi \approx \phi$. This enters very strongly into the regulator cost function and also into the observation equation for the KF. The bank angle instability exhibited in the nonlinear simulations is believed to result from combining this bank

angle nonlinearity with a system designed to give neutral (linear) stability and a KF which is very slow at estimating bank angle. Because the neutral stability of the bank angle is part of the cause of the instability it is possible that by directly penalizing the bank angle in the regulator cost function, bank angle would be kept small, thereby not leaving the region of validity of the linearization. A second approach, at least for the KF part of the problem, may be to create a linear pseudo-observation of lateral acceleration such as

$$\tilde{Z}(k) = Z(k) + \sin \hat{\phi} \tag{1}$$

where $\tilde{Z}(k)$ is the new pseudo-observation of lateral acceleration, $Z(k)$ is the acceleration sensor's output and $\hat{\phi}$ is the KF state estimate of bank angle.

In summary, the main points of this section are:

1) We have demonstrated the feasibility of using regulators in aircraft control design. Specifically we have been able to formulate a cost criterion that reflects the usual handling qualities criteria. The problem remains to develop some method for incorporating pilot inputs. (See the next section).
2) The use of Kalman filters in aircraft control design is hindered by the presence of a slow pole in the filter due to a lack of strong observability.
3) The MMAC method provides good response when the model is correctly identified. However, when identification is poor, the response can also be poor if the chosen model is mismatch unstable.
4) Neutral stability of the bank angle for a linear model can lead to an unstable bank angle response when the method is applied to a nonlinear model.

5) Both the determinant dominance effect and the effects of nonlinearities can severly degrade performance.

7.3 Pilot Inputs

It should be noted that in the present design, no capability for pilot commands is included. That is, the present system regulates the state with the reference taken to be the zero state. It is envisioned that pilot commands could enter by making the reference the output of some ideal model driven by pilot inputs. Research is presently continuing to implement such a system. It is not at all clear, however, that the present design combined with a varying reference will prove to be satisfactory, as regulator systems are not usually employed with "dynamic" references.

7.4 Suggestions for Future Research

The list of possible directions for future research is almost endless. A few of the possible areas are given below.

1) As mentioned in Chapter 2, no theory has been developed to prove stability of the MMAC method when the true model is not among the available candidates. It is imperative that this be done.

2) New filters need to be developed either using measurements considered unusable in the present work or using a filter designed with a pole constraint to speed up the filter response. Breza and Bryson have presented one method of accomplishing the latter [3].

3) One approach to curing the divergence of bank angle appears to be to redesign the regulators to include an explicit penalty on bank angle. This would tend to hold the angle near zero and thus would also assist in eliminating problems due to nonlinearities. Note that this would tend to

damp out the coordinated turns effect of the control system (a characteristic of the near neutral stability of the bank angle).

4) Further investigation is needed to determine how the lateral and longitudinal systems aid each other in identification of the model. It may be that the longitudinal system can provide sufficient information to render the lateral identification calculations unnecessary.

5) Additional work also needs to be done on exactly how the determinant in equation (4) of Chapter 2 affects the identification. The determinant dominance effect is highly undesirable (see the simulations of Chapter 6), and it may prove to be necessary to modify the probability calculations to avoid this problem.

This list is by no means exhaustive as there are many small parameters which affect any practical design. However, it is felt that this list points out several crucial directions in which research is needed before any type of advanced control philosophy can be transformed into a practical aircraft control system design methodology.

APPENDIX A

LATERAL DYNAMICS

PLANT MATRICES

FLIGHT CONDITION 5 DYNAMIC PRESSURE 133 PSF MACH 0.30 ALTITUDE 0 FT

SYSTEM MATRIX (A)

-2.6533	0.4064	-22.7939	0.0	9.8486	3.8587	0.0	0.0	-22.7939
-0.0841	-0.2620	2.2666	0.0	0.3508	-1.6798	0.0	0.0	2.2666
0.1403	-0.9855	-0.2292	0.0962	0.0	0.0467	0.0	0.0	-0.2292
0.9900	0.1409	0.0	0.0	0.0	0.0	0.0	0.0	0.0
0.0	0.0	0.0	0.0	-30.0000	0.0	30.0000	0.0	0.0
0.0	0.0	0.0	0.0	0.0	-25.0000	0.0	25.0000	0.0
0.0	0.0	0.0	0.0	0.0	0.0	0.0	0.0	0.0
0.0	0.0	0.0	0.0	0.0	0.0	0.0	0.0	0.0
0.0	0.0	0.0	0.0	0.0	0.0	0.0	0.0	-3.3493

INPUT MATRIX (B)

0.0	0.0
0.0	0.0
0.0	0.0
0.0	0.0
0.0	0.0
0.0	0.0
1.000	0.0
0.0	1.000
0.0	0.0

POLES OF OPEN-LOOP SYSTEM

REAL PART =	-0.441	IMAG PART =	2.136
REAL PART =	-0.441	IMAG PART =	-2.136
REAL PART =	-2.228	IMAG PART =	0.0
REAL PART =	-0.035	IMAG PART =	0.0
REAL PART =	-30.000	IMAG PART =	0.0
REAL PART =	-25.000	IMAG PART =	0.0
REAL PART =	0.0	IMAG PART =	0.0
REAL PART =	0.0	IMAG PART =	0.0
REAL PART =	-3.349	IMAG PART =	0.0

OBSERVATION MATRIX (C)

-0.01166	0.15030	-2.38430	0.00064	0.0	0.48618	0.0	0.0	0.0
1.00000	0.0	0.0	0.0	0.0	0.0	0.0	0.0	0.0
0.0	1.00000	0.0	0.0	0.0	0.0	0.0	0.0	0.0
0.0	0.0	0.0	0.0	1.00000	0.0	0.0	0.0	0.0
0.0	0.0	0.0	0.0	0.0	1.00000	0.0	0.0	0.0

FLIGHT CONDITION 5 CONTINUED

DISCRETE TIME SYSTEM MATRIX (AD) DT=.125 SEC

0.6967	0.1950	-2.3467	-0.0151	0.2472	0.1034	0.7948	0.2804	-1.8894
-0.0064	0.9503	0.2840	0.0017	0.0093	-0.0625	0.0288	-0.1439	0.2319
0.0157	-0.1173	0.9320	0.0117	0.0029	0.0090	0.0046	0.0132	-0.0578
0.1043	0.0265	-0.1529	0.9994	0.0264	0.0103	0.0422	0.0137	-0.1330
0.0	0.0	0.0	0.0	0.0235	0.0	0.9765	0.0	0.0
0.0	0.0	0.0	0.0	0.0	0.0439	0.0	0.9561	0.0
0.0	0.0	0.0	0.0	0.0	0.0	1.0000	0.0	0.0
0.0	0.0	0.0	0.0	0.0	0.0	0.0	1.0000	0.0
0.0	0.0	0.0	0.0	0.0	0.0	0.0	0.0	0.6579

DISCRETE TIME INPUT MATRIX (BD) DT=.125 SEC

0.042	0.015
0.002	-0.007
0.000	0.001
0.002	0.000
0.092	0.0
0.0	0.087
0.125	0.0
0.0	0.125
0.0	0.0

POLES OF DISCRETE TIME OPEN-LOOP SYSTEM DT=.125 SEC

REAL PART =	0.913	IMAG PART =	0.250
REAL PART =	0.913	IMAG PART =	-0.250
REAL PART =	0.757	IMAG PART =	0.0
REAL PART =	0.996	IMAG PART =	0.0
REAL PART =	0.024	IMAG PART =	0.0
REAL PART =	0.044	IMAG PART =	0.0
REAL PART =	1.000	IMAG PART =	0.0
REAL PART =	1.000	IMAG PART =	0.0
REAL PART =	0.658	IMAG PART =	0.0

FLIGHT CONDITION 6 DYNAMIC PRESSURE 416 PSF MACH 0.53 ALTITUDE 0 FT

SYSTEM MATRIX (A)

-4.4953	0.3397	-54.3350	0.0	26.8795	10.4212	0.0	0.0	-54.3350
-0.0950	-0.4772	7.8455	0.0	1.1063	-4.7476	0.0	0.0	7.8455
0.0538	-0.9940	-0.3905	0.0545	0.0	0.0716	0.0	0.0	-0.3905
0.9985	0.0541	0.0	0.0	0.0	0.0	0.0	0.0	0.0
0.0	0.0	0.0	0.0	-30.0000	0.0	30.0000	0.0	0.0
0.0	0.0	0.0	0.0	0.0	-25.0000	0.0	25.0000	0.0
0.0	0.0	0.0	0.0	0.0	0.0	0.0	0.0	0.0
0.0	0.0	0.0	0.0	0.0	0.0	0.0	0.0	0.0
0.0	0.0	0.0	0.0	0.0	0.0	0.0	0.0	-5.9172

INPUT MATRIX (B)

0.0	0.0
0.0	0.0
0.0	0.0
0.0	0.0
0.0	0.0
0.0	0.0
1.000	0.0
0.0	1.000
0.0	0.0

POLES OF OPEN-LOOP SYSTEM

REAL PART =	-4.332	IMAG PART =	0.0
REAL PART =	-0.026	IMAG PART =	0.0
REAL PART =	-0.503	IMAG PART =	3.178
REAL PART =	-0.503	IMAG PART =	-3.178
REAL PART =	-30.000	IMAG PART =	0.0
REAL PART =	-25.000	IMAG PART =	0.0
REAL PART =	0.0	IMAG PART =	0.0
REAL PART =	0.0	IMAG PART =	0.0
REAL PART =	-5.917	IMAG PART =	0.0

OBSERVATION MATRIX (C)

-0.00505	0.11063	-7.17580	0.00096	0.0	1.31520	0.0	0.0	0.0
1.00000	0.0	0.0	0.0	0.0	0.0	0.0	0.0	0.0
0.0	1.00000	0.0	0.0	0.0	0.0	0.0	0.0	0.0
0.0	0.0	0.0	0.0	1.00000	0.0	0.0	0.0	0.0
0.0	0.0	0.0	0.0	0.0	1.00000	0.0	0.0	0.0

FLIGHT CONDITION 6 CONTINUED

DISCRETE TIME SYSTEM MATRIX (AD) DT=.125 SEC

0.5527	0.3652	-4.8866	-0.0187	0.5748	0.2117	1.9934	0.6716	-3.2973
-0.0058	0.8838	0.9354	0.0033	0.0286	-0.1678	0.0900	-0.3973	0.6557
0.0058	-0.1143	0.8750	0.0065	0.0008	0.0196	0.0013	0.0279	-0.0946
0.0947	0.0234	-0.3395	0.9992	0.0665	0.0260	0.1092	0.0360	-0.2656
0.0	0.0	0.0	0.0	0.0235	0.0	0.9765	0.0	0.0
0.0	0.0	0.0	0.0	0.0	0.0439	0.0	0.9561	0.0
0.0	0.0	0.0	0.0	0.0	0.0	1.0000	0.0	0.0
0.0	0.0	0.0	0.0	0.0	0.0	0.0	1.0000	0.0
0.0	0.0	0.0	0.0	0.0	0.0	0.0	0.0	0.4773

DISCRETE TIME INPUT MATRIX (BD) DT=.125 SEC

0.109	0.037
0.005	-0.020
0.000	0.001
0.004	0.001
0.092	0.0
0.0	0.087
0.125	0.0
0.0	0.125
0.0	0.0

POLES OF DISCRETE TIME OPEN-LOOP SYSTEM DT=.125 SEC

REAL PART =	0.582	IMAG PART =	0.0
REAL PART =	0.997	IMAG PART =	0.0
REAL PART =	0.866	IMAG PART =	0.363
REAL PART =	0.866	IMAG PART =	-0.363
REAL PART =	0.024	IMAG PART =	0.0
REAL PART =	0.044	IMAG PART =	0.0
REAL PART =	1.000	IMAG PART =	0.0
REAL PART =	1.000	IMAG PART =	0.0
REAL PART =	0.477	IMAG PART =	0.0

FLIGHT CONDITION 7 DYNAMIC PRESSURE 726 PSF MACH 0.70 ALTITUDE 0 FT

SYSTEM MATRIX (A)

-5.9383	0.2922	-80.5645	0.0	41.6520	14.9656	0.0	0.0	-80.5645
-0.0911	-0.6424	13.9832	0.0	1.6644	-7.1693	0.0	0.0	13.9832
0.0330	-0.9948	-0.5079	0.0412	0.0	0.0783	0.0	0.0	-0.5079
0.9995	0.0331	0.0	0.0	0.0	0.0	0.0	0.0	0.0
0.0	0.0	0.0	0.0	-30.0000	0.0	30.0000	0.0	0.0
0.0	0.0	0.0	0.0	0.0	-25.0000	0.0	25.0000	0.0
0.0	0.0	0.0	0.0	0.0	0.0	0.0	0.0	0.0
0.0	0.0	0.0	0.0	0.0	0.0	0.0	0.0	0.0
0.0	0.0	0.0	0.0	0.0	0.0	0.0	0.0	-7.8151

INPUT MATRIX (B)

0.0	0.0
0.0	0.0
0.0	0.0
0.0	0.0
0.0	0.0
0.0	0.0
1.000	0.0
0.0	1.000
0.0	0.0

POLES OF OPEN-LOOP SYSTEM

REAL PART =	-5.846	IMAG PART =	0.0
REAL PART =	-0.019	IMAG PART =	0.0
REAL PART =	-0.612	IMAG PART =	4.012
REAL PART =	-0.612	IMAG PART =	-4.012
REAL PART =	-30.000	IMAG PART =	0.0
REAL PART =	-25.000	IMAG PART =	0.0
REAL PART =	0.0	IMAG PART =	0.0
REAL PART =	0.0	IMAG PART =	0.0
REAL PART =	-7.815	IMAG PART =	0.0

OBSERVATION MATRIX (C)

-0.00391	0.12596	-12.32800	-0.00053	0.0	1.89990	0.0	0.0	0.0
1.00000	0.0	0.0	0.0	0.0	0.0	0.0	0.0	0.0
0.0	1.00000	0.0	0.0	0.0	0.0	0.0	0.0	0.0
0.0	0.0	0.0	0.0	1.00000	0.0	0.0	0.0	0.0
0.0	0.0	0.0	0.0	0.0	1.00000	0.0	0.0	0.0

FLIGHT CONDITION 7 CONTINUED

DISCRETE TIME SYSTEM MATRIX (AD) DT=.125 SEC

0.4614	0.4842	-6.4983	-0.0196	0.7876	0.2360	2.8972	0.8757	-3.8091
-0.0045	0.8222	1.5999	0.0043	0.0418	-0.2412	0.1338	-0.5872	1.0018
0.0034	-0.1108	0.8212	0.0048	-0.0010	0.0268	-0.0015	0.0377	-0.1252
0.0875	0.0264	-0.4718	0.9991	0.0967	0.0342	0.1618	0.0492	-0.3414
0.0	0.0	0.0	0.0	0.0235	0.0	0.9765	0.0	0.0
0.0	0.0	0.0	0.0	0.0	0.0439	0.0	0.9561	0.0
0.0	0.0	0.0	0.0	0.0	0.0	1.0000	0.0	0.0
0.0	0.0	0.0	0.0	0.0	0.0	0.0	1.0000	0.0
0.0	0.0	0.0	0.0	0.0	0.0	0.0	0.0	0.3765

DISCRETE TIME INPUT MATRIX (BD) DT=.125 SEC

0.162	0.050
0.007	-0.030
-0.000	0.001
0.006	0.002
0.092	0.0
0.0	0.087
0.125	0.0
0.0	0.125
0.0	0.0

POLES OF DISCRETE TIME OPEN-LOOP SYSTEM DT=.125 SEC

REAL PART =	0.482	IMAG PART =	0.0
REAL PART =	0.998	IMAG PART =	0.0
REAL PART =	0.812	IMAG PART =	0.445
REAL PART =	0.812	IMAG PART =	-0.445
REAL PART =	0.024	IMAG PART =	0.0
REAL PART =	0.044	IMAG PART =	0.0
REAL PART =	1.000	IMAG PART =	0.0
REAL PART =	1.000	IMAG PART =	0.0
REAL PART =	0.376	IMAG PART =	0.0

FLIGHT CONDITION 8 DYNAMIC PRESSURE 1098 PSF MACH 0.86 ALTITUDE 0 FT

SYSTEM MATRIX (A)

-7.9192	0.2787	-115.6782	0.0	48.4070	15.5433	0.0	0.0	-115.6782
-0.1155	-0.8086	20.7316	0.0	1.7529	-7.8529	0.0	0.0	20.7316
0.0261	-0.9951	-0.6435	0.0335	0.0	0.0662	0.0	0.0	-0.6435
0.9997	0.0262	0.0	0.0	0.0	0.0	0.0	0.0	0.0
0.0	0.0	0.0	0.0	-30.0000	0.0	30.0000	0.0	0.0
0.0	0.0	0.0	0.0	0.0	-25.0000	0.0	25.0000	0.0
0.0	0.0	0.0	0.0	0.0	0.0	0.0	0.0	0.0
0.0	0.0	0.0	0.0	0.0	0.0	0.0	0.0	0.0
0.0	0.0	0.0	0.0	0.0	0.0	0.0	0.0	-9.6015

INPUT MATRIX (B)

0.0	0.0
0.0	0.0
0.0	0.0
0.0	0.0
0.0	0.0
0.0	0.0
1.000	0.0
0.0	1.000
0.0	0.0

POLES OF OPEN-LOOP SYSTEM

REAL PART =	-7.852	IMAG PART =	0.0
REAL PART =	-0.015	IMAG PART =	0.0
REAL PART =	-0.752	IMAG PART =	4.814
REAL PART =	-0.752	IMAG PART =	-4.814
REAL PART =	-30.000	IMAG PART =	0.0
REAL PART =	-25.000	IMAG PART =	0.0
REAL PART =	0.0	IMAG PART =	0.0
REAL PART =	0.0	IMAG PART =	0.0
REAL PART =	-9.601	IMAG PART =	0.0

OBSERVATION MATRIX (C)

-0.00357	0.14581	-19.18700	-0.00079	0.0	1.97370	0.0	0.0	0.0
1.00000	0.0	0.0	0.0	0.0	0.0	0.0	0.0	0.0
0.0	1.00000	0.0	0.0	0.0	0.0	0.0	0.0	0.0
0.0	0.0	0.0	0.0	1.00000	0.0	0.0	0.0	0.0
0.0	0.0	0.0	0.0	0.0	1.00000	0.0	0.0	0.0

FLIGHT CONDITION 8 CONTINUED

DISCRETE TIME SYSTEM MATRIX (AD) DT=.125 SEC

0.3566	0.6201	-8.0868	-0.0209	0.7709	0.1585	3.0874	0.7920	-4.0636
-0.0050	0.7584	2.2939	0.0051	0.0399	-0.2517	0.1340	-0.6303	1.2922
0.0026	-0.1067	0.7596	0.0038	-0.0015	0.0275	-0.0023	0.0385	-0.1567
0.0786	0.0323	-0.6209	0.9990	0.1030	0.0310	0.1769	0.0470	-0.4161
0.0	0.0	0.0	0.0	0.0235	0.0	0.9765	0.0	0.0
0.0	0.0	0.0	0.0	0.0	0.0439	0.0	0.9561	0.0
0.0	0.0	0.0	0.0	0.0	0.0	1.0000	0.0	0.0
0.0	0.0	0.0	0.0	0.0	0.0	0.0	1.0000	0.0
0.0	0.0	0.0	0.0	0.0	0.0	0.0	0.0	0.3011

DISCRETE TIME INPUT MATRIX (BD) DT=.125 SEC

0.177	0.048
0.007	-0.033
-0.000	0.001
0.007	0.002
0.092	0.0
0.0	0.087
0.125	0.0
0.0	0.125
0.0	0.0

POLES OF DISCRETE TIME OPEN-LOOP SYSTEM DT=.125 SEC

REAL PART =	0.375	IMAG PART =	0.0
REAL PART =	0.998	IMAG PART =	0.0
REAL PART =	0.750	IMAG PART =	0.515
REAL PART =	0.750	IMAG PART =	-0.515
REAL PART =	0.024	IMAG PART =	0.0
REAL PART =	0.044	IMAG PART =	0.0
REAL PART =	1.000	IMAG PART =	0.0
REAL PART =	1.000	IMAG PART =	0.0
REAL PART =	0.301	IMAG PART =	0.0

FLIGHT CONDITION 9 DYNAMIC PRESSURE 1480 PSF MACH 1.00 ALTITUDE 0 FT

SYSTEM MATRIX (A)

-7.6563	0.0747	-147.1262	0.0	16.4470	8.7581	0.0	0.0	-147.1262
-0.1238	-0.9751	24.3374	0.0	0.6475	-4.4033	0.0	0.0	24.3374
0.0208	-0.9952	-0.7786	0.0288	0.0	0.0307	0.0	0.0	-0.7786
0.9998	0.0209	0.0	0.0	0.0	0.0	0.0	0.0	0.0
0.0	0.0	0.0	0.0	-30.0000	0.0	30.0000	0.0	0.0
0.0	0.0	0.0	0.0	0.0	-25.0000	0.0	25.0000	0.0
0.0	0.0	0.0	0.0	0.0	0.0	0.0	0.0	0.0
0.0	0.0	0.0	0.0	0.0	0.0	0.0	0.0	0.0
0.0	0.0	0.0	0.0	0.0	0.0	0.0	0.0	-11.1640

INPUT MATRIX (B)

0.0	0.0
0.0	0.0
0.0	0.0
0.0	0.0
0.0	0.0
0.0	0.0
1.000	0.0
0.0	1.000
0.0	0.0

POLES OF OPEN-LOOP SYSTEM

REAL PART =	-7.673	IMAG PART =	0.0
REAL PART =	-0.018	IMAG PART =	0.0
REAL PART =	-0.859	IMAG PART =	5.233
REAL PART =	-0.859	IMAG PART =	-5.233
REAL PART =	-30.000	IMAG PART =	0.0
REAL PART =	-25.000	IMAG PART =	0.0
REAL PART =	0.0	IMAG PART =	0.0
REAL PART =	0.0	IMAG PART =	0.0
REAL PART =	-11.164	IMAG PART =	0.0

OBSERVATION MATRIX (C)

-0.00360	0.16643	-26.99699	-0.00005	0.0	1.06510	0.0	0.0	0.0
1.00000	0.0	0.0	0.0	0.0	0.0	0.0	0.0	0.0
0.0	1.00000	0.0	0.0	0.0	0.0	0.0	0.0	0.0
0.0	0.0	0.0	0.0	1.00000	0.0	0.0	0.0	0.0
0.0	0.0	0.0	0.0	0.0	0.0	0.0	0.0	0.0

FLIGHT CONDITION 9 CONTINUED

DISCRETE TIME SYSTEM MATRIX (AD) DT=.125 SEC

0.3678	0.7623	-10.2401	-0.0229	0.2703	0.0781	1.0636	0.4387	-4.6280
-0.0057	0.7180	2.6306	0.0050	0.0141	-0.1369	0.0486	-0.3488	1.3544
0.0022	-0.1037	0.7217	0.0032	-0.0008	0.0148	-0.0013	0.0206	-0.1699
0.0797	0.0379	-0.7911	0.9990	0.0355	0.0173	0.0606	0.0264	-0.5002
0.0	0.0	0.0	0.0	0.0235	0.0	0.9765	0.0	0.0
0.0	0.0	0.0	0.0	0.0	0.0439	0.0	0.9561	0.0
0.0	0.0	0.0	0.0	0.0	0.0	1.0000	0.0	0.0
0.0	0.0	0.0	0.0	0.0	0.0	0.0	1.0000	0.0
0.0	0.0	0.0	0.0	0.0	0.0	0.0	0.0	0.2477

DISCRETE TIME INPUT MATRIX (BD) DT=.125 SEC

0.061	0.027
0.003	-0.018
-0.000	0.001
0.002	0.001
0.092	0.0
0.0	0.087
0.125	0.0
0.0	0.125
0.0	0.0

POLES OF DISCRETE TIME OPEN-LOOP SYSTEM DT=.125 SEC

REAL PART =	0.383	IMAG PART =	0.0
REAL PART =	0.998	IMAG PART =	0.0
REAL PART =	0.713	IMAG PART =	0.547
REAL PART =	0.713	IMAG PART =	-0.547
REAL PART =	0.024	IMAG PART =	0.0
REAL PART =	0.044	IMAG PART =	0.0
REAL PART =	1.000	IMAG PART =	0.0
REAL PART =	1.000	IMAG PART =	0.0
REAL PART =	0.248	IMAG PART =	0.0

FLIGHT CONDITION 10 DYNAMIC PRESSURE 109 PSF MACH 0.40 ALTITUDE 20000 FT

SYSTEM MATRIX (A)

-1.7458	0.3138	-18.0314	0.0	7.7616	3.3622	0.0	0.0	-18.0314
-0.0665	-0.1757	1.5046	0.0	0.4238	-1.4372	0.0	0.0	1.5046
0.1698	-0.9830	-0.1694	0.0778	0.0	0.0322	0.0	0.0	-0.1694
0.9854	0.1702	0.0	0.0	0.0	0.0	0.0	0.0	0.0
0.0	0.0	0.0	0.0	-30.0000	0.0	30.0000	0.0	0.0
0.0	0.0	0.0	0.0	0.0	-25.0000	0.0	25.0000	0.0
0.0	0.0	0.0	0.0	0.0	0.0	0.0	0.0	0.0
0.0	0.0	0.0	0.0	0.0	0.0	0.0	0.0	0.0
0.0	0.0	0.0	0.0	0.0	0.0	0.0	0.0	-0.3318

INPUT MATRIX (B)

0.0	0.0
0.0	0.0
0.0	0.0
0.0	0.0
0.0	0.0
0.0	0.0
1.000	0.0
0.0	1.000
0.0	0.0

POLES OF OPEN-LOOP SYSTEM

REAL PART =	-0.371	IMAG PART =	2.004
REAL PART =	-0.371	IMAG PART =	-2.004
REAL PART =	-1.321	IMAG PART =	0.0
REAL PART =	-0.028	IMAG PART =	0.0
REAL PART =	-30.000	IMAG PART =	0.0
REAL PART =	-25.000	IMAG PART =	0.0
REAL PART =	0.0	IMAG PART =	0.0
REAL PART =	0.0	IMAG PART =	0.0
REAL PART =	-0.332	IMAG PART =	0.0

OBSERVATION MATRIX (C)

-0.01625	0.21898	-2.18190	0.00151	0.0	0.41451	0.0	0.0	0.0
1.00000	0.0	0.0	0.0	0.0	0.0	0.0	0.0	0.0
0.0	1.00000	0.0	0.0	0.0	0.0	0.0	0.0	0.0
0.0	0.0	0.0	0.0	1.00000	0.0	0.0	0.0	0.0
0.0	0.0	0.0	0.0	0.0	1.00000	0.0	0.0	0.0

FLIGHT CONDITION 10 CONTINUED

DISCRETE TIME SYSTEM MATRIX (AD) DT=.125 SEC

0.7827	0.1606	-1.9750	-0.0101	0.2125	0.1009	0.6553	0.2584	-1.9327
-0.0054	0.9666	0.1905	0.0009	0.0123	-0.0541	0.0368	-0.1238	0.1866
0.0196	-0.1184	0.9452	0.0095	0.0026	0.0078	0.0040	0.0111	-0.0539
0.1097	0.0285	-0.1254	0.9996	0.0217	0.0093	0.0343	0.0122	-0.1236
0.0	0.0	0.0	0.0	0.0235	0.0	0.9765	0.0	0.0
0.0	0.0	0.0	0.0	0.0	0.0439	0.0	0.9561	0.0
0.0	0.0	0.0	0.0	0.0	0.0	1.0000	0.0	0.0
0.0	0.0	0.0	0.0	0.0	0.0	0.0	1.0000	0.0
0.0	0.0	0.0	0.0	0.0	0.0	0.0	0.0	0.9594

DISCRETE TIME INPUT MATRIX (BD) DT=.125 SEC

0.035	0.013
0.002	-0.006
0.000	0.000
0.001	0.000
0.092	0.0
0.0	0.087
0.125	0.0
0.0	0.125
0.0	0.0

POLES OF DISCRETE TIME OPEN-LOOP SYSTEM DT=.125 SEC

REAL PART =	0.925	IMAG PART =	0.237
REAL PART =	0.925	IMAG PART =	-0.237
REAL PART =	0.848	IMAG PART =	0.0
REAL PART =	0.996	IMAG PART =	0.0
REAL PART =	0.024	IMAG PART =	0.0
REAL PART =	0.044	IMAG PART =	0.0
REAL PART =	1.000	IMAG PART =	0.0
REAL PART =	1.000	IMAG PART =	0.0
REAL PART =	0.959	IMAG PART =	0.0

FLIGHT CONDITION 11 DYNAMIC PRESSURE 254 PSF MACH 0.60 ALTITUDE 20000 FT

SYSTEM MATRIX (A)

-2.5805	0.2514	-37.7795	0.0	17.2369	7.0158	0.0	0.0	-37.7795
-0.0753	-0.2725	4.3579	0.0	0.8157	-3.1758	0.0	0.0	4.3579
0.0782	-0.9944	-0.2293	0.0517	0.0	0.0456	0.0	0.0	-0.2293
0.9969	0.0785	0.0	0.0	0.0	0.0	0.0	0.0	0.0
0.0	0.0	0.0	0.0	-30.0000	0.0	30.0000	0.0	0.0
0.0	0.0	0.0	0.0	0.0	-25.0000	0.0	25.0000	0.0
0.0	0.0	0.0	0.0	0.0	0.0	0.0	0.0	0.0
0.0	0.0	0.0	0.0	0.0	0.0	0.0	0.0	0.0
0.0	0.0	0.0	0.0	0.0	0.0	0.0	0.0	-0.4977

INPUT MATRIX (B)

0.0	0.0
0.0	0.0
0.0	0.0
0.0	0.0
0.0	0.0
0.0	0.0
1.000	0.0
0.0	1.000
0.0	0.0

POLES OF OPEN-LOOP SYSTEM

REAL PART =	-2.380	IMAG PART =	0.0
REAL PART =	-0.025	IMAG PART =	0.0
REAL PART =	-0.338	IMAG PART =	2.620
REAL PART =	-0.338	IMAG PART =	-2.620
REAL PART =	-30.000	IMAG PART =	0.0
REAL PART =	-25.000	IMAG PART =	0.0
REAL PART =	0.0	IMAG PART =	0.0
REAL PART =	0.0	IMAG PART =	0.0
REAL PART =	-0.498	IMAG PART =	0.0

OBSERVATION MATRIX (C)

-0.00559	0.10839	-4.43030	-0.00049	0.0	0.88107	0.0	0.0	0.0
1.00000	0.0	0.0	0.0	0.0	0.0	0.0	0.0	0.0
0.0	1.00000	0.0	0.0	0.0	0.0	0.0	0.0	0.0
0.0	0.0	0.0	0.0	1.00000	0.0	0.0	0.0	0.0
0.0	0.0	0.0	0.0	0.0	1.00000	0.0	0.0	0.0

FLIGHT CONDITION 11 CONTINUED

DISCRETE TIME SYSTEM MATRIX (AD) DT=.125 SEC

0.7046	0.2820	-3.8887	-0.0135	0.4383	0.1837	1.3990	0.5074	-3.7618
-0.0054	0.9331	0.5374	0.0018	0.0228	-0.1166	0.0692	-0.2706	0.5209
0.0089	-0.1180	0.9176	0.0063	0.0015	0.0140	0.0023	0.0195	-0.0804
0.1056	0.0223	-0.2569	0.9994	0.0467	0.0194	0.0746	0.0259	-0.2515
0.0	0.0	0.0	0.0	0.0235	0.0	0.9765	0.0	0.0
0.0	0.0	0.0	0.0	0.0	0.0439	0.0	0.9561	0.0
0.0	0.0	0.0	0.0	0.0	0.0	1.0000	0.0	0.0
0.0	0.0	0.0	0.0	0.0	0.0	0.0	1.0000	0.0
0.0	0.0	0.0	0.0	0.0	0.0	0.0	0.0	0.9397

DISCRETE TIME INPUT MATRIX (BD) DT=.125 SEC

0.075	0.027
0.004	-0.014
0.000	0.001
0.003	0.001
0.092	0.0
0.0	0.087
0.125	0.0
0.0	0.125
0.0	0.0

POLES OF DISCRETE TIME OPEN-LOOP SYSTEM DT=.125 SEC

REAL PART =	0.743	IMAG PART =	0.0
REAL PART =	0.997	IMAG PART =	0.0
REAL PART =	0.908	IMAG PART =	0.308
REAL PART =	0.908	IMAG PART =	-0.308
REAL PART =	0.024	IMAG PART =	0.0
REAL PART =	0.044	IMAG PART =	0.0
REAL PART =	1.000	IMAG PART =	0.0
REAL PART =	1.000	IMAG PART =	0.0
REAL PART =	0.940	IMAG PART =	0.0

FLIGHT CONDITION 12 DYNAMIC PRESSURE 434 PSF MACH 0.80 ALTITUDE 20000 FT

SYSTEM MATRIX (A)

-3.6595	0.2071	-53.3336	0.0	27.9092	10.9683	0.0	0.0	-53.3336
-0.0752	-0.3785	8.3027	0.0	1.2640	-5.1245	0.0	0.0	8.3027
0.0435	-0.9964	-0.3170	0.0389	0.0	0.0526	0.0	0.0	-0.3170
0.9991	0.0436	0.0	0.0	0.0	0.0	0.0	0.0	0.0
0.0	0.0	0.0	0.0	-30.0000	0.0	30.0000	0.0	0.0
0.0	0.0	0.0	0.0	0.0	-25.0000	0.0	25.0000	0.0
0.0	0.0	0.0	0.0	0.0	0.0	0.0	0.0	0.0
0.0	0.0	0.0	0.0	0.0	0.0	0.0	0.0	0.0
0.0	0.0	0.0	0.0	0.0	0.0	0.0	0.0	-0.6636

INPUT MATRIX (B)

0.0	0.0
0.0	0.0
0.0	0.0
0.0	0.0
0.0	0.0
0.0	0.0
1.000	0.0
0.0	1.000
0.0	0.0

POLES OF OPEN-LOOP SYSTEM

REAL PART =	-3.570	IMAG PART =	0.0
REAL PART =	-0.018	IMAG PART =	0.0
REAL PART =	-0.383	IMAG PART =	3.211
REAL PART =	-0.383	IMAG PART =	-3.211
REAL PART =	-30.000	IMAG PART =	0.0
REAL PART =	-25.000	IMAG PART =	0.0
REAL PART =	0.0	IMAG PART =	0.0
REAL PART =	0.0	IMAG PART =	0.0
REAL PART =	-0.664	IMAG PART =	0.0

OBSERVATION MATRIX (C)

-0.00343	0.09223	-8.16640	0.00138	0.0	1.35530	0.0	0.0	0.0
1.00000	0.0	0.0	0.0	0.0	0.0	0.0	0.0	0.0
0.0	1.00000	0.0	0.0	0.0	0.0	0.0	0.0	0.0
0.0	0.0	0.0	0.0	1.00000	0.0	0.0	0.0	0.0
0.0	0.0	0.0	0.0	0.0	1.00000	0.0	0.0	0.0

FLIGHT CONDITION 12 CONTINUED

DISCRETE TIME SYSTEM MATRIX (AD) DT=.125 SEC

0.6182	0.3625	-5.0689	-0.0136	0.6468	0.2478	2.1555	0.7431	-4.8436
-0.0047	0.8916	0.9925	0.0025	0.0343	-0.1825	0.1059	-0.4307	0.9516
0.0049	-0.1159	0.8833	0.0046	-0.0002	0.0202	-0.0003	0.0278	-0.1129
0.0996	0.0216	-0.3462	0.9994	0.0719	0.0289	0.1167	0.0395	-0.3364
0.0	0.0	0.0	0.0	0.0235	0.0	0.9765	0.0	0.0
0.0	0.0	0.0	0.0	0.0	0.0439	0.0	0.9561	0.0
0.0	0.0	0.0	0.0	0.0	0.0	1.0000	0.0	0.0
0.0	0.0	0.0	0.0	0.0	0.0	0.0	1.0000	0.0
0.0	0.0	0.0	0.0	0.0	0.0	0.0	0.0	0.9204

DISCRETE TIME INPUT MATRIX (BD) DT=.125 SEC

0.117	0.040
0.006	-0.022
-0.000	0.001
0.004	0.001
0.092	0.0
0.0	0.087
0.125	0.0
0.0	0.125
0.0	0.0

POLES OF DISCRETE TIME OPEN-LOOP SYSTEM DT=.125 SEC

REAL PART =	0.640	IMAG PART =	0.0
REAL PART =	0.998	IMAG PART =	0.0
REAL PART =	0.877	IMAG PART =	0.372
REAL PART =	0.877	IMAG PART =	-0.372
REAL PART =	0.024	IMAG PART =	0.0
REAL PART =	0.044	IMAG PART =	0.0
REAL PART =	1.000	IMAG PART =	0.0
REAL PART =	1.000	IMAG PART =	0.0
REAL PART =	0.920	IMAG PART =	0.0

FLIGHT CONDITION 13 DYNAMIC PRESSURE 550 PSF MACH 0.90 ALTITUDE 20000 FT

SYSTEM MATRIX (A)

-4.5877	0.1788	-69.2185	0.0	30.6474	11.3638	0.0	0.0	-69.2185
-0.0957	-0.4412	11.2003	0.0	1.2882	-5.4219	0.0	0.0	11.2003
0.0400	-0.9965	-0.3644	0.0345	0.0	0.0474	0.0	0.0	-0.3644
0.9992	0.0401	0.0	0.0	0.0	0.0	0.0	0.0	0.0
0.0	0.0	0.0	0.0	-30.0000	0.0	30.0000	0.0	0.0
0.0	0.0	0.0	0.0	0.0	-25.0000	0.0	25.0000	0.0
0.0	0.0	0.0	0.0	0.0	0.0	0.0	0.0	0.0
0.0	0.0	0.0	0.0	0.0	0.0	0.0	0.0	0.0
0.0	0.0	0.0	0.0	0.0	0.0	0.0	0.0	-0.7466

INPUT MATRIX (B)

0.0	0.0
0.0	0.0
0.0	0.0
0.0	0.0
0.0	0.0
0.0	0.0
1.000	0.0
0.0	1.000
0.0	0.0

POLES OF OPEN-LOOP SYSTEM

REAL PART =	-4.494	IMAG PART =	0.0
REAL PART =	-0.015	IMAG PART =	0.0
REAL PART =	-0.442	IMAG PART =	3.682
REAL PART =	-0.442	IMAG PART =	-3.682
REAL PART =	-30.000	IMAG PART =	0.0
REAL PART =	-25.000	IMAG PART =	0.0
REAL PART =	0.0	IMAG PART =	0.0
REAL PART =	0.0	IMAG PART =	0.0
REAL PART =	-0.747	IMAG PART =	0.0

OBSERVATION MATRIX (C)

-0.00355	0.10202	-10.56300	0.00076	0.0	1.37520	0.0	0.0	0.0
1.00000	0.0	0.0	0.0	0.0	0.0	0.0	0.0	0.0
0.0	1.00000	0.0	0.0	0.0	0.0	0.0	0.0	0.0
0.0	0.0	0.0	0.0	1.00000	0.0	0.0	0.0	0.0
0.0	0.0	0.0	0.0	0.0	1.00000	0.0	0.0	0.0

FLIGHT CONDITION 13 CONTINUED

DISCRETE TIME SYSTEM MATRIX (AD) DT=.125 SEC

0.5470	0.4411	-6.1513	-0.0150	0.6526	0.2202	2.2659	0.7234	-5.8373
-0.0056	0.8632	1.3245	0.0029	0.0330	-0.1895	0.1046	-0.4522	1.2631
0.0044	-0.1142	0.8544	0.0041	-0.0003	0.0206	-0.0004	0.0283	-0.1405
0.0943	0.0247	-0.4309	0.9993	0.0756	0.0282	0.1242	0.0393	-0.4170
0.0	0.0	0.0	0.0	0.0235	0.0	0.9765	0.0	0.0
0.0	0.0	0.0	0.0	0.0	0.0439	0.0	0.9561	0.0
0.0	0.0	0.0	0.0	0.0	0.0	1.0000	0.0	0.0
0.0	0.0	0.0	0.0	0.0	0.0	0.0	1.0000	0.0
0.0	0.0	0.0	0.0	0.0	0.0	0.0	0.0	0.9109

DISCRETE TIME INPUT MATRIX (BD) DT=.125 SEC

0.124	0.040
0.006	-0.023
-0.000	0.001
0.005	0.001
0.092	0.0
0.0	0.087
0.125	0.0
0.0	0.125
0.0	0.0

POLES OF DISCRETE TIME OPEN-LOOP SYSTEM DT=.125 SEC

REAL PART =	0.570	IMAG PART =	0.0
REAL PART =	0.998	IMAG PART =	0.0
REAL PART =	0.848	IMAG PART =	0.420
REAL PART =	0.848	IMAG PART =	-0.420
REAL PART =	0.024	IMAG PART =	0.0
REAL PART =	0.044	IMAG PART =	0.0
REAL PART =	1.000	IMAG PART =	0.0
REAL PART =	1.000	IMAG PART =	0.0
REAL PART =	0.911	IMAG PART =	0.0

FLIGHT CONDITION 14 DYNAMIC PRESSURE 978 PSF MACH 1.20 ALTITUDE 20000 FT

SYSTEM MATRIX (A)

-4.1459	0.1921	-103.5909	C.C	18.6579	7.1883	0.0	0.0	-103.5909
-0.0212	-0.6885	17.6901	0.0	0.6223	-2.8727	0.0	0.0	17.6901
0.0296	-0.9966	-0.4458	0.0259	0.0	0.0182	0.0	0.0	-0.4458
0.9996	0.0297	0.0	0.0	0.0	0.0	0.0	0.0	0.0
0.0	0.0	0.0	0.0	-30.0000	0.0	30.0000	0.0	0.0
0.0	0.0	0.0	0.C	0.0	-25.0000	0.0	25.0000	0.0
0.0	0.0	0.0	0.0	C.0	0.0	0.0	0.0	0.0
0.0	0.0	0.0	0.0	0.0	0.0	0.0	0.0	0.0
0.0	0.0	0.0	0.0	0.0	0.0	0.0	0.0	-0.9955

INPUT MATRIX (B)

0.0	0.0
0.0	0.0
0.0	C.0
0.0	0.0
C.0	0.0
0.0	0.0
1.00C	0.0
0.0	1.000
C.0	0.0

POLES OF OPEN-LOOP SYSTEM

REAL PART =	-3.950	IMAG PART =	0.0
REAL PART =	-0.021	IMAG PART =	0.0
REAL PART =	-0.654	IMAG PART =	4.472
REAL PART =	-0.654	IMAG PART =	-4.472
REAL PART =	-30.000	IMAG PART =	0.0
REAL PART =	-25.00C	IMAG PART =	0.0
REAL PART =	0.0	IMAG PART =	0.0
REAL PART =	0.0	IMAG PART =	0.0
REAL PART =	-0.995	IMAG PART =	0.0

OBSERVATION MATRIX (C)

-0.C0350	0.13216	-17.22800	0.00163	0.0	0.70485	0.0	0.0	C.0
1.C0000	0.0	0.0	0.C	0.0	0.0	0.0	0.0	0.0
0.0	1.00000	0.0	0.C	C.0	0.0	0.0	0.0	0.0
C.C	0.0	0.0	0.0	1.00000	0.0	0.0	0.0	C.0
0.0	0.0	0.0	0.C	0.0	1.00000	0.0	0.0	0.0

FLIGHT CONDITION 14 CONTINUED

DISCRETE TIME SYSTEM MATRIX (AD) DT=.125 SEC

0.5782	0.6494	-9.2131	-0.0169	0.4145	0.1386	1.4091	0.4608	-8.5905
0.0015	0.7927	1.9650	0.0033	0.0178	-0.0939	0.0537	-0.2323	1.8419
0.0029	-0.1099	0.8000	0.0030	-0.0003	0.0103	-0.0005	0.0140	-0.1907
0.0967	0.0327	-0.6491	0.9993	0.0470	0.0181	0.0767	0.0253	-0.6215
0.0	0.0	0.0	0.0	0.0235	0.0	0.9765	0.0	0.0
0.0	0.0	0.0	0.0	0.0	0.0439	0.0	0.9561	0.0
0.0	0.0	0.0	0.0	0.0	0.0	1.0000	0.0	0.0
0.0	0.0	0.0	0.0	0.0	0.0	0.0	1.0000	0.0
0.0	0.0	0.0	0.0	0.0	0.0	0.0	0.0	0.8830

DISCRETE TIME INPUT MATRIX (BD) DT=.125 SEC

0.077	0.026
0.003	-0.012
-0.000	0.001
0.003	0.001
0.092	0.0
0.0	0.087
0.125	0.0
0.0	0.125
0.0	0.0

POLES OF DISCRETE TIME OPEN-LOOP SYSTEM DT=.125 SEC

REAL PART =	0.610	IMAG PART =	0.0
REAL PART =	0.997	IMAG PART =	0.0
REAL PART =	0.781	IMAG PART =	0.489
REAL PART =	0.781	IMAG PART =	-0.489
REAL PART =	0.024	IMAG PART =	0.0
REAL PART =	0.044	IMAG PART =	0.0
REAL PART =	1.000	IMAG PART =	0.0
REAL PART =	1.000	IMAG PART =	0.0
REAL PART =	0.883	IMAG PART =	0.0

FLIGHT CONDITION 15 DYNAMIC PRESSURE 135 PSF MACH 0.70 ALTITUDE 40000 FT

SYSTEM MATRIX (A)

-1.3523	0.2002	-24.8738	0.0	9.8344	4.3847	0.0	0.0	-24.8738
-0.0440	-0.1406	2.3205	0.0	0.5462	-1.9424	0.0	0.0	2.3205
0.1269	-0.9907	-0.1206	0.0476	0.0	0.0258	0.0	0.0	-0.1206
0.9919	0.127.1	0.0	0.0	0.0	0.0	0.0	0.0	0.0
0.0	0.0	0.0	0.0	-30.0000	0.0	30.0000	0.0	0.0
0.0	0.0	0.0	0.0	0.0	-25.0000	0.0	25.0000	0.0
0.0	0.0	0.0	0.0	0.0	0.0	0.0	0.0	0.0
0.0	0.0	0.0	C.0	0.0	0.0	0.0	0.0	0.0
0.0	0.0	0.0	0.0	0.0	0.0	0.0	0.0	-0.5421

INPUT MATRIX (B)

0.0	0.0
C.0	0.0
0.0	0.0
0.0	0.0
0.0	0.0
0.0	0.0
1.000	0.0
0.0	1.000
0.0	0.0

POLES OF OPEN-LOOP SYSTEM

REAL PART =	-0.259	IMAG PART =	2.275
REAL PART =	-0.259	IMAG PART =	-2.275
REAL PART =	-1.075	IMAG PART =	0.0
REAL PART =	-0.021	IMAG PART =	0.0
REAL PART =	-30.000	IMAG PART =	0.0
REAL PART =	-25.000	IMAG PART =	0.0
REAL PART =	0.0	IMAG PART =	0.0
REAL PART =	0.0	IMAG PART =	0.0
REAL PART =	-0.542	IMAG PART =	0.0

OBSERVATION MATRIX (C)

-0.C1070	C.19635	-2.53800	0.00070	0.0	0.54276	0.0	0.0	0.0
1.00000	0.0	0.0	0.C	0.0	0.0	0.0	0.0	0.0
0.0	1.00000	0.0	0.0	0.0	0.0	0.0	0.0	0.0
0.0	C.0	0.0	0.0	1.00000	0.0	0.0	0.0	0.0
0.0	0.0	0.0	0.C	0.0	1.00000	0.0	0.0	0.0

FLIGHT CONDITION 15 CONTINUED

DISCRETE TIME SYSTEM MATRIX (AD) DT=.125 SEC

0.8220	0.2013	-2.7938	-0.0086	0.2796	0.1351	0.8469	0.3427	-2.6977
-0.0028	0.9647	0.2893	0.0009	0.0166	-0.0728	0.0485	-0.1670	0.2797
0.0149	-0.1199	0.9439	0.0058	0.0020	0.0093	0.0032	0.0128	-0.0547
0.1131	0.0246	-0.1777	0.9996	0.0282	0.0127	0.0443	0.0166	-0.1736
0.0	0.0	0.0	0.0	0.0235	0.0	0.9765	0.0	0.0
0.0	0.0	0.0	0.0	0.0	0.0439	0.0	0.9561	0.0
0.0	0.0	0.0	0.0	0.0	0.0	1.0000	0.0	0.0
0.0	0.0	0.0	0.0	0.0	0.0	0.0	1.0000	0.0
0.0	0.0	0.0	0.0	0.0	0.0	0.0	0.0	0.9345

DISCRETE TIME INPUT MATRIX (BD) DT=.125 SEC

0.044	0.018
0.003	-0.008
0.000	0.000
0.002	0.001
0.092	0.0
0.0	0.087
0.125	0.0
0.0	0.125
0.0	0.0

POLES OF DISCRETE TIME OPEN-LOOP SYSTEM DT=.125 SEC

REAL PART =	0.929	IMAG PART =	0.272
REAL PART =	0.929	IMAG PART =	-0.272
REAL PART =	0.997	IMAG PART =	0.0
REAL PART =	0.874	IMAG PART =	0.0
REAL PART =	0.024	IMAG PART =	0.0
REAL PART =	0.044	IMAG PART =	0.0
REAL PART =	1.000	IMAG PART =	0.0
REAL PART =	1.000	IMAG PART =	0.0
REAL PART =	0.934	IMAG PART =	0.0

FLIGHT CONDITION 16 DYNAMIC PRESSURE 176 PSF MACH 0.80 ALTITUDE 40000 FT

SYSTEM MATRIX (A)

-1.6215	0.1666	-31.2874	0.0	12.9218	5.5535	0.0	0.0	-31.2874
-0.0560	-0.1666	3.7470	0.0	0.6202	-2.5084	0.0	0.0	3.7470
0.0940	-0.9943	-0.1442	0.0415	0.0	0.0285	0.0	0.0	-0.1442
0.9956	0.0941	0.0	0.0	0.0	0.0	0.0	0.0	0.0
0.0	0.0	0.0	0.0	-30.0000	0.0	30.0000	0.0	0.0
0.0	0.0	0.0	0.0	0.0	-25.0000	0.0	25.0000	0.0
0.0	0.0	0.0	0.0	0.0	0.0	0.0	0.0	0.0
0.0	0.0	0.0	0.0	0.0	0.0	0.0	0.0	0.0
0.0	0.0	0.0	0.0	0.0	0.0	0.0	0.0	-0.6196

INPUT MATRIX (B)

0.0	0.0
0.0	0.0
0.0	0.0
0.0	0.0
0.0	0.0
0.0	0.0
1.000	0.0
0.0	1.000
0.0	0.0

POLES OF OPEN-LOOP SYSTEM

REAL PART =	-1.449	IMAG PART =	0.0
REAL PART =	-0.017	IMAG PART =	0.0
REAL PART =	-0.233	IMAG PART =	2.538
REAL PART =	-0.233	IMAG PART =	-2.538
REAL PART =	-30.000	IMAG PART =	0.0
REAL PART =	-25.000	IMAG PART =	0.0
REAL PART =	0.0	IMAG PART =	0.0
REAL PART =	0.0	IMAG PART =	0.0
REAL PART =	-0.620	IMAG PART =	0.0

OBSERVATION MATRIX (C)

-0.00643	0.13709	-3.46750	-0.00186	0.0	0.68475	0.0	0.0	0.0
1.00000	0.0	0.0	0.0	0.0	0.0	0.0	0.0	0.0
0.0	1.00000	0.0	0.0	0.0	0.0	0.0	0.0	0.0
0.0	0.0	0.0	0.0	1.00000	0.0	0.0	0.0	0.0
0.0	0.0	0.0	0.0	0.0	1.00000	0.0	0.0	0.0

FLIGHT CONDITION 16 CONTINUED

DISCRETE TIME SYSTEM MATRIX (AD) DT=.125 SEC

0.7958	0.2407	-3.4398	-0.0093	0.3587	0.1642	1.0985	0.4260	-3.3039
-0.0036	0.9505	0.4640	0.0012	0.0182	-0.0932	0.0540	-0.2149	0.4464
0.0110	-0.1197	0.9319	0.0051	0.0017	0.0112	0.0027	0.0153	-0.0662
0.1117	0.0222	-0.2214	0.9996	0.0366	0.0162	0.0577	0.0211	-0.2157
0.0	0.0	0.0	0.0	0.0235	0.0	0.9765	0.0	0.0
0.0	0.0	0.0	0.0	0.0	0.0439	0.0	0.9561	0.0
0.0	0.0	0.0	0.0	0.0	0.0	1.0000	0.0	0.0
0.0	0.0	0.0	0.0	0.0	0.0	0.0	1.0000	0.0
0.0	0.0	0.0	0.0	0.0	0.0	0.0	0.0	0.9255

DISCRETE TIME INPUT MATRIX (BD) DT=.125 SEC

0.058	0.022
0.003	-0.011
0.000	0.001
0.002	0.001
0.092	0.0
0.0	0.087
0.125	0.0
0.0	0.125
0.0	0.0

POLES OF DISCRETE TIME OPEN-LOOP SYSTEM DT=.125 SEC

REAL PART = 0.834 IMAG PART = 0.0
REAL PART = 0.998 IMAG PART = 0.0
REAL PART = 0.923 IMAG PART = 0.303
REAL PART = 0.923 IMAG PART = -0.303
REAL PART = 0.024 IMAG PART = 0.0
REAL PART = 0.044 IMAG PART = 0.0
REAL PART = 1.000 IMAG PART = 0.0
REAL PART = 1.000 IMAG PART = 0.0
REAL PART = 0.925 IMAG PART = 0.0

FLIGHT CONDITION 17 DYNAMIC PRESSURE 223 PSF MACH 0.90 ALTITUDE 40000 FT

SYSTEM MATRIX (A)

-2.0595	0.1350	-38.0375	0.0	16.4553	6.4544	0.0	0.0	-38.0375
-0.0548	-0.1962	5.4886	0.0	0.6475	-2.9261	0.0	0.0	5.4886
0.0731	-0.9960	-0.1685	0.0370	0.0	0.0280	0.0	0.0	-0.1685
0.9973	0.0732	0.0	0.0	0.0	0.0	0.0	0.0	0.0
0.0	0.0	0.0	0.0	-30.0000	0.0	30.0000	0.0	0.0
0.0	0.0	0.0	0.0	0.0	-25.0000	0.0	25.0000	0.0
0.0	0.0	0.0	0.0	0.0	0.0	0.0	0.0	0.0
0.0	0.0	0.0	0.0	0.0	0.0	0.0	0.0	0.0
0.0	0.0	0.0	0.0	0.0	0.0	0.0	0.0	-0.6970

INPUT MATRIX (B)

0.0	0.0
0.0	0.0
0.0	0.0
0.0	0.0
0.0	0.0
0.0	0.0
1.000	0.0
0.0	1.000
0.0	0.0

POLES OF OPEN-LOOP SYSTEM

REAL PART =	-1.889	IMAG PART =	0.0
REAL PART =	-0.014	IMAG PART =	0.0
REAL PART =	-0.260	IMAG PART =	2.820
REAL PART =	-0.260	IMAG PART =	-2.820
REAL PART =	-30.000	IMAG PART =	0.0
REAL PART =	-25.000	IMAG PART =	0.0
REAL PART =	0.0	IMAG PART =	0.0
REAL PART =	0.0	IMAG PART =	0.0
REAL PART =	-0.697	IMAG PART =	0.0

OBSERVATION MATRIX (C)

-0.00442	0.10850	-4.55820	0.00007	0.0	0.75790	0.0	0.0	0.0
1.00000	0.0	0.0	0.0	0.0	0.0	0.0	0.0	0.0
0.0	1.00000	0.0	0.0	0.0	0.0	0.0	0.0	0.0
0.0	0.0	0.0	0.0	1.00000	0.0	0.0	0.0	0.0
0.0	0.0	0.0	0.0	0.0	1.00000	0.0	0.0	0.0

FLIGHT CONDITION 17 CONTINUED

DISCRETE TIME SYSTEM MATRIX (AD) DT=.125 SEC

0.7540	0.2793	-4.0480	-0.0099	0.4387	0.1803	1.3692	0.4822	-3.8666
-0.0030	0.9339	0.6710	0.0016	0.0187	-0.1073	0.0558	-0.2494	0.6423
0.0084	-0.1190	0.9173	0.0045	0.0016	0.0123	0.0025	0.0167	-0.0800
0.1091	0.0212	-0.2643	0.9996	0.0457	0.0185	0.0724	0.0244	-0.2565
0.0	0.0	0.0	0.0	0.0235	0.0	0.9765	0.0	0.0
0.0	0.0	0.0	0.0	0.0	0.0439	0.0	0.9561	0.0
0.0	0.0	0.0	0.0	0.0	0.0	1.0000	0.0	0.0
0.0	0.0	0.0	0.0	0.0	0.0	0.0	1.0000	0.0
0.0	0.0	0.0	0.0	0.0	0.0	0.0	0.0	0.9166

DISCRETE TIME INPUT MATRIX (BD) DT=.125 SEC

0.072	0.025
0.003	-0.013
0.000	0.001
0.003	0.001
0.092	0.0
0.0	0.087
0.125	0.0
0.0	0.125
0.0	0.0

POLES OF DISCRETE TIME OPEN-LOOP SYSTEM DT=.125 SEC

REAL PART =	0.790	IMAG PART =	0.0
REAL PART =	0.998	IMAG PART =	0.0
REAL PART =	0.908	IMAG PART =	0.334
REAL PART =	0.908	IMAG PART =	-0.334
REAL PART =	0.024	IMAG PART =	0.0
REAL PART =	0.044	IMAG PART =	0.0
REAL PART =	1.000	IMAG PART =	0.0
REAL PART =	1.000	IMAG PART =	0.0
REAL PART =	0.917	IMAG PART =	0.0

FLIGHT CONDITION 18 DYNAMIC PRESSURE 397 PSF MACH 1.20 ALTITUDE 40000 FT

SYSTEM MATRIX (A)

-2.1285	0.1748	-55.7635	0.0	12.1947	5.5097	0.0	0.0	-55.7635
-0.0137	-0.3230	9.2954	0.0	0.3276	-2.1190	0.0	0.0	9.2954
0.0540	-0.9969	-0.2119	0.0277	0.0	0.0153	0.0	0.0	-0.2119
0.9985	0.0541	0.0	0.0	0.0	0.0	0.0	0.0	0.0
0.0	0.0	0.0	0.0	-30.0000	0.0	30.0000	0.0	0.0
0.0	0.0	0.0	0.0	0.0	-25.0000	0.0	25.0000	0.0
0.0	0.0	0.0	0.0	0.0	0.0	0.0	0.0	0.0
0.0	0.0	0.0	0.0	0.0	0.0	0.0	0.0	0.0
0.0	0.0	0.0	0.0	0.0	0.0	0.0	0.0	-0.9294

INPUT MATRIX (B)

0.0	0.0
0.0	0.0
0.0	0.0
0.0	0.0
0.0	0.0
0.0	0.0
1.000	0.0
0.0	1.000
0.0	0.0

POLES OF OPEN-LOOP SYSTEM

REAL PART =	-1.897	IMAG PART =	0.0
REAL PART =	-0.019	IMAG PART =	0.0
REAL PART =	-0.374	IMAG PART =	3.447
REAL PART =	-0.374	IMAG PART =	-3.447
REAL PART =	-30.000	IMAG PART =	0.0
REAL PART =	-25.000	IMAG PART =	0.0
REAL PART =	0.0	IMAG PART =	0.0
REAL PART =	0.0	IMAG PART =	0.0
REAL PART =	-0.929	IMAG PART =	0.0

OBSERVATION MATRIX (C)

-0.00415	0.11004	-7.64340	-0.00174	0.0	0.55054	0.0	0.0	0.0
1.00000	0.0	0.0	0.0	0.0	0.0	0.0	0.0	0.0
0.0	1.00000	0.0	0.0	0.0	0.0	0.0	0.0	0.0
0.0	0.0	0.0	0.0	1.00000	0.0	0.0	0.0	0.0
0.0	0.0	0.0	0.0	0.0	1.00000	0.0	0.0	0.0

FLIGHT CONDITION 18 CONTINUED

DISCRETE TIME SYSTEM MATRIX (AD) DT=.125 SEC

0.7465	0.4011	-5.8247	-0.0108	0.3227	0.1494	1.0109	0.4070	-5.4772
0.0021	0.8915	1.0937	0.0019	0.0103	-0.0747	0.0295	-0.1773	1.0310
0.0059	-0.1167	0.8833	0.0033	0.0009	0.0085	0.0014	0.0114	-0.1118
0.1087	0.0242	-0.3846	0.9995	0.0337	0.0159	0.0535	0.0210	-0.3697
0.0	0.0	0.0	0.0	0.0235	0.0	0.9765	0.0	0.0
0.0	0.0	0.0	0.0	0.0	0.0439	0.0	0.9561	0.0
0.0	0.0	0.0	0.0	0.0	0.0	1.0000	0.0	0.0
0.0	0.0	0.0	0.0	0.0	0.0	0.0	1.0000	0.0
0.0	0.0	0.0	0.0	0.0	0.0	0.0	0.0	0.8903

DISCRETE TIME INPUT MATRIX (BD) DT=.125 SEC

0.054	0.022
0.002	-0.009
0.000	0.000
0.002	0.001
0.092	0.0
0.0	0.087
0.125	0.0
0.0	0.125
0.0	0.0

POLES OF DISCRETE TIME OPEN-LOOP SYSTEM DT=.125 SEC

REAL PART =	0.789	IMAG PART =	0.0
REAL PART =	0.998	IMAG PART =	0.0
REAL PART =	0.867	IMAG PART =	0.399
REAL PART =	0.867	IMAG PART =	-0.399
REAL PART =	0.024	IMAG PART =	0.0
REAL PART =	0.044	IMAG PART =	0.0
REAL PART =	1.000	IMAG PART =	0.0
REAL PART =	1.000	IMAG PART =	0.0
REAL PART =	0.890	IMAG PART =	0.0

FLIGHT CONDITION 19 DYNAMIC PRESSURE 537 PSF MACH 1.40 ALTITUDE 40000 FT

SYSTEM MATRIX (A)

-2.2793	0.1869	-73.9007	0.0	11.2794	5.2266	0.0	0.0	-73.9007
0.0019	-0.3451	8.2936	0.0	0.2940	-2.1305	0.0	0.0	8.2936
0.0523	-0.9974	-0.2233	0.0238	0.0	0.0128	0.0	0.0	-0.2233
0.9986	0.0523	0.0	0.0	0.0	0.0	0.0	0.0	0.0
0.0	0.0	0.0	0.0	-30.0000	0.0	30.0000	0.0	0.0
0.0	0.0	0.0	0.0	0.0	-25.0000	0.0	25.0000	0.0
0.0	0.0	0.0	0.0	0.0	0.0	0.0	0.0	0.0
0.0	0.0	0.0	0.0	0.0	0.0	0.0	0.0	0.0
0.0	0.0	0.0	0.0	0.0	0.0	0.0	0.0	-1.0842

INPUT MATRIX (B)

0.0	0.0
0.0	0.0
0.0	0.0
0.0	0.0
0.0	0.0
0.0	0.0
1.000	0.0
0.0	1.000
0.0	0.0

POLES OF OPEN-LOOP SYSTEM

REAL PART = -1.851 IMAG PART = 0.0
REAL PART = -0.025 IMAG PART = 0.0
REAL PART = -0.486 IMAG PART = 3.377
REAL PART = -0.486 IMAG PART = -3.377
REAL PART = -30.000 IMAG PART = 0.0
REAL PART = -25.000 IMAG PART = 0.0
REAL PART = 0.0 IMAG PART = 0.0
REAL PART = 0.0 IMAG PART = 0.0
REAL PART = -1.084 IMAG PART = 0.0

OBSERVATION MATRIX (C)

-0.00377	0.11112	-9.39800	0.00049	0.0	0.53707	0.0	0.0	0.0
1.00000	0.0	0.0	0.0	0.0	0.0	0.0	0.0	0.0
0.0	1.00000	0.0	0.0	0.0	0.0	0.0	0.0	0.0
0.0	0.0	0.0	0.0	1.00000	0.0	0.0	0.0	0.0
0.0	0.0	0.0	0.0	0.0	1.00000	0.0	0.0	0.0

FLIGHT CONDITION 19 CONTINUED

DISCRETE TIME SYSTEM MATRIX (AD) DT=.125 SEC

0.7273	0.5233	-7.6521	-0.0122	0.2938	0.1315	0.9275	0.3757	-7.1215
0.0032	0.8966	0.9687	0.0015	0.0097	-0.0753	0.0272	-0.1783	0.9042
0.0056	-0.1165	0.8839	0.0028	0.0007	0.0083	0.0012	0.0111	-0.1104
0.1075	0.0293	-0.5085	0.9995	0.0309	0.0146	0.0492	0.0196	-0.4856
0.0	0.0	0.0	0.0	0.0235	0.0	0.9765	0.0	0.0
0.0	0.0	0.0	0.0	0.0	0.0439	0.0	0.9561	0.0
0.0	0.0	0.0	0.0	0.0	0.0	1.0000	0.0	0.0
0.0	0.0	0.0	0.0	0.0	0.0	0.0	1.0000	0.0
0.0	0.0	0.0	0.0	0.0	0.0	0.0	0.0	0.8733

DISCRETE TIME INPUT MATRIX (BD) DT=.125 SEC

0.049	0.020
0.001	-0.009
0.000	0.000
0.002	0.001
0.092	0.0
0.0	0.087
0.125	0.0
0.0	0.125
0.0	0.0

POLES OF DISCRETE TIME OPEN-LOOP SYSTEM DT=.125 SEC

REAL PART =	0.793	IMAG PART =	0.0
REAL PART =	0.997	IMAG PART =	0.0
REAL PART =	0.859	IMAG PART =	0.386
REAL PART =	0.859	IMAG PART =	-0.396
REAL PART =	0.024	IMAG PART =	0.0
REAL PART =	0.044	IMAG PART =	0.0
REAL PART =	1.000	IMAG PART =	0.0
REAL PART =	1.000	IMAG PART =	0.0
REAL PART =	0.873	IMAG PART =	0.0

FLIGHT CONDITION 20 DYNAMIC PRESSURE 703 PSF MACH 1.60 ALTITUDE 40000 FT

SYSTEM MATRIX (A)

-2.4566	0.1810	-85.4735	0.0	10.4824	5.0385	0.0	0.0	-85.4735
0.0058	-0.3589	7.9205	0.0	0.3012	-2.2665	0.0	0.0	7.9205
0.0470	-0.9977	-0.2433	0.0208	0.0	0.0114	0.0	0.0	-0.2433
0.9989	0.0471	0.0	0.0	0.0	0.0	0.0	0.0	0.0
0.0	0.0	0.0	0.0	-30.0000	0.0	30.0000	0.0	0.0
0.0	0.0	0.0	0.0	0.0	-25.0000	0.0	25.0000	0.0
0.0	0.0	0.0	0.0	0.0	0.0	0.0	0.0	0.0
0.0	0.0	0.0	0.0	0.0	0.0	0.0	0.0	0.0
0.0	0.0	0.0	0.0	0.0	0.0	0.0	0.0	-1.2390

INPUT MATRIX (B)

0.0	0.0
0.0	0.0
0.0	0.0
0.0	0.0
0.0	0.0
0.0	0.0
1.000	0.0
0.0	1.000
0.0	0.0

POLES OF OPEN-LOOP SYSTEM

REAL PART =	-1.941	IMAG PART =	0.0
REAL PART =	-0.027	IMAG PART =	0.0
REAL PART =	-0.545	IMAG PART =	3.316
REAL PART =	-0.545	IMAG PART =	-3.316
REAL PART =	-30.000	IMAG PART =	0.0
REAL PART =	-25.000	IMAG PART =	0.0
REAL PART =	0.0	IMAG PART =	0.0
REAL PART =	0.0	IMAG PART =	0.0
REAL PART =	-1.239	IMAG PART =	0.0

OBSERVATION MATRIX (C)

-0.00355	0.11016	-11.70200	0.00055	0.0	0.54838	0.0	0.0	0.0
1.00000	0.0	0.0	0.0	0.0	0.0	0.0	0.0	0.0
0.0	1.00000	0.0	0.0	0.0	0.0	0.0	0.0	0.0
0.0	0.0	0.0	0.0	1.00000	0.0	0.0	0.0	0.0
0.0	0.0	0.0	0.0	0.0	1.00000	0.0	0.0	0.0

FLIGHT CONDITION 20 CONTINUED

DISCRETE TIME SYSTEM MATRIX (AD) DT=.125 SEC

0.7103	0.5968	-8.7529	-0.0122	0.2692	0.1177	0.8552	0.3528	-8.0614
0.0032	0.8979	0.9213	0.0012	0.0098	-0.0803	0.0278	-0.1898	0.8516
0.0049	-0.1164	0.8836	0.0025	0.0004	0.0086	0.0007	0.0114	-0.1098
0.1064	0.0319	-0.5849	0.9995	0.0285	0.0137	0.0455	0.0186	-0.5548
0.0	0.0	0.0	0.0	0.0235	0.0	0.9765	0.0	0.0
0.0	0.0	0.0	0.0	0.0	0.0439	0.0	0.9561	0.0
0.0	0.0	0.0	0.0	0.0	0.0	1.0000	0.0	0.0
0.0	0.0	0.0	0.0	0.0	0.0	0.0	1.0000	0.0
0.0	0.0	0.0	0.0	0.0	0.0	0.0	0.0	0.8565

DISCRETE TIME INPUT MATRIX (BD) DT=.125 SEC

0.045	0.019
0.001	-0.010
0.000	0.000
0.002	0.001
0.092	0.0
0.0	0.087
0.125	0.0
0.0	0.125
0.0	0.0

POLES OF DISCRETE TIME OPEN-LOOP SYSTEM DT=.125 SEC

REAL PART = 0.785 IMAG PART = 0.0
REAL PART = 0.997 IMAG PART = 0.0
REAL PART = 0.855 IMAG PART = 0.376
REAL PART = 0.855 IMAG PART = -0.376
REAL PART = 0.024 IMAG PART = 0.0
REAL PART = 0.044 IMAG PART = 0.0
REAL PART = 1.000 IMAG PART = 0.0
REAL PART = 1.000 IMAG PART = 0.0
REAL PART = 0.857 IMAG PART = 0.0

APPENDIX B

LATERAL DYNAMICS
REGULATOR MATRICES

FLIGHT CONDITION 5 DYNAMIC PRESSURE 133 PSF MACH 0.30 ALTITUDE 0 FT

STATE WEIGHTING MATRIX (Q)

2.39E-03	-2.80E-02	4.45E-01	-1.20E-04	0.0	-9.07E-02	0.0	0.0	0.0
-2.80E-02	3.61E-01	-5.73E+00	1.55E-03	0.0	1.17E+00	0.0	0.0	0.0
4.45E-01	-5.73E+00	1.00E+02	-2.45E-02	0.0	-1.85E+01	0.0	0.0	0.0
-1.20E-04	1.55E-03	-2.45E-02	6.61E-06	0.0	5.00E-03	0.0	0.0	0.0
0.0	0.0	0.0	0.0	0.0	0.0	0.0	0.0	0.0
-9.07E-02	1.17E+00	-1.85E+01	5.00E-03	0.0	3.78E+00	0.0	0.0	0.0
0.0	0.0	0.0	0.0	0.0	0.0	0.0	0.0	0.0
0.0	0.0	0.0	0.0	0.0	0.0	0.0	0.0	0.0
0.0	0.0	0.0	0.0	0.0	0.0	0.0	0.0	0.0

CONTROL WEIGHTING MATRIX (R)

3.78E-01	0.0
0.0	6.71E-01

REGULATOR CLOSED-LOOP MATRIX (ACL)

-2.6533	0.4064	-22.7939	0.0	9.8486	3.8587	0.0	0.0	-22.7939
-0.0841	-0.2620	2.2666	0.0	0.3508	-1.6798	0.0	0.0	2.2666
0.1403	-0.9855	-0.2292	0.0962	0.0	0.0467	0.0	0.0	-0.2292
0.9900	0.1409	0.0	0.0	0.0	0.0	0.0	0.0	0.0
0.0	0.0	0.0	0.0	-30.0000	0.0	30.0000	0.0	0.0
0.0	0.0	0.0	0.0	0.0	-25.0000	0.0	25.0000	0.0
-0.4190	4.2430	-1.6960	-0.4207	-0.0886	-0.3413	-1.6980	-2.0790	0.0000
-0.2114	2.4970	4.3310	-0.2649	-0.0457	-0.3048	-1.1710	-3.5790	-0.0000
0.0	0.0	0.0	0.0	0.0	0.0	0.0	0.0	-3.3493

REGULATOR GAIN MATRIX (G)

0.4190	-4.2430	1.6960	0.4207	0.0886	0.3413	1.6980	2.0790	-0.0000
0.2114	-2.4970	-4.3310	0.2649	0.0457	0.3048	1.1710	3.5790	0.0000

FLIGHT CONDITION 5 CONTINUED

POLES OF CLOSED-LOOP SYSTEM - REGULATOR

REAL PART =	-30.000	IMAG PART =	0.0
REAL PART =	-24.890	IMAG PART =	0.0
REAL PART =	-1.961	IMAG PART =	2.746
REAL PART =	-1.961	IMAG PART =	-2.746
REAL PART =	-0.254	IMAG PART =	0.120
REAL PART =	-0.254	IMAG PART =	-0.120
REAL PART =	-1.499	IMAG PART =	0.0
REAL PART =	-2.604	IMAG PART =	0.0
REAL PART =	-3.349	IMAG PART =	0.0

DISCRETE TIME REGULATOR MATRIX (ACLD) DT=.125 SEC

0.6786	0.3846	-2.3387	-0.0343	0.2434	0.0875	0.7119	0.1477	-1.8606
-0.0059	0.9425	0.2521	0.0026	0.0094	-0.0615	0.0337	-0.1232	0.2311
0.0156	-0.1156	0.9339	0.0115	0.0028	0.0088	0.0037	0.0111	-0.0576
0.1037	0.0335	-0.1529	0.9987	0.0262	0.0097	0.0392	0.0090	-0.1322
-0.0330	0.3368	-0.1017	-0.0338	0.0165	-0.0272	0.8321	-0.1793	0.0737
-0.0108	0.1423	0.3508	-0.0156	-0.0023	0.0295	-0.0817	0.6839	0.0258
-0.0430	0.4394	-0.1233	-0.0442	-0.0091	-0.0354	0.8085	-0.2382	0.1167
-0.0132	0.1812	0.4943	-0.0202	-0.0028	-0.0178	-0.1109	0.6224	0.0419
0.0	0.0	0.0	0.0	0.0	0.0	0.0	0.0	0.6579

POLES OF DISCRETE TIME REGULATOR DT=.125 SEC

REAL PART =	0.024	IMAG PART =	0.0
REAL PART =	0.045	IMAG PART =	0.0
REAL PART =	0.737	IMAG PART =	0.263
REAL PART =	0.737	IMAG PART =	-0.263
REAL PART =	0.969	IMAG PART =	0.015
REAL PART =	0.969	IMAG PART =	-0.015
REAL PART =	0.829	IMAG PART =	0.0
REAL PART =	0.722	IMAG PART =	0.0
REAL PART =	0.658	IMAG PART =	0.0

FLIGHT CONDITION 5 CONTINUED

DISCRETE TIME CONTROL GAIN (GD)

0.3512	-3.5860	1.0390	0.3603	0.0742	0.2897	1.5490	1.9270	-0.8634
0.1130	-1.5220	-3.9790	0.1685	0.0238	0.1511	0.9073	3.0630	-0.3147

FLIGHT CONDITION 6 DYNAMIC PRESSURE 416 PSF MACH 0.53 ALTITUDE 0 FT

STATE WEIGHTING MAIRIX (Q)

4.49E-04	-8.94E-03	5.80E-01	-7.75E-05	0.0	-1.06E-01	0.0	0.0	0.0
-8.94E-03	1.96E-01	-1.27E+01	1.70E-03	0.0	2.33E+00	0.0	0.0	0.0
5.80E-01	-1.27E+01	9.06E+02	-1.10E-01	0.0	-1.51E+02	0.0	0.0	0.0
-7.75E-05	1.70E-03	-1.10E-01	1.47E-05	0.0	2.02E-02	0.0	0.0	0.0
0.0	0.0	0.0	0.0	0.0	0.0	0.0	0.0	0.0
-1.06E-01	2.33E+00	-1.51E+02	2.02E-02	0.0	2.77E+01	0.0	0.0	0.0
0.0	0.0	0.0	0.0	0.0	0.0	0.0	0.0	0.0
0.0	0.0	0.0	0.0	0.0	0.0	0.0	0.0	0.0
0.0	0.0	0.0	0.0	0.0	0.0	0.0	0.0	0.0

CONTROL WEIGHTING MATRIX (R)

3.78E-01	0.0
0.0	6.71E-01

DUE TC NUMERICAL PROBLEMS, WE WERE UNABLE TO

SOLVE THE RICCATI EQUATICN FOR THIS FLIGHT CONDITION

FLIGHT CONDITION 7 DYNAMIC PRESSURE 726 PSF MACH 0.70 ALTITUDE 0 FT

STATE WEIGHTING MATRIX (Q)

2.69E-04	-7.88E-03	7.71E-01	3.35E-05	0.0	-1.19E-01	0.0	0.0	0.0
-7.88E-03	2.54E-01	-2.48E+01	-1.08E-03	0.0	3.83E+00	0.0	0.0	0.0
7.71E-01	-2.48E+01	2.67E+03	1.06E-01	0.0	-3.75E+02	0.0	0.0	0.0
3.35E-05	-1.08E-03	1.06E-01	4.58E-06	0.0	-1.63E-02	0.0	0.0	0.0
0.0	0.0	0.0	0.0	0.0	0.0	0.0	0.0	0.0
-1.19E-01	3.83E+00	-3.75E+02	-1.63E-02	0.0	5.78E+01	0.0	0.0	0.0
0.0	0.0	0.0	0.0	0.0	0.0	0.0	0.0	0.0
0.0	0.0	0.0	0.0	0.0	0.0	0.0	0.0	0.0
0.0	0.0	0.0	0.0	0.0	0.0	0.0	0.0	0.0

CONTROL WEIGHTING MATRIX (R)

3.78E-01	0.0
0.0	6.71E-01

REGULATOR CLOSED-LOOP MATRIX (ACL)

-5.9383	0.2922	-80.5645	0.0	41.6520	14.9656	0.0	0.0	-80.5645
-0.0911	-0.6424	13.9832	0.0	1.6644	-7.1693	0.0	0.0	13.9832
0.0330	-0.9948	-0.5079	0.0412	0.0	0.0783	0.0	0.0	-0.5079
0.9995	0.0331	0.0	0.0	0.0	0.0	0.0	0.0	0.0
0.0	0.0	0.0	0.0	-30.0000	0.0	30.0000	0.0	0.0
0.0	0.0	0.0	0.0	0.0	-25.0000	0.0	25.0000	0.0
0.1087	-3.8270	8.3960	0.1659	-0.0566	0.9939	-0.7815	2.2230	-0.0000
-0.3437	12.2200	4.3830	-0.5820	0.1962	-4.6140	1.2520	-15.1000	-0.0000
0.0	0.0	0.0	0.0	0.0	0.0	0.0	0.0	-7.8151

REGULATOR GAIN MATRIX (G)

-0.1087	3.8270	-8.3960	-0.1659	0.0566	-0.9939	0.7815	-2.2230	0.0000
0.3437	-12.2200	-4.3830	0.5820	-0.1962	4.6140	-1.2520	15.1000	0.0000

FLIGHT CONDITION 7 CONTINUED

POLES OF CLOSED-LOOP SYSTEM - REGULATOR

REAL PART =	-30.000	IMAG PART =	0.0
REAL PART =	-23.291	IMAG PART =	0.0
REAL PART =	-6.788	IMAG PART =	5.632
REAL PART =	-6.788	IMAG PART =	-5.632
REAL PART =	-5.770	IMAG PART =	0.0
REAL PART =	-0.118	IMAG PART =	0.0
REAL PART =	-0.403	IMAG PART =	0.0
REAL PART =	-4.811	IMAG PART =	0.0
REAL PART =	-7.815	IMAG PART =	0.0

DISCRETE TIME REGULATOR MATRIX (ACLD) DT=.125 SEC

0.4665	0.3102	-5.1017	-0.0141	0.7857	0.2538	2.8212	0.6312	-3.9019
0.0015	0.6044	1.4337	0.0149	0.0381	-0.1672	0.1036	-0.2422	0.8873
0.0031	-0.1000	0.8306	0.0043	-0.0008	0.0230	-0.0002	0.0207	-0.1206
0.0877	0.0209	-0.4183	0.9993	0.0966	0.0344	0.1590	0.0391	-0.3439
0.0072	-0.2540	0.5356	0.0109	0.0197	0.0660	0.9115	0.1585	-0.1908
-0.0112	0.4090	0.6474	-0.0206	0.0073	-0.0955	0.0602	0.1316	0.3320
0.0090	-0.3180	0.6672	0.0136	-0.0048	0.0825	0.9140	0.2012	-0.2878
-0.0115	0.4276	0.9423	-0.0222	0.0080	-0.1438	0.0737	-0.0381	0.4798
0.0	0.0	0.0	0.0	0.0	0.0	0.0	0.0	0.3765

POLES OF DISCRETE TIME REGULATOR DT=.125 SEC

REAL PART =	0.985	IMAG PART =	0.0
REAL PART =	0.951	IMAG PART =	0.0
REAL PART =	0.326	IMAG PART =	0.277
REAL PART =	0.326	IMAG PART =	-0.277
REAL PART =	0.548	IMAG PART =	0.0
REAL PART =	0.024	IMAG PART =	0.0
REAL PART =	0.054	IMAG PART =	0.0
REAL PART =	0.486	IMAG PART =	0.0
REAL PART =	0.376	IMAG PART =	0.0

FLIGHT CONDITION 7 CONTINUED

DISCRETE TIME CONTROL GAIN (GD)

-0.0698	2.4720	-5.9060	-0.1051	0.0371	-0.6070	0.6811	-1.4430	1.9890
0.1086	-4.0000	-7.6170	0.2046	-0.0733	1.3630	-0.6362	8.8560	-3.8860

FLIGHT CONDITION 8 DYNAMIC PRESSURE 1098 PSF MACH 0.86 ALTITUDE 0 FT

STATE WEIGHTING MATRIX (Q)

2.25E-04	-8.34E-03	1.10E+00	4.52E-05	0.0	-1.13E-01	0.0	0.0	0.0
-8.34E-03	3.40E-01	-4.48E+01	-1.85E-03	0.0	4.60E+00	0.0	0.0	0.0
1.10E+00	-4.48E+01	6.48E+03	2.43E-01	0.0	-6.06E+02	0.0	0.0	0.0
4.52E-05	-1.85E-03	2.43E-01	1.00E-05	0.0	-2.50E-02	0.0	0.0	0.0
0.0	0.0	0.0	0.0	0.0	0.0	0.0	0.0	0.0
-1.13E-01	4.60E+00	-6.06E+02	-2.50E-02	0.0	6.23E+01	0.0	0.0	0.0
0.0	0.0	0.0	0.0	0.0	0.0	0.0	0.0	0.0
0.0	0.0	0.0	0.0	0.0	0.0	0.0	0.0	0.0
0.0	0.0	0.0	0.0	0.0	0.0	0.0	0.0	0.0

CONTROL WEIGHTING MATRIX (R)

3.78E-01	0.0
0.0	6.71E-01

REGULATOR CLOSED-LOOP MATRIX (ACL)

-7.9192	0.2787	-115.6782	0.0	48.4070	15.5433	0.0	0.0	-115.6782
-0.1155	-0.8086	20.7316	0.0	1.7529	-7.8529	0.0	0.0	20.7316
0.0261	-0.9951	-0.6435	0.0335	0.0	0.0662	0.0	0.0	-0.6435
0.9997	0.0262	0.0	0.0	0.0	0.0	0.0	0.0	0.0
0.0	0.0	0.0	0.0	-30.0000	0.0	30.0000	0.0	0.0
0.0	0.0	0.0	0.0	0.0	-25.0000	0.0	25.0000	0.0
0.1315	-5.6960	14.5600	0.2051	-0.1099	1.5770	-0.9937	3.1550	-0.0000
-0.3543	15.5200	5.0830	-0.6075	0.3290	-5.9300	1.7770	-17.0500	-0.0000
0.0	0.0	0.0	0.0	0.0	0.0	0.0	0.0	-9.6015

REGULATOR GAIN MATRIX (G)

-0.1315	5.6960	-14.5600	-0.2051	0.1099	-1.5770	0.9937	-3.1550	0.0000
0.3543	-15.5200	-5.0830	0.6075	-0.3290	5.9300	-1.7770	17.0500	0.0000

FLIGHT CONDITION 8 CONTINUED

POLES OF CLOSED-LOOP SYSTEM - REGULATOR

REAL PART =	-30.000	IMAG PART =	0.0
REAL PART =	-23.368	IMAG PART =	0.0
REAL PART =	-7.384	IMAG PART =	7.422
REAL PART =	-7.384	IMAG PART =	-7.422
REAL PART =	-7.803	IMAG PART =	0.0
REAL PART =	-0.088	IMAG PART =	0.0
REAL PART =	-0.453	IMAG PART =	0.0
REAL PART =	-5.936	IMAG PART =	0.0
REAL PART =	-9.601	IMAG PART =	0.0

DISCRETE TIME REGULATOR MATRIX (ACLD) DT=.125 SEC

0.3663	0.2066	-5.7489	-0.0079	0.7640	0.2432	2.9833	0.6831	-4.3736
0.0011	0.4850	2.0246	0.0161	0.0338	-0.1537	0.0911	-0.2231	1.0892
0.0023	-0.0936	0.7733	0.0033	-0.0012	0.0227	-0.0005	0.0195	-0.1490
0.0789	0.0177	-0.5282	0.9995	0.1028	0.0336	0.1730	0.0416	-0.4251
0.0080	-0.3478	0.8389	0.0124	0.0167	0.0965	0.8984	0.2133	-0.3638
-0.0097	0.4355	0.9827	-0.0184	0.0103	-0.1165	0.0788	0.0803	0.5069
0.0098	-0.4264	1.0219	0.0152	-0.0084	0.1182	0.8980	0.2670	-0.5365
-0.0091	0.4141	1.4256	-0.0184	0.0104	-0.1543	0.0937	-0.0810	0.6928
0.0	0.0	0.0	0.0	0.0	0.0	0.0	0.0	0.3011

POLES OF DISCRETE TIME REGULATOR DT=.125 SEC

REAL PART =	0.989	IMAG PART =	0.0
REAL PART =	0.945	IMAG PART =	0.0
REAL PART =	0.238	IMAG PART =	0.318
REAL PART =	0.238	IMAG PART =	-0.318
REAL PART =	0.476	IMAG PART =	0.0
REAL PART =	0.054	IMAG PART =	0.0
REAL PART =	0.024	IMAG PART =	0.0
REAL PART =	0.377	IMAG PART =	0.0
REAL PART =	0.301	IMAG PART =	0.0

FLIGHT CONDITION 8 CONTINUED

DISCRETE TIME CONTROL GAIN (GD)

-0.0803	3.4950	-9.4020	-0.1240	0.0680	-0.9338	0.8190	-2.0410	3.6830
0.0894	-4.0530	-11.5800	0.1757	-0.0991	1.5100	-0.8188	9.2970	-5.7600

FLIGHT CONDITION 9 DYNAMIC PRESSURE 1480 PSF MACH 1.00 ALTITUDE 0 FT

STATE WEIGHTING MATRIX (Q)

2.28E-04	-9.59E-03	1.56E+00	2.85E-06	0.0	-6.14E-02	0.0	0.0	0.0
-9.59E-03	4.43E-01	-7.19E+01	-1.32E-04	0.0	2.84E+00	0.0	0.0	0.0
1.56E+00	-7.19E+01	1.28E+04	2.14E-02	0.0	-4.60E+02	0.0	0.0	0.0
2.85E-06	-1.32E-04	2.14E-02	3.92E-08	0.0	-8.43E-04	0.0	0.0	0.0
0.0	0.0	0.0	0.0	0.0	0.0	0.0	0.0	0.0
-6.14E-02	2.84E+00	-4.60E+02	-8.43E-04	0.0	1.82E+01	0.0	0.0	0.0
0.0	0.0	0.0	0.0	0.0	0.0	0.0	0.0	0.0
0.0	0.0	0.0	0.0	0.0	0.0	0.0	0.0	0.0
0.0	0.0	0.0	0.0	0.0	0.0	0.0	0.0	0.0

CONTROL WEIGHTING MATRIX (R)

3.78E-01	0.0
0.0	6.71E-01

REGULATOR CLOSED-LOOP MATRIX (ACL)

-7.6563	0.0747	-147.1262	0.0	16.4470	8.7581	0.0	0.0	-147.1262
-0.1238	-0.9751	24.3374	0.0	0.6475	-4.4033	0.0	0.0	24.3374
0.0208	-0.9952	-0.7786	0.0288	0.0	0.0307	0.0	0.0	-0.7786
0.9998	0.0209	0.0	0.0	0.0	0.0	0.0	0.0	0.0
0.0	0.0	0.0	0.0	-30.0000	0.0	30.0000	0.0	0.0
0.0	0.0	0.0	0.0	0.0	-25.0000	0.0	25.0000	0.0
0.1013	-4.5690	8.1380	0.1446	-0.0410	0.7586	-0.4266	2.0120	0.0000
-0.4404	19.4000	13.3000	-0.6756	0.1827	-3.8760	1.1330	-13.8400	0.0000
0.0	0.0	0.0	0.0	0.0	0.0	0.0	0.0	-11.1640

REGULATOR GAIN MATRIX (G)

-0.1013	4.5690	-8.1380	-0.1446	0.0410	-0.7586	0.4266	-2.0120	-0.0000
0.4404	-19.4000	-13.3000	0.6756	-0.1827	3.8760	-1.1330	13.8400	-0.0000

FLIGHT CONDITION 9 CONTINUED

POLES OF CLOSED-LOOP SYSTEM - REGULATOR

REAL PART = -30.000	IMAG PART = 0.0
REAL PART = -24.623	IMAG PART = 0.0
REAL PART = -5.162	IMAG PART = 7.803
REAL PART = -5.162	IMAG PART = -7.803
REAL PART = -7.678	IMAG PART = 0.0
REAL PART = -0.117	IMAG PART = 0.026
REAL PART = -0.117	IMAG PART = -0.026
REAL PART = -5.819	IMAG PART = 0.0
REAL PART = -11.164	IMAG PART = 0.0

DISCRETE TIME REGULATOR MATRIX (ACLD) DT=.125 SEC

0.3661	0.8248	-9.3999	-0.0263	0.2710	0.0585	1.0610	0.2651	-4.5668
-0.0012	0.5206	2.2862	0.0122	0.0122	-0.0973	0.0333	-0.1555	1.1931
0.0020	-0.0943	0.7363	0.0029	-0.0007	0.0129	-0.0006	0.0119	-0.1637
0.0796	0.0419	-0.7588	0.9988	0.0355	0.0162	0.0606	0.0191	-0.4978
0.0060	-0.2697	0.3822	0.0085	0.0211	0.0454	0.9424	0.1403	-0.3133
-0.0152	0.6526	1.7802	-0.0248	0.0064	-0.0901	0.0584	0.1620	0.7954
0.0072	-0.3264	0.4420	0.0102	-0.0030	0.0550	0.9554	0.1766	-0.4547
-0.0159	0.6712	2.5550	-0.0268	0.0067	-0.1414	0.0724	-0.0131	1.1098
0.0	0.0	0.0	0.0	0.0	0.0	0.0	0.0	0.2477

POLES OF DISCRETE TIME REGULATOR DT=.125 SEC

REAL PART = 0.985	IMAG PART = 0.003
REAL PART = 0.985	IMAG PART = -0.003
REAL PART = 0.294	IMAG PART = 0.434
REAL PART = 0.294	IMAG PART = -0.434
REAL PART = 0.483	IMAG PART = 0.0
REAL PART = 0.383	IMAG PART = 0.0
REAL PART = 0.046	IMAG PART = 0.0
REAL PART = 0.024	IMAG PART = 0.0
REAL PART = 0.248	IMAG PART = 0.0

FLIGHT CONDITION 9 CONTINUED

DISCRETE TIME CONTROL GAIN (GD)

-0.0575	2.5933	-3.8860	-0.0811	0.0235	-0.4316	0.3553	-1.3807	3.4729
0.1459	-6.1931	-20.5160	0.2420	-0.0612	1.2907	-0.6155	8.5069	-8.9991

FLIGHT CONDITION 10 DYNAMIC PRESSURE 109 PSF MACH 0.40 ALTITUDE 20000 FT

STATE WEIGHTING MATRIX (Q)

4.65E-03	-5.69E-02	5.67E-01	-3.92E-04	0.0	-1.08E-01	0.0	0.0	0.0
-5.69E-02	7.67E-01	-7.64E+00	5.28E-03	0.0	1.45E+00	0.0	0.0	0.0
5.67E-01	-7.64E+00	8.38E+01	-5.26E-02	0.0	-1.45E+01	0.0	0.0	0.0
-3.92E-04	5.28E-03	-5.26E-02	3.63E-05	0.0	9.99E-03	0.0	0.0	0.0
0.0	0.0	0.0	0.0	0.0	0.0	0.0	0.0	0.0
-1.08E-01	1.45E+00	-1.45E+01	9.99E-03	0.0	2.75E+00	0.0	0.0	0.0
0.0	0.0	0.0	0.0	0.0	0.0	0.0	0.0	0.0
0.0	0.0	0.0	0.0	0.0	0.0	0.0	0.0	0.0
0.0	0.0	0.0	0.0	0.0	0.0	0.0	0.0	0.0

CONTROL WEIGHTING MATRIX (R)

3.78E-01	0.0
0.0	6.71E-01

REGULATOR CLOSED-LOOP MATRIX (ACL)

-1.7458	0.3138	-18.0314	0.0	7.7616	3.3622	0.0	0.0	-18.0314
-0.0665	-0.1757	1.5046	0.0	0.4238	-1.4372	0.0	0.0	1.5046
0.1698	-0.9830	-0.1694	0.0778	0.0	0.0322	0.0	0.0	-0.1694
0.9854	0.1702	0.0	0.0	0.0	0.0	0.0	0.0	0.0
0.0	0.0	0.0	0.0	-30.0000	0.0	30.0000	0.0	0.0
0.0	0.0	0.0	0.0	0.0	-25.0000	0.0	25.0000	0.0
-0.5108	4.0840	-1.5460	-0.3054	-0.0748	-0.2965	-1.5360	-1.9430	0.0000
-0.3813	3.4400	2.9930	-0.2433	-0.0540	-0.3253	-1.0940	-3.7600	-0.0000
0.0	0.0	0.0	0.0	0.0	0.0	0.0	0.0	-0.3318

REGULATOR GAIN MATRIX (G)

0.5108	-4.0840	1.5460	0.3054	0.0748	0.2965	1.5360	1.9430	-0.0000
0.3813	-3.4400	-2.9930	0.2433	0.0540	0.3253	1.0940	3.7600	0.0000

FLIGHT CONDITION 10 CONTINUED

POLES OF CLOSED-LOOP SYSTEM - REGULATOR

REAL PART =	-30.000	IMAG PART =	0.0
REAL PART =	-24.920	IMAG PART =	0.0
REAL PART =	-1.776	IMAG PART =	2.655
REAL PART =	-1.776	IMAG PART =	-2.655
REAL PART =	-0.324	IMAG PART =	0.230
REAL PART =	-0.324	IMAG PART =	-0.230
REAL PART =	-1.233	IMAG PART =	0.0
REAL PART =	-2.033	IMAG PART =	0.0
REAL PART =	-0.332	IMAG PART =	0.0

DISCRETE TIME REGULATOR MATRIX (ACLD) DT=.125 SEC

0.7630	0.3234	-1.9742	-0.0222	0.2096	0.0886	0.5923	0.1488	-1.9106
-0.0045	0.9565	0.1696	0.0016	0.0125	-0.0532	0.0399	-0.1059	0.1855
0.0194	-0.1166	0.9464	0.0094	0.0025	0.0077	0.0034	0.0094	-0.0537
0.1090	0.0344	-0.1256	0.9991	0.0216	0.0089	0.0321	0.0084	-0.1230
-0.0400	0.3210	-0.0924	-0.0244	0.0177	-0.0234	0.8451	-0.1651	0.0651
-0.0224	0.2145	0.2600	-0.0152	-0.0031	0.0262	-0.0775	0.6688	0.0383
-0.0520	0.4177	-0.1118	-0.0319	-0.0076	-0.0304	0.8255	-0.2186	0.1050
-0.0289	0.2818	0.3722	-0.0199	-0.0039	-0.0228	-0.1057	0.6004	0.0651
0.0	0.0	0.0	0.0	0.0	0.0	0.0	0.0	0.9594

POLES OF DISCRETE TIME REGULATOR DT=.125 SEC

REAL PART =	0.024	IMAG PART =	0.0
REAL PART =	0.044	IMAG PART =	0.0
REAL PART =	0.757	IMAG PART =	0.261
REAL PART =	0.757	IMAG PART =	-0.261
REAL PART =	0.960	IMAG PART =	0.028
REAL PART =	0.960	IMAG PART =	-0.028
REAL PART =	0.857	IMAG PART =	0.0
REAL PART =	0.776	IMAG PART =	0.0
REAL PART =	0.959	IMAG PART =	0.0

FLIGHT CONDITION 10 CONTINUED

DISCRETE TIME CONTROL GAIN (GD)

0.4243	-3.4070	0.9411	0.2600	0.0622	0.2483	1.4090	1.7690	-0.7758
0.2412	-2.3340	-2.9800	0.1651	0.0329	0.1902	0.8628	3.2370	-0.4882

FLIGHT CONDITION 11 DYNAMIC PRESSURE 254 PSF MACH 0.60 ALTITUDE 20000 FT

STATE WEIGHTING MATRIX (Q)

5.51E-04	-9.70E-03	3.97E-01	4.39E-05	0.0	-7.89E-02	0.0	0.0	0.0
-9.70E-03	1.88E-01	-7.68E+00	-8.50E-04	0.0	1.53E+00	0.0	0.0	0.0
3.97E-01	-7.68E+00	3.45E+02	3.47E-02	0.0	-6.25E+01	0.0	0.0	0.0
4.39E-05	-8.50E-04	3.47E-02	3.84E-06	0.0	-6.91E-03	0.0	0.0	0.0
0.0	0.0	0.0	0.0	0.0	0.0	0.0	0.0	0.0
-7.89E-02	1.53E+00	-6.25E+01	-6.91E-03	0.0	1.24E+01	0.0	0.0	0.0
0.0	0.0	0.0	0.0	0.0	0.0	0.0	0.0	0.0
0.0	0.0	0.0	0.0	0.0	0.0	0.0	0.0	0.0
0.0	0.0	0.0	0.0	0.0	0.0	0.0	0.0	0.0

CONTROL WEIGHTING MATRIX (R)

3.78E-01	0.0
0.0	6.71E-01

REGULATOR CLOSED-LOOP MATRIX (ACL)

-2.5805	0.2514	-37.7795	0.0	17.2369	7.0158	0.0	0.0	-37.7795
-0.0753	-0.2725	4.3579	0.0	0.8157	-3.1758	0.0	0.0	4.3579
0.0782	-0.9944	-0.2293	0.0517	0.0	0.0456	0.0	0.0	-0.2293
0.9969	0.0785	0.0	0.0	0.0	0.0	0.0	0.0	0.0
0.0	0.0	0.0	0.0	-30.0000	0.0	30.0000	0.0	0.0
0.0	0.0	0.0	0.0	0.0	-25.0000	0.0	25.0000	0.0
-0.2242	3.3410	-3.4990	-0.1838	-0.0373	-0.4534	-0.6684	-1.7850	0.0000
-0.4307	6.6640	4.3630	-0.3755	-0.0706	-1.2490	-1.0050	-7.7890	-0.0000
0.0	0.0	0.0	0.0	0.0	0.0	0.0	0.0	-0.4977

REGULATOR GAIN MATRIX (G)

0.2242	-3.3410	3.4990	0.1838	0.0373	0.4534	0.6684	1.7850	-0.0000
0.4307	-6.6640	-4.3630	0.3755	0.0706	1.2490	1.0050	7.7890	0.0000

FLIGHT CONDITION 11 CONTINUED

POLES OF CLOSED-LOOP SYSTEM - REGULATOR

REAL PART =	-30.000	IMAG PART =	0.0
REAL PART =	-24.639	IMAG PART =	0.0
REAL PART =	-3.265	IMAG PART =	3.473
REAL PART =	-3.265	IMAG PART =	-3.473
REAL PART =	-2.362	IMAG PART =	0.0
REAL PART =	-0.154	IMAG PART =	0.117
REAL PART =	-0.154	IMAG PART =	-0.117
REAL PART =	-2.699	IMAG PART =	0.0
REAL PART =	-0.498	IMAG PART =	0.0

DISCRETE TIME REGULATOR MATRIX (ACLD) DT=.125 SEC

0.6819	0.6275	-3.9807	-0.0328	0.4346	0.1326	1.3307	0.2067	-3.6721
-0.0020	0.8791	0.4642	0.0049	0.0233	-0.1071	0.0778	-0.1861	0.5077
0.0087	-0.1140	0.9208	0.0060	0.0014	0.0133	0.0017	0.0143	-0.0796
0.1048	0.0352	-0.2608	0.9987	0.0465	0.0174	0.0721	0.0149	-0.2489
-0.0172	0.2566	-0.2479	-0.0142	0.0207	-0.0349	0.9198	-0.1464	0.0973
-0.0220	0.3487	0.3997	-0.0201	-0.0035	-0.0133	-0.0622	0.4236	0.1322
-0.0222	0.3323	-0.3157	-0.0185	-0.0037	-0.0452	0.9249	-0.1922	0.1566
-0.0270	0.4334	0.5727	-0.0252	-0.0042	-0.0698	-0.0817	0.2827	0.2199
0.0	0.0	0.0	0.0	0.0	0.0	0.0	0.0	0.9397

POLES OF DISCRETE TIME REGULATOR DT=.125 SEC

REAL PART =	0.603	IMAG PART =	0.280
REAL PART =	0.603	IMAG PART =	-0.280
REAL PART =	0.981	IMAG PART =	0.014
REAL PART =	0.981	IMAG PART =	-0.014
REAL PART =	0.744	IMAG PART =	0.0
REAL PART =	0.046	IMAG PART =	0.0
REAL PART =	0.714	IMAG PART =	0.0
REAL PART =	0.024	IMAG PART =	0.0
REAL PART =	0.940	IMAG PART =	0.0

FLIGHT CONDITION 11 CONTINUED

DISCREIE TIME CONTROL GAIN (GD)

0.1882	-2.8100	2.6390	0.1559	0.0313	0.3859	0.6168	1.6170	-1.0750
0.2317	-3.6970	-4.5690	0.2139	0.0361	0.6002	0.6798	5.8980	-1.6390

FLIGHT CONDITION 12 DYNAMIC PRESSURE 434 PSF MACH 0.80 ALTITUDE 20000 FT

STATE WEIGHTING MATRIX (Q)

2.07E-04	-5.06E-03	4.48E-01	-7.55E-05	0.0	-7.43E-02	0.0	0.0	0.0
-5.06E-03	1.36E-01	-1.21E+01	2.03E-03	0.0	2.00E+00	0.0	0.0	0.0
4.48E-01	-1.21E+01	1.17E+03	-1.80E-01	0.0	-1.77E+02	0.0	0.0	0.0
-7.55E-05	2.03E-03	-1.80E-01	3.03E-05	0.0	2.99E-02	0.0	0.0	0.0
0.0	0.0	0.0	0.0	0.0	0.0	0.0	0.0	0.0
-7.43E-02	2.00E+00	-1.77E+02	2.99E-02	0.0	2.94E+01	0.0	0.0	0.0
0.0	0.0	0.0	0.0	0.0	0.0	0.0	0.0	0.0
0.0	0.0	0.0	0.0	0.0	0.0	0.0	0.0	0.0
0.0	0.0	0.0	0.0	0.0	0.0	0.0	0.0	0.0

CONTROL WEIGHTING MATRIX (R)

3.78E-01	0.0
0.0	6.71E-01

DUE TO NUMERICAL PROBLEMS, WE WERE UNABLE TO

SOLVE THE RICCATI EQUATION FOR THIS FLIGHT CONDITION

FLIGHT CONDITION 13 DYNAMIC PRESSURE 550 PSF MACH 0.90 ALTITUDE 20000 FT

STATE WEIGHTING MATRIX (Q)

2.22E-04	-5.79E-03	6.00E-01	-4.34E-05	0.0	-7.81E-02	0.0	0.0	0.0
-5.79E-03	1.67E-01	-1.72E+01	1.25E-03	0.0	2.24E+00	0.0	0.0	0.0
6.00E-01	-1.72E+01	1.96E+03	-1.29E-01	0.0	-2.32E+02	0.0	0.0	0.0
-4.34E-05	1.25E-03	-1.29E-01	9.36E-06	0.0	1.68E-02	0.0	0.0	0.0
0.0	0.0	0.0	0.0	0.0	0.0	0.0	0.0	0.0
-7.81E-02	2.24E+00	-2.32E+02	1.68E-02	0.0	3.03E+01	0.0	0.0	0.0
0.0	0.0	0.0	0.0	0.0	0.0	0.0	0.0	0.0
0.0	0.0	0.0	0.0	0.0	0.0	0.0	0.0	0.0
0.0	0.0	0.0	0.0	0.0	0.0	0.0	0.0	0.0

CONTROL WEIGHTING MATRIX (R)

3.78E-01	0.0
0.0	6.71E-01

REGULATOR CLOSED-LOOP MATRIX (ACL)

-4.5877	0.1788	-69.2185	0.0	30.6474	11.3638	0.0	0.0	-69.2185
-0.0957	-0.4412	11.2003	0.0	1.2882	-5.4219	0.0	0.0	11.2003
0.0400	-0.9965	-0.3644	0.0345	0.0	0.0474	0.0	0.0	-0.3644
0.9992	0.0401	0.0	0.0	0.0	0.0	0.0	0.0	0.0
0.0	0.0	0.0	0.0	-30.0000	0.0	30.0000	0.0	0.0
0.0	0.0	0.0	0.0	0.0	-25.0000	0.0	25.0000	0.0
0.0596	-1.6980	3.1080	0.0597	-0.0110	0.3468	-0.3187	0.9982	-0.0000
-0.4289	12.3000	2.7290	-0.4655	0.0858	-3.3630	0.5622	-12.9500	-0.0000
0.0	0.0	0.0	0.0	0.0	0.0	0.0	0.0	-0.7466

REGULATOR GAIN MATRIX (G)

-0.0596	1.6980	-3.1080	-0.0597	0.0110	-0.3468	0.3187	-0.9982	0.0000
0.4289	-12.3000	-2.7290	0.4655	-0.0858	3.3630	-0.5622	12.9500	0.0000

FLIGHT CONDITION 13 CONTINUED

POLES OF CLOSED-LOOP SYSTEM - REGULATOR

REAL PART =	-30.000	IMAG PART =	0.0
REAL PART =	-24.159	IMAG PART =	0.0
REAL PART =	-5.238	IMAG PART =	5.399
REAL PART =	-5.238	IMAG PART =	-5.399
REAL PART =	-0.077	IMAG PART =	0.0
REAL PART =	-4.379	IMAG PART =	0.160
REAL PART =	-4.379	IMAG PART =	-0.160
REAL PART =	-0.192	IMAG PART =	0.0
REAL PART =	-0.747	IMAG PART =	0.0

DISCRETE TIME REGUIATOR MATRIX (ACLD) DT=.125 SEC

0.5430	0.5612	-5.6196	-0.0203	0.6537	0.1807	2.2441	0.4304	-5.7686
0.0005	0.6868	1.2074	0.0097	0.0317	-0.1445	0.0934	-0.2180	1.1707
0.0041	-0.1055	0.8600	0.0037	-0.0002	0.0184	0.0001	0.0171	-0.1369
0.0941	0.0301	-0.4115	0.9991	0.0757	0.0264	0.1235	0.0280	-0.4149
0.0040	-0.1140	0.2016	0.0040	0.0228	0.0233	0.9484	0.0721	-0.0896
-0.0167	0.4907	0.5498	-0.0192	0.0039	-0.0801	0.0311	0.1911	0.4137
0.0050	-0.1431	0.2522	0.0050	-0.0010	0.0292	0.9625	0.0919	-0.1415
-0.0186	0.5519	0.8327	-0.0219	0.0046	-0.1383	0.0397	0.0132	0.6595
0.0	0.0	0.0	0.0	0.0	0.0	0.0	0.0	0.9109

POLES OF DISCRETE TIME REGULATOR DT=.125 SEC

REAL PART =	0.990	IMAG PART =	0.0
REAL PART =	0.976	IMAG PART =	0.0
REAL PART =	0.406	IMAG PART =	0.325
REAL PART =	0.406	IMAG PART =	-0.325
REAL PART =	0.049	IMAG PART =	0.0
REAL PART =	0.578	IMAG PART =	0.012
REAL PART =	0.578	IMAG PART =	-0.012
REAL PART =	0.024	IMAG PART =	0.0
REAL PART =	0.911	IMAG PART =	0.0

FLIGHT CONDITION 13 CONTINUED

DISCRETE TIME CONTROL GAIN (GD)

-0.0339	0.9745	-2.1110	-0.0334	0.0066	-0.1821	0.2950	-0.5928	1.0780
0.1578	-4.9480	-6.5450	0.1951	-0.0405	1.2470	-0.3346	8.2910	-5.0770

FLIGHT CONDITION 14 DYNAMIC PRESSURE 978 PSF MACH 1.20 ALTITUDE 20000 FT

STATE WEIGHTING MATRIX (Q)

2.15E-04	-7.39E-03	9.64E-01	-9.14E-05	0.0	-3.94E-02	0.0	0.0	0.0
-7.39E-03	2.79E-01	-3.64E+01	3.46E-03	0.0	1.49E+00	0.0	0.0	0.0
9.64E-01	-3.64E+01	5.22E+03	-4.51E-01	0.0	-1.94E+02	0.0	0.0	0.0
-9.14E-05	3.46E-03	-4.51E-01	4.28E-05	0.0	1.84E-02	0.0	0.0	0.0
0.0	0.0	0.0	0.0	0.0	0.0	0.0	0.0	0.0
-3.94E-02	1.49E+00	-1.94E+02	1.84E-02	0.0	7.95E+00	0.0	0.0	0.0
0.0	0.0	0.0	0.0	0.0	0.0	0.0	0.0	0.0
0.0	0.0	0.0	0.0	0.0	0.0	0.0	0.0	0.0
0.0	0.0	0.0	0.0	0.0	0.0	0.0	0.0	0.0

CONTROL WEIGHTING MATRIX (R)

3.78E-01	0.0
0.0	6.71E-01

REGULATOR CLOSED-LOOP MATRIX (ACL)

-4.1459	0.1921	-103.5909	0.0	18.6579	7.1883	0.0	0.0	-103.5909
-0.0212	-0.6885	17.6901	0.0	0.6223	-2.8727	0.0	0.0	17.6901
0.0296	-0.9966	-0.4458	0.0259	0.0	0.0182	0.0	0.0	-0.4458
0.9996	0.0297	0.0	0.0	0.0	0.0	0.0	0.0	0.0
0.0	0.0	0.0	0.0	-30.0000	0.0	30.0000	0.0	0.0
0.0	0.0	0.0	0.0	0.0	-25.0000	0.0	25.0000	0.0
0.0536	-2.5460	1.7960	0.0726	-0.0184	0.2910	-0.3580	1.3150	-0.0000
-0.2956	14.6600	18.1000	-0.4460	0.1165	-1.9770	0.7406	-9.8920	-0.0000
0.0	0.0	0.0	0.0	0.0	0.0	0.0	0.0	-0.9955

REGULATOR GAIN MATRIX (G)

-0.0536	2.5460	-1.7960	-0.0726	0.0184	-0.2910	0.3580	-1.3150	0.0000
0.2956	-14.6600	-18.1000	0.4460	-0.1165	1.9770	-0.7406	9.8920	0.0000

FLIGHT CONDITION 14 CONTINUED

POLES OF CLOSED-LOOP SYSTEM - REGULATOR

REAL PART =	-30.000	IMAG PART =	0.0
REAL PART =	-24.812	IMAG PART =	0.0
REAL PART =	-3.633	IMAG PART =	6.081
REAL PART =	-3.633	IMAG PART =	-6.081
REAL PART =	-4.101	IMAG PART =	0.384
REAL PART =	-4.101	IMAG PART =	-0.384
REAL PART =	-0.060	IMAG PART =	0.0
REAL PART =	-0.192	IMAG PART =	0.0
REAL PART =	-0.995	IMAG PART =	0.0

DISCRETE TIME REGULATOR MATRIX (ACLD) DT=.125 SEC

0.5768	0.7367	-8.6299	-0.0201	0.4155	0.1240	1.3985	0.3384	-8.5243
0.0037	0.6771	1.7339	0.0070	0.0167	-0.0785	0.0455	-0.1324	1.7576
0.0028	-0.1045	0.8102	0.0028	-0.0003	0.0096	-0.0001	0.0096	-0.1877
0.0967	0.0366	-0.6276	0.9991	0.0470	0.0175	0.0764	0.0206	-0.6195
0.0031	-0.1535	0.0763	0.0044	0.0223	0.0176	0.9458	0.0937	-0.1746
-0.0115	0.6348	1.6915	-0.0206	0.0060	-0.0417	0.0479	0.3153	0.7267
0.0038	-0.1870	0.0870	0.0054	-0.0014	0.0214	0.9592	0.1189	-0.2713
-0.0126	0.7297	2.3899	-0.0243	0.0074	-0.0994	0.0638	0.1514	1.1644
0.0	0.0	0.0	0.0	0.0	0.0	0.0	0.0	0.8830

POLES OF DISCRETE TIME REGULATOR DT=.125 SEC

REAL PART =	0.993	IMAG PART =	0.0
REAL PART =	0.976	IMAG PART =	0.0
REAL PART =	0.460	IMAG PART =	0.438
REAL PART =	0.460	IMAG PART =	-0.438
REAL PART =	0.598	IMAG PART =	0.029
REAL PART =	0.598	IMAG PART =	-0.029
REAL PART =	0.045	IMAG PART =	0.0
REAL PART =	0.024	IMAG PART =	0.0
REAL PART =	0.883	IMAG PART =	0.0

FLIGHT CONDITION 14 CONTINUED

DISCRETE TIME CONTROL GAIN (GD)

-0.0294	1.4480	-0.8220	-0.0415	0.0112	-0.1633	0.3258	-0.9311	2.0830
0.1123	-6.3760	-19.2700	0.2097	-0.0631	0.8651	-0.5257	7.0060	-8.9900

FLIGHT CONDITION 15 DYNAMIC PRESSURE 135 PSF MACH 0.70 ALTITUDE 40000 FT

STATE WEIGHTING MATRIX (Q)

2.02E-03	-3.36E-02	4.35E-01	-1.20E-04	0.0	-9.29E-02	0.0	0.0	0.0
-3.36E-02	6.17E-01	-7.97E+00	2.20E-03	0.0	1.71E+00	0.0	0.0	0.0
4.35E-01	-7.97E+00	1.13E+02	-2.84E-02	0.0	-2.20E+01	0.0	0.0	0.0
-1.20E-04	2.20E-03	-2.84E-02	7.82E-06	0.0	6.07E-03	0.0	0.0	0.0
0.0	0.0	0.0	0.0	0.0	0.0	0.0	0.0	0.0
-9.29E-02	1.71E+00	-2.20E+01	6.07E-03	0.0	4.71E+00	0.0	0.0	0.0
0.0	0.0	0.0	0.0	0.0	0.0	0.0	0.0	0.0
0.0	0.0	0.0	0.0	0.0	0.0	0.0	0.0	0.0
0.0	0.0	0.0	0.0	0.0	0.0	0.0	0.0	0.0

CONTROL WEIGHTING MATRIX (R)

3.78E-01	0.0
0.0	6.71E-01

REGULATOR CLOSED-LOOP MATRIX (ACL)

-1.3523	0.2002	-24.8738	0.0	9.8344	4.3847	0.0	0.0	-24.8738
-0.0440	-0.1406	2.3205	0.0	0.5462	-1.9424	0.0	0.0	2.3205
0.1269	-0.9907	-0.1206	0.0476	0.0	0.0258	0.0	0.0	-0.1206
0.9919	0.1271	0.0	0.0	0.0	0.0	0.0	0.0	0.0
0.0	0.0	0.0	0.0	-30.0000	0.0	30.0000	0.0	0.0
0.0	0.0	0.0	0.0	0.0	-25.0000	0.0	25.0000	0.0
-0.3393	3.3110	-1.0930	-0.1562	-0.0511	-0.3055	-1.1760	-1.7290	0.0000
-0.3953	4.2710	4.3190	-0.1830	-0.0559	-0.5266	-0.9736	-4.9640	-0.0000
0.0	0.0	0.0	0.0	0.0	0.0	0.0	0.0	-0.5421

REGULATOR GAIN MATRIX (G)

0.3393	-3.3110	1.0930	0.1562	0.0511	0.3055	1.1760	1.7290	-0.0000
0.3953	-4.2710	-4.3190	0.1830	0.0559	0.5266	0.9736	4.9640	0.0000

FLIGHT CONDITION 15 CONTINUED

POLES OF CLOSED-LOOP SYSTEM - REGULATOR

REAL PART =	-30.000	IMAG PART =	0.0
REAL PART =	-24.863	IMAG PART =	0.0
REAL PART =	-2.070	IMAG PART =	2.814
REAL PART =	-2.070	IMAG PART =	-2.814
REAL PART =	-1.229	IMAG PART =	0.0
REAL PART =	-0.340	IMAG PART =	0.221
REAL PART =	-0.340	IMAG PART =	-0.221
REAL PART =	-1.840	IMAG PART =	0.0
REAL PART =	-0.542	IMAG PART =	0.0

DISCRETE TIME REGULATOR MATRIX (ACLD) DT=.125 SEC

0.8034	0.3901	-2.7533	-0.0174	0.2769	0.1165	0.7826	0.1918	-2.6648
-0.0010	0.9442	0.2521	0.0017	0.0168	-0.0703	0.0526	-0.1336	0.2765
0.0147	-0.1179	0.9458	0.0057	0.0020	0.0091	0.0027	0.0104	-0.0544
0.1124	0.0315	-0.1765	0.9993	0.0281	0.0121	0.0420	0.0113	-0.1727
-0.0264	0.2572	-0.0601	-0.0124	0.0195	-0.0238	0.8750	-0.1448	0.0668
-0.0226	0.2554	0.3584	-0.0109	-0.0031	0.0164	-0.0667	0.5878	0.0622
-0.0342	0.3337	-0.0709	-0.0162	-0.0052	-0.0309	0.8649	-0.1911	0.1076
-0.0288	0.3311	0.5073	-0.0141	-0.0039	-0.0350	-0.0902	0.4921	0.1053
0.0	0.0	0.0	0.0	0.0	0.0	0.0	0.0	0.9345

POLES OF DISCRETE TIME REGULATOR DT=.125 SEC

REAL PART =	0.725	IMAG PART =	0.266
REAL PART =	0.725	IMAG PART =	-0.266
REAL PART =	0.958	IMAG PART =	0.026
REAL PART =	0.958	IMAG PART =	-0.026
REAL PART =	0.858	IMAG PART =	0.0
REAL PART =	0.045	IMAG PART =	0.0
REAL PART =	0.024	IMAG PART =	0.0
REAL PART =	0.795	IMAG PART =	0.0
REAL PART =	0.934	IMAG PART =	0.0

FLIGHT CONDITION 15 CONTINUED

DISCRETE TIME CONTROL GAIN (GD)

0.2810	-2.7420	0.6060	0.1323	0.0425	0.2544	1.0920	1.5580	-0.7833
0.2418	-2.7600	-4.0790	0.1176	0.0327	0.2939	0.7394	4.1300	-0.7891

FLIGHT CONDITION 16 DYNAMIC PRESSURE 176 PSF MACH 0.80 ALTITUDE 40000 FT

STATE WEIGHTING MATRIX (Q)

7.28E-04	-1.41E-02	3.57E-01	1.91E-04	0.0	-7.05E-02	0.0	0.0	0.0
-1.41E-02	3.01E-01	-7.61E+00	-4.07E-03	0.0	1.50E+00	0.0	0.0	0.0
3.57E-01	-7.61E+00	2.12E+02	1.03E-01	0.0	-3.80E+01	0.0	0.0	0.0
1.91E-04	-4.07E-03	1.03E-01	5.51E-05	0.0	-2.03E-02	0.0	0.0	0.0
0.0	0.0	0.0	0.0	0.0	0.0	0.0	0.0	0.0
-7.05E-02	1.50E+00	-3.80E+01	-2.03E-02	0.0	7.50E+00	0.0	0.0	0.0
0.0	0.0	0.0	0.0	0.0	0.0	0.0	0.0	0.0
0.0	0.0	0.0	0.0	0.0	0.0	0.0	0.0	0.0
0.0	0.0	0.0	0.0	0.0	0.0	0.0	0.0	0.0

CONTROL WEIGHTING MATRIX (R)

3.78E-01	0.0
0.0	6.71E-01

REGULATOR CLOSED-LOOP MATRIX (ACL)

-1.6215	0.1666	-31.2874	0.0	12.9218	5.5535	0.0	0.0	-31.2874
-0.0560	-0.1666	3.7470	0.0	0.6202	-2.5084	0.0	0.0	3.7470
0.0940	-0.9943	-0.1442	0.0415	0.0	0.0285	0.0	0.0	-0.1442
0.9956	0.0941	0.0	0.0	0.0	0.0	0.0	0.0	0.0
0.0	0.0	0.0	0.0	-30.0000	0.0	30.0000	0.0	0.0
0.0	0.0	0.0	0.0	0.0	-25.0000	0.0	25.0000	0.0
-0.3000	3.6950	-2.1290	-0.1586	-0.0522	-0.4141	-0.9199	-2.0150	0.0000
-0.4109	5.2180	5.6160	-0.2254	-0.0733	-0.8039	-1.1350	-6.1570	-0.0000
0.0	0.0	0.0	0.0	0.0	0.0	0.0	0.0	-0.6196

REGULATOR GAIN MATRIX (G)

0.3000	-3.6950	2.1290	0.1586	0.0522	0.4141	0.9199	2.0150	-0.0000
0.4109	-5.2180	-5.6160	0.2254	0.0733	0.8039	1.1350	6.1570	0.0000

FLIGHT CONDITION 16 CONTINUED

POLES OF CLOSED-LOOP SYSTEM - REGULATOR

REAL PART =	-30.000	IMAG PART =	0.0
REAL PART =	-24.783	IMAG PART =	0.0
REAL PART =	-2.570	IMAG PART =	3.183
REAL PART =	-2.570	IMAG PART =	-3.183
REAL PART =	-1.539	IMAG PART =	0.0
REAL PART =	-0.178	IMAG PART =	0.117
REAL PART =	-0.178	IMAG PART =	-0.117
REAL PART =	-2.190	IMAG PART =	0.0
REAL PART =	-0.620	IMAG PART =	0.0

DISCRETE TIME REGULATOR MATRIX (ACLD) DT=.125 SEC

0.7740	0.5142	-3.4152	-0.0212	0.3549	0.1312	1.0278	0.1983	-3.2410
-0.0011	0.9181	0.4002	0.0026	0.0186	-0.0884	0.0618	-0.1618	0.4392
0.0108	-0.1170	0.9349	0.0049	0.0017	0.0108	0.0021	0.0119	-0.0657
0.1109	0.0323	-0.2209	0.9992	0.0365	0.0149	0.0551	0.0130	-0.2139
-0.0231	0.2854	-0.1395	-0.0123	0.0195	-0.0320	0.8987	-0.1669	0.0961
-0.0221	0.2885	0.4641	-0.0126	-0.0039	0.0047	-0.0750	0.5161	0.0975
-0.0299	0.3699	-0.1741	-0.0160	-0.0052	-0.0415	0.8970	-0.2197	0.1545
-0.0277	0.3646	0.6546	-0.0160	-0.0049	-0.0487	-0.1003	0.3997	0.1634
0.0	0.0	0.0	0.0	0.0	0.0	0.0	0.0	0.9255

POLES OF DISCRETE TIME REGULATOR DT=.125 SEC

REAL PART =	0.669	IMAG PART =	0.281
REAL PART =	0.669	IMAG PART =	-0.281
REAL PART =	0.978	IMAG PART =	0.014
REAL PART =	0.978	IMAG PART =	-0.014
REAL PART =	0.825	IMAG PART =	0.0
REAL PART =	0.045	IMAG PART =	0.0
REAL PART =	0.760	IMAG PART =	0.0
REAL PART =	0.024	IMAG PART =	0.0
REAL PART =	0.925	IMAG PART =	0.0

FLIGHT CONDITION 16 CONTINUED

DISCRETE TIME CONTROL GAIN (GD)

0.2486	-3.0700	1.4550	0.1329	0.0433	0.3464	0.8396	1.8080	-1.1010
0.2348	-3.0800	-5.2660	0.1352	0.0413	0.4141	0.8269	4.9060	-1.2200

FLIGHT CONDITION 17 DYNAMIC PRESSURE 223 PSF MACH 0.90 ALTITUDE 40000 FT

STATE WEIGHTING MATRIX (Q)

3.44E-04	-7.68E-03	3.23E-01	-4.79E-06	0.0	-5.36E-02	0.0	0.0	0.0
-7.68E-03	1.88E-01	-7.91E+00	1.18E-04	0.0	1.32E+00	0.0	0.0	0.0
3.23E-01	-7.91E+00	3.66E+02	-4.94E-03	0.0	-5.53E+01	0.0	0.0	0.0
-4.79E-06	1.18E-04	-4.94E-03	7.34E-08	0.0	8.21E-04	0.0	0.0	0.0
0.0	0.0	0.0	0.0	0.0	0.0	0.0	0.0	0.0
-5.36E-02	1.32E+00	-5.53E+01	8.21E-04	0.0	9.19E+00	0.0	0.0	0.0
0.0	0.0	0.0	0.0	0.0	0.0	0.0	0.0	0.0
0.0	0.0	0.0	0.0	0.0	0.0	0.0	0.0	0.0
0.0	0.0	0.0	0.0	0.0	0.0	0.0	0.0	0.0

CONTROL WEIGHTING MATRIX (R)

3.78E-01	0.0
0.0	6.71E-01

REGULATOR CLOSED-LOOP MATRIX (ACL)

-2.0595	0.1350	-38.0375	0.0	16.4553	6.4544	0.0	0.0	-38.0375
-0.0548	-0.1962	5.4886	0.0	0.6475	-2.9261	0.0	0.0	5.4886
0.0731	-0.9960	-0.1685	0.0370	0.0	0.0280	0.0	0.0	-0.1685
0.9973	0.0732	0.0	0.0	0.0	0.0	0.0	0.0	0.0
0.0	0.0	0.0	0.0	-30.0000	0.0	30.0000	0.0	0.0
0.0	0.0	0.0	0.0	0.0	-25.0000	0.0	25.0000	0.0
-0.2229	3.5710	-2.6710	-0.1390	-0.0447	-0.4461	-0.8182	-1.8910	0.0000
-0.3835	6.4820	6.4770	-0.2473	-0.0757	-1.0800	-1.0650	-7.2090	-0.0000
0.0	0.0	0.0	0.0	0.0	0.0	0.0	0.0	-0.6970

REGULATOR GAIN MATRIX (G)

0.2229	-3.5710	2.6710	0.1390	0.0447	0.4461	0.8182	1.8910	-0.0000
0.3835	-6.4820	-6.4770	0.2473	0.0757	1.0800	1.0650	7.2090	0.0000

FLIGHT CONDITION 17 CONTINUED

POLES OF CLOSED-LOOP SYSTEM - REGULATOR

REAL PART =	-30.000	IMAG PART =	0.0
REAL PART =	-24.736	IMAG PART =	0.0
REAL PART =	-2.921	IMAG PART =	3.634
REAL PART =	-2.921	IMAG PART =	-3.634
REAL PART =	-1.926	IMAG PART =	0.0
REAL PART =	-0.199	IMAG PART =	0.163
REAL PART =	-0.199	IMAG PART =	-0.163
REAL PART =	-2.550	IMAG PART =	0.0
REAL PART =	-0.697	IMAG PART =	0.0

DISCRETE TIME REGULATOR MATRIX (ACLD) DT=.125 SEC

0.7332	0.6215	-4.0359	-0.0233	0.4346	0.1342	1.2917	0.1991	-3.7673
-0.0002	0.8846	0.5842	0.0035	0.0192	-0.0995	0.0644	-0.1764	0.6286
0.0082	-0.1156	0.9212	0.0043	0.0015	0.0118	0.0018	0.0126	-0.0792
0.1083	0.0340	-0.2644	0.9991	0.0455	0.0168	0.0696	0.0141	-0.2538
-0.0169	0.2705	-0.1730	-0.0107	0.0201	-0.0339	0.9071	-0.1547	0.1147
-0.0195	0.3423	0.5477	-0.0132	-0.0037	-0.0074	-0.0674	0.4547	0.1466
-0.0217	0.3489	-0.2153	-0.0138	-0.0044	-0.0437	0.9079	-0.2030	0.1838
-0.0240	0.4259	0.7739	-0.0166	-0.0045	-0.0629	-0.0890	0.3213	0.2437
0.0	0.0	0.0	0.0	0.0	0.0	0.0	0.0	0.9166

POLES OF DISCRETE TIME REGULATOR DT=.125 SEC

REAL PART =	0.624	IMAG PART =	0.305
REAL PART =	0.624	IMAG PART =	-0.305
REAL PART =	0.975	IMAG PART =	0.020
REAL PART =	0.975	IMAG PART =	-0.020
REAL PART =	0.786	IMAG PART =	0.0
REAL PART =	0.045	IMAG PART =	0.0
REAL PART =	0.727	IMAG PART =	0.0
REAL PART =	0.024	IMAG PART =	0.0
REAL PART =	0.917	IMAG PART =	0.0

FLIGHT CONDITION 17 CONTINUED

DISCRETE TIME CONTROL GAIN (GD)

0.1836	-2.9470	1.8180	0.1163	0.0369	0.3721	0.7538	1.6970	-1.2720
0.2056	-3.6290	-6.2170	0.1407	0.0389	0.5392	0.7386	5.5680	-1.8190

FLIGHT CONDITION 18 DYNAMIC PRESSURE 397 PSF MACH 1.20 ALTITUDE 40000 FT

STATE WEIGHTING MATRIX (Q)

3.03E-04	-7.30E-03	5.07E-01	1.15E-04	0.0	-3.65E-02	0.0	0.0	0.0
-7.30E-03	1.94E-01	-1.35E+01	-3.06E-03	0.0	9.69E-01	0.0	0.0	0.0
5.07E-01	-1.35E+01	1.03E+03	2.12E-01	0.0	-6.73E+01	0.0	0.0	0.0
1.15E-04	-3.06E-03	2.12E-01	4.82E-05	0.0	-1.53E-02	0.0	0.0	0.0
0.0	0.0	0.0	0.0	0.0	0.0	0.0	0.0	0.0
-3.65E-02	9.69E-01	-6.73E+01	-1.53E-02	0.0	4.85E+00	0.0	0.0	0.0
0.0	0.0	0.0	0.0	0.0	0.0	0.0	0.0	0.0
0.0	0.0	0.0	0.0	0.0	0.0	0.0	0.0	0.0
0.0	0.0	0.0	0.0	0.0	0.0	0.0	0.0	0.0

CONTROL WEIGHTING MATRIX (R)

3.78E-01	0.0
0.0	6.71E-01

REGULATOR CLOSED-LOOP MATRIX (ACL)

-2.1285	0.1748	-55.7635	0.0	12.1947	5.5097	0.0	0.0	-55.7635
-0.0137	-0.3230	9.2954	0.0	0.3276	-2.1190	0.0	0.0	9.2954
0.0540	-0.9969	-0.2119	0.0277	0.0	0.0153	0.0	0.0	-0.2119
0.9985	0.0541	0.0	0.0	0.0	0.0	0.0	0.0	0.0
0.0	0.0	0.0	0.0	-30.0000	0.0	30.0000	0.0	0.0
0.0	0.0	0.0	0.0	0.0	-25.0000	0.0	25.0000	0.0
-0.1367	3.3040	-1.0820	-0.1017	-0.0202	-0.2990	-0.3916	-1.3720	0.0000
-0.3138	8.3870	13.6200	-0.2651	-0.0429	-0.9242	-0.7730	-6.7190	-0.0000
0.0	0.0	0.0	0.0	0.0	0.0	0.0	0.0	-0.9294

REGULATOR GAIN MATRIX (G)

0.1367	-3.3040	1.0820	0.1017	0.0202	0.2990	0.3916	1.3720	-0.0000
0.3138	-8.3870	-13.6200	0.2651	0.0429	0.9242	0.7730	6.7190	0.0000

FLIGHT CONDITION 18 CONTINUED

POLES OF CLOSED-LOOP SYSTEM - REGULATOR

REAL PART =	-30.000	IMAG PART =	0.0
REAL PART =	-24.869	IMAG PART =	0.0
REAL PART =	-2.551	IMAG PART =	4.319
REAL PART =	-2.551	IMAG PART =	-4.319
REAL PART =	-1.970	IMAG PART =	0.0
REAL PART =	-0.087	IMAG PART =	0.086
REAL PART =	-0.087	IMAG PART =	-0.086
REAL PART =	-2.660	IMAG PART =	0.0
REAL PART =	-0.929	IMAG PART =	0.0

DISCRETE TIME REGULATOR MATRIX (ACLD) DT=.125 SEC

0.7358	0.6814	-5.5651	-0.0196	0.3213	0.1220	0.9776	0.2126	-5.3596
0.0038	0.8420	0.9740	0.0035	0.0105	-0.0694	0.0347	-0.1265	1.0110
0.0058	-0.1138	0.8889	0.0032	0.0009	0.0082	0.0011	0.0088	-0.1109
0.1083	0.0348	-0.3757	0.9992	0.0336	0.0148	0.0523	0.0139	-0.3664
-0.0100	0.2466	-0.0237	-0.0077	0.0221	-0.0225	0.9432	-0.1145	0.1518
-0.0150	0.4390	1.1185	-0.0144	-0.0018	-0.0022	-0.0498	0.4792	0.2712
-0.0128	0.3165	-0.0144	-0.0099	-0.0019	-0.0289	0.9559	-0.1507	0.2424
-0.0179	0.5428	1.5689	-0.0180	-0.0020	-0.0569	-0.0660	0.3509	0.4483
0.0	0.0	0.0	0.0	0.0	0.0	0.0	0.0	0.8903

POLES OF DISCRETE TIME REGULATOR DT=.125 SEC

REAL PART =	0.624	IMAG PART =	0.374
REAL PART =	0.624	IMAG PART =	-0.374
REAL PART =	0.989	IMAG PART =	0.011
REAL PART =	0.989	IMAG PART =	-0.011
REAL PART =	0.782	IMAG PART =	0.0
REAL PART =	0.045	IMAG PART =	0.0
REAL PART =	0.717	IMAG PART =	0.0
REAL PART =	0.024	IMAG PART =	0.0
REAL PART =	0.890	IMAG PART =	0.0

FLIGHT CONDITION 18 CONTINUED

DISCRETE TIME CONTROL GAIN (GD)

0.1084	-2.6640	0.1740	0.0830	0.0158	0.2440	0.3602	1.2470	-1.7280
0.1543	-4.6160	-12.6600	0.1524	0.0177	0.4847	0.5451	5.3060	-3.3890

FLIGHT CONDITION 19 DYNAMIC PRESSURE 537 PSF MACH 1.40 ALTITUDE 40000 FT

STATE WEIGHTING MATRIX (Q)

2.51E-04	-6.71E-03	5.68E-01	-2.95E-05	0.0	-3.24E-02	0.0	0.0	0.0
-6.71E-03	1.98E-01	-1.67E+01	8.70E-04	0.0	9.55E-01	0.0	0.0	0.0
5.68E-01	-1.67E+01	1.55E+03	-7.36E-02	0.0	-8.08E+01	0.0	0.0	0.0
-2.95E-05	8.70E-04	-7.36E-02	3.83E-06	0.0	4.20E-03	0.0	0.0	0.0
0.0	0.0	0.0	0.0	0.0	0.0	0.0	0.0	0.0
-3.24E-02	9.55E-01	-8.08E+01	4.20E-03	0.0	4.62E+00	0.0	0.0	0.0
0.0	0.0	0.0	0.0	0.0	0.0	0.0	0.0	0.0
0.0	0.0	0.0	0.0	0.0	0.0	0.0	0.0	0.0
0.0	0.0	0.0	0.0	0.0	0.0	0.0	0.0	0.0

CONTROL WEIGHTING MATRIX (R)

3.78E-01	0.0
0.0	6.71E-01

REGULATOR CLOSED-LOOP MATRIX (ACL)

-2.2793	0.1869	-73.9007	0.0	11.2794	5.2266	0.0	0.0	-73.9007
0.0019	-0.3451	8.2936	0.0	0.2940	-2.1305	0.0	0.0	8.2936
0.0523	-0.9974	-0.2233	0.0238	0.0	0.0128	0.0	0.0	-0.2233
0.9986	0.0523	0.0	0.0	0.0	0.0	0.0	0.0	0.0
0.0	0.0	0.0	0.0	-30.0000	0.0	30.0000	0.0	0.0
0.0	0.0	0.0	0.0	0.0	-25.0000	0.0	25.0000	0.0
-0.1175	3.1900	-2.5370	-0.0838	-0.0138	-0.2827	-0.3826	-1.0980	0.0000
-0.3681	11.5500	8.7340	-0.3005	-0.0327	-1.1820	-0.6183	-7.6440	-0.0000
0.0	0.0	0.0	0.0	0.0	0.0	0.0	0.0	-1.0842

REGULATOR GAIN MATRIX (G)

0.1175	-3.1900	2.5370	0.0838	0.0138	0.2827	0.3826	1.0980	-0.0000
0.3681	-11.5500	-8.7340	0.3005	0.0327	1.1820	0.6183	7.6440	0.0000

FLIGHT CONDITION 19 CONTINUED

POLES OF CLOSED-LOOP SYSTEM - REGULATOR

REAL PART =	-30.000	IMAG PART =	0.0
REAL PART =	-24.879	IMAG PART =	0.0
REAL PART =	-2.765	IMAG PART =	4.587
REAL PART =	-2.765	IMAG PART =	-4.587
REAL PART =	-2.214	IMAG PART =	0.0
REAL PART =	-0.124	IMAG PART =	0.098
REAL PART =	-0.124	IMAG PART =	-0.098
REAL PART =	-3.004	IMAG PART =	0.0
REAL PART =	-1.084	IMAG PART =	0.0

DISCRETE TIME REGULATOR MATRIX (ACLD) DT=.125 SEC

0.7175	0.8230	-7.5348	-0.0201	0.2929	0.1030	0.8998	0.1934	-7.0021
0.0053	0.8257	0.8765	0.0034	0.0098	-0.0682	0.0310	-0.1202	0.8772
0.0055	-0.1128	0.8878	0.0027	0.0007	0.0079	0.0010	0.0083	-0.1092
0.1072	0.0407	-0.5049	0.9992	0.0309	0.0135	0.0482	0.0129	-0.4822
-0.0085	0.2367	-0.1279	-0.0063	0.0226	-0.0212	0.9432	-0.0915	0.1390
-0.0174	0.6095	0.8812	-0.0163	-0.0011	-0.0164	-0.0375	0.4242	0.3530
-0.0109	0.3033	-0.1469	-0.0082	-0.0012	-0.0272	0.9556	-0.1204	0.2215
-0.0206	0.7569	1.2788	-0.0204	-0.0010	-0.0747	-0.0486	0.2798	0.5833
0.0	0.0	0.0	0.0	0.0	0.0	0.0	0.0	0.8733

POLES OF DISCRETE TIME REGULATOR DT=.125 SEC

REAL PART =	0.045	IMAG PART =	0.0
REAL PART =	0.024	IMAG PART =	0.0
REAL PART =	0.595	IMAG PART =	0.384
REAL PART =	0.595	IMAG PART =	-0.384
REAL PART =	0.758	IMAG PART =	0.0
REAL PART =	0.985	IMAG PART =	0.012
REAL PART =	0.985	IMAG PART =	-0.012
REAL PART =	0.687	IMAG PART =	0.0
REAL PART =	0.873	IMAG PART =	0.0

FLIGHT CONDITION 19 CONTINUED

DISCRETE TIME CONTROL GAIN (GD)

0.0922	-2.5630	1.2970	0.0686	0.0104	0.2302	0.3610	1.0010	-1.5810
0.1780	-6.4160	-10.1800	0.1723	0.0095	0.6340	0.4049	5.8960	-4.4270

FLIGHT CONDITION 2C DYNAMIC PRESSURE 703 PSF MACH 1.60 ALTITUDE 40000 FT

STATE WEIGHTING MATRIX (Q)

2.21E-04	-6.25E-03	6.64E-01	-3.12E-05	0.0	-3.11E-02	0.0	0.0	0.0
-6.25E-03	1.94E-01	-2.06E+01	9.68E-04	0.0	9.67E-01	0.0	0.0	0.0
6.64E-01	-2.06E+01	2.41E+03	-1.03E-01	0.0	-1.03E+02	0.0	0.0	0.0
-3.12E-05	9.68E-04	-1.03E-01	4.83E-06	0.0	4.82E-03	0.0	0.0	0.0
0.0	0.0	0.0	0.0	0.0	0.0	0.0	0.0	0.0
-3.11E-02	9.67E-01	-1.03E+02	4.82E-03	0.0	4.81E+00	0.0	0.0	0.0
0.0	0.0	0.0	0.0	0.0	0.0	0.0	0.0	0.0
0.0	0.0	0.0	0.0	0.0	0.0	0.0	0.0	0.0
0.0	0.0	0.0	0.0	0.0	0.0	0.0	0.0	0.0

CONTROL WEIGHTING MATRIX (R)

3.78E-01	0.0
0.0	6.71E-01

REGULATOR CLOSED-LOOP MATRIX (ACL)

-2.4566	0.1810	-85.4735	0.0	10.4824	5.0385	0.0	0.0	-85.4735
0.0058	-0.3589	7.9205	0.0	0.3012	-2.2665	0.0	0.0	7.9205
0.0470	-0.9977	-0.2433	0.0208	0.0	0.0114	0.0	0.0	-0.2433
0.9989	0.0471	0.0	0.0	0.0	0.0	0.0	0.0	0.0
0.0	0.0	0.0	0.0	-30.0000	0.0	30.0000	0.0	0.0
0.0	0.0	0.0	0.0	0.0	-25.0000	0.0	25.0000	0.0
-0.0680	2.0240	-2.5710	-0.0479	-0.0040	-0.1855	-0.2704	-0.5468	0.0000
-0.4394	15.3400	1.3650	-0.3463	-0.0067	-1.5740	-0.3079	-8.8610	-0.0000
0.0	0.0	0.0	0.0	0.0	0.0	0.0	0.0	-1.2390

REGULATOR GAIN MATRIX (G)

0.0680	-2.0240	2.5710	0.0479	0.0040	0.1855	0.2704	0.5468	-0.0000
0.4394	-15.3400	-1.3650	0.3463	0.0067	1.5740	0.3079	8.8610	0.0000

FLIGHT CONDITION 20 CONTINUED

POLES OF CIOSED-LOCP SYSTEM - REGULATOR

REAL PART =	-30.000	IMAG PART =	0.0
REAL PART =	-24.878	IMAG PART =	0.0
REAL PART =	-3.062	IMAG PART =	4.932
REAL PART =	-3.062	IMAG PART =	-4.932
REAL PART =	-3.514	IMAG PART =	0.0
REAL PART =	-2.444	IMAG PART =	0.0
REAL PART =	-0.115	IMAG PART =	0.080
REAL PART =	-0.115	IMAG PART =	-0.080
REAL PART =	-1.239	IMAG PART =	0.0

DISCRETE TIME REGULATOR MATRIX (ACLD) DT=.125 SEC

0.7022	0.8808	-8.7352	-0.0188	0.2691	0.0897	0.8390	0.1869	-7.9498
0.0059	0.7964	0.8684	0.0036	0.0098	-0.0700	0.0296	-0.1186	0.8134
0.0048	-0.1115	0.8854	0.0024	0.0004	0.0081	0.0006	0.0082	-0.1084
0.1061	0.0428	-0.5851	0.9992	0.0285	0.0127	0.0449	0.0125	-0.5517
-0.0050	0.1523	-0.1460	-0.0037	0.0232	-0.0141	0.9521	-0.0472	0.0878
-0.0204	0.7908	0.5517	-0.0183	0.0004	-0.0355	-0.0163	0.3572	0.4534
-0.0064	0.1954	-0.1742	-0.0048	-0.0003	-0.0182	0.9673	-0.0624	0.1398
-0.0242	0.9751	0.8879	-0.0227	0.0008	-0.0979	-0.0200	0.1954	0.7459
0.0	0.0	0.0	0.0	0.0	0.0	0.0	0.0	0.8565

POLES OF DISCRETE TIME REGULATOR DT=.125 SEC

REAL PART =	0.045	IMAG PART =	0.0
REAL PART =	0.024	IMAG PART =	0.0
REAL PART =	0.556	IMAG PART =	0.394
REAL PART =	0.556	IMAG PART =	-0.394
REAL PART =	0.737	IMAG PART =	0.0
REAL PART =	0.986	IMAG PART =	0.010
REAL PART =	0.986	IMAG PART =	-0.010
REAL PART =	0.644	IMAG PART =	0.0
REAL PART =	0.857	IMAG PART =	0.0

FLIGHT CONDITION 20 CONTINUED

DISCRETE TIME CONTROL GAIN (GD)

0.0551	-1.6840	1.5390	0.0407	0.0029	0.1571	0.2642	0.5316	-1.0790
0.2086	-8.2790	-6.8200	0.1923	-0.0056	0.8315	0.1701	6.6040	-6.3440

APPENDIX C

LATERAL DYNAMICS
KALMAN FILTER MATRICES

FLIGHT CONDITION 5 DYNAMIC PRESSURE 133 PSF MACH 0.30 ALTITUDE 0 FT

PLANT NOISE COVARIANCE (XI)

1.100E-01	0.0	0.0	0.0	0.0	0.0	0.0
0.0	7.600E-04	0.0	0.0	0.0	0.0	0.0
0.0	0.0	1.400E-05	0.0	0.0	0.0	0.0
0.0	0.0	0.0	2.500E-05	0.0	0.0	0.0
0.0	0.0	0.0	0.0	1.000E-07	0.0	0.0
0.0	0.0	0.0	0.0	0.0	1.000E-07	0.0
0.0	0.0	0.0	0.0	0.0	0.0	6.540E-02

OBSERVATION NOISE COVARIANCE (THETA)

1.750E-03	0.0	0.0	0.0	0.0
0.0	1.218E-03	0.0	0.0	0.0
0.0	0.0	7.610E-05	0.0	0.0
0.0	0.0	0.0	3.000E-06	0.0
0.0	0.0	0.0	0.0	3.000E-06

KALMAN FILTER GAINS (H)

-5.242E-01	1.376E+01	-1.600E+01	1.201E-03	2.484E-04
1.656E-01	-1.000E+00	5.587E+00	-1.181E-04	-2.833E-05
-3.674E-01	1.586E-01	-1.029E+00	6.424E-06	1.595E-05
-8.163E-01	6.353E-01	2.521E-01	3.698E-05	8.754E-05
-8.823E-08	2.959E-06	-4.657E-06	5.556E-04	2.274E-11
5.231E-07	6.118E-07	-1.117E-06	2.274E-11	6.667E-04
4.631E-01	-4.310E+00	9.422E+00	7.921E-05	5.339E-05

FLIGHT CONDITION 5 CONTINUED

KF CLOSED-LOOP MATRIX (ACL)

-16.4200	16.4900	-24.0400	0.0003	9.8470	4.1130	-22.7900
0.9178	-5.8740	2.6610	-0.0001	0.3509	-1.7600	2.2670
-0.0227	0.0990	-1.1050	0.0964	-0.0000	0.2254	-0.2292
0.3452	0.0114	-1.9460	0.0005	-0.0000	0.3968	0.0000
-0.0000	0.0000	-0.0000	0.0000	-30.0000	0.0000	-0.0000
-0.0000	0.0000	0.0000	-0.0000	-0.0000	-25.0000	-0.0000
4.3160	-9.4910	1.1040	-0.0003	-0.0001	-0.2252	-3.3490

KF POLES

REAL PART =	-10.511	IMAG PART =	8.267
REAL PART =	-10.511	IMAG PART =	-8.267
REAL PART =	-4.803	IMAG PART =	0.0
REAL PART =	-0.342	IMAG PART =	0.0
REAL PART =	-0.580	IMAG PART =	0.0
REAL PART =	-30.000	IMAG PART =	0.0
REAL PART =	-25.000	IMAG PART =	0.0

STATE ESTIMATION ERROR COVARIANCE MATRIX

1.676E-02	-1.218E-03	1.932E-04	7.738E-04	3.604E-09	7.452E-10	-5.250E-03
-1.218E-03	4.252E-04	-7.833E-05	1.919E-05	-3.544E-10	-8.499E-11	7.170E-04
1.932E-04	-7.833E-05	2.408E-04	5.462E-04	1.927E-11	4.786E-11	-2.400E-04
7.738E-04	1.919E-05	5.462E-04	3.604E-03	1.109E-10	2.626E-10	-3.992E-04
3.604E-09	-3.544E-10	1.927E-11	1.109E-10	1.667E-09	6.821E-17	2.376E-10
7.452E-10	-8.499E-11	4.786E-11	2.626E-10	6.821E-17	2.000E-09	1.602E-10
-5.250E-03	7.170E-04	-2.400E-04	-3.992E-04	2.376E-10	1.602E-10	5.325E-03

FLIGHT CONDITION 5 CONTINUED

DISCRETE TIME PLANT NOISE COVARIANCE MATRIX (XID) DT=.125 SEC

2.208E-02	-1.445E-03	3.795E-04	1.200E-03	4.838E-10	2.534E-10	-6.857E-03
-1.445E-03	2.544E-04	-3.996E-05	-7.229E-05	1.735E-11	-1.220E-10	7.768E-04
3.795E-04	-3.996E-05	1.059E-05	2.303E-05	1.500E-12	8.339E-12	-1.506E-04
1.200E-03	-7.229E-05	2.303E-05	8.943E-05	1.398E-11	7.540E-12	-2.859E-04
4.838E-10	1.735E-11	1.500E-12	1.398E-11	1.666E-09	0.0	0.0
2.534E-10	-1.220E-10	8.339E-12	7.540E-12	0.0	1.996E-09	0.0
-6.857E-03	7.768E-04	-1.506E-04	-2.859E-04	0.0	0.0	5.537E-03

DISCRETE TIME KF GAINS (HD) DT=.125 SEC

-2.451E-02	9.387E-01	-2.993E-01	1.180E-05	-1.170E-07
1.390E-02	-1.870E-02	7.669E-01	4.517E-06	-1.260E-05
-5.853E-02	9.016E-03	-8.421E-02	-6.021E-07	1.743E-05
-1.386E-01	5.140E-02	9.384E-02	-4.423E-06	4.688E-05
3.384E-09	2.907E-08	1.781E-07	5.552E-04	4.123E-12
4.808E-07	-2.863E-10	-4.969E-07	4.123E-12	6.662E-04
4.924E-02	-2.025E-01	1.157E+00	2.652E-05	5.164E-05

DISCRETE TIME KF CLOSED-LOOP MATRIX DT=.125 SEC

-0.3140	2.2384	-2.2703	-0.0151	0.2471	0.0879	-1.8894
0.0618	-0.0261	0.3029	0.0017	0.0093	-0.0663	0.2319
-0.0226	0.1307	0.7865	0.0117	0.0029	0.0386	-0.0578
-0.0716	0.1054	-0.4826	0.9995	0.0264	0.0775	-0.1330
-0.0000	-0.0000	0.0000	-0.0000	0.0235	-0.0000	0.0000
0.0000	0.0000	0.0000	-0.0000	-0.0000	0.0439	0.0000
0.1336	-0.7659	0.0773	-0.0000	-0.0000	-0.0158	0.6579

FLIGHT CONDITION 5 CONTINUED

DISCRETE TIME KF POLES DT=.125 SEC

REAL PART =	0.024	IMAG PART =	0.129
REAL PART =	0.024	IMAG PART =	-0.129
REAL PART =	0.892	IMAG PART =	0.0
REAL PART =	0.963	IMAG PART =	0.0
REAL PART =	0.200	IMAG PART =	0.0
REAL PART =	0.024	IMAG PART =	0.0
REAL PART =	0.044	IMAG PART =	0.0

STATE PREDICTION COVARIANCE MATRIX DT=.125 SEC

3.439E-02	-3.010E-03	7.256E-04	1.906E-03	4.907E-10	2.438E-10	-1.082E-02
-3.010E-03	5.122E-04	-9.673E-05	-1.470E-04	1.844E-11	-1.268E-10	1.307E-03
7.256E-04	-9.673E-05	6.805E-05	1.560E-04	1.437E-12	1.114E-11	-2.974E-04
1.906E-03	-1.470E-04	1.560E-04	1.076E-03	1.455E-11	1.332E-11	-5.673E-04
4.907E-10	1.844E-11	1.437E-12	1.455E-11	1.667E-09	1.278E-20	1.231E-12
2.438E-10	-1.268E-10	1.114E-11	1.332E-11	1.278E-20	2.000E-09	4.478E-12
-1.082E-02	1.307E-03	-2.974E-04	-5.673E-04	1.231E-12	4.478E-12	6.897E-03

INVERSE OF DISCRETE TIME OBSERVATION ERROR COVARIANCE MATRIX DT=.125 SEC

4.904E+02	2.013E+01	-1.826E+02	-1.128E-03	-1.603E-01
2.013E+01	5.031E+01	2.457E+02	-9.690E-03	9.546E-05
-1.826E+02	2.457E+02	3.063E+03	-5.936E-02	1.656E-01
-1.128E-03	-9.690E-03	-5.936E-02	3.331E+05	-1.374E-06
-1.603E-01	9.546E-05	1.656E-01	-1.374E-06	3.331E+05

DETERMINANT OF OBSERVATION COVARIANCE MATRIX = 0.218E-18

FLIGHT CONDITION 6 DYNAMIC PRESSURE 416 PSF MACH 0.53 ALTITUDE 0 FT

PLANT NOISE COVARIANCE (XI)

1.100E-01	0.0	0.0	0.0	0.0	0.0	0.0
0.0	7.600E-04	0.0	0.0	0.0	0.0	0.0
0.0	0.0	1.400E-05	0.0	0.0	0.0	0.0
0.0	0.0	0.0	2.500E-05	0.0	0.0	0.0
0.0	0.0	0.0	0.0	1.000E-07	0.0	0.0
0.0	0.0	0.0	0.0	0.0	1.000E-07	0.0
0.0	0.0	0.0	0.0	0.0	0.0	4.920E-02

OBSERVATION NOISE COVARIANCE (THETA)

1.750E-03	0.0	0.0	0.0	0.0
0.0	1.218E-03	0.0	0.0	0.0
0.0	0.0	7.610E-05	0.0	0.0
0.0	0.0	0.0	3.000E-06	0.0
0.0	0.0	0.0	0.0	3.000E-06

KALMAN FILTER GAINS (H)

-8.806E-01	1.557E+01	-2.955E+01	1.868E-03	1.035E-03
4.050E-01	-1.846E+00	8.989E+00	-1.777E-04	-2.625E-04
-2.733E-01	1.219E-01	-1.027E+00	4.016E-05	2.697E-05
-8.216E-01	6.374E-01	-4.151E-02	1.073E-04	-2.241E-04
-5.947E-07	4.601E-06	-7.005E-06	5.556E-04	4.828E-10
1.216E-06	2.550E-06	-1.035E-05	4.828E-10	6.667E-04
4.021E-01	-3.332E+00	9.426E+00	2.852E-04	-6.030E-05

FLIGHT CONDITION 6 CONTINUED

KF CLOSED-LOOP MATRIX (ACL)

-20.0700	29.9900	-60.6500	0.0008	26.8800	11.5800	-54.3400
1.7530	-9.5110	10.7500	-0.0004	1.1060	-5.2800	7.8460
-0.0694	0.0634	-2.3520	0.0547	-0.0000	0.4310	-0.3905
0.3570	0.1865	-5.8960	0.0008	-0.0001	1.0810	0.0000
-0.0000	0.0000	-0.0000	0.0000	-30.0000	0.0000	-0.0000
-0.0000	0.0000	0.0000	-0.0000	-0.0000	-25.0000	0.0000
3.3340	-9.4710	2.8850	-0.0004	-0.0003	-0.5287	-5.9170

KF POLES

REAL PART =	-14.940	IMAG PART =	13.236
REAL PART =	-14.940	IMAG PART =	-13.236
REAL PART =	-0.176	IMAG PART =	0.0
REAL PART =	-5.952	IMAG PART =	0.0
REAL PART =	-1.840	IMAG PART =	0.0
REAL PART =	-30.000	IMAG PART =	0.0
REAL PART =	-25.000	IMAG PART =	0.0

STATE ESTIMATION ERROR COVARIANCE MATRIX

1.896E-02	-2.249E-03	1.484E-04	7.764E-04	5.605E-09	3.106E-09	-4.059E-03
-2.249E-03	6.841E-04	-7.817E-05	-3.159E-06	-5.331E-10	-7.875E-10	7.173E-04
1.484E-04	-7.817E-05	5.966E-05	1.833E-04	1.205E-10	8.092E-11	-7.575E-05
7.764E-04	-3.159E-06	1.833E-04	5.187E-03	3.219E-10	-6.724E-10	-1.468E-04
5.605E-09	-5.331E-10	1.205E-10	3.219E-10	1.667E-09	1.448E-15	8.557E-10
3.106E-09	-7.875E-10	8.092E-11	-6.724E-10	1.448E-15	2.000E-09	-1.809E-10
-4.059E-03	7.173E-04	-7.575E-05	-1.468E-04	8.557E-10	-1.809E-10	2.421E-03

FLIGHT CONDITION 6 CONTINUED

DISCRETE TIME PLANT NOISE COVARIANCE MATRIX (XID) DT=.125 SEC

4.213E-02	-6.126E-03	7.208E-04	2.251E-03	1.259E-09	6.386E-10	-8.468E-03
-6.126E-03	1.187E-03	-1.320E-04	-3.258E-04	5.445E-11	-3.402E-10	1.469E-03
7.208E-04	-1.320E-04	1.737E-05	4.176E-05	4.543E-13	1.695E-11	-1.533E-04
2.251E-03	-3.258E-04	4.176E-05	1.528E-04	3.678E-11	2.021E-11	-3.614E-04
1.259E-09	5.445E-11	4.543E-13	3.678E-11	1.666E-09	0.0	0.0
6.386E-10	-3.402E-10	1.695E-11	2.021E-11	0.0	1.996E-09	0.0
-8.468E-03	1.469E-03	-1.533E-04	-3.614E-04	0.0	0.0	3.210E-03

DISCRETE TIME KF GAINS (HD) DT=.125 SEC

-1.642E-02	9.191E-01	-3.697E-01	4.149E-05	-1.344E-05
2.409E-02	-2.309E-02	8.292E-01	1.312E-05	-3.468E-05
-4.115E-02	2.292E-03	-6.415E-02	3.080E-07	3.277E-05
-1.367E-01	5.089E-02	1.109E-01	-1.107E-05	1.247E-04
-1.678E-09	1.022E-07	5.172E-07	5.552E-04	4.098E-11
1.093E-06	-3.309E-08	-1.367E-06	4.098E-11	6.662E-04
-2.237E-02	-1.027E-01	5.059E-01	3.421E-05	9.875E-05

DISCRETE TIME KF CLOSED-LOOP MATRIX DT=.125 SEC

-0.2718	1.5928	-2.8979	-0.0190	0.5746	-0.1524	-3.2973
0.0848	-0.1197	0.7042	0.0033	0.0286	-0.1254	0.6557
-0.0144	0.0901	0.6050	0.0065	0.0008	0.0691	-0.0946
-0.0697	0.0538	-1.1835	0.9993	0.0665	0.1806	-0.2656
-0.0000	-0.0000	-0.0000	0.0000	0.0235	0.0000	0.0000
0.0000	0.0000	0.0000	-0.0000	-0.0000	0.0439	0.0000
0.0489	-0.2403	-0.0766	0.0000	-0.0000	0.0140	0.4773

FLIGHT CONDITION 6 CONTINUED

DISCRETE TIME KF POLES DT=.125 SEC

REAL PART =	0.977	IMAG PART =	0.0
REAL PART =	0.722	IMAG PART =	0.0
REAL PART =	-0.145	IMAG PART =	0.0
REAL PART =	0.167	IMAG PART =	0.0
REAL PART =	-0.031	IMAG PART =	0.0
REAL PART =	0.024	IMAG PART =	0.0
REAL PART =	0.044	IMAG PART =	0.0

STATE PREDICTION COVARIANCE MATRIX DT=.125 SEC

5.947E-02	-9.557E-03	1.146E-03	3.338E-03	1.275E-09	5.901E-10	-1.085E-02
-9.557E-03	1.930E-03	-2.290E-04	-5.241E-04	5.798E-11	-3.463E-10	1.954E-03
1.146E-03	-2.290E-04	4.053E-05	1.105E-04	1.813E-13	2.183E-11	-2.202E-04
3.338E-03	-5.241E-04	1.105E-04	1.722E-03	3.825E-11	3.371E-11	-5.271E-04
1.275E-09	5.798E-11	1.813E-13	3.825E-11	1.667E-09	1.270E-19	1.152E-12
5.901E-10	-3.463E-10	2.183E-11	3.371E-11	1.270E-19	2.000E-09	6.217E-12
-1.085E-02	1.954E-03	-2.202E-04	-5.271E-04	1.152E-12	6.217E-12	3.549E-03

INVERSE OF DISCRETE TIME OBSERVATION ERROR COVARIANCE MATRIX DT=.125 SEC

4.012E+02	1.349E+01	-3.166E+02	5.593E-04	-3.642E-01
1.349E+01	6.640E+01	3.035E+02	-3.406E-02	1.103E-02
-3.166E+02	3.035E+02	2.244E+03	-1.724E-01	4.558E-01
5.593E-04	-3.406E-02	-1.724E-01	3.331E+05	-1.366E-05
-3.642E-01	1.103E-02	4.558E-01	-1.366E-05	3.331E+05

DETERMINANT OF OBSERVATION COVARIANCE MATRIX = 0.683E-18

FLIGHT CONDITION 7 DYNAMIC PRESSURE 726 PSF MACH 0.70 ALTITUDE 0 FT

PLANT NOISE COVARIANCE (XI)

1.100E-01	0.0	0.0	0.0	0.0	0.0	0.0
0.0	7.600E-04	0.0	0.0	0.0	0.0	0.0
0.0	0.0	1.400E-05	0.0	0.0	0.0	0.0
0.0	0.0	0.0	2.500E-05	0.0	0.0	0.0
0.0	0.0	0.0	0.0	1.000E-07	0.0	0.0
0.0	0.0	0.0	0.0	0.0	1.000E-07	0.0
0.0	0.0	0.0	0.0	0.0	0.0	4.281E-02

OBSERVATION NOISE COVARIANCE (THETA)

1.750E-03	0.0	0.0	0.0	0.0
0.0	1.218E-03	0.0	0.0	0.0
0.0	0.0	7.610E-05	0.0	0.0
0.0	0.0	0.0	3.000E-06	0.0
0.0	0.0	0.0	0.0	3.000E-06

KALMAN FILTER GAINS (H)

-1.337E+00	1.582E+01	-3.764E+01	-8.884E-04	4.688E-04
6.573E-01	-2.352E+00	1.173E+01	3.399E-04	-1.983E-04
-2.581E-01	1.134E-01	-9.893E-01	-1.980E-05	2.205E-05
-8.078E-01	5.990E-01	-1.445E-01	-1.631E-04	-1.382E-04
5.447E-07	-2.188E-06	1.340E-05	5.555E-04	-2.705E-10
1.815E-06	1.155E-06	-7.815E-06	-2.705E-10	6.667E-04
4.317E-01	-2.845E+00	9.332E+00	4.611E-04	4.990E-05

FLIGHT CONDITION 7 CONTINUED

KF CLOSED-LOOP MATRIX (ACL)

-21.7600	38.1000	-97.0500	-0.0007	41.6500	17.5100	-80.5600
2.2630	-12.4500	22.0900	0.0004	1.6640	-8.4180	13.9800
-0.0814	0.0270	-3.6900	0.0410	0.0000	0.5686	-0.5079
0.3973	0.2794	-9.9580	-0.0004	0.0002	1.5350	0.0000
0.0000	-0.0000	0.0000	0.0000	-30.0000	-0.0000	-0.0000
-0.0000	0.0000	0.0000	0.0000	0.0000	-25.0000	-0.0000
2.8460	-9.3860	5.3220	0.0002	-0.0005	-0.8202	-7.8150

KF POLES

REAL PART = -17.841 IMAG PART = 16.221
REAL PART = -17.841 IMAG PART = -16.221
REAL PART = -0.127 IMAG PART = 0.0
REAL PART = -6.688 IMAG PART = 0.0
REAL PART = -3.220 IMAG PART = 0.0
REAL PART = -30.000 IMAG PART = 0.0
REAL PART = -25.000 IMAG PART = 0.0

STATE ESTIMATION ERROR COVARIANCE MATRIX

1.927E-02	-2.865E-03	1.381E-04	7.296E-04	-2.665E-09	1.406E-09	-3.465E-03
-2.865E-03	8.923E-04	-7.528E-05	-1.100E-05	1.020E-09	-5.948E-10	7.102E-04
1.381E-04	-7.528E-05	3.268E-05	1.042E-04	-5.941E-11	6.616E-11	-4.767E-05
7.296E-04	-1.100E-05	1.042E-04	6.407E-03	-4.892E-10	-4.146E-10	-9.002E-05
-2.665E-09	1.020E-09	-5.941E-11	-4.892E-10	1.667E-09	-8.114E-16	1.383E-09
1.406E-09	-5.948E-10	6.616E-11	-4.146E-10	-8.114E-16	2.000E-09	1.497E-10
-3.465E-03	7.102E-04	-4.767E-05	-9.002E-05	1.383E-09	1.497E-10	1.665E-03

FLIGHT CONDITION 7 CONTINUED

DISCRETE TIME PLANT NOISE COVARIANCE MATRIX (XID) DT=.125 SEC

5.421E-02	-1.072E-02	1.016E-03	2.939E-03	1.881E-09	8.687E-10	-8.373E-03
-1.072E-02	2.537E-03	-2.391E-04	-5.951E-04	8.146E-11	-5.076E-10	1.815E-03
1.016E-03	-2.391E-04	2.550E-05	6.151E-05	-4.701E-13	2.247E-11	-1.529E-04
2.939E-03	-5.951E-04	6.151E-05	2.008E-04	5.517E-11	2.804E-11	-3.590E-04
1.881E-09	8.146E-11	-4.701E-13	5.517E-11	1.666E-09	0.0	0.0
8.687E-10	-5.076E-10	2.247E-11	2.804E-11	0.0	1.996E-09	0.0
-8.373E-03	1.815E-03	-1.529E-04	-3.590E-04	0.0	0.0	2.351E-03

DISCRETE TIME KF GAINS (HD) DT=.125 SEC

-5.418E-03	9.028E-01	-3.777E-01	7.266E-05	-3.251E-05
3.052E-02	-2.359E-02	8.456E-01	1.930E-05	-5.441E-05
-3.670E-02	1.024E-04	-4.818E-02	1.204E-06	4.257E-05
-1.320E-01	4.766E-02	1.352E-01	-1.437E-05	1.742E-04
-2.176E-08	1.790E-07	7.607E-07	5.552E-04	1.068E-10
1.259E-06	-8.003E-08	-2.145E-06	1.068E-10	6.662E-04
-6.898E-02	-8.949E-02	3.242E-01	4.800E-05	1.579E-04

DISCRETE TIME KF CLOSED-LOOP MATRIX DT=.125 SEC

-0.2809	1.1084	-0.1358	-0.0193	0.7873	-0.7437	-3.8091
0.1078	-0.1100	0.3268	0.0042	0.0417	-0.0450	1.0018
-0.0139	0.0669	0.5064	0.0048	-0.0010	0.0753	-0.1252
-0.0693	0.0014	-1.5902	0.9991	0.0966	0.2065	-0.3414
-0.0000	-0.0000	-0.0000	-0.0000	0.0235	0.0000	0.0000
0.0000	0.0000	0.0000	0.0000	-0.0000	0.0439	0.0000
0.0336	-0.1188	-0.3201	-0.0000	-0.0000	0.0493	0.3765

FLIGHT CONDITION 7 CONTINUED

DISCRETE TIME KF POLES DT=.125 SEC

REAL PART =	0.982	IMAG PART =	0.0
REAL PART =	0.570	IMAG PART =	0.0
REAL PART =	-0.195	IMAG PART =	0.0
REAL PART =	0.144	IMAG PART =	0.0
REAL PART =	-0.010	IMAG PART =	0.0
REAL PART =	0.024	IMAG PART =	0.0
REAL PART =	0.044	IMAG PART =	0.0

STATE PREDICTION COVARIANCE MATRIX DT=.125 SEC

7.118E-02	-1.512E-02	1.491E-03	4.121E-03	1.901E-09	7.678E-10	-9.963E-03
-1.512E-02	3.744E-03	-3.746E-04	-8.841E-04	8.772E-11	-5.047E-10	2.237E-03
1.491E-03	-3.746E-04	4.625E-05	1.214E-04	-1.002E-12	2.772E-11	-2.018E-04
4.121E-03	-8.841E-04	1.214E-04	2.244E-03	5.723E-11	4.367E-11	-4.789E-04
1.901E-09	8.772E-11	-1.002E-12	5.723E-11	1.667E-09	3.304E-19	1.276E-12
7.678E-10	-5.047E-10	2.772E-11	4.367E-11	3.304E-19	2.000E-09	7.842E-12
-9.963E-03	2.237E-03	-2.018E-04	-4.789E-04	1.276E-12	7.842E-12	2.504E-03

INVERSE OF DISCRETE TIME OBSERVATION ERROR COVARIANCE MATRIX DT=.125 SEC

3.106E+02	4.453E+00	-4.011E+02	7.252E-03	-4.195E-01
4.453E+00	7.984E+01	3.100E+02	-5.966E-02	2.668E-02
-4.011E+02	3.100E+02	2.030E+03	-2.536E-01	7.151E-01
7.252E-03	-5.966E-02	-2.536E-01	3.331E+05	-3.560E-05
-4.195E-01	2.668E-02	7.151E-01	-3.560E-05	3.331E+05

DETERMINANT OF OBSERVATION COVARIANCE MATRIX = 0.139E-17

FLIGHT CONDITION 8 DYNAMIC PRESSURE 1098 PSF MACH 0.86 ALTITUDE 0 FT

PLANT NOISE COVARIANCE (XI)

1.100E-01	0.0	0.0	0.0	0.0	0.0	0.0
0.0	7.600E-04	0.0	0.0	0.0	0.0	0.0
0.0	0.0	1.400E-05	0.0	0.0	0.0	0.0
0.0	0.0	0.0	2.500E-05	0.0	0.0	0.0
0.0	0.0	0.0	0.0	1.000E-07	0.0	0.0
0.0	0.0	0.0	0.0	0.0	1.000E-07	0.0
0.0	0.0	0.0	0.0	0.0	0.0	3.862E-02

OBSERVATION NOISE COVARIANCE (THETA)

1.750E-03	0.0	0.0	0.0	0.0
0.0	1.218E-03	0.0	0.0	0.0
0.0	0.0	7.610E-05	0.0	0.0
0.0	0.0	0.0	3.000E-06	0.0
0.0	0.0	0.0	0.0	3.000E-06

KALMAN FILTER GAINS (H)

-2.061E+00	1.662E+01	-4.443E+01	6.091E-04	5.644E-04
9.586E-01	-2.776E+00	1.345E+01	1.044E-04	-2.705E-04
-2.532E-01	1.169E-01	-9.399E-01	1.140E-06	2.366E-05
-7.828E-01	5.448E-01	-3.300E-01	2.986E-04	-9.734E-05
-1.699E-08	1.500E-06	4.115E-06	5.555E-04	-1.241E-10
1.538E-06	1.390E-06	-1.066E-05	-1.241E-10	6.667E-04
4.853E-01	-2.623E+00	8.781E+00	1.930E-04	1.425E-05

FLIGHT CONDITION 8 CONTINUED

KF CLOSED-LOOP MATRIX (ACL)

-24.5500	45.0100	-155.2000	-0.0016	48.4100	19.6100	-115.7000
2.6640	-14.4000	39.1200	0.0008	1.7530	-9.7450	20.7300
-0.0917	-0.0183	-5.5020	0.0333	-0.0000	0.5659	-0.6435
0.4521	0.4703	-15.0200	-0.0006	-0.0003	1.5450	0.0000
-0.0000	-0.0000	-0.0000	-0.0000	-30.0000	0.0000	-0.0000
-0.0000	0.0000	0.0000	0.0000	0.0000	-25.0000	-0.0000
2.6250	-8.8520	9.3120	0.0004	-0.0002	-0.9579	-9.6010

KF ECLES

REAL PART =	-20.876	IMAG PART =	19.160
REAL PART =	-20.876	IMAG PART =	-19.160
REAL PART =	-0.094	IMAG PART =	0.0
REAL PART =	-6.060	IMAG PART =	0.0
REAL PART =	-6.147	IMAG PART =	0.0
REAL PART =	-30.000	IMAG PART =	0.0
REAL PART =	-25.000	IMAG PART =	0.0

STATE ESTIMATION ERROR COVARIANCE MATRIX

2.025E-02	-3.381E-03	1.424E-04	6.635E-04	1.827E-09	1.693E-09	-3.195E-03
-3.381E-03	1.024E-03	-7.152E-05	-2.511E-05	3.132E-10	-8.114E-10	6.682E-04
1.424E-04	-7.152E-05	2.054E-05	6.467E-05	3.419E-12	7.099E-11	-3.479E-05
6.635E-04	-2.511E-05	6.467E-05	7.057E-03	8.959E-10	-2.920E-10	-6.326E-05
1.827E-09	3.132E-10	3.419E-12	8.959E-10	1.667E-09	-3.723E-16	5.790E-10
1.693E-09	-8.114E-10	7.099E-11	-2.920E-10	-3.723E-16	2.000E-09	4.275E-11
-3.195E-03	6.682E-04	-3.479E-05	-6.326E-05	5.790E-10	4.275E-11	1.250E-03

FLIGHT CONDITION 8 CONTINUED

DISCRETE TIME PLANT NOISE COVARIANCE MATRIX (XID) DT=.125 SEC

6.720E-02	-1.561E-02	1.355E-03	3.712E-03	2.082E-09	8.370E-10	-8.340E-03
-1.561E-02	4.118E-03	-3.643E-04	-9.111E-04	8.341E-11	-5.501E-10	1.988E-03
1.355E-03	-3.643E-04	3.590E-05	8.758E-05	-7.550E-13	2.267E-11	-1.524E-04
3.712E-03	-9.111E-04	8.758E-05	2.620E-04	6.136E-11	2.744E-11	-3.588E-04
2.082E-09	8.341E-11	-7.550E-13	6.136E-11	1.666E-09	0.0	0.0
8.370E-10	-5.501E-10	2.267E-11	2.744E-11	0.0	1.996E-09	0.0
-8.340E-03	1.988E-03	-1.524E-04	-3.588E-04	0.0	0.0	1.829E-03

DISCRETE TIME KF GAINS (HD) DT=.125 SEC

1.251E-02	8.927E-01	-4.053E-01	8.722E-05	-6.119E-05
3.383E-02	-2.532E-02	8.310E-01	2.246E-05	-6.212E-05
-3.269E-02	-1.297E-03	-3.417E-02	1.825E-06	3.959E-05
-1.216E-01	4.077E-02	1.582E-01	-1.079E-05	1.677E-04
-5.492E-08	2.148E-07	8.855E-07	5.552E-04	1.694E-10
9.366E-07	-1.507E-07	-2.449E-06	1.694E-10	6.662E-04
-9.108E-02	-9.625E-02	2.427E-01	6.129E-05	1.703E-04

DISCRETE TIME KF CLOSED-LOOP MATRIX DT=.125 SEC

-0.3444	0.8661	4.6245	-0.0204	0.7707	-1.1481	-4.0636
0.1452	-0.0855	-0.9240	0.0049	0.0398	0.0792	1.2922
-0.0167	0.0485	0.4794	0.0038	-0.0015	0.0563	-0.1567
-0.0726	-0.0320	-1.7958	0.9990	0.1030	0.1518	-0.4161
-0.0000	-0.0000	-0.0000	-0.0000	0.0235	0.0000	0.0000
0.0000	0.0000	0.0000	0.0000	-0.0000	0.0439	0.0000
0.0289	-0.0691	-0.5263	-0.0000	-0.0000	0.0541	0.3011

FLIGHT CONDITION 8 CONTINUED

DISCRETE TIME KF POLES DT=.125 SEC

REAL PART =	0.986	IMAG PART =	0.0
REAL PART =	0.412	IMAG PART =	0.0
REAL PART =	-0.180	IMAG PART =	0.0
REAL PART =	0.137	IMAG PART =	0.0
REAL PART =	-0.005	IMAG PART =	0.0
REAL PART =	0.044	IMAG PART =	0.0
REAL PART =	0.024	IMAG PART =	0.0

STATE PREDICTION COVARIANCE MATRIX DT=.125 SEC

8.168E-02	-2.013E-02	1.841E-03	4.883E-03	2.096E-09	7.092E-10	-9.355E-03
-2.013E-02	5.595E-03	-5.278E-04	-1.263E-03	9.204E-11	-5.373E-10	2.311E-03
1.841E-03	-5.278E-04	5.726E-05	1.464E-04	-1.551E-12	2.647E-11	-1.891E-04
4.883E-03	-1.263E-03	1.464E-04	2.697E-03	6.328E-11	3.877E-11	-4.473E-04
2.096E-09	9.204E-11	-1.551E-12	6.328E-11	1.667E-09	5.287E-19	1.304E-12
7.092E-10	-5.373E-10	2.647E-11	3.877E-11	5.287E-19	2.000E-09	6.749E-12
-9.355E-03	2.311E-03	-1.891E-04	-4.473E-04	1.304E-12	6.749E-12	1.902E-03

INVERSE OF DISCRETE TIME OBSERVATION ERROR COVARIANCE MATRIX DT=.125 SEC

2.101E+02	-1.027E+01	-4.446E+02	1.831E-02	-3.122E-01
-1.027E+01	8.809E+01	3.327E+02	-7.160E-02	5.022E-02
-4.446E+02	3.327E+02	2.221E+03	-2.952E-01	8.163E-01
1.831E-02	-7.160E-02	-2.952E-01	3.331E+05	-5.646E-05
-3.122E-01	5.022E-02	8.163E-01	-5.646E-05	3.331E+05

DETERMINANT OF OBSERVATION COVARIANCE MATRIX = 0.278E-17

FLIGHT CONDITION 9 DYNAMIC PRESSURE 1480 PSF MACH 1.00 ALTITUDE 0 FT

PLANT NOISE COVARIANCE (XI)

1.100E-01	0.0	0.0	0.0	0.0	0.0	0.0
0.0	7.600E-04	0.0	0.0	0.0	0.0	0.0
0.0	0.0	1.400E-05	0.0	0.0	0.0	0.0
0.0	0.0	0.0	2.500E-05	0.0	0.0	0.0
0.0	0.0	0.0	0.0	1.000E-07	0.0	0.0
0.0	0.0	0.0	0.0	0.0	1.000E-07	0.0
0.0	0.0	0.0	0.0	0.0	0.0	3.582E-02

OBSERVATION NOISE COVARIANCE (THETA)

1.750E-03	0.0	0.0	0.0	0.0
0.0	1.218E-03	0.0	0.0	0.0
0.0	0.0	7.610E-05	0.0	0.0
0.0	0.0	0.0	3.000E-06	0.0
0.0	0.0	0.0	0.0	3.000E-06

KALMAN FILTER GAINS (H)

-3.107E+00	1.888E+01	-4.744E+01	5.348E-04	-7.900E-05
1.181E+00	-2.964E+00	1.268E+01	-1.390E-04	-5.905E-05
-2.477E-01	1.304E-01	-8.355E-01	2.017E-05	1.319E-05
-8.011E-01	5.797E-01	-8.340E-02	-2.382E-04	3.365E-05
-1.068E-06	1.317E-06	-5.479E-06	5.555E-04	-6.374E-12
6.460E-07	-1.946E-07	-2.328E-06	-6.374E-12	6.667E-04
5.481E-01	-2.541E+00	7.691E+00	-2.384E-06	1.161E-04

FLIGHT CONDITION 9 CONTINUED

KF CLOSED-LOOP MATRIX (ACL)

-26.5500	48.0300	-231.0000	-0.0002	16.4500	12.0700	-147.1000
2.8440	-13.8500	56.2300	0.0001	0.6476	-5.6610	24.3400
-0.1104	-0.1185	-7.4660	0.0288	-0.0000	0.2946	-0.7786
0.4172	0.2377	-21.6300	-0.0000	0.0002	0.8532	0.0000
-0.0000	0.0000	-0.0000	-0.0000	-30.0000	0.0000	0.0000
0.0000	0.0000	0.0000	0.0000	0.0000	-25.0000	-0.0000
2.5420	-7.7820	14.8000	0.0000	0.0000	-0.5839	-11.1600

KF ECLES

REAL PART = -22.819 IMAG PART = 21.004
REAL PART = -22.819 IMAG PART = -21.004
REAL PART = -0.082 IMAG PART = 0.0
REAL PART = -6.653 IMAG PART = 2.313
REAL PART = -6.653 IMAG PART = -2.313
REAL PART = -30.000 IMAG PART = 0.0
REAL PART = -25.000 IMAG PART = 0.0

STATE ESTIMATION ERROR COVARIANCE MATRIX

2.300E-02	-3.610E-03	1.588E-04	7.061E-04	1.604E-09	-2.370E-10	-3.094E-03
-3.610E-03	9.649E-04	-6.358E-05	-6.346E-06	-4.169E-10	-1.772E-10	5.853E-04
1.588E-04	-6.358E-05	1.427E-05	4.733E-05	6.051E-11	3.956E-11	-2.846E-05
7.061E-04	-6.346E-06	4.733E-05	8.178E-03	-7.147E-10	1.010E-10	-4.803E-05
1.604E-09	-4.169E-10	6.051E-11	-7.147E-10	1.667E-09	-1.912E-17	-7.151E-12
-2.370E-10	-1.772E-10	3.956E-11	1.010E-10	-1.912E-17	2.000E-09	3.484E-10
-3.094E-03	5.853E-04	-2.846E-05	-4.803E-05	-7.151E-12	3.484E-10	1.029E-03

FLIGHT CONDITION 9 CONTINUED

DISCRETE TIME PLANT NOISE COVARIANCE MATRIX (XID) DT=.125 SEC

8.717E-02	-1.882E-02	1.648E-03	4.859E-03	7.124E-10	4.698E-10	-8.484E-03
-1.882E-02	4.512E-03	-4.045E-04	-1.113E-03	3.057E-11	-3.062E-10	1.834E-03
1.648E-03	-4.045E-04	4.032E-05	1.087E-04	-4.266E-13	1.207E-11	-1.404E-04
4.859E-03	-1.113E-03	1.087E-04	3.459E-04	2.098E-11	1.550E-11	-3.588E-04
7.124E-10	3.057E-11	-4.266E-13	2.098E-11	1.666E-09	0.0	0.0
4.698E-10	-3.062E-10	1.207E-11	1.550E-11	0.0	1.996E-09	0.0
-8.484E-03	1.834E-03	-1.404E-04	-3.588E-04	0.0	0.0	1.506E-03

DISCRETE TIME KF GAINS (HD) DT=.125 SEC

1.560E-02	9.013E-01	-4.300E-01	2.827E-05	0.0
3.262E-02	-2.686E-02	7.925E-01	8.490E-06	0.0
-2.787E-02	-1.116E-03	-2.285E-02	4.900E-07	0.0
-1.118E-01	4.016E-02	2.126E-01	-3.947E-06	0.0
-2.042E-08	6.962E-08	3.347E-07	5.552E-04	0.0
3.600E-07	-9.580E-08	-1.411E-06	3.598E-11	0.0
-8.683E-02	-8.501E-02	2.522E-01	1.827E-05	0.0

DISCRETE TIME KF CLOSED-LOOP MATRIX DT=.125 SEC

-0.3446	1.1344	9.2088	-0.0229	0.2702	-0.6892	-4.6280
0.1360	-0.1080	-1.9088	0.0050	0.0140	0.0422	1.3544
-0.0164	0.0396	0.4769	0.0032	-0.0008	0.0245	-0.1699
-0.0748	-0.0549	-1.9705	0.9990	0.0355	0.0638	-0.5002
-0.0000	-0.0000	-0.0000	-0.0000	0.0235	0.0000	0.0000
0.0000	0.0000	0.0000	0.0000	-0.0000	0.0439	0.0000
0.0210	-0.0589	-0.5807	-0.0000	-0.0000	0.0229	0.2477

FLIGHT CONDITION 9 CONTINUED

DISCRETE TIME KF POLES DT=.125 SEC

REAL PART =	0.987	IMAG PART =	0.0
REAL PART =	-0.158	IMAG PART =	0.0
REAL PART =	0.288	IMAG PART =	0.0
REAL PART =	0.157	IMAG PART =	0.0
REAL PART =	-0.003	IMAG PART =	0.0
REAL PART =	0.044	IMAG PART =	0.0
REAL PART =	0.024	IMAG PART =	0.0

STATE PREDICTION COVARIANCE MATRIX DT=.125 SEC

1.026E-01	-2.325E-02	2.155E-03	6.203E-03	7.179E-10	3.933E-10	-9.267E-03
-2.325E-02	5.849E-03	-5.610E-04	-1.485E-03	3.337E-11	-2.997E-10	2.064E-03
2.155E-03	-5.610E-04	6.070E-05	1.691E-04	-7.096E-13	1.369E-11	-1.679E-04
6.203E-03	-1.485E-03	1.691E-04	3.244E-03	2.160E-11	2.015E-11	-4.317E-04
7.179E-10	3.337E-11	-7.096E-13	2.160E-11	1.667E-09	1.116E-19	3.197E-13
3.933E-10	-2.997E-10	1.369E-11	2.015E-11	1.116E-19	2.000E-09	2.830E-12
-9.267E-03	2.064E-03	-1.679E-04	-4.317E-04	3.197E-13	2.830E-12	1.547E-03

INVERSE OF DISCRETE TIME OBSERVATION ERROR COVARIANCE MATRIX DT=.125 SEC

1.384E+02	-1.280E+01	-4.287E+02	6.808E-03	0.0
-1.280E+01	8.102E+01	3.530E+02	-2.321E-02	0.0
-4.287E+02	3.530E+02	2.727E+03	-1.116E-01	0.0
6.808E-03	-2.321E-02	-1.116E-01	3.331E+05	0.0
0.0	0.0	0.0	0.0	3.333E+05

DETERMINANT OF OBSERVATION COVARIANCE MATRIX = 0.483E-17

FLIGHT CONDITION 10 DYNAMIC PRESSURE 109 PSF MACH 0.40 ALTITUDE 20000 FT

PLANT NOISE COVARIANCE (XI)

1.100E-01	0.0	0.0	0.0	0.0	0.0	0.0
0.0	7.600E-04	0.0	0.0	0.0	0.0	0.0
0.0	0.0	1.400E-05	0.0	0.0	0.0	0.0
0.0	0.0	0.0	2.500E-05	0.0	0.0	0.0
0.0	0.0	0.0	0.0	1.000E-07	0.0	0.0
0.0	0.0	0.0	0.0	0.0	1.000E-07	0.0
0.0	0.0	0.0	0.0	0.0	0.0	1.662E-02

OBSERVATION NOISE COVARIANCE (THETA)

1.750E-03	0.0	0.0	0.0	0.0
0.0	1.218E-03	0.0	0.0	0.0
0.0	0.0	7.610E-05	0.0	0.0
0.0	0.0	0.0	3.000E-06	0.0
0.0	0.0	0.0	0.0	3.000E-06

KALMAN FILTER GAINS (H)

-5.877E-01	1.186E+01	-9.707E+00	7.498E-04	4.561E-04
1.598E-01	-6.065E-01	4.516E+00	-3.017E-05	-3.848E-05
-3.798E-01	2.051E-01	-1.014E+00	5.753E-06	1.594E-05
-8.462E-01	7.609E-01	3.619E-01	4.505E-05	6.827E-05
-5.864E-08	1.847E-06	-1.189E-06	5.555E-04	5.046E-11
4.234E-07	1.124E-06	-1.517E-06	5.046E-11	6.667E-04
5.270E-01	-2.937E+00	6.705E+00	4.682E-05	9.218E-06

FLIGHT CONDITION 10 CONTINUED

KF CLOSED-LOOP MATRIX (ACL)

-13.6200	10.1500	-19.3100	0.0009	7.7610	3.6050	-18.0300
0.5426	-4.7260	1.8530	-0.0002	0.4238	-1.5030	1.5050
-0.0415	0.1144	-0.9980	0.0783	-0.0000	0.1896	-0.1694
0.2107	-0.0064	-1.8460	0.0013	-0.0000	0.3507	0.0000
-0.0000	0.0000	-0.0000	0.0000	-30.0000	0.0000	-0.0000
-0.0000	0.0000	0.0000	-0.0000	-0.0000	-25.0000	-0.0000
2.9460	-6.8200	1.1500	-0.0008	-0.0000	-0.2185	-0.3318

KF POLES

REAL PART =	-6.973	IMAG PART =	3.686
REAL PART =	-6.973	IMAG PART =	-3.686
REAL PART =	-4.907	IMAG PART =	0.0
REAL PART =	-0.256	IMAG PART =	0.0
REAL PART =	-0.565	IMAG PART =	0.0
REAL PART =	-30.000	IMAG PART =	0.0
REAL PART =	-25.000	IMAG PART =	0.0

STATE ESTIMATION ERROR COVARIANCE MATRIX

1.445E-02	-7.387E-04	2.498E-04	9.268E-04	2.249E-09	1.368E-09	-3.578E-03
-7.387E-04	3.436E-04	-7.718E-05	2.754E-05	-9.051E-11	-1.154E-10	5.102E-04
2.498E-04	-7.718E-05	2.693E-04	6.193E-04	1.726E-11	4.781E-11	-3.090E-04
9.268E-04	2.754E-05	6.193E-04	4.145E-03	1.352E-10	2.048E-10	-5.649E-04
2.249E-09	-9.051E-11	1.726E-11	1.352E-10	1.667E-09	1.514E-16	1.405E-10
1.368E-09	-1.154E-10	4.781E-11	2.048E-10	1.514E-16	2.000E-09	2.765E-11
-3.578E-03	5.102E-04	-3.090E-04	-5.649E-04	1.405E-10	2.765E-11	3.386E-03

FLIGHT CONDITION 10 CONTINUED

DISCRETE TIME PLANT NOISE COVARIANCE MATRIX (XID) DT=.125 SEC

1.378E-02	-2.935E-04	1.804E-04	8.034E-04	3.910E-10	2.285E-10	-2.062E-03
-2.935E-04	1.167E-04	-1.196E-05	-1.430E-05	2.164E-11	-1.047E-10	1.895E-04
1.804E-04	-1.196E-05	5.466E-06	1.336E-05	1.324E-12	6.839E-12	-4.371E-05
8.034E-04	-1.430E-05	1.336E-05	6.834E-05	1.126E-11	6.652E-12	-8.523E-05
3.910E-10	2.164E-11	1.324E-12	1.126E-11	1.666E-09	0.0	0.0
2.285E-10	-1.047E-10	6.839E-12	6.652E-12	0.0	1.996E-09	0.0
-2.062E-03	1.895E-04	-4.371E-05	-8.523E-05	0.0	0.0	1.994E-03

DISCRETE TIME KF GAINS (HD) DT=.125 SEC

-2.974E-02	9.359E-01	-2.051E-01	9.991E-06	5.029E-06
1.468E-02	-1.281E-02	7.244E-01	3.793E-06	-1.295E-05
-5.862E-02	1.137E-02	-8.042E-02	-5.512E-07	1.457E-05
-1.366E-01	5.248E-02	1.042E-01	-4.012E-06	3.937E-05
3.197E-09	2.461E-08	1.495E-07	5.552E-04	2.801E-12
4.140E-07	1.239E-08	-5.104E-07	2.801E-12	6.662E-04
8.130E-02	-1.856E-01	1.126E+00	1.661E-05	3.544E-05

DISCRETE TIME KF CLOSED-LOOP MATRIX DT=.125 SEC

-0.2845	2.2363	-2.1079	-0.0100	0.2124	0.1262	-1.9327
0.0447	0.0665	0.2302	0.0009	0.0123	-0.0616	0.1866
-0.0225	0.1210	0.8069	0.0096	0.0026	0.0341	-0.0539
-0.0689	0.0865	-0.4354	0.9998	0.0217	0.0682	-0.1236
-0.0000	-0.0000	0.0000	-0.0000	0.0235	-0.0000	-0.0000
-0.0000	0.0000	0.0000	-0.0000	-0.0000	0.0439	0.0000
0.1793	-1.0972	0.1702	-0.0001	-0.0000	-0.0324	0.9594

FLIGHT CONDITION 10 CONTINUED

DISCRETE TIME KF POLES DT=.125 SEC

REAL PART =	0.293	IMAG PART =	0.156
REAL PART =	0.293	IMAG PART =	-0.156
REAL PART =	0.896	IMAG PART =	0.0
REAL PART =	0.972	IMAG PART =	0.0
REAL PART =	0.093	IMAG PART =	0.0
REAL PART =	0.024	IMAG PART =	0.0
REAL PART =	0.044	IMAG PART =	0.0

STATE PREDICTION COVARIANCE MATRIX DT=.125 SEC

2.232E-02	-1.180E-03	4.572E-04	1.333E-03	3.977E-10	2.247E-10	-5.828E-03
-1.180E-03	2.650E-04	-5.203E-05	-5.245E-05	2.259E-11	-1.099E-10	6.186E-04
4.572E-04	-5.203E-05	6.518E-05	1.511E-04	1.304E-12	9.353E-12	-2.115E-04
1.333E-03	-5.245E-05	1.511E-04	1.171E-03	1.177E-11	1.187E-11	-3.808E-04
3.977E-10	2.259E-11	1.304E-12	1.177E-11	1.667E-09	8.684E-21	1.124E-12
2.247E-10	-1.099E-10	9.353E-12	1.187E-11	8.684E-21	2.000E-09	4.482E-12
-5.828E-03	6.186E-04	-2.115E-04	-3.808E-04	1.124E-12	4.482E-12	3.838E-03

INVERSE OF DISCRETE TIME OBSERVATION ERROR COVARIANCE MATRIX DT=.125 SEC

4.963E+02	2.442E+01	-1.929E+02	-1.066E-03	-1.380E-01
2.442E+01	5.261E+01	1.684E+02	-8.202E-03	-4.129E-03
-1.929E+02	1.684E+02	3.622E+03	-4.984E-02	1.701E-01
-1.066E-03	-8.202E-03	-4.984E-02	3.331E+05	-9.337E-07
-1.380E-01	-4.129E-03	1.701E-01	-9.337E-07	3.331E+05

DETERMINANT OF OBSERVATION COVARIANCE MATRIX = 0.120E-18

FLIGHT CONDITION 11 DYNAMIC PRESSURE 254 PSF MACH 0.60 ALTITUDE 20000 FT

PLANT NOISE COVARIANCE (XI)

1.100E-01	0.0	0.0	0.0	0.0	0.0	0.0
0.0	7.600E-04	0.0	0.0	0.0	0.0	0.0
0.0	0.0	1.400E-05	0.0	0.0	0.0	0.0
0.0	0.0	0.0	2.500E-05	0.0	0.0	0.0
0.0	0.0	0.0	0.0	1.000E-07	0.0	0.0
0.0	0.0	0.0	0.0	0.0	1.000E-07	0.0
0.0	0.0	0.0	0.0	0.0	0.0	1.357E-02

OBSERVATION NOISE COVARIANCE (THETA)

1.750E-03	0.0	0.0	0.0	0.0
0.0	1.218E-03	0.0	0.0	0.0
0.0	0.0	7.610E-05	0.0	0.0
0.0	0.0	0.0	3.000E-06	0.0
0.0	0.0	0.0	0.0	3.000E-06

KALMAN FILTER GAINS (H)

-5.753E-01	1.353E+01	-1.784E+01	4.053E-03	1.036E-03
2.467E-01	-1.115E+00	6.295E+00	-1.974E-04	-1.988E-04
-2.903E-01	1.261E-01	-9.944E-01	3.958E-05	6.923E-05
-8.587E-01	7.824E-01	1.006E-01	6.624E-04	4.817E-04
-4.120E-07	9.983E-06	-7.781E-06	5.556E-04	1.223E-09
4.746E-07	2.551E-06	-7.835E-06	1.223E-09	6.667E-04
3.857E-01	-2.556E+00	6.910E+00	-1.508E-04	-5.391E-05

FLIGHT CONDITION 11 CONTINUED

KF CLOSED-LOOP MATRIX (ACL)

-16.1200	18.1500	-40.3300	-0.0003	17.2300	7.5220	-37.7800
1.0410	-6.5940	5.4510	0.0001	0.8159	-3.3930	4.3580
-0.0495	0.0315	-1.5160	0.0516	-0.0000	0.3013	-0.2293
0.2097	0.0709	-3.8040	-0.0004	-0.0007	0.7561	0.0000
-0.0000	0.0000	-0.0000	-0.0000	-30.0000	0.0000	0.0000
-0.0000	0.0000	0.0000	0.0000	-0.0000	-25.0000	0.0000
2.5580	-6.9510	1.7090	0.0002	0.0002	-0.3398	-0.4977

KF POLES

REAL PART =	-9.068	IMAG PART =	7.104
REAL PART =	-9.068	IMAG PART =	-7.104
REAL PART =	-5.309	IMAG PART =	0.0
REAL PART =	-0.177	IMAG PART =	0.0
REAL PART =	-1.106	IMAG PART =	0.0
REAL PART =	-30.000	IMAG PART =	0.0
REAL PART =	-25.000	IMAG PART =	0.0

STATE ESTIMATION ERROR COVARIANCE MATRIX

1.648E-02	-1.358E-03	1.536E-04	9.530E-04	1.216E-08	3.107E-09	-3.113E-03
-1.358E-03	4.791E-04	-7.567E-05	7.657E-06	-5.921E-10	-5.963E-10	5.258E-04
1.536E-04	-7.567E-05	1.028E-04	3.085E-04	1.187E-10	2.077E-10	-1.225E-04
9.530E-04	7.657E-06	3.085E-04	5.785E-03	1.987E-09	1.445E-09	-3.001E-04
1.216E-08	-5.921E-10	1.187E-10	1.987E-09	1.667E-09	3.669E-15	-4.524E-10
3.107E-09	-5.963E-10	2.077E-10	1.445E-09	3.669E-15	2.000E-09	-1.617E-10
-3.113E-03	5.258E-04	-1.225E-04	-3.001E-04	-4.524E-10	-1.617E-10	1.752E-03

FLIGHT CONDITION 11 CONTINUED

DISCRETE TIME PLANT NOISE COVARIANCE MATRIX (XID) DT=.125 SEC

1.905E-02	-1.225E-03	1.993E-04	1.051E-03	8.490E-10	4.604E-10	-3.321E-03
-1.225E-03	2.481E-04	-2.563E-05	-6.052E-05	4.112E-11	-2.299E-10	4.320E-04
1.993E-04	-2.563E-05	5.153E-06	1.217E-05	7.734E-13	1.169E-11	-5.180E-05
1.051E-03	-6.052E-05	1.217E-05	8.149E-05	2.466E-11	1.423E-11	-1.411E-04
8.490E-10	4.112E-11	7.734E-13	2.466E-11	1.666E-09	0.0	0.0
4.604E-10	-2.299E-10	1.169E-11	1.423E-11	0.0	1.996E-09	0.0
-3.321E-03	4.320E-04	-5.180E-05	-1.411E-04	0.0	0.0	1.595E-03

DISCRETE TIME KF GAINS (HD) DT=.125 SEC

-1.882E-02	9.341E-01	-3.012E-01	2.324E-05	-3.862E-06
1.712E-02	-1.882E-02	7.856E-01	8.515E-06	-2.372E-05
-4.383E-02	4.458E-03	-6.928E-02	-1.094E-07	2.337E-05
-1.351E-01	5.489E-02	1.066E-01	-8.880E-06	8.346E-05
2.198E-09	5.725E-08	3.357E-07	5.552E-04	1.707E-11
8.243E-07	-9.508E-09	-9.351E-07	1.707E-11	6.662E-04
3.719E-02	-1.130E-01	8.019E-01	2.139E-05	6.156E-05

DISCRETE TIME KF CLOSED-LOOP MATRIX DT=.125 SEC

-0.3553	3.0188	-3.7826	-0.0135	0.4382	0.1629	-3.7618
0.0737	-0.1835	0.5890	0.0018	0.0227	-0.1268	0.5209
-0.0154	0.1098	0.7128	0.0062	0.0015	0.0547	-0.0804
-0.0755	0.1285	-0.8539	0.9994	0.0467	0.1380	-0.2515
-0.0000	-0.0000	0.0000	0.0000	0.0235	-0.0000	0.0000
0.0000	0.0000	0.0000	0.0000	-0.0000	0.0439	0.0
0.1064	-0.7573	0.1548	0.0000	-0.0000	-0.0308	0.9397

FLIGHT CONDITION 11 CONTINUED

DISCRETE TIME KF POLES DT=.125 SEC

REAL PART =	0.978	IMAG PART =	0.0
REAL PART =	0.821	IMAG PART =	0.0
REAL PART =	0.082	IMAG PART =	0.158
REAL PART =	0.082	IMAG PART =	-0.158
REAL PART =	0.150	IMAG PART =	0.0
REAL PART =	0.024	IMAG PART =	0.0
REAL PART =	0.044	IMAG PART =	0.0

STATE PREDICTION COVARIANCE MATRIX DT=.125 SEC

3.260E-02	-3.184E-03	4.895E-04	1.881E-03	8.619E-10	4.326E-10	-6.476E-03
-3.184E-03	5.931E-04	-7.961E-05	-1.622E-04	4.334E-11	-2.372E-10	9.127E-04
4.895E-04	-7.961E-05	3.148E-05	9.210E-05	6.423E-13	1.553E-11	-1.378E-04
1.881E-03	-1.622E-04	9.210E-05	1.682E-03	2.567E-11	2.397E-11	-3.665E-04
8.619E-10	4.334E-11	6.423E-13	2.567E-11	1.667E-09	5.291E-20	1.418E-12
4.326E-10	-2.372E-10	1.553E-11	2.397E-11	5.291E-20	2.000E-09	7.624E-12
-6.476E-03	9.127E-04	-1.378E-04	-3.665E-04	1.418E-12	7.624E-12	2.376E-03

INVERSE OF DISCRETE TIME OBSERVATION ERROR COVARIANCE MATRIX DT=.125 SEC

4.593E+02	1.545E+01	-2.250E+02	-7.325E-04	-2.748E-01
1.545E+01	5.408E+01	2.473E+02	-1.908E-02	3.169E-03
-2.250E+02	2.473E+02	2.817E+03	-1.119E-01	3.117E-01
-7.325E-04	-1.908E-02	-1.119E-01	3.331E+05	-5.690E-06
-2.748E-01	3.170E-03	3.117E-01	-5.690E-06	3.331E+05

DETERMINANT OF OBSERVATION COVARIANCE MATRIX = 0.245E-18

FLIGHT CONDITION 12 DYNAMIC PRESSURE 434 PSF MACH 0.80 ALTITUDE 20000 FT

PLANT NOISE COVARIANCE (XI)

1.100E-01	0.0	0.0	0.0	0.0	0.0	0.0
0.0	7.600E-04	0.0	0.0	0.0	0.0	0.0
0.0	0.0	1.400E-05	0.0	0.0	0.0	0.0
0.0	0.0	0.0	2.500E-05	0.0	0.0	0.0
0.0	0.0	0.0	0.0	1.000E-07	0.0	0.0
0.0	0.0	0.0	0.0	0.0	1.000E-07	0.0
0.0	0.0	0.0	0.0	0.0	0.0	1.175E-02

OBSERVATION NOISE COVARIANCE (THETA)

1.750E-03	0.0	0.0	0.0	0.0
0.0	1.218E-03	0.0	0.0	0.0
0.0	0.0	7.610E-05	0.0	0.0
0.0	0.0	0.0	3.000E-06	0.0
0.0	0.0	0.0	0.0	3.000E-06

KALMAN FILTER GAINS (H)

-7.933E-01	1.327E+01	-2.410E+01	2.741E-03	1.638E-04
4.244E-01	-1.505E+00	8.567E+00	-2.619E-04	-1.863E-04
-2.643E-01	1.052E-01	-9.857E-01	5.493E-05	3.058E-05
-8.532E-01	7.492E-01	2.191E-02	3.864E-04	1.777E-04
-9.031E-07	6.751E-06	-1.032E-05	5.556E-04	4.297E-11
1.193E-06	4.034E-07	-7.345E-06	4.297E-11	6.667E-04
3.898E-01	-2.173E+00	7.389E+00	-2.831E-05	3.047E-05

FLIGHT CONDITION 12 CONTINUED

KF CLOSED-LOOP MATRIX (ACL)

-16.9300	24.3800	-59.8100	0.0011	27.9100	12.0400	-53.3300
1.4320	-8.9840	11.7700	-0.0006	1.2640	-5.6990	8.3030
-0.0626	0.0136	-2.4750	0.0392	-0.0001	0.4107	-0.3170
0.2469	0.1004	-6.9680	0.0012	-0.0004	1.1560	0.0000
-0.0000	0.0000	-0.0000	0.0000	-30.0000	0.0000	0.0000
-0.0000	0.0000	0.0000	-0.0000	-0.0000	-25.0000	-0.0000
2.1750	-7.4250	3.1840	-0.0005	0.0000	-0.5284	-0.6636

KF POLES

REAL PART = -10.336 IMAG PART = 9.022
REAL PART = -10.336 IMAG PART = -9.022
REAL PART = -6.218 IMAG PART = 0.0
REAL PART = -0.131 IMAG PART = 0.0
REAL PART = -2.031 IMAG PART = 0.0
REAL PART = -30.000 IMAG PART = 0.0
REAL PART = -25.000 IMAG PART = 0.0

STATE ESTIMATION ERROR COVARIANCE MATRIX

1.616E-02	-1.834E-03	1.281E-04	9.126E-04	8.222E-09	4.914E-10	-2.647E-03
-1.834E-03	6.519E-04	-7.501E-05	1.667E-06	-7.857E-10	-5.590E-10	5.623E-04
1.281E-04	-7.501E-05	5.090E-05	1.681E-04	1.648E-10	9.173E-11	-6.895E-05
9.126E-04	1.667E-06	1.681E-04	7.456E-03	1.159E-09	5.330E-10	-1.760E-04
8.222E-09	-7.857E-10	1.648E-10	1.159E-09	1.667E-09	1.289E-16	-8.494E-11
4.914E-10	-5.590E-10	9.173E-11	5.330E-10	1.289E-16	2.000E-09	9.141E-11
-2.647E-03	5.623E-04	-6.895E-05	-1.760E-04	-8.494E-11	9.141E-11	1.208E-03

FLIGHT CONDITION 12 CONTINUED

DISCRETE TIME PLANT NOISE COVARIANCE MATRIX (XID) DT=.125 SEC

2.264E-02	-2.554E-03	2.653E-04	1.218E-03	1.337E-09	6.928E-10	-3.781E-03
-2.554E-03	5.555E-04	-5.032E-05	-1.279E-04	6.332E-11	-3.682E-10	6.850E-04
2.653E-04	-5.032E-05	6.736E-06	1.495E-05	-9.502E-14	1.636E-11	-6.215E-05
1.218E-03	-1.279E-04	1.495E-05	9.000E-05	3.896E-11	2.196E-11	-1.635E-04
1.337E-09	6.332E-11	-9.502E-14	3.896E-11	1.666E-09	0.0	0.0
6.928E-10	-3.682E-10	1.636E-11	2.196E-11	0.0	1.996E-09	0.0
-3.781E-03	6.850E-04	-6.215E-05	-1.635E-04	0.0	0.0	1.354E-03

DISCRETE TIME KF GAINS (HD) DT=.125 SEC

-1.462E-02	9.189E-01	-3.318E-01	4.408E-05	-1.191E-05
2.357E-02	-2.073E-02	8.309E-01	1.311E-05	-3.630E-05
-3.746E-02	1.962E-03	-5.682E-02	3.187E-07	3.075E-05
-1.273E-01	5.577E-02	1.291E-01	-1.438E-05	1.221E-04
-2.683E-09	1.086E-07	5.166E-07	5.552E-04	4.356E-11
1.112E-06	-2.934E-08	-1.431E-06	4.357E-11	6.662E-04
1.629E-02	-7.612E-02	6.194E-01	2.103E-05	8.312E-05

DISCRETE TIME KF CLOSED-LOOP MATRIX DT=.125 SEC

-0.2999	2.9700	-4.1525	-0.0137	0.6465	0.0962	-4.8436
0.0884	-0.3840	0.9851	0.0025	0.0343	-0.1812	0.9516
-0.0127	0.1051	0.5704	0.0047	-0.0002	0.0721	-0.1129
-0.0726	0.1075	-1.3321	0.9996	0.0719	0.1925	-0.3364
-0.0000	-0.0000	-0.0000	0.0000	0.0235	0.0000	0.0000
0.0000	0.0000	0.0000	-0.0000	-0.0000	0.0439	0.0000
0.0701	-0.5715	0.1224	-0.0000	-0.0000	-0.0204	0.9204

FLIGHT CONDITION 12 CONTINUED

DISCRETE TIME KF POLES DT=.125 SEC

REAL PART =	0.983	IMAG PART =	0.0
REAL PART =	0.702	IMAG PART =	0.0
REAL PART =	-0.009	IMAG PART =	0.135
REAL PART =	-0.009	IMAG PART =	-0.135
REAL PART =	0.140	IMAG PART =	0.0
REAL PART =	0.024	IMAG PART =	0.0
REAL PART =	0.044	IMAG PART =	0.0

STATE PREDICTION COVARIANCE MATRIX DT=.125 SEC

3.708E-02	-5.451E-03	5.884E-04	2.124E-03	1.357E-09	6.381E-10	-6.380E-03
-5.451E-03	1.205E-03	-1.273E-04	-2.875E-04	6.690E-11	-3.740E-10	1.227E-03
5.884E-04	-1.273E-04	2.432E-05	7.113E-05	-3.487E-13	2.110E-11	-1.300E-04
2.124E-03	-2.875E-04	7.113E-05	2.234E-03	4.059E-11	3.523E-11	-3.419E-04
1.357E-09	6.690E-11	-3.487E-13	4.059E-11	1.667E-09	1.351E-19	1.365E-12
6.381E-10	-3.740E-10	2.110E-11	3.523E-11	1.351E-19	2.000E-09	1.008E-11
-6.380E-03	1.227E-03	-1.300E-04	-3.419E-04	1.365E-12	1.008E-11	1.843E-03

INVERSE OF DISCRETE TIME OBSERVATION ERROR COVARIANCE MATRIX DT=.125 SEC

3.954E+02	1.200E+01	-3.097E+02	8.945E-04	-3.707E-01
1.200E+01	6.659E+01	2.724E+02	-3.619E-02	9.779E-03
-3.097E+02	2.724E+02	2.222E+03	-1.722E-01	4.770E-01
8.945E-04	-3.619E-02	-1.722E-01	3.331E+05	-1.452E-05
-3.707E-01	9.779E-03	4.770E-01	-1.452E-05	3.331E+05

DETERMINANT OF OBSERVATION COVARIANCE MATRIX = 0.441E-18

FLIGHT CONDITION 13 DYNAMIC PRESSURE 550 PSF MACH 0.90 ALTITUDE 20000 FT

PLANT NOISE COVARIANCE (XI)

1.100E-01	0.0	0.0	0.0	0.0	0.0	0.0
0.0	7.600E-04	0.0	0.0	0.0	0.0	0.0
0.0	0.0	1.400E-05	0.0	0.0	0.0	0.0
0.0	0.0	0.0	2.500E-05	0.0	0.0	0.0
0.0	0.0	0.0	0.0	1.000E-07	0.0	0.0
0.0	0.0	0.0	0.0	0.0	1.000E-07	0.0
0.0	0.0	0.0	0.0	0.0	0.0	1.108E-02

OBSERVATION NOISE COVARIANCE (THETA)

1.750E-03	0.0	0.0	0.0	0.0
0.0	1.218E-03	0.0	0.0	0.0
0.0	0.0	7.610E-05	0.0	0.0
0.0	0.0	0.0	3.000E-06	0.0
0.0	0.0	0.0	0.0	3.000E-06

KALMAN FILTER GAINS (H)

-1.010E+00	1.374E+01	-2.822E+01	6.005E-04	2.383E-04
5.327E-01	-1.763E+00	9.575E+00	-3.054E-05	-1.871E-04
-2.582E-01	1.040E-01	-9.584E-01	1.820E-05	3.730E-05
-8.436E-01	7.122E-01	-1.269E-01	1.760E-04	4.027E-04
-3.700E-07	1.479E-06	-1.204E-06	5.555E-04	5.068E-11
9.435E-07	5.870E-07	-7.376E-06	5.068E-11	6.667E-04
3.975E-01	-2.099E+00	7.229E+00	1.060E-04	1.571E-05

FLIGHT CONDITION 13 CONTINUED

KF CLOSED-LOOP MATRIX (ACL)

-18.3300	28.5000	-79.8900	0.0008	30.6500	12.7500	-69.2200
1.6690	-10.0700	16.8300	-0.0004	1.2880	-6.1540	11.2000
-0.0649	-0.0117	-3.0920	0.0347	-0.0000	0.4025	-0.3644
0.2840	0.2531	-8.9110	0.0006	-0.0002	1.1600	0.0000
-0.0000	0.0000	-0.0000	0.0000	-30.0000	0.0000	-0.0000
-0.0000	0.0000	0.0000	-0.0000	-0.0000	-25.0000	-0.0000
2.1010	-7.2690	4.1990	-0.0003	-0.0001	-0.5467	-0.7466

KF POLES

REAL PART = -11.519 IMAG PART = 10.453
REAL PART = -11.519 IMAG PART = -10.453
REAL PART = -0.113 IMAG PART = 0.0
REAL PART = -6.426 IMAG PART = 0.0
REAL PART = -2.661 IMAG PART = 0.0
REAL PART = -30.000 IMAG PART = 0.0
REAL PART = -25.000 IMAG PART = 0.0

STATE ESTIMATION ERROR COVARIANCE MATRIX

1.673E-02	-2.147E-03	1.267E-04	8.675E-04	1.801E-09	7.149E-10	-2.557E-03
-2.147E-03	7.287E-04	-7.293E-05	-9.660E-06	-9.161E-11	-5.613E-10	5.501E-04
1.267E-04	-7.293E-05	3.837E-05	1.280E-04	5.459E-11	1.119E-10	-5.405E-05
8.675E-04	-9.660E-06	1.280E-04	7.972E-03	5.280E-10	1.208E-09	-1.410E-04
1.801E-09	-9.161E-11	5.459E-11	5.280E-10	1.667E-09	1.520E-16	3.179E-10
7.149E-10	-5.613E-10	1.119E-10	1.208E-09	1.520E-16	2.000E-09	4.712E-11
-2.557E-03	5.501E-04	-5.405E-05	-1.410E-04	3.179E-10	4.712E-11	9.936E-04

FLIGHT CONDITION 13 CONTINUED

DISCRETE TIME PLANT NOISE COVARIANCE MATRIX (XID) DT=.125 SEC

2.774E-02	-3.951E-03	3.660E-04	1.463E-03	1.432E-09	6.929E-10	-4.390E-03
-3.951E-03	8.726E-04	-7.537E-05	-2.006E-04	6.340E-11	-3.880E-10	8.578E-04
3.660E-04	-7.537E-05	8.716E-06	2.045E-05	-1.218E-13	1.653E-11	-7.178E-05
1.463E-03	-2.006E-04	2.045E-05	1.030E-04	4.186E-11	2.212E-11	-1.921E-04
1.432E-09	6.340E-11	-1.218E-13	4.186E-11	1.666E-09	0.0	0.0
6.929E-10	-3.880E-10	1.653E-11	2.212E-11	0.0	1.996E-09	0.0
-4.390E-03	8.578E-04	-7.178E-05	-1.921E-04	0.0	0.0	1.264E-03

DISCRETE TIME KF GAINS (HD) DT=.125 SEC

-1.340E-02	9.112E-01	-3.570E-01	5.097E-05	-1.690E-05
2.643E-02	-2.231E-02	8.361E-01	1.441E-05	-3.860E-05
-3.521E-02	1.306E-03	-4.933E-02	4.091E-07	2.943E-05
-1.230E-01	5.409E-02	1.354E-01	-1.444E-05	1.197E-04
-5.217E-09	1.255E-07	5.682E-07	5.552E-04	5.224E-11
1.031E-06	-4.163E-08	-1.522E-06	5.224E-11	6.662E-04
3.154E-03	-6.775E-02	4.927E-01	2.213E-05	7.875E-05

DISCRETE TIME KF CLOSED-LOOP MATRIX DT=.125 SEC

-0.3275	2.8213	-3.9928	-0.0152	0.6524	-0.0603	-5.8373
0.1024	-0.4159	1.1119	0.0029	0.0330	-0.1618	1.2631
-0.0131	0.0971	0.4941	0.0041	-0.0003	0.0675	-0.1405
-0.0732	0.0978	-1.5892	0.9994	0.0756	0.1789	-0.4170
-0.0000	-0.0000	-0.0000	0.0000	0.0235	0.0000	-0.0000
0.0000	0.0000	0.0000	-0.0000	-0.0000	0.0439	0.0000
0.0617	-0.4491	0.0303	-0.0000	-0.0000	-0.0040	0.9109

FLIGHT CONDITION 13 CONTINUED

DISCRETE TIME KF POLES DT=.125 SEC

REAL PART =	0.985	IMAG PART =	0.0
REAL PART =	0.633	IMAG PART =	0.0
REAL PART =	-0.050	IMAG PART =	0.097
REAL PART =	-0.050	IMAG PART =	-0.097
REAL PART =	0.142	IMAG PART =	0.0
REAL PART =	0.024	IMAG PART =	0.0
REAL PART =	0.044	IMAG PART =	0.0

STATE PREDICTION COVARIANCE MATRIX DT=.125 SEC

4.484E-02	-7.705E-03	7.538E-04	2.543E-03	1.451E-09	6.241E-10	-6.945E-03
-7.705E-03	1.764E-03	-1.721E-04	-4.166E-04	6.755E-11	-3.907E-10	1.435E-03
7.538E-04	-1.721E-04	2.545E-05	7.362E-05	-4.327E-13	2.083E-11	-1.369E-04
2.543E-03	-4.166E-04	7.362E-05	2.478E-03	4.350E-11	3.402E-11	-3.664E-04
1.451E-09	6.755E-11	-4.327E-13	4.350E-11	1.667E-09	1.619E-19	1.422E-12
6.241E-10	-3.907E-10	2.083E-11	3.402E-11	1.619E-19	2.000E-09	9.455E-12
-6.945E-03	1.435E-03	-1.369E-04	-3.664E-04	1.422E-12	9.455E-12	1.658E-03

INVERSE OF DISCRETE TIME OBSERVATION ERROR COVARIANCE MATRIX DT=.125 SEC

3.574E+02	1.101E+01	-3.473E+02	1.739E-03	-3.437E-01
1.101E+01	7.288E+01	2.931E+02	-4.185E-02	1.388E-02
-3.473E+02	2.931E+02	2.153E+03	-1.894E-01	5.072E-01
1.739E-03	-4.185E-02	-1.894E-01	3.331E+05	-1.741E-05
-3.437E-01	1.388E-02	5.072E-01	-1.741E-05	3.331E+05

DETERMINANT OF OBSERVATION COVARIANCE MATRIX = 0.639E-18

FLIGHT CONDITION 14 DYNAMIC PRESSURE 978 PSF MACH 1.20 ALTITUDE 20000 FT

PLANT NOISE COVARIANCE (XI)

1.100E-01	0.0	0.0	0.0	0.0	0.0	0.0
0.0	7.600E-04	0.0	0.0	0.0	0.0	0.0
0.0	0.0	1.400E-05	0.0	0.0	0.0	0.0
0.0	0.0	0.0	2.500E-05	0.0	0.0	0.0
0.0	0.0	0.0	0.0	1.000E-07	0.0	0.0
0.0	0.0	0.0	0.0	0.0	1.000E-07	0.0
0.0	0.0	0.0	0.0	0.0	0.0	9.597E-03

OBSERVATION NOISE COVARIANCE (THETA)

1.750E-03	0.0	0.0	0.0	0.0
0.0	1.218E-03	0.0	0.0	0.0
0.0	0.0	7.610E-05	0.0	0.0
0.0	0.0	0.0	3.000E-06	0.0
0.0	0.0	0.0	0.0	3.000E-06

KALMAN FILTER GAINS (H)

-1.658E+00	1.609E+01	-3.468E+01	2.788E-04	3.367E-04
7.559E-01	-2.166E+00	1.064E+01	1.271E-04	-1.099E-04
-2.455E-01	1.066E-01	-8.338E-01	6.295E-07	2.253E-05
-8.575E-01	7.782E-01	3.053E-01	5.414E-04	3.075E-04
1.100E-08	6.868E-07	5.011E-06	5.555E-04	1.792E-10
1.248E-07	8.293E-07	-4.331E-06	1.792E-10	6.667E-04
4.171E-01	-1.948E+00	6.589E+00	1.742E-04	4.628E-05

FLIGHT CONDITION 14 CONTINUED

KF CLOSED-LOOP MATRIX (ACL)

-20.2400	35.0900	-132.1000	0.0027	18.6600	8.3560	-103.6000
2.1480	-11.4300	30.7100	-0.0012	0.6221	-3.4050	17.6900
-0.0778	-0.1303	-4.6750	0.0263	-0.0000	0.1912	-0.4458
0.2184	-0.1623	-14.7700	0.0014	-0.0005	0.6041	0.0000
-0.0000	-0.0000	0.0000	-0.0000	-30.0000	-0.0000	-0.0000
-0.0000	0.0000	0.0000	-0.0000	-0.0000	-25.0000	-0.0000
1.9490	-6.6440	7.1860	-0.0007	-0.0002	-0.2940	-0.9955

KF POLES

REAL PART = -13.443 IMAG PART = 12.921
REAL PART = -13.443 IMAG PART = -12.921
REAL PART = -0.088 IMAG PART = 0.0
REAL PART = -5.183 IMAG PART = 0.649
REAL PART = -5.183 IMAG PART = -0.649
REAL PART = -25.000 IMAG PART = 0.0
REAL PART = -30.000 IMAG PART = 0.0

STATE ESTIMATION ERROR COVARIANCE MATRIX

1.959E-02	-2.639E-03	1.298E-04	9.478E-04	8.365E-10	1.010E-09	-2.372E-03
-2.639E-03	8.099E-04	-6.345E-05	2.323E-05	3.813E-10	-3.296E-10	5.014E-04
1.298E-04	-6.345E-05	2.229E-05	8.065E-05	1.888E-12	6.759E-11	-3.442E-05
9.478E-04	2.323E-05	8.065E-05	1.083E-02	1.624E-09	9.226E-10	-9.159E-05
8.365E-10	3.813E-10	1.888E-12	1.624E-09	1.667E-09	5.377E-16	5.226E-10
1.010E-09	-3.296E-10	6.759E-11	9.226E-10	5.377E-16	2.000E-09	1.388E-10
-2.372E-03	5.014E-04	-3.442E-05	-9.159E-05	5.226E-10	1.388E-10	7.000E-04

FLIGHT CONDITION 14 CONTINUED

DISCRETE TIME PLANT NOISE COVARIANCE MATRIX (XID) DT=.125 SEC

4.600E-02	-7.527E-03	6.163E-04	2.383E-03	8.822E-10	4.413E-10	-5.543E-03
-7.527E-03	1.600E-03	-1.274E-04	-3.800E-04	3.173E-11	-2.019E-10	1.094E-03
6.163E-04	-1.274E-04	1.249E-05	3.376E-05	-1.347E-13	8.093E-12	-8.210E-05
2.383E-03	-3.800E-04	3.376E-05	1.541E-04	2.574E-11	1.422E-11	-2.431E-04
8.822E-10	3.173E-11	-1.347E-13	2.574E-11	1.666E-09	0.0	0.0
4.413E-10	-2.019E-10	8.093E-12	1.422E-11	0.0	1.996E-09	0.0
-5.543E-03	1.094E-03	-8.210E-05	-2.431E-04	0.0	0.0	1.062E-03

DISCRETE TIME KF GAINS (HD) DT=.125 SEC

-1.160E-02	9.171E-01	-3.501E-01	2.870E-05	-7.784E-06
3.002E-02	-2.187E-02	8.284E-01	8.398E-06	-2.070E-05
-3.062E-02	6.190E-04	-3.363E-02	1.609E-07	1.331E-05
-1.142E-01	5.525E-02	1.897E-01	-9.451E-06	5.790E-05
-3.049E-09	7.069E-08	3.311E-07	5.552E-04	1.404E-11
4.073E-07	-1.916E-08	-8.159E-07	1.404E-11	6.662E-04
-2.056E-02	-4.940E-02	3.747E-01	1.069E-05	4.113E-05

DISCRETE TIME KF CLOSED-LOOP MATRIX DT=.125 SEC

-0.3539	3.1633	-1.0567	-0.0177	0.4143	-0.1948	-8.5905
0.1068	-0.4782	0.6792	0.0035	0.0177	-0.0413	1.8419
-0.0123	0.0832	0.3822	0.0030	-0.0003	0.0274	-0.1907
-0.0771	0.0718	-2.0553	0.9994	0.0470	0.0756	-0.6215
-0.0000	-0.0000	-0.0000	0.0000	0.0235	0.0000	0.0000
0.0000	0.0000	0.0000	-0.0000	-0.0000	0.0439	0.0000
0.0436	-0.3284	-0.3127	0.0000	-0.0000	0.0128	0.8830

FLIGHT CONDITION 14 CONTINUED

DISCRETE TIME KF POLES DT=.125 SEC

REAL PART =	0.989	IMAG PART =	0.0
REAL PART =	0.475	IMAG PART =	0.0
REAL PART =	-0.131	IMAG PART =	0.0
REAL PART =	0.148	IMAG PART =	0.0
REAL PART =	-0.049	IMAG PART =	0.0
REAL PART =	0.024	IMAG PART =	0.0
REAL PART =	0.044	IMAG PART =	0.0

STATE PREDICTION COVARIANCE MATRIX DT=.125 SEC

7.324E-02	-1.341E-02	1.183E-03	4.129E-03	8.934E-10	3.882E-10	-8.241E-03
-1.341E-02	2.935E-03	-2.601E-04	-7.308E-04	3.431E-11	-1.989E-10	1.690E-03
1.183E-03	-2.601E-04	2.910E-05	8.967E-05	-3.433E-13	9.684E-12	-1.425E-04
4.129E-03	-7.308E-04	8.967E-05	3.384E-03	2.666E-11	1.874E-11	-4.236E-04
8.934E-10	3.431E-11	-3.433E-13	2.666E-11	1.667E-09	4.353E-20	6.664E-13
3.882E-10	-1.989E-10	9.684E-12	1.874E-11	4.353E-20	2.000E-09	4.788E-12
-8.241E-03	1.690E-03	-1.425E-04	-4.236E-04	6.664E-13	4.788E-12	1.336E-03

INVERSE OF DISCRETE TIME OBSERVATION ERROR COVARIANCE MATRIX DT=.125 SEC

2.678E+02	9.527E+00	-3.945E+02	1.016E-03	-1.358E-01
9.527E+00	6.805E+01	2.874E+02	-2.356E-02	6.385E-03
-3.945E+02	2.874E+02	2.255E+03	-1.104E-01	2.720E-01
1.016E-03	-2.356E-02	-1.104E-01	3.331E+05	-4.681E-06
-1.358E-01	6.385E-03	2.720E-01	-4.681E-06	3.331E+05

DETERMINANT OF OBSERVATION COVARIANCE MATRIX = 0.150E-17

FLIGHT CONDITION 15 DYNAMIC PRESSURE 135 PSF MACH 0.70 ALTITUDE 40000 FT

PLANT NOISE COVARIANCE (XI)

1.100E-01	0.0	0.0	0.0	0.0	0.0	0.0
0.0	7.600E-04	0.0	0.0	0.0	0.0	0.0
0.0	0.0	1.400E-05	0.0	0.0	0.0	0.0
0.0	0.0	0.0	2.500E-05	0.0	0.0	0.0
0.0	0.0	0.0	0.0	1.000E-07	0.0	0.0
0.0	0.0	0.0	0.0	0.0	1.000E-07	0.0
0.0	0.0	0.0	0.0	0.0	0.0	1.300E-02

OBSERVATION NOISE COVARIANCE (THETA)

1.750E-03	0.0	0.0	0.0	0.0
0.0	1.218E-03	0.0	0.0	0.0
0.0	0.0	7.610E-05	0.0	0.0
0.0	0.0	0.0	3.000E-06	0.0
0.0	0.0	0.0	0.0	3.000E-06

KALMAN FILTER GAINS (H)

-4.644E-01	1.284E+01	-1.147E+01	1.857E-03	2.286E-04
1.597E-01	-7.169E-01	4.946E+00	-4.273E-05	-1.047E-04
-3.154E-01	1.310E-01	-8.914E-01	1.276E-05	2.888E-06
-8.531E-01	7.898E-01	4.960E-01	2.191E-04	-8.225E-05
-1.134E-07	4.573E-06	-1.685E-06	5.556E-04	7.379E-11
6.215E-07	5.631E-07	-4.127E-06	7.379E-11	6.667E-04
3.853E-01	-2.503E+00	5.981E+00	-1.062E-04	3.714E-07

FLIGHT CONDITION 15 CONTINUED

KF CLOSED-LOOP MATRIX (ACL)

-14.1900	11.7700	-26.0500	0.0003	9.8330	4.6370	-24.8700
0.6747	-5.1180	2.7260	-0.0001	0.5462	-2.0290	2.3210
-0.0075	-0.0373	-0.9212	0.0478	-0.0000	0.1970	-0.1206
0.1929	-0.2015	-2.1650	0.0006	-0.0002	0.4631	0.0000
-0.0000	0.0000	-0.0000	0.0000	-30.0000	0.0000	0.0000
-0.0000	0.0000	0.0000	-0.0000	-0.0000	-25.0000	-0.0000
2.5070	-6.0570	0.9780	-0.0003	0.0001	-0.2091	-0.5421

KF POLES

REAL PART =	-7.536	IMAG PART =	4.818
REAL PART =	-7.536	IMAG PART =	-4.818
REAL PART =	-4.889	IMAG PART =	0.0
REAL PART =	-0.161	IMAG PART =	0.0
REAL PART =	-0.648	IMAG PART =	0.0
REAL PART =	-30.000	IMAG PART =	0.0
REAL PART =	-25.000	IMAG PART =	0.0

STATE ESTIMATION ERROR COVARIANCE MATRIX

1.564E-02	-8.732E-04	1.596E-04	9.620E-04	5.570E-09	6.858E-10	-3.049E-03
-8.732E-04	3.764E-04	-6.784E-05	3.775E-05	-1.282E-10	-3.141E-10	4.552E-04
1.596E-04	-6.784E-05	1.931E-04	5.384E-04	3.829E-11	8.664E-12	-1.950E-04
9.620E-04	3.775E-05	5.384E-04	6.228E-03	6.573E-10	-2.467E-10	-4.759E-04
5.570E-09	-1.282E-10	3.829E-11	6.573E-10	1.667E-09	2.214E-16	-3.185E-10
6.858E-10	-3.141E-10	8.664E-12	-2.467E-10	2.214E-16	2.000E-09	1.114E-12
-3.049E-03	4.552E-04	-1.950E-04	-4.759E-04	-3.185E-10	1.114E-12	2.226E-03

FLIGHT CONDITION 15 CONTINUED

DISCRETE TIME PLANT NOISE COVARIANCE MATRIX (XID) DT=.125 SEC

1.575E-02	-4.459E-04	1.579E-04	9.100E-04	5.009E-10	3.014E-10	-2.206E-03
-4.459E-04	1.357E-04	-1.256E-05	-2.121E-05	2.824E-11	-1.413E-10	2.206E-04
1.579E-04	-1.256E-05	4.335E-06	1.128E-05	1.045E-12	7.534E-12	-3.244E-05
9.100E-04	-2.121E-05	1.128E-05	7.483E-05	1.447E-11	9.000E-12	-9.165E-05
5.009E-10	2.824E-11	1.045E-12	1.447E-11	1.666E-09	0.0	0.0
3.014E-10	-1.413E-10	7.534E-12	9.000E-12	0.0	1.996E-09	0.0
-2.206E-03	2.206E-04	-3.244E-05	-9.165E-05	0.0	0.0	1.520E-03

DISCRETE TIME KF GAINS (HD) DT=.125 SEC

-2.142E-02	9.413E-01	-2.244E-01	1.216E-05	2.000E-06
1.381E-02	-1.402E-02	7.455E-01	4.894E-06	-1.587E-05
-4.936E-02	7.089E-03	-6.646E-02	-2.477E-07	1.639E-05
-1.391E-01	5.497E-02	1.063E-01	-5.449E-06	5.268E-05
2.495E-09	2.995E-08	1.929E-07	5.552E-04	5.726E-12
5.433E-07	4.927E-09	-6.256E-07	5.725E-12	6.662E-04
5.007E-02	-1.408E-01	9.383E-01	1.505E-05	4.444E-05

DISCRETE TIME KF CLOSED-LOOP MATRIX DT=.125 SEC

-0.3085	2.5843	-2.8213	-0.0086	0.2795	0.1410	-2.6977
0.0508	-0.0009	0.3222	0.0009	0.0165	-0.0798	0.2797
-0.0161	0.0965	0.8116	0.0059	0.0020	0.0376	-0.0547
-0.0727	0.1042	-0.5356	0.9997	0.0282	0.0892	-0.1736
-0.0000	-0.0000	0.0000	-0.0000	0.0235	-0.0000	0.0000
0.0000	0.0000	0.0000	-0.0000	-0.0000	0.0439	0.0000
0.1321	-0.8860	0.1188	-0.0000	-0.0000	-0.0254	0.9345

FLIGHT CONDITION 15 CONTINUED

DISCRETE TIME KF POLES DT=.125 SEC

REAL PART =	0.981	IMAG PART =	0.0
REAL PART =	0.890	IMAG PART =	0.0
REAL PART =	0.230	IMAG PART =	0.166
REAL PART =	0.230	IMAG PART =	-0.166
REAL PART =	0.105	IMAG PART =	0.0
REAL PART =	0.024	IMAG PART =	0.0
REAL PART =	0.044	IMAG PART =	0.0

STATE PREDICTION COVARIANCE MATRIX DT=.125 SEC

2.619E-02	-1.593E-03	3.766E-04	1.552E-03	5.098E-10	2.912E-10	-5.431E-03
-1.593E-03	3.215E-04	-4.765E-05	-7.327E-05	2.951E-11	-1.475E-10	6.075E-04
3.766E-04	-4.765E-05	4.588E-05	1.303E-04	1.019E-12	1.037E-11	-1.325E-04
1.552E-03	-7.327E-05	1.303E-04	1.711E-03	1.511E-11	1.564E-11	-3.486E-04
5.098E-10	2.951E-11	1.019E-12	1.511E-11	1.667E-09	1.775E-20	9.923E-13
2.912E-10	-1.475E-10	1.037E-11	1.564E-11	1.775E-20	2.000E-09	5.474E-12
-5.431E-03	6.075E-04	-1.325E-04	-3.486E-04	9.923E-13	5.474E-12	2.622E-03

INVERSE OF DISCRETE TIME OBSERVATION ERROR COVARIANCE MATRIX DT=.125 SEC

4.982E+02	1.759E+01	-1.814E+02	-8.318E-04	-1.811E-01
1.759E+01	4.819E+01	1.842E+02	-9.983E-03	-1.642E-03
-1.814E+02	1.842E+02	3.345E+03	-6.431E-02	2.085E-01
-8.318E-04	-9.983E-03	-6.431E-02	3.331E+05	-1.909E-06
-1.811E-01	-1.642E-03	2.085E-01	-1.909E-06	3.331E+05

DETERMINANT OF OBSERVATION COVARIANCE MATRIX = 0.151E-18

FLIGHT CONDITION 16 DYNAMIC PRESSURE 176 PSF MACH 0.80 ALTITUDE 40000 FT

PLANT NOISE COVARIANCE (XI)

1.100E-01	0.0	0.0	0.0	0.0	0.0	0.0
0.0	7.600E-04	0.0	0.0	0.0	0.0	0.0
0.0	0.0	1.400E-05	0.0	0.0	0.0	0.0
0.0	0.0	0.0	2.500E-05	0.0	0.0	0.0
0.0	0.0	0.0	0.0	1.000E-07	0.0	0.0
0.0	0.0	0.0	0.0	0.0	1.000E-07	0.0
0.0	0.0	0.0	0.0	0.0	0.0	1.216E-02

OBSERVATION NOISE COVARIANCE (THETA)

1.750E-03	0.0	0.0	0.0	0.0
0.0	1.218E-03	0.0	0.0	0.0
0.0	0.0	7.610E-05	0.0	0.0
0.0	0.0	0.0	3.000E-06	0.0
0.0	0.0	0.0	0.0	3.000E-06

KALMAN FILTER GAINS (H)

-4.499E-01	1.304E+01	-1.524E+01	1.327E-03	5.087E-04
1.969E-01	-9.519E-01	6.090E+00	-3.567E-05	-1.289E-04
-2.887E-01	1.082E-01	-9.252E-01	1.275E-05	1.375E-06
-8.587E-01	7.997E-01	3.839E-01	2.448E-04	-3.345E-04
-1.089E-07	3.268E-06	-1.406E-06	5.556E-04	1.390E-10
8.089E-07	1.253E-06	-5.082E-06	1.390E-10	6.667E-04
3.472E-01	-2.300E+00	6.630E+00	7.451E-05	-3.469E-06

FLIGHT CONDITION 16 CONTINUED

KF CLOSED-LOOP MATRIX (ACL)

-14.6700	15.4600	-32.8500	-0.0008	12.9200	5.8610	-31.2900
0.8972	-6.2840	4.4300	0.0004	0.6202	-2.6430	3.7470
-0.0161	-0.0295	-1.1450	0.0410	-0.0000	0.2261	-0.1442
0.1903	-0.1721	-2.9770	-0.0016	-0.0002	0.5883	0.0000
-0.0000	0.0000	-0.0000	-0.0000	-30.0000	0.0000	-0.0000
-0.0000	0.0000	0.0000	0.0000	-0.0000	-25.0000	0.0000
2.3030	-6.6770	1.2040	0.0006	-0.0001	-0.2377	-0.6196

KF POLES

REAL PART =	-8.133	IMAG PART =	6.022
REAL PART =	-8.133	IMAG PART =	-6.022
REAL PART =	-5.443	IMAG PART =	0.0
REAL PART =	-0.144	IMAG PART =	0.0
REAL PART =	-0.866	IMAG PART =	0.0
REAL PART =	-30.000	IMAG PART =	0.0
REAL PART =	-25.000	IMAG PART =	0.0

STATE ESTIMATION ERROR COVARIANCE MATRIX

1.589E-02	-1.159E-03	1.318E-04	9.741E-04	3.981E-09	1.526E-09	-2.802E-03
-1.159E-03	4.635E-04	-7.041E-05	2.922E-05	-1.070E-10	-3.867E-10	5.045E-04
1.318E-04	-7.041E-05	1.300E-04	3.918E-04	3.825E-11	4.124E-12	-1.349E-04
9.741E-04	2.922E-05	3.918E-04	7.076E-03	7.343E-10	-1.004E-09	-3.517E-04
3.981E-09	-1.070E-10	3.825E-11	7.343E-10	1.667E-09	4.170E-16	2.235E-10
1.526E-09	-3.867E-10	4.124E-12	-1.004E-09	4.170E-16	2.000E-09	-1.041E-11
-2.802E-03	5.045E-04	-1.349E-04	-3.517E-04	2.235E-10	-1.041E-11	1.760E-03

FLIGHT CONDITION 16 CONTINUED

DISCRETE TIME PLANT NOISE COVARIANCE MATRIX (XID) DT=.125 SEC

1.721E-02	-8.157E-04	1.586E-04	9.781E-04	6.533E-10	3.777E-10	-2.536E-03
-8.157E-04	1.955E-04	-1.797E-05	-3.950E-05	3.173E-11	-1.822E-10	3.287E-04
1.586E-04	-1.797E-05	4.259E-06	1.050E-05	8.823E-13	8.941E-12	-3.643E-05
9.781E-04	-3.950E-05	1.050E-05	7.841E-05	1.891E-11	1.151E-11	-1.062E-04
6.533E-10	3.173E-11	8.823E-13	1.891E-11	1.666E-09	0.0	0.0
3.777E-10	-1.822E-10	8.941E-12	1.151E-11	0.0	1.996E-09	0.0
-2.536E-03	3.287E-04	-3.643E-05	-1.062E-04	0.0	0.0	1.409E-03

DISCRETE TIME KF GAINS (HD) DT=.125 SEC

-1.750E-02	9.367E-01	-2.621E-01	1.690E-05	-1.291E-06
1.452E-02	-1.637E-02	7.867E-01	6.007E-06	-1.770E-05
-4.478E-02	4.836E-03	-6.477E-02	-1.147E-07	1.877E-05
-1.380E-01	5.643E-02	1.062E-01	-7.219E-06	6.614E-05
1.930E-09	4.164E-08	2.368E-07	5.552E-04	9.040E-12
6.661E-07	-3.177E-09	-6.980E-07	9.040E-12	6.662E-04
3.739E-02	-1.084E-01	8.760E-01	1.466E-05	5.392E-05

DISCRETE TIME KF CLOSED-LOOP MATRIX DT=.125 SEC

-0.2867	2.9295	-3.3658	-0.0093	0.3585	0.1497	-3.3039
0.0615	-0.1606	0.4973	0.0012	0.0182	-0.0997	0.4464
-0.0135	0.1016	0.7695	0.0050	0.0017	0.0432	-0.0662
-0.0722	0.1213	-0.6990	0.9994	0.0366	0.1104	-0.2157
-0.0000	-0.0000	0.0000	0.0000	0.0235	-0.0000	0.0000
0.0000	0.0000	0.0000	0.0000	-0.0000	0.0439	0.0
0.1006	-0.8155	0.1200	0.0001	-0.0000	-0.0237	0.9255

FLIGHT CONDITION 16 CONTINUED

DISCRETE TIME KF POLES DT=.125 SEC

REAL PART =	0.983	IMAG PART =	0.0
REAL PART =	0.857	IMAG PART =	0.0
REAL PART =	0.144	IMAG PART =	0.176
REAL PART =	0.144	IMAG PART =	-0.176
REAL PART =	0.119	IMAG PART =	0.0
REAL PART =	0.024	IMAG PART =	0.0
REAL PART =	0.044	IMAG PART =	0.0

STATE PREDICTION COVARIANCE MATRIX DT=.125 SEC

2.853E-02	-2.408E-03	3.823E-04	1.677E-03	6.650E-10	3.593E-10	-5.404E-03
-2.408E-03	4.855E-04	-6.120E-05	-1.169E-04	3.329E-11	-1.883E-10	7.641E-04
3.823E-04	-6.120E-05	3.393E-05	1.017E-04	8.336E-13	1.208E-11	-1.159E-04
1.677E-03	-1.169E-04	1.017E-04	1.969E-03	1.976E-11	1.950E-11	-3.229E-04
6.650E-10	3.329E-11	8.336E-13	1.976E-11	1.667E-09	2.802E-20	9.572E-13
3.593E-10	-1.883E-10	1.208E-11	1.950E-11	2.802E-20	2.000E-09	6.578E-12
-5.404E-03	7.641E-04	-1.159E-04	-3.229E-04	9.572E-13	6.578E-12	2.203E-03

INVERSE OF DISCRETE TIME OBSERVATION ERROR COVARIANCE MATRIX DT=.125 SEC

4.814E+02	1.437E+01	-1.908E+02	-6.434E-04	-2.220E-01
1.437E+01	5.193E+01	2.152E+02	-1.388E-02	1.059E-03
-1.908E+02	2.152E+02	2.803E+03	-7.893E-02	2.327E-01
-6.434E-04	-1.388E-02	-7.893E-02	3.331E+05	-3.013E-06
-2.220E-01	1.059E-03	2.327E-01	-3.013E-06	3.331E+05

DETERMINANT OF OBSERVATION COVARIANCE MATRIX = 0.204E-18

FLIGHT CONDITION 17 DYNAMIC PRESSURE 223 PSF MACH 0.90 ALTITUDE 40000 FT

PLANT NOISE COVARIANCE (XI)

1.100E-01	0.0	0.0	0.0	0.0	0.0	0.0
0.0	7.600E-04	0.0	0.0	0.0	0.0	0.0
0.0	0.0	1.400E-05	0.0	0.0	0.0	0.0
0.0	0.0	0.0	2.500E-05	0.0	0.0	0.0
0.0	0.0	0.0	0.0	1.000E-07	0.0	0.0
0.0	0.0	0.0	0.0	0.0	1.000E-07	0.0
0.0	0.0	0.0	0.0	0.0	0.0	1.147E-02

OBSERVATION NOISE COVARIANCE (THETA)

1.750E-03	0.0	0.0	0.0	0.0
0.0	1.218E-03	0.0	0.0	0.0
0.0	0.0	7.610E-05	0.0	0.0
0.0	0.0	0.0	3.000E-06	0.0
0.0	0.0	0.0	0.0	3.000E-06

KALMAN FILTER GAINS (H)

-4.647E-01	1.301E+01	-1.854E+01	2.215E-03	9.167E-04
2.450E-01	-1.159E+00	7.302E+00	-4.941E-05	-1.534E-04
-2.735E-01	9.371E-02	-9.382E-01	-3.378E-06	9.332E-06
-8.597E-01	7.939E-01	2.967E-01	1.152E-04	-3.182E-04
4.584E-10	5.455E-06	-1.948E-06	5.556E-04	4.265E-10
8.288E-07	2.258E-06	-6.048E-06	4.265E-10	6.667E-04
3.297E-01	-2.128E+00	7.033E+00	-3.020E-05	-1.892E-05

FLIGHT CONDITION 17 CONTINUED

KF CLOSED-LOOP MATRIX (ACL)

-15.0800	18.7300	-40.1600	0.0000	16.4500	6.8060	-38.0400
1.1050	-7.5240	6.6050	-0.0000	0.6475	-3.1120	5.4890
-0.0218	-0.0281	-1.4150	0.0370	0.0000	0.2352	-0.1685
0.1997	-0.1302	-3.9190	0.0001	-0.0001	0.6519	0.0000
-0.0000	0.0000	0.0000	-0.0000	-30.0000	-0.0000	0.0000
-0.0000	0.0000	0.0000	-0.0000	-0.0000	-25.0000	0.0000
2.1300	-7.0690	1.5030	-0.0000	0.0000	-0.2499	-0.6970

KF POLES

REAL PART =	-8.766	IMAG PART =	7.117
REAL PART =	-8.766	IMAG PART =	-7.117
REAL PART =	-5.931	IMAG PART =	0.0
REAL PART =	-0.129	IMAG PART =	0.0
REAL PART =	-1.124	IMAG PART =	0.0
REAL PART =	-30.000	IMAG PART =	0.0
REAL PART =	-25.000	IMAG PART =	0.0

STATE ESTIMATION ERROR COVARIANCE MATRIX

1.585E-02	-1.411E-03	1.141E-04	9.669E-04	6.644E-09	2.750E-09	-2.592E-03
-1.411E-03	5.557E-04	-7.140E-05	2.258E-05	-1.482E-10	-4.602E-10	5.352E-04
1.141E-04	-7.140E-05	9.418E-05	3.015E-04	-1.013E-11	2.800E-11	-1.005E-04
9.669E-04	2.258E-05	3.015E-04	7.922E-03	3.456E-10	-9.547E-10	-2.775E-04
6.644E-09	-1.482E-10	-1.013E-11	3.456E-10	1.667E-09	1.280E-15	-9.060E-11
2.750E-09	-4.602E-10	2.800E-11	-9.547E-10	1.280E-15	2.000E-09	-5.677E-11
-2.592E-03	5.352E-04	-1.005E-04	-2.775E-04	-9.060E-11	-5.677E-11	1.444E-03

FLIGHT CONDITION 17 CONTINUED

DISCRETE TIME PLANT NOISE COVARIANCE MATRIX (XID) DT=.125 SEC

1.862E-02	-1.299E-03	1.735E-04	1.040E-03	8.220E-10	4.321E-10	-2.820E-03
-1.299E-03	2.957E-04	-2.574E-05	-6.317E-05	3.292E-11	-2.119E-10	4.461E-04
1.735E-04	-2.574E-05	4.585E-06	1.075E-05	8.135E-13	9.729E-12	-4.116E-05
1.040E-03	-6.317E-05	1.075E-05	8.141E-05	2.383E-11	1.337E-11	-1.190E-04
8.220E-10	3.292E-11	8.135E-13	2.383E-11	1.666E-09	0.0	0.0
4.321E-10	-2.119E-10	9.729E-12	1.337E-11	0.0	1.996E-09	0.0
-2.820E-03	4.461E-04	-4.116E-05	-1.190E-04	0.0	0.0	1.316E-03

DISCRETE TIME KF GAINS (HD) DT=.125 SEC

-1.494E-02	9.308E-01	-2.832E-01	2.255E-05	-3.960E-06
1.598E-02	-1.770E-02	8.200E-01	7.035E-06	-1.823E-05
-4.185E-02	3.385E-03	-6.081E-02	-3.840E-08	1.939E-05
-1.361E-01	5.734E-02	1.085E-01	-9.095E-06	7.222E-05
1.436E-09	5.555E-08	2.773E-07	5.552E-04	1.184E-11
7.107E-07	-9.751E-09	-7.187E-07	1.184E-11	6.662E-04
2.784E-02	-8.623E-02	7.819E-01	1.532E-05	5.725E-05

DISCRETE TIME KF CLOSED-LOOP MATRIX DT=.125 SEC

-0.2618	3.0359	-3.7913	-0.0099	0.4385	0.1378	-3.8666
0.0694	-0.2948	0.6917	0.0016	0.0186	-0.1107	0.6423
-0.0120	0.1035	0.7202	0.0045	0.0016	0.0451	-0.0800
-0.0712	0.1252	-0.8722	0.9996	0.0456	0.1195	-0.2565
-0.0000	-0.0000	0.0000	-0.0000	0.0235	-0.0000	-0.0000
0.0000	0.0000	0.0000	-0.0000	-0.0000	0.0439	0.0000
0.0792	-0.7194	0.1163	-0.0000	-0.0000	-0.0194	0.9166

FLIGHT CONDITION 17 CONTINUED

DISCRETE TIME KF POLES DT=.125 SEC

REAL PART =	0.984	IMAG PART =	0.0
REAL PART =	0.820	IMAG PART =	0.0
REAL PART =	0.075	IMAG PART =	0.173
REAL PART =	-0.075	IMAG PART =	-0.173
REAL PART =	0.126	IMAG PART =	0.0
REAL PART =	0.024	IMAG PART =	0.0
REAL PART =	0.044	IMAG PART =	0.0

STATE PREDICTION COVARIANCE MATRIX DT=.125 SEC

3.050E-02	-3.328E-03	4.084E-04	1.779E-03	8.363E-10	4.073E-10	-5.403E-03
-3.328E-03	7.136E-04	-7.802E-05	-1.660E-04	3.480E-11	-2.170E-10	9.169E-04
4.084E-04	-7.802E-05	2.782E-05	8.600E-05	7.372E-13	1.288E-11	-1.092E-04
1.779E-03	-1.660E-04	8.600E-05	2.228E-03	2.488E-11	2.179E-11	-3.092E-04
8.363E-10	3.480E-11	7.372E-13	2.488E-11	1.667E-09	3.669E-20	9.906E-13
4.073E-10	-2.170E-10	1.288E-11	2.179E-11	3.669E-20	2.000E-09	6.916E-12
-5.403E-03	9.169E-04	-1.092E-04	-3.092E-04	9.906E-13	6.916E-12	1.922E-03

INVERSE OF DISCRETE TIME OBSERVATION ERROR COVARIANCE MATRIX DT=.125 SEC

4.614E+02	1.226E+01	-2.099E+02	-4.788E-04	-2.369E-01
1.226E+01	5.683E+01	2.325E+02	-1.852E-02	3.251E-03
-2.099E+02	2.325E+02	2.365E+03	-9.244E-02	2.396E-01
-4.788E-04	-1.852E-02	-9.244E-02	3.331E+05	-3.946E-06
-2.369E-01	3.251E-03	2.396E-01	-3.946E-06	3.331E+05

DETERMINANT OF OBSERVATION COVARIANCE MATRIX = 0.273E-18

FLIGHT CONDITION 18 DYNAMIC PRESSURE 397 PSF MACH 1.20 ALTITUDE 40000 FT

PLANT NOISE COVARIANCE (XI)

1.100E-01	0.0	0.0	0.0	0.0	0.0	0.0
0.0	7.600E-04	0.0	0.0	0.0	0.0	0.0
0.0	0.0	1.400E-05	0.0	0.0	0.0	0.0
0.0	0.0	0.0	2.500E-05	0.0	0.0	0.0
0.0	0.0	0.0	0.0	1.000E-07	0.0	0.0
0.0	0.0	0.0	0.0	0.0	1.000E-07	0.0
0.0	0.0	0.0	0.0	0.0	0.0	9.932E-03

OBSERVATION NOISE COVARIANCE (THETA)

1.750E-03	0.0	0.0	0.0	0.0
0.0	1.218E-03	0.0	0.0	0.0
0.0	0.0	7.610E-05	0.0	0.0
0.0	0.0	0.0	3.000E-06	0.0
0.0	0.0	0.0	0.0	3.000E-06

KALMAN FILTER GAINS (H)

-6.721E-01	1.407E+01	-2.354E+01	1.087E-03	4.657E-04
3.719E-01	-1.471E+00	8.756E+00	-2.592E-05	-8.200E-05
-2.544E-01	8.652E-02	-8.843E-01	1.016E-05	3.725E-05
-8.633E-01	8.315E-01	4.702E-01	2.459E-04	7.788E-04
-1.602E-07	2.678E-06	-1.022E-06	5.556E-04	2.207E-10
1.312E-07	1.147E-06	-3.233E-06	2.207E-10	6.667E-04
3.224E-01	-1.908E+00	6.759E+00	6.079E-05	6.165E-05

FLIGHT CONDITION 18 CONTINUED

KF CLOSED-LOOP MATRIX (ACL)

-16.2000	23.7900	-60.9000	-0.0012	12.1900	5.8790	-55.7600
1.4580	-9.1200	12.1400	0.0006	0.3276	-2.3240	9.2950
-0.0336	-0.0846	-2.1570	0.0272	-0.0000	0.1553	-0.2119
0.1634	-0.3211	-6.5990	-0.0015	-0.0002	0.4745	0.0000
-0.0000	0.0000	-0.0000	-0.0000	-30.0000	0.0000	-0.0000
-0.0000	0.0000	0.0000	0.0000	-0.0000	-25.0000	-0.0000
1.9100	-6.7940	2.4640	0.0006	-0.0001	-0.1775	-0.9294

KF POLES

REAL PART = -10.142 IMAG PART = 9.087
REAL PART = -10.142 IMAG PART = -9.087
REAL PART = -6.140 IMAG PART = 0.0
REAL PART = -0.098 IMAG PART = 0.0
REAL PART = -1.887 IMAG PART = 0.0
REAL PART = -25.000 IMAG PART = 0.0
REAL PART = -30.000 IMAG PART = 0.0

STATE ESTIMATION ERROR COVARIANCE MATRIX

1.713E-02	-1.791E-03	1.054E-04	1.013E-03	3.262E-09	1.397E-09	-2.324E-03
-1.791E-03	6.663E-04	-6.730E-05	3.578E-05	-7.776E-11	-2.460E-10	5.143E-04
1.054E-04	-6.730E-05	5.220E-05	1.783E-04	3.048E-11	1.117E-10	-5.878E-05
1.013E-03	3.578E-05	1.783E-04	1.044E-02	7.378E-10	2.336E-09	-1.688E-04
3.262E-09	-7.776E-11	3.048E-11	7.378E-10	1.667E-09	6.622E-16	1.824E-10
1.397E-09	-2.460E-10	1.117E-10	2.336E-09	6.622E-16	2.000E-09	1.850E-10
-2.324E-03	5.143E-04	-5.878E-05	-1.688E-04	1.824E-10	1.850E-10	9.975E-04

FLIGHT CONDITION 18 CONTINUED

DISCRETE TIME PLANT NOISE COVARIANCE MATRIX (XID) DT=.125 SEC

2.476E-02	-2.579E-03	2.500E-04	1.339E-03	6.079E-10	3.668E-10	-3.444E-03
-2.579E-03	5.601E-04	-4.482E-05	-1.248E-04	1.706E-11	-1.519E-10	6.209E-04
2.500E-04	-4.482E-05	5.823E-06	1.425E-05	4.711E-13	6.537E-12	-4.848E-05
1.339E-03	-1.248E-04	1.425E-05	9.731E-05	1.762E-11	1.153E-11	-1.463E-04
6.079E-10	1.706E-11	4.711E-13	1.762E-11	1.666E-09	0.0	0.0
3.668E-10	-1.519E-10	6.537E-12	1.153E-11	0.0	1.996E-09	0.0
-3.444E-03	6.209E-04	-4.848E-05	-1.463E-04	0.0	0.0	1.108E-03

DISCRETE TIME KF GAINS (HD) DT=.125 SEC

-1.483E-02	9.300E-01	-2.923E-01	1.619E-05	-1.882E-06
2.065E-02	-1.826E-02	8.450E-01	4.737E-06	-1.283E-05
-3.733E-02	2.006E-03	-4.983E-02	-1.924E-08	1.270E-05
-1.304E-01	5.812E-02	1.356E-01	-6.840E-06	5.018E-05
1.051E-09	3.987E-08	1.867E-07	5.552E-04	4.617E-12
4.598E-07	-4.634E-09	-5.058E-07	4.617E-12	6.662E-04
1.107E-02	-5.991E-02	5.876E-01	8.932E-06	3.449E-05

DISCRETE TIME KF CLOSED-LOOP MATRIX DT=.125 SEC

-0.2556	3.1930	-4.6369	-0.0105	0.3226	0.0640	-5.4773
0.0758	-0.4115	1.0074	0.0019	0.0103	-0.0685	1.0310
-0.0105	0.0970	0.5994	0.0032	0.0009	0.0289	-0.1118
-0.0719	0.1114	-1.3106	0.9993	0.0337	0.0825	-0.3697
-0.0000	-0.0000	0.0000	0.0000	0.0235	-0.0000	-0.0000
0.0000	0.0000	0.0000	0.0000	-0.0000	0.0439	0.0000
0.0534	-0.5242	0.0753	0.0000	-0.0000	-0.0055	0.8903

FLIGHT CONDITION 18 CONTINUED

DISCRETE TIME KF POLES DT=.125 SEC

REAL PART =	0.988	IMAG PART =	0.0
REAL PART =	0.719	IMAG PART =	0.0
REAL PART =	-0.011	IMAG PART =	0.139
REAL PART =	-0.011	IMAG PART =	-0.139
REAL PART =	0.136	IMAG PART =	0.0
REAL PART =	0.044	IMAG PART =	0.0
REAL PART =	0.024	IMAG PART =	0.0

STATE PREDICTION COVARIANCE MATRIX DT=.125 SEC

4.055E-02	-5.583E-03	5.476E-04	2.319E-03	6.181E-10	3.443E-10	-5.838E-03
-5.583E-03	1.209E-03	-1.134E-04	-2.837E-04	1.842E-11	-1.534E-10	1.101E-03
5.476E-04	-1.134E-04	2.209E-05	6.972E-05	4.001E-13	8.469E-12	-1.034E-04
2.319E-03	-2.837E-04	6.972E-05	2.970E-03	1.836E-11	1.714E-11	-3.097E-04
6.181E-10	1.842E-11	4.001E-13	1.836E-11	1.667E-09	1.431E-20	5.612E-13
3.443E-10	-1.534E-10	8.469E-12	1.714E-11	1.431E-20	2.000E-09	4.048E-12
-5.838E-03	1.101E-03	-1.034E-04	-3.097E-04	5.612E-13	4.048E-12	1.493E-03

INVERSE OF DISCRETE TIME OBSERVATION ERROR COVARIANCE MATRIX DT=.125 SEC

4.069E+02	1.217E+01	-2.713E+02	-3.503E-04	-1.533E-01
1.217E+01	5.747E+01	2.400E+02	-1.329E-02	1.545E-03
-2.713E+02	2.400E+02	2.037E+03	-6.225E-02	1.686E-01
-3.503E-04	-1.329E-02	-6.225E-02	3.331E+05	-1.539E-06
-1.533E-01	1.545E-03	1.686E-01	-1.539E-06	3.331E+05

DETERMINANT OF OBSERVATION COVARIANCE MATRIX = 0.498E-18

FLIGHT CONDITION 19 DYNAMIC PRESSURE 537 PSF MACH 1.40 ALTITUDE 40000 FT

PLANT NOISE COVARIANCE (XI)

1.100E-01	0.0	0.0	0.0	0.0	0.0	0.0
0.0	7.600E-04	0.0	0.0	0.0	0.0	0.0
0.0	0.0	1.400E-05	0.0	0.0	0.0	0.0
0.0	0.0	0.0	2.500E-05	0.0	0.0	0.0
0.0	0.0	0.0	0.0	1.000E-07	0.0	0.0
0.0	0.0	0.0	0.0	0.0	1.000E-07	0.0
0.0	0.0	0.0	0.0	0.0	0.0	9.195E-03

OBSERVATION NOISE COVARIANCE (THETA)

1.750E-03	0.0	0.0	0.0	0.0
0.0	1.218E-03	0.0	0.0	0.0
0.0	0.0	7.610E-05	0.0	0.0
0.0	0.0	0.0	3.000E-06	0.0
0.0	0.0	0.0	0.0	3.000E-06

KALMAN FILTER GAINS (H)

-8.235E-01	1.665E+01	-2.207E+01	-2.525E-04	2.808E-04
3.785E-01	-1.379E+00	6.485E+00	5.266E-05	-5.418E-05
-2.456E-01	9.215E-02	-7.613E-01	-1.181E-06	2.005E-05
-8.616E-01	8.636E-01	6.790E-01	1.110E-04	3.322E-04
3.366E-08	-6.220E-07	2.076E-06	5.556E-04	-1.831E-11
3.050E-07	6.916E-07	-2.136E-06	-1.831E-11	6.667E-04
3.082E-01	-2.085E+00	4.987E+00	1.241E-04	3.602E-05

FLIGHT CONDITION 19 CONTINUED

KF CLOSED-LOOP MATRIX (ACL)

-18.9300	22.3500	-81.6400	0.0004	11.2800	5.6690	-73.9000
1.3830	-6.8730	11.8500	-0.0002	0.2940	-2.3340	8.2940
-0.0408	-0.2088	-2.5310	0.0239	0.0000	0.1446	-0.2233
0.1318	-0.5309	-8.0970	0.0004	-0.0001	0.4624	0.0000
0.0000	-0.0000	0.0000	-0.0000	-30.0000	-0.0000	-0.0000
-0.0000	0.0000	0.0000	-0.0000	0.0000	-25.0000	-0.0000
2.0870	-5.0210	2.8970	-0.0002	-0.0001	-0.1656	-1.0840

KF POLES

REAL PART =	-11.091	IMAG PART =	9.768
REAL PART =	-11.091	IMAG PART =	-9.768
REAL PART =	-4.694	IMAG PART =	0.0
REAL PART =	-0.084	IMAG PART =	0.0
REAL PART =	-2.458	IMAG PART =	0.0
REAL PART =	-25.000	IMAG PART =	0.0
REAL PART =	-30.000	IMAG PART =	0.0

STATE ESTIMATION ERROR COVARIANCE MATRIX

2.028E-02	-1.680E-03	1.122E-04	1.052E-03	-7.576E-10	8.424E-10	-2.540E-03
-1.680E-03	4.935E-04	-5.793E-05	5.167E-05	1.580E-10	-1.625E-10	3.795E-04
1.122E-04	-5.793E-05	4.109E-05	1.475E-04	-3.542E-12	6.015E-11	-4.698E-05
1.052E-03	5.167E-05	1.475E-04	1.197E-02	3.330E-10	9.965E-10	-1.439E-04
-7.576E-10	1.580E-10	-3.542E-12	3.330E-10	1.667E-09	-5.493E-17	3.724E-10
8.424E-10	-1.625E-10	6.015E-11	9.965E-10	-5.493E-17	2.000E-09	1.081E-10
-2.540E-03	3.795E-04	-4.698E-05	-1.439E-04	3.724E-10	1.081E-10	8.546E-04

FLIGHT CONDITION 19 CONTINUED

DISCRETE TIME PLANT NOISE COVARIANCE MATRIX (XID) DT=.125 SEC

3.284E-02	-2.738E-03	2.904E-04	1.732E-03	5.598E-10	3.431E-10	-4.122E-03
-2.738E-03	4.272E-04	-3.723E-05	-1.332E-04	1.554E-11	-1.526E-10	5.007E-04
2.904E-04	-3.723E-05	5.492E-06	1.636E-05	4.103E-13	6.320E-12	-4.414E-05
1.732E-03	-1.332E-04	1.636E-05	1.181E-04	1.624E-11	1.081E-11	-1.759E-04
5.598E-10	1.554E-11	4.103E-13	1.624E-11	1.666E-09	0.0	0.0
3.431E-10	-1.526E-10	6.320E-12	1.081E-11	0.0	1.996E-09	0.0
-4.122E-03	5.007E-04	-4.414E-05	-1.759E-04	0.0	0.0	1.007E-03

DISCRETE TIME KF GAINS (HD) DT=.125 SEC

-1.725E-02	9.456E-01	-3.102E-01	1.200E-05	-4.848E-06
2.312E-02	-1.938E-02	7.804E-01	4.922E-06	-1.694E-05
-3.549E-02	2.031E-03	-4.722E-02	-5.030E-08	1.164E-05
-1.278E-01	5.569E-02	1.587E-01	-5.961E-06	4.933E-05
1.665E-09	2.956E-08	1.940E-07	5.552E-04	6.477E-12
4.227E-07	-1.194E-08	-6.679E-07	6.477E-12	6.662E-04
9.658E-03	-7.059E-02	4.701E-01	1.091E-05	2.982E-05

DISCRETE TIME KF CLOSED-LOOP MATRIX DT=.125 SEC

-0.4360	3.3060	-5.7362	-0.0123	0.2937	0.0222	-7.1215
0.0793	-0.1810	0.9203	0.0015	0.0096	-0.0725	0.9042
-0.0118	0.0732	0.5495	0.0029	0.0007	0.0274	-0.1104
-0.0829	0.0983	-1.5942	0.9995	0.0309	0.0766	-0.4856
-0.0000	-0.0000	0.0000	-0.0000	0.0235	-0.0000	0.0000
0.0000	0.0000	0.0000	-0.0000	-0.0000	0.0439	0.0000
0.0617	-0.4114	0.0793	-0.0000	-0.0000	-0.0046	0.8733

FLIGHT CONDITION 19 CONTINUED

DISCRETE TIME KF POLES DT=.125 SEC

REAL PART =	0.989	IMAG PART =	0.0
REAL PART =	0.666	IMAG PART =	0.0
REAL PART =	-0.022	IMAG PART =	0.114
REAL PART =	-0.022	IMAG PART =	-0.114
REAL PART =	0.193	IMAG PART =	0.0
REAL PART =	0.024	IMAG PART =	0.0
REAL PART =	0.044	IMAG PART =	0.0

STATE PREDICTION COVARIANCE MATRIX DT=.125 SEC

5.641E-02	-5.801E-03	6.322E-04	3.157E-03	5.667E-10	3.132E-10	-6.860E-03
-5.801E-03	8.862E-04	-9.226E-05	-2.965E-04	1.692E-11	-1.562E-10	8.713E-04
6.322E-04	-9.226E-05	1.898E-05	6.905E-05	3.143E-13	8.247E-12	-9.118E-05
3.157E-03	-2.965E-04	6.905E-05	3.465E-03	1.676E-11	1.578E-11	-3.554E-04
5.667E-10	1.692E-11	3.143E-13	1.676E-11	1.667E-09	2.008E-20	6.722E-13
3.132E-10	-1.562E-10	8.247E-12	1.578E-11	2.008E-20	2.000E-09	3.433E-12
-6.860E-03	8.713E-04	-9.118E-05	-3.554E-04	6.722E-13	3.433E-12	1.339E-03

INVERSE OF DISCRETE TIME OBSERVATION ERROR COVARIANCE MATRIX DT=.125 SEC

3.794E+02	1.416E+01	-3.039E+02	-5.551E-04	-1.409E-01
1.416E+01	4.466E+01	2.547E+02	-9.852E-03	3.979E-03
-3.039E+02	2.547E+02	2.886E+03	-6.468E-02	2.226E-01
-5.551E-04	-9.852E-03	-6.468E-02	3.331E+05	-2.159E-06
-1.409E-01	3.979E-03	2.226E-01	-2.159E-06	3.331E+05

DETERMINANT OF OBSERVATION COVARIANCE MATRIX = 0.518E-18

FLIGHT CONDITION 20 DYNAMIC PRESSURE 703 PSF MACH 1.60 ALTITUDE 40000 FT

PLANT NOISE COVARIANCE (XI)

1.100E-01	0.0	0.0	0.0	0.0	0.0	0.0
0.0	7.600E-04	0.0	0.0	0.0	0.0	0.0
0.0	0.0	1.400E-05	0.0	0.0	0.0	0.0
0.0	0.0	0.0	2.500E-05	0.0	0.0	0.0
0.0	0.0	0.0	0.0	1.000E-07	0.0	0.0
0.0	0.0	0.0	0.0	0.0	1.000E-07	0.0
0.0	0.0	0.0	0.0	0.0	0.0	8.601E-03

OBSERVATION NOISE COVARIANCE (THETA)

1.750E-03	0.0	0.0	0.0	0.0
0.0	1.218E-03	0.0	0.0	0.0
0.0	0.0	7.610E-05	0.0	0.0
0.0	0.0	0.0	3.000E-06	0.0
0.0	0.0	0.0	0.0	3.000E-06

KALMAN FILTER GAINS (H)

-1.262E+00	1.971E+01	-2.435E+01	7.400E-04	-6.011E-04
4.445E-01	-1.521E+00	5.988E+00	-1.154E-04	1.349E-05
-2.415E-01	1.214E-01	-7.348E-01	2.506E-05	-5.987E-07
-8.686E-01	9.702E-01	7.000E-01	2.643E-04	-1.703E-04
1.974E-08	-1.481E-06	5.318E-07	-2.421E-10	5.555E-04
1.070E-07	1.823E-06	-4.549E-06	6.667E-04	-2.421E-10
3.902E-01	-2.665E+00	5.258E+00	2.611E-05	1.715E-05

FLIGHT CONDITION 20 CONTINUED

KF CLOSED-LOOP MATRIX (ACL)

-22.1700	24.6700	-100.2000	0.0007	10.4800	5.7300	-85.4700
1.5290	-6.3960	13.1200	-0.0002	0.3012	-2.5100	7.9200
-0.0752	-0.2363	-3.0690	0.0209	0.0000	0.1438	-0.2433
0.0256	-0.5573	-10.1600	0.0005	0.0002	0.4760	0.0000
0.0000	-0.0000	0.0000	-0.0000	-30.0000	-0.0000	-0.0000
-0.0000	0.0000	0.0000	-0.0000	0.0000	-25.0000	-0.0000
2.6660	-5.3010	4.5660	-0.0002	-0.0000	-0.2140	1.2390

KF POLES

REAL PART = -11.603 IMAG PART = 10.208
REAL PART = -11.603 IMAG PART = -10.208
REAL PART = -3.558 IMAG PART = 0.637
REAL PART = -3.558 IMAG PART = -0.637
REAL PART = -0.074 IMAG PART = 0.0
REAL PART = -25.000 IMAG PART = 0.0
REAL PART = -30.000 IMAG PART = 0.0

STATE ESTIMATION ERROR COVARIANCE MATRIX

2.401E-02	-1.853E-03	1.479E-04	1.182E-03	-1.803E-09	2.220E-09	-3.246E-03
-1.853E-03	4.557E-04	-5.592E-05	5.327E-05	4.047E-11	-3.462E-10	4.001E-04
1.479E-04	-5.592E-05	3.245E-05	1.195E-04	-1.796E-12	7.520E-11	-4.861E-05
1.182E-03	5.327E-05	1.195E-04	1.368E-02	-5.108E-10	7.930E-10	-1.517E-04
-1.803E-09	4.047E-11	-1.796E-12	-5.108E-10	1.667E-09	-7.263E-16	5.144E-11
2.220E-09	-3.462E-10	7.520E-11	7.930E-10	-7.263E-16	2.000E-09	7.832E-11
-3.246E-03	4.001E-04	-4.861E-05	-1.517E-04	5.144E-11	7.832E-11	9.676E-04

FLIGHT CONDITION 20 CONTINUED

DISCRETE TIME PLANT NOISE COVARIANCE MATRIX (XID) DT=.125 SEC

3.743E-02	-2.754E-03	3.032E-04	1.958E-03	5.179E-10	3.263E-10	-4.343E-03
-2.754E-03	3.714E-04	-3.357E-05	-1.348E-04	1.593E-11	-1.624E-10	4.377E-04
3.032E-04	-3.357E-05	5.259E-06	1.696E-05	2.561E-13	6.444E-12	-4.102E-05
1.958E-03	-1.348E-04	1.696E-05	1.303E-04	1.503E-11	1.032E-11	-1.860E-04
5.179E-10	1.593E-11	2.561E-13	1.503E-11	1.666E-09	0.0	0.0
3.263E-10	-1.624E-10	6.444E-12	1.032E-11	0.0	1.996E-09	0.0
-4.343E-03	4.377E-04	-4.102E-05	-1.860E-04	0.0	0.0	9.246E-04

DISCRETE TIME KF GAINS (HD) DT=.125 SEC

-1.908E-02	9.529E-01	-3.022E-01	9.937E-06	-6.049E-06
2.557E-02	-1.888E-02	7.438E-01	4.778E-06	-2.079E-05
-3.338E-02	1.879E-03	-4.314E-02	-4.818E-08	1.110E-05
-1.232E-01	5.433E-02	1.795E-01	-5.428E-06	4.992E-05
1.803E-09	2.448E-08	1.883E-07	5.552E-04	7.544E-12
3.998E-07	-1.489E-08	-8.196E-07	7.544E-12	6.662E-04
7.911E-03	-7.238E-02	3.974E-01	1.055E-05	2.767E-05

DISCRETE TIME KF CLOSED-LOOP MATRIX DT=.125 SEC

-0.5208	3.1700	-6.0431	-0.0124	0.2691	-0.0091	-8.0614
0.0769	-0.0677	0.9065	0.0012	0.0098	-0.0795	0.8516
-0.0118	0.0567	0.4888	0.0025	0.0004	0.0271	-0.1098
-0.0881	0.0682	-1.8634	0.9995	0.0285	0.0736	-0.5548
-0.0000	-0.0000	0.0000	-0.0000	0.0235	-0.0000	-0.0000
0.0000	0.0000	0.0000	-0.0000	-0.0000	0.0439	0.0000
0.0620	-0.3411	0.0793	-0.0000	-0.0000	-0.0037	0.8565

FLIGHT CONDITION 20 CONTINUED

DISCRETE TIME KF POLES DT=.125 SEC

REAL PART =	0.991	IMAG PART =	0.0
REAL PART =	0.602	IMAG PART =	0.0
REAL PART =	-0.031	IMAG PART =	0.102
REAL PART =	-0.031	IMAG PART =	-0.102
REAL PART =	0.225	IMAG PART =	0.0
REAL PART =	0.024	IMAG PART =	0.0
REAL PART =	0.044	IMAG PART =	0.0

STATE PREDICTION COVARIANCE MATRIX DT=.125 SEC

6.464E-02	-5.701E-03	6.535E-04	3.603E-03	5.232E-10	2.922E-10	-7.099E-03
-5.701E-03	7.463E-04	-8.140E-05	-2.921E-04	1.725E-11	-1.675E-10	7.478E-04
6.535E-04	-8.140E-05	1.653E-05	6.484E-05	1.519E-13	8.421E-12	-8.214E-05
3.603E-03	-2.921E-04	6.484E-05	3.991E-03	1.544E-11	1.505E-11	-3.631E-04
5.232E-10	1.725E-11	1.519E-13	1.544E-11	1.667E-09	2.338E-20	6.377E-13
2.922E-10	-1.675E-10	8.421E-12	1.505E-11	2.338E-20	2.000E-09	3.124E-12
-7.099E-03	7.478E-04	-8.214E-05	-3.631E-04	6.377E-13	3.124E-12	1.214E-03

INVERSE OF DISCRETE TIME OBSERVATION ERROR COVARIANCE MATRIX DT=.125 SEC

3.466E+02	1.567E+01	-3.360E+02	-6.011E-04	-1.333E-01
1.567E+01	3.868E+01	2.481E+02	-8.159E-03	4.965E-03
-3.360E+02	2.481E+02	3.367E+03	-6.278E-02	2.732E-01
-6.011E-04	-8.159E-03	-6.278E-02	3.331E+05	-2.515E-06
-1.333E-01	4.965E-03	2.732E-01	-2.515E-06	3.331E+05

DETERMINANT OF OBSERVATION COVARIANCE MATRIX = 0.563E-18

APPENDIX D

LATERAL DYNAMICS
LINEAR SIMULATION RESULTS

Conditions for the Simulation of Figure D.1

True model: FC 11

Altitude: 20,000 feet

Speed: Mach .6

Dynamic Pressure: 245 ft.

Initial Condition on the state: a two degree sideslip angle

Both an open loop (x) and closed loop (y) simulation are shown. The simulation is deterministic with full state feedback using the matched control gains.

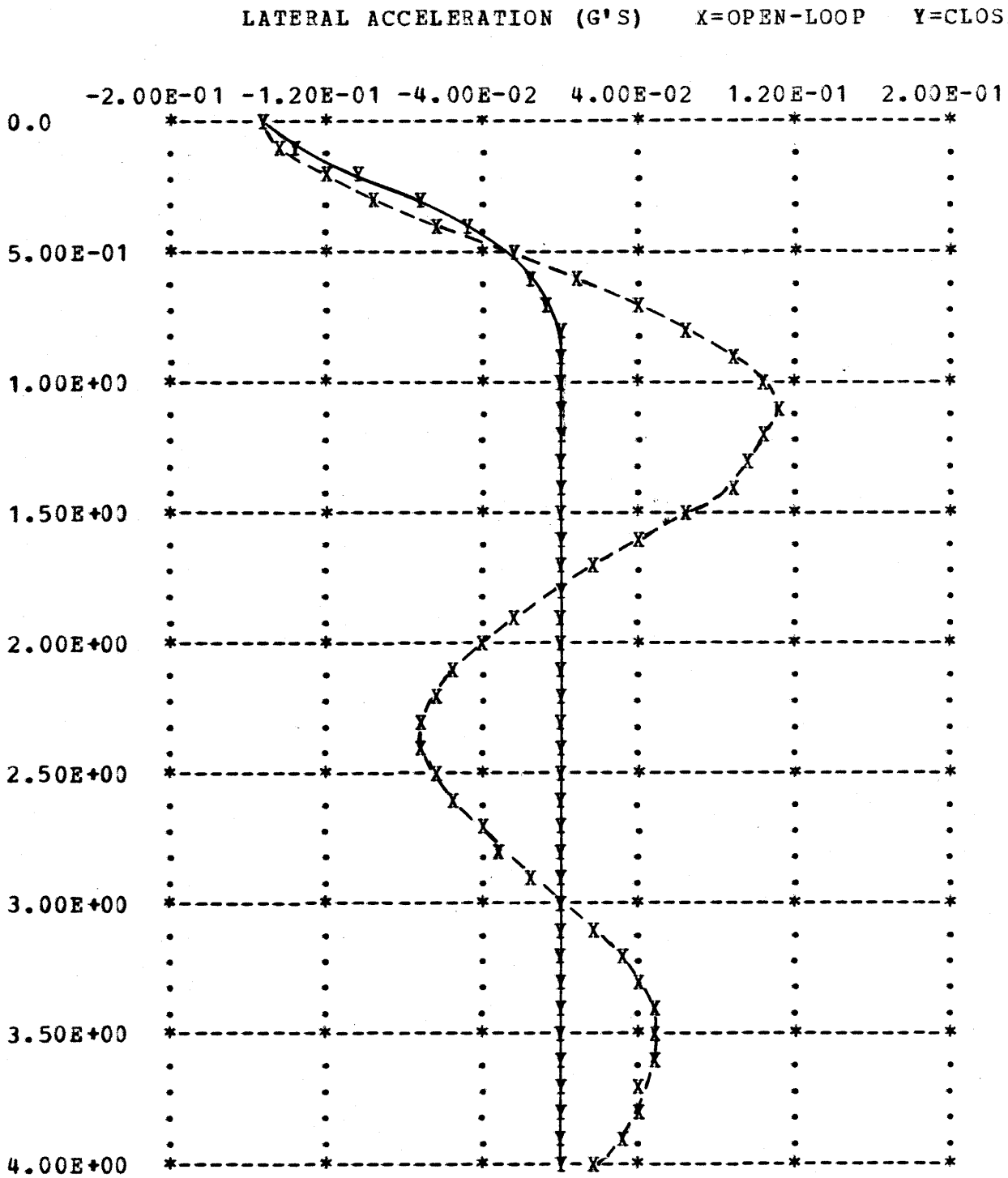

Figure D.1 (a)
Regulator Simulation
Open and Closed Loop

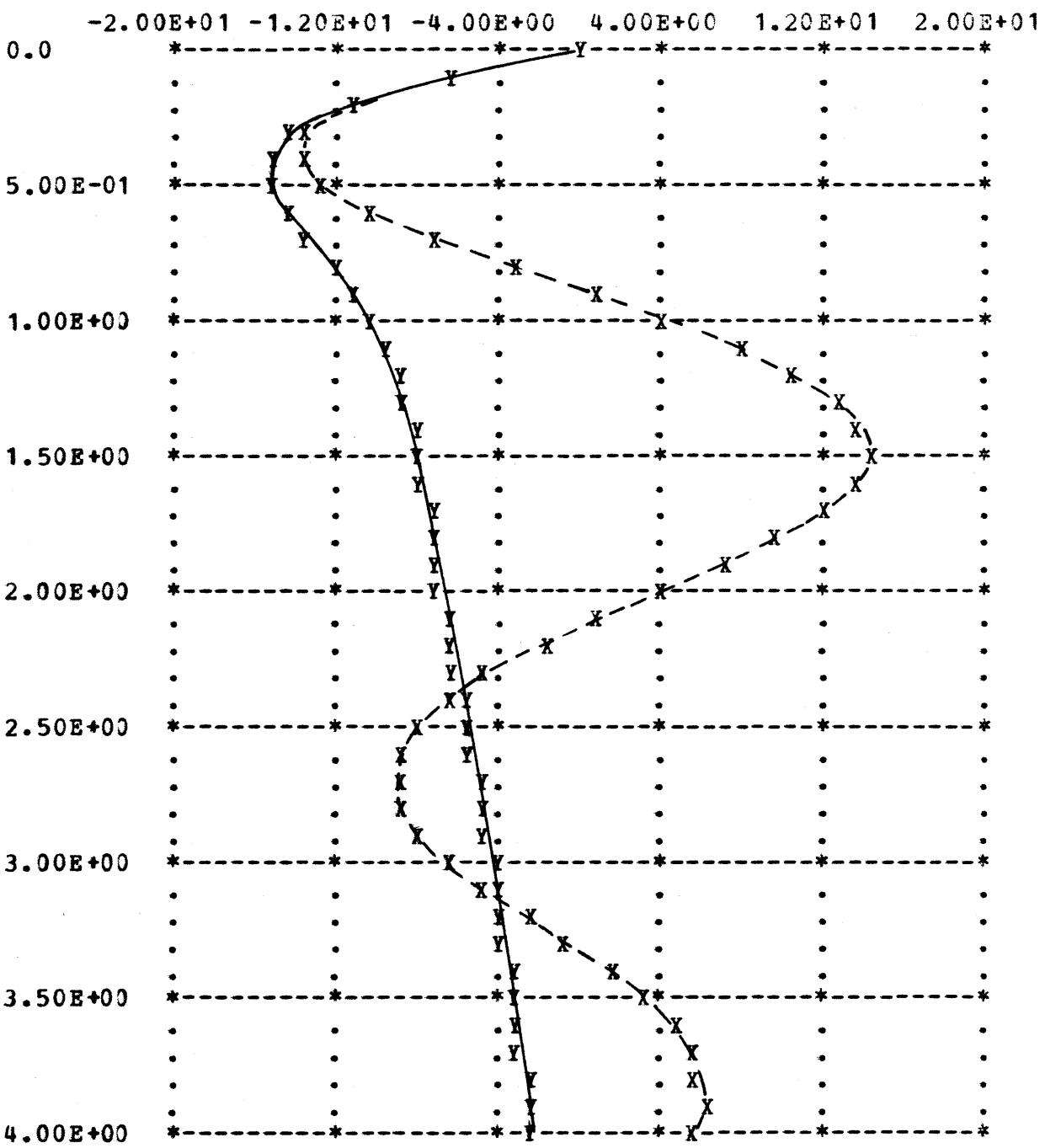

Figure D.I (b)
Regulator Simulation
Open and Closed Loop

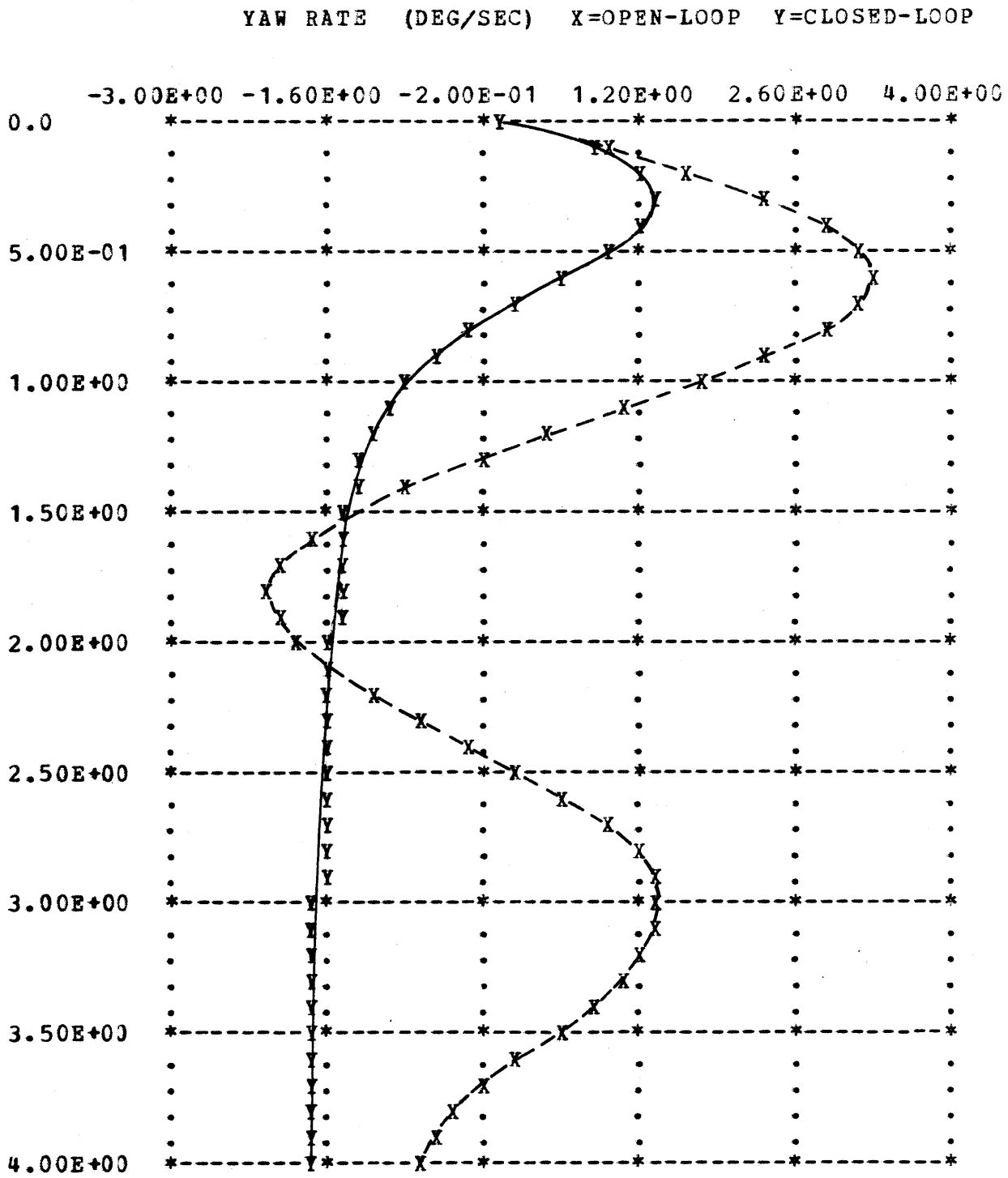

Figure D.1 (c)
Regulator Simulation
Open and Closed Loop

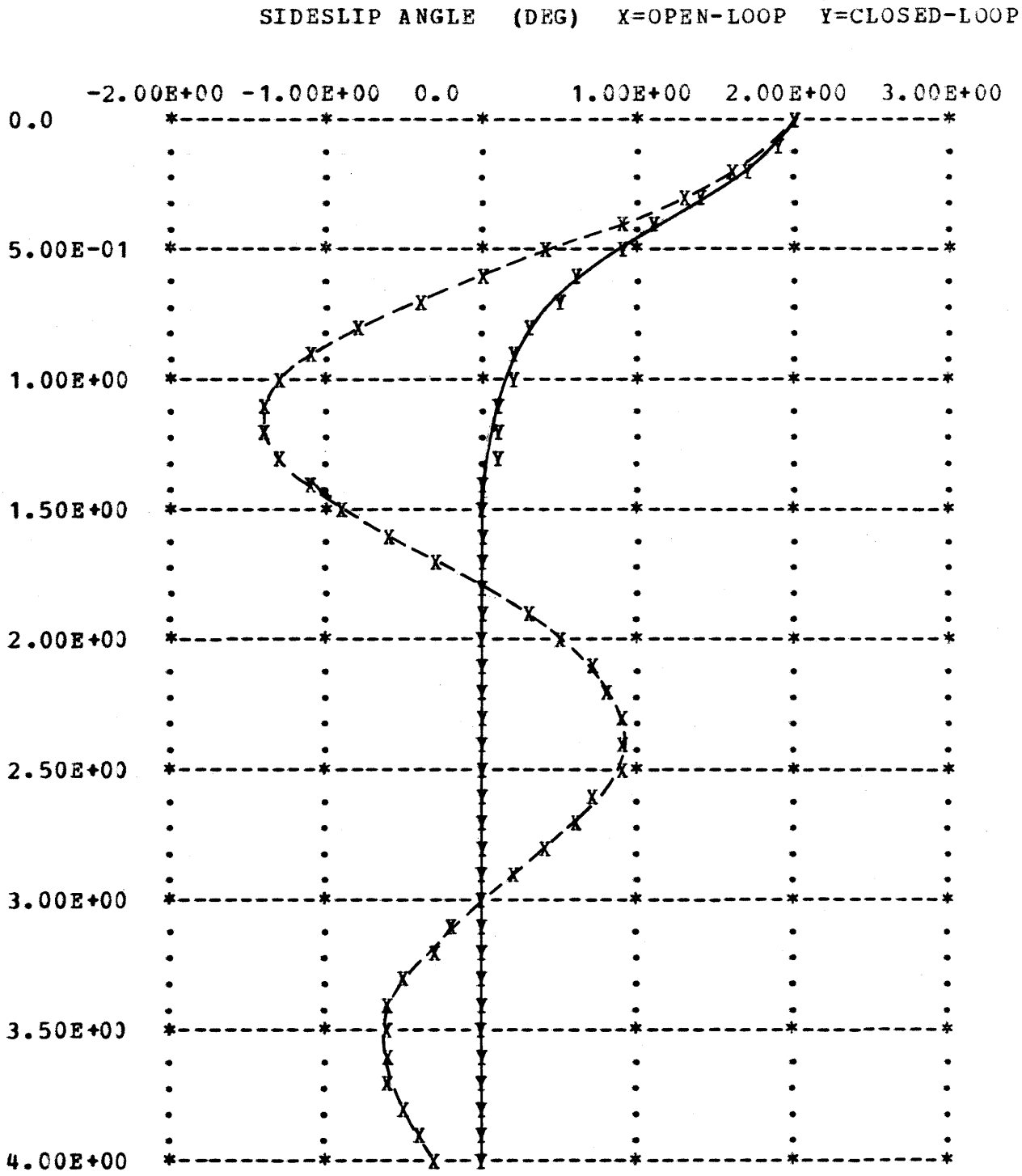

Figure D.I (d)
Regulator Simulation
Open and Closed Loop

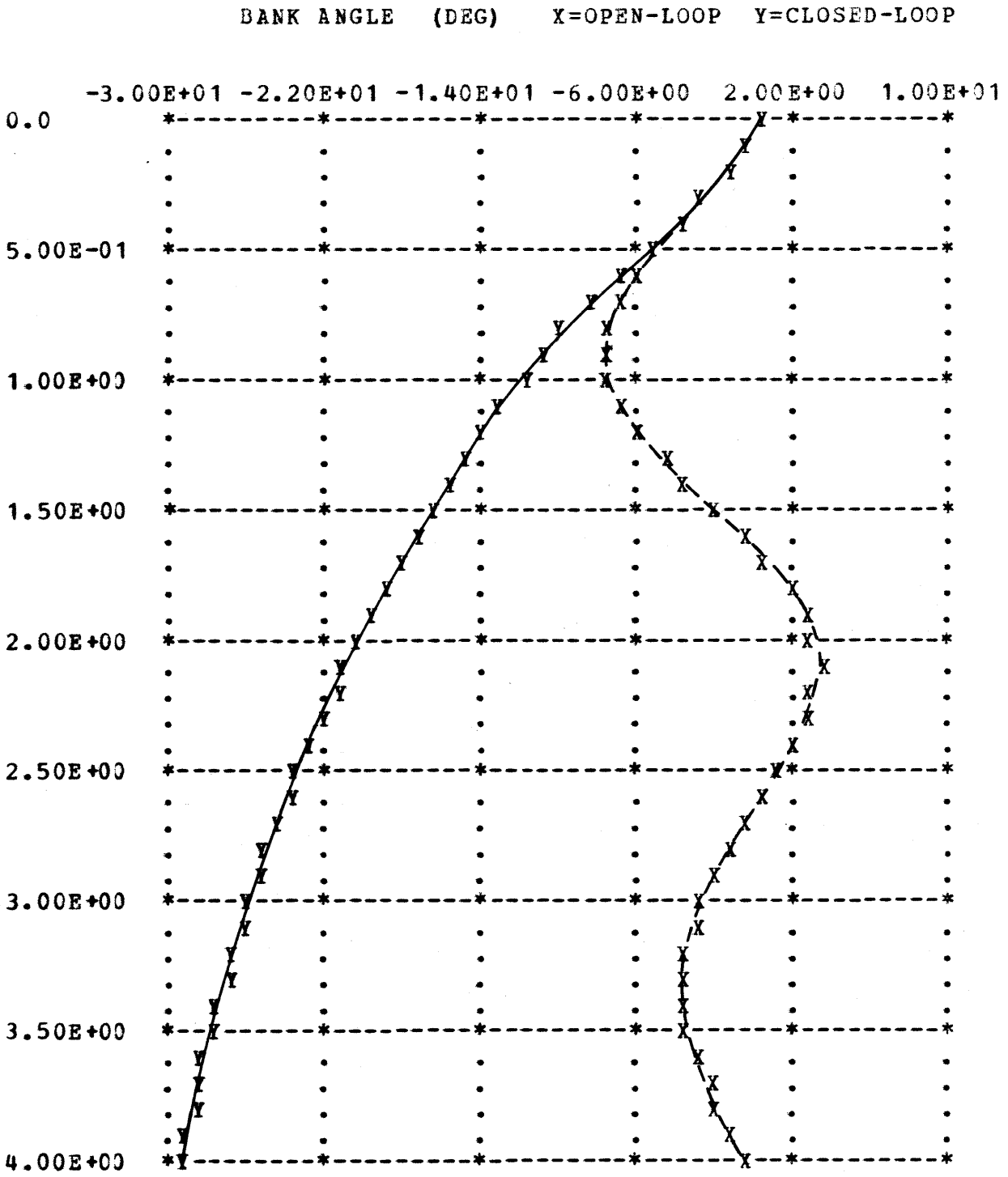

Figure D.1 (e)
Regulator Simulation
Open and Closed Loop

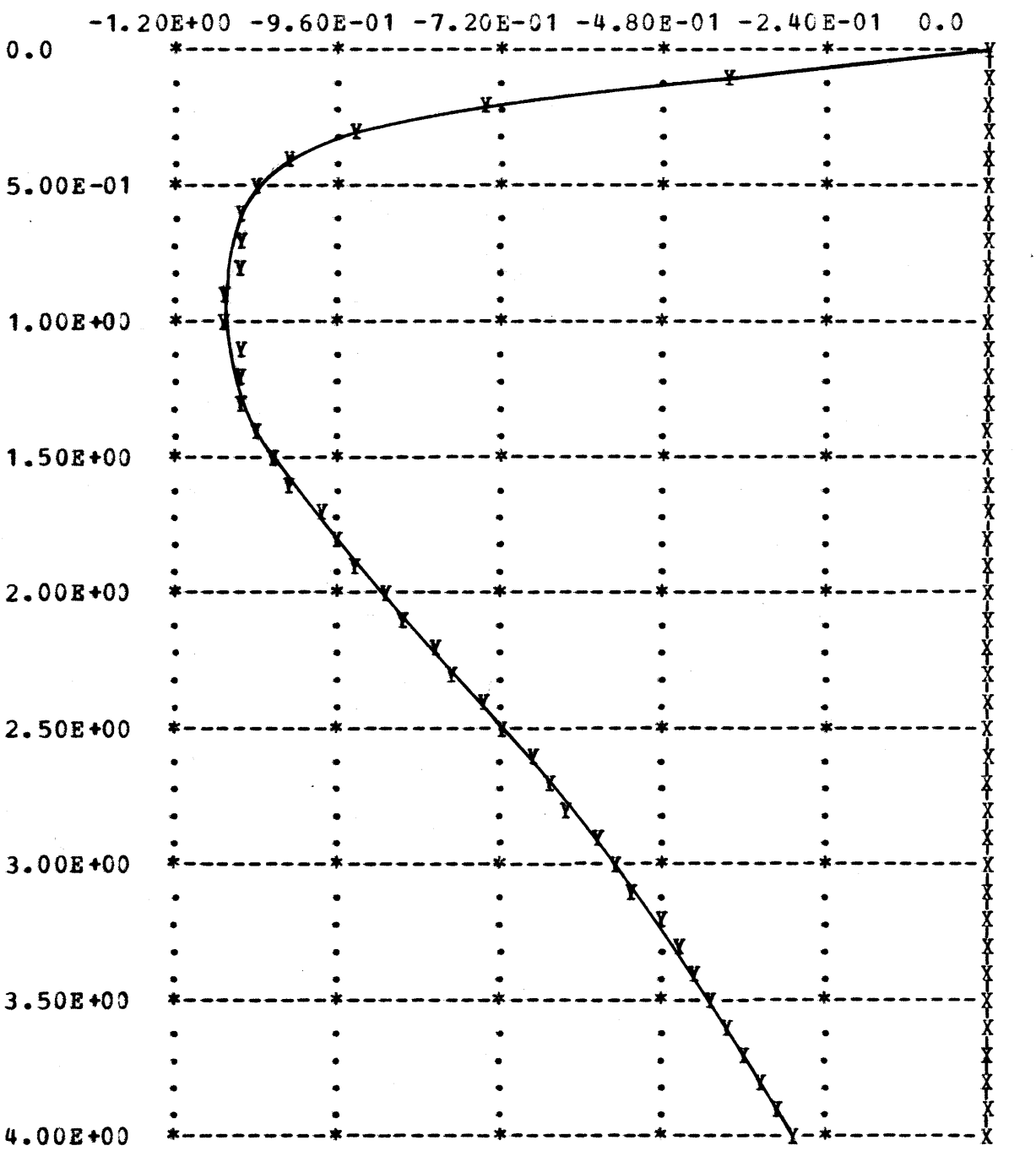

Figure D.I (f)
Regulator Simulation
Open and Closed Loop

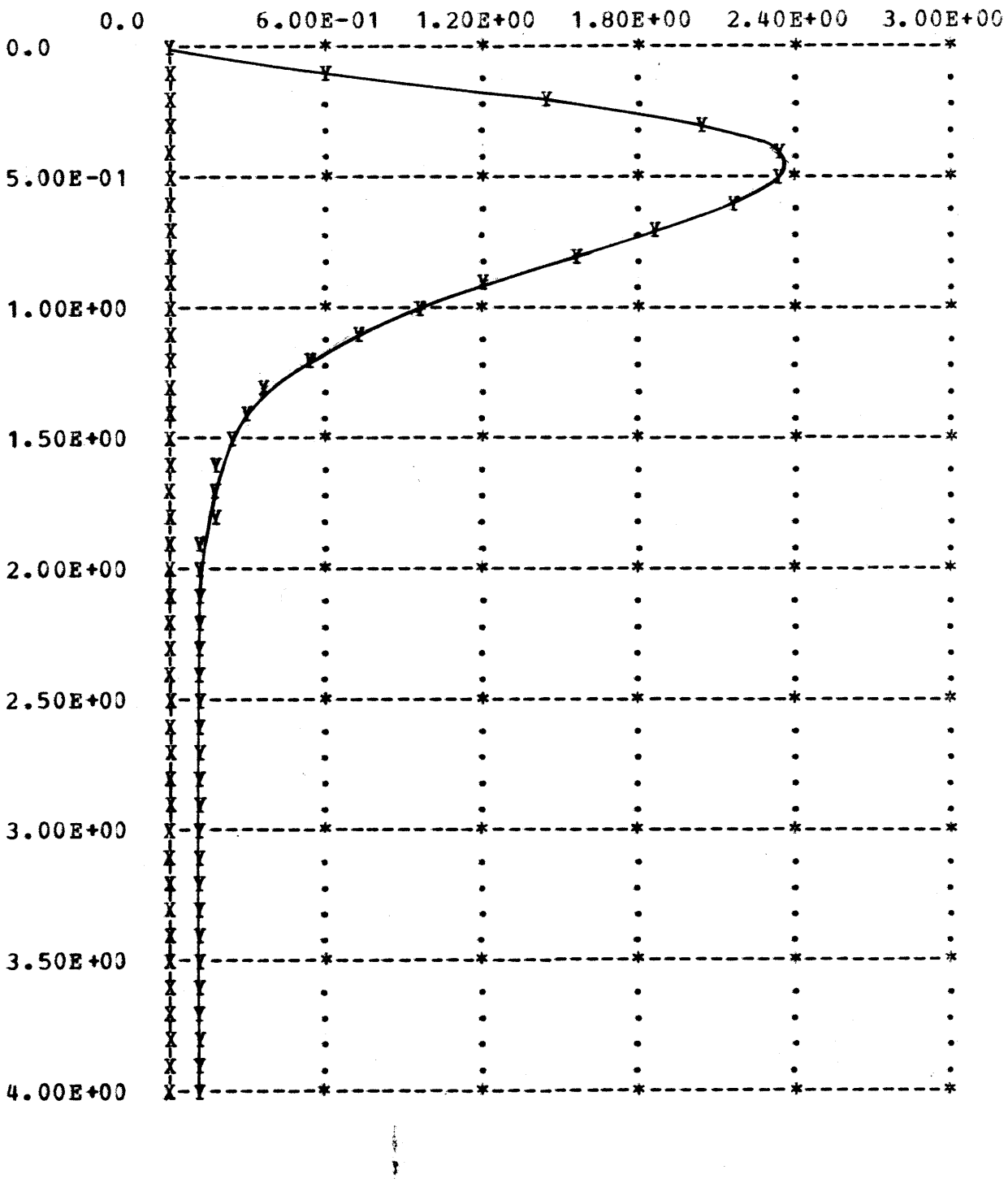

Figure D.1 (g)
Regulator Simulation
Open and Closed Loop

Condition for the Simulation of Figure D.2

True model: FC 19

Altitude: 40,000

Speed: Mach 1.4

Dynamic Pressure: 537 psf

Initial Conditions on the state: 45 degree bank angle (all others zero)

Initial Conditions on the filter: zero

This is a matched simulation in which the filter and control gains for the true model are used. Observation noise is included, but plant noise is not included.

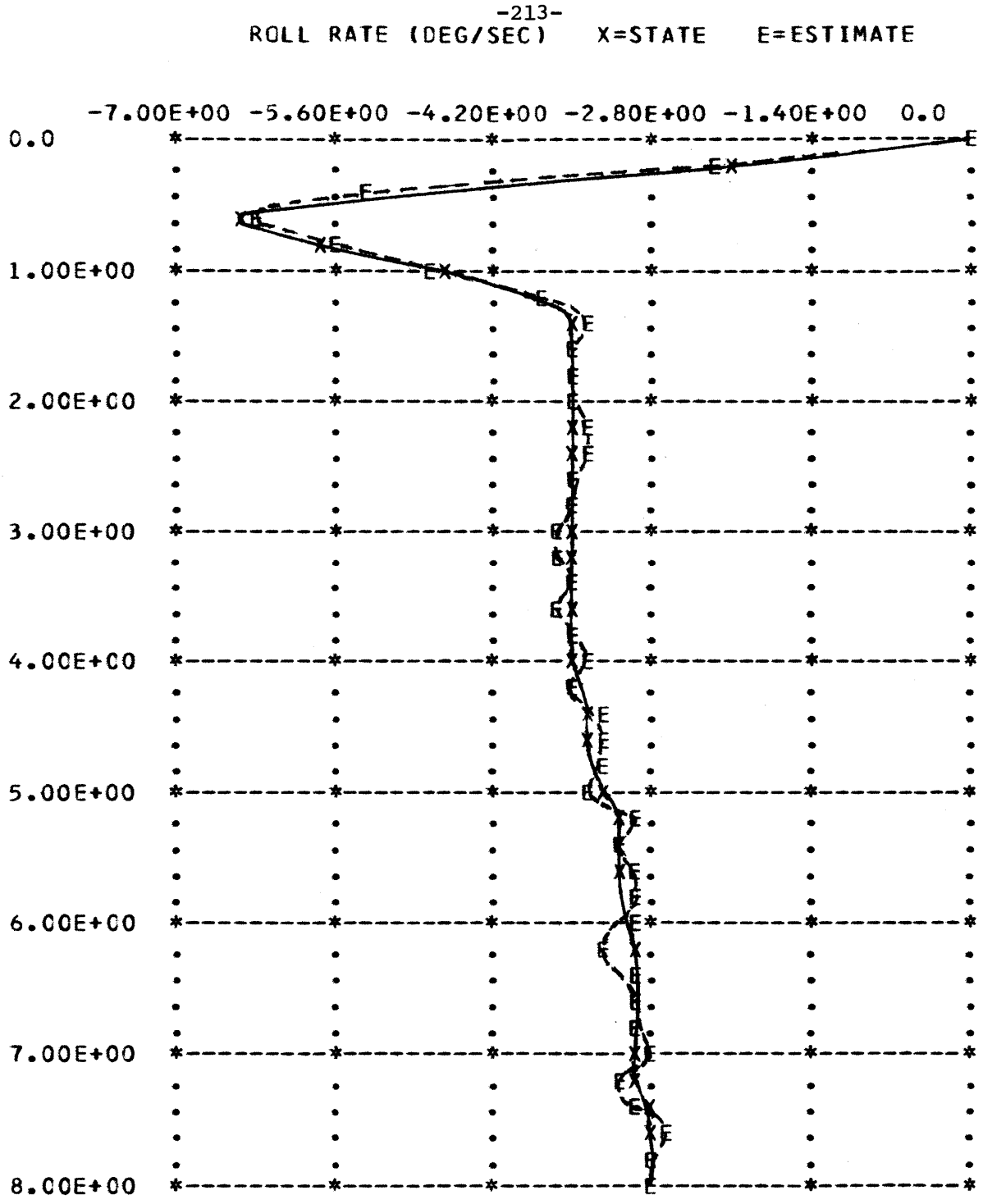

Figure D.2 (a)
KF Simulation I

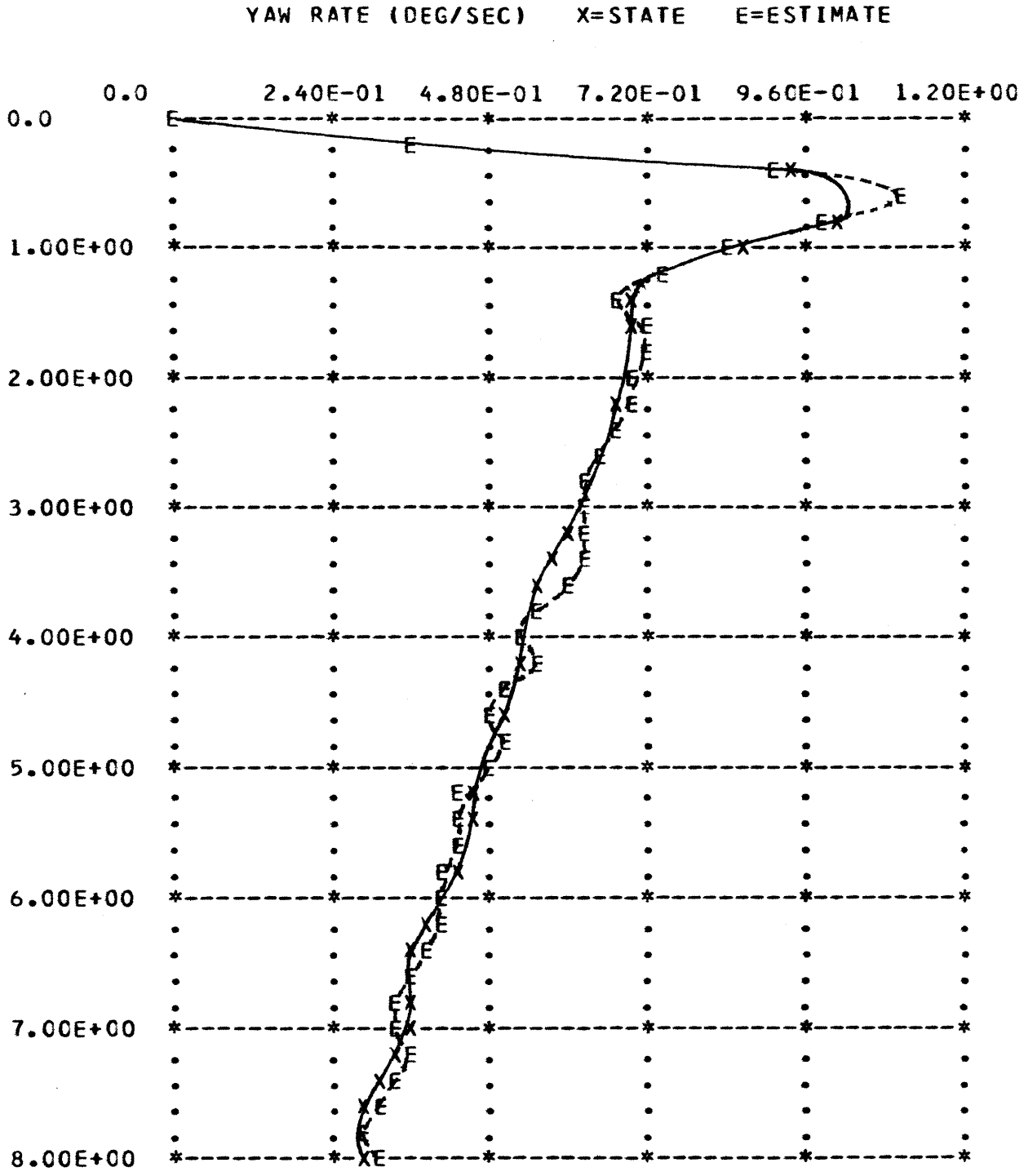

Figure D.2 (b)
KF Simulation I

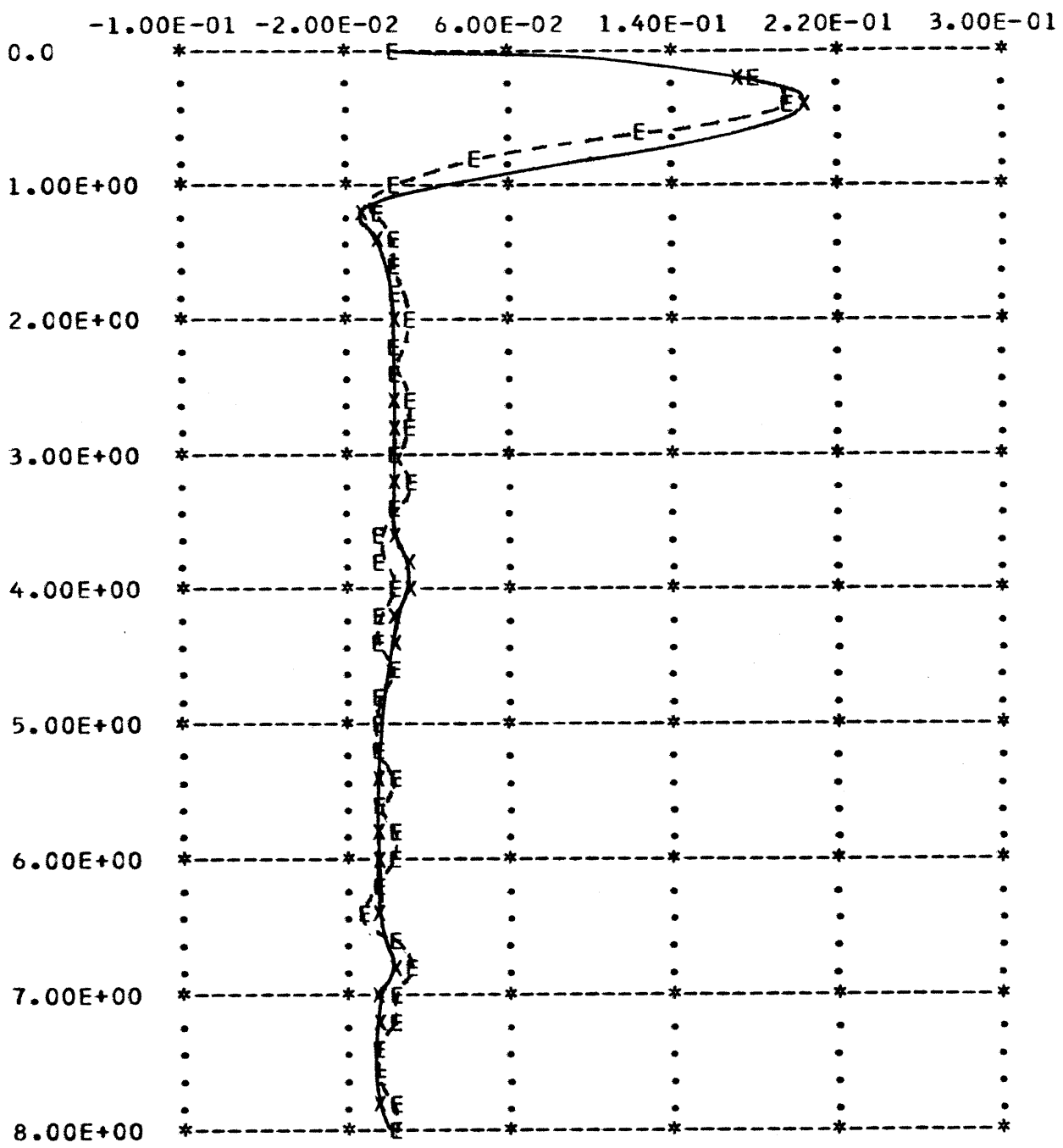

Figure D.2 (c)
KF Simulation I

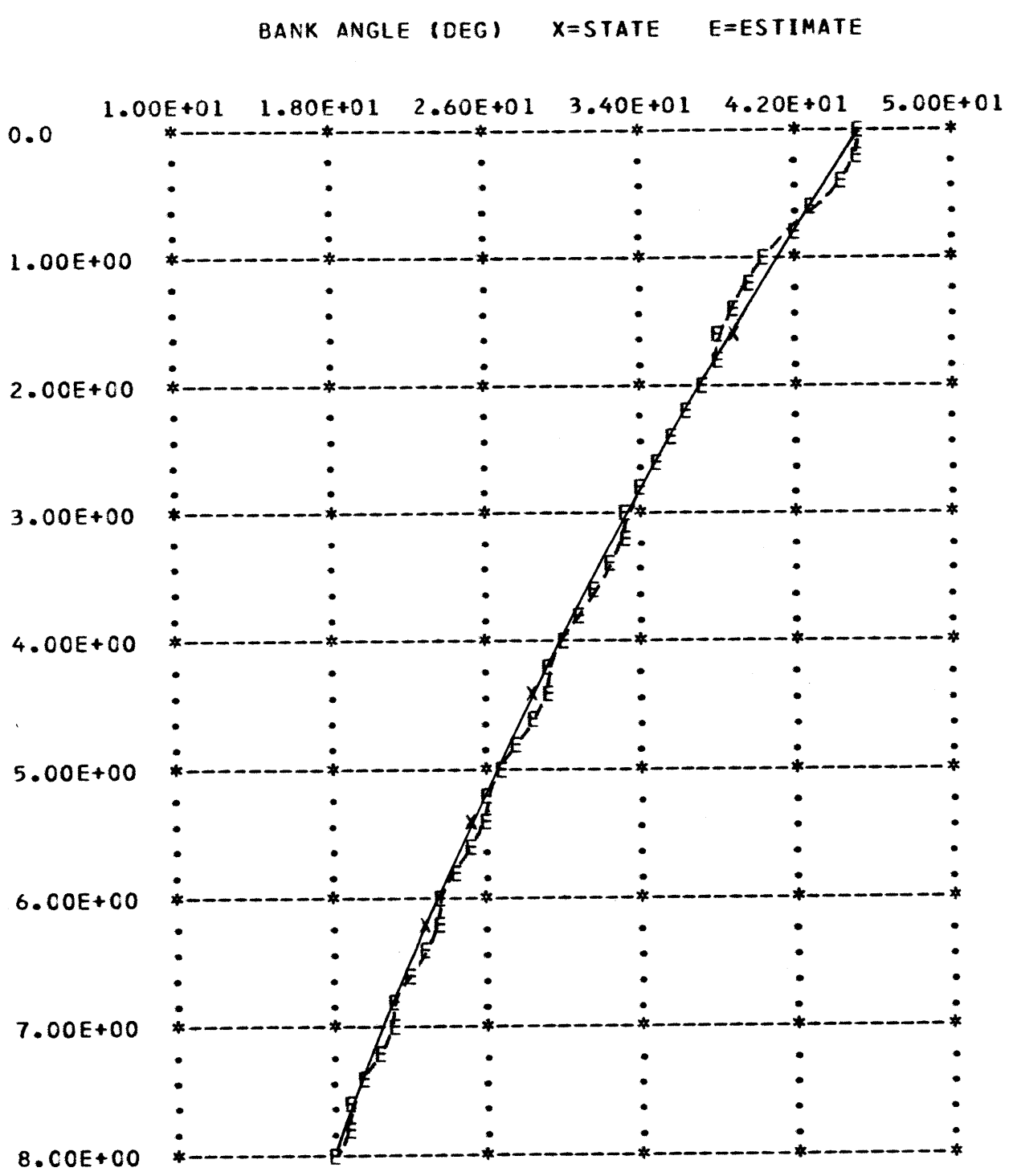

Figure D.2 (d)
KF Simulation I

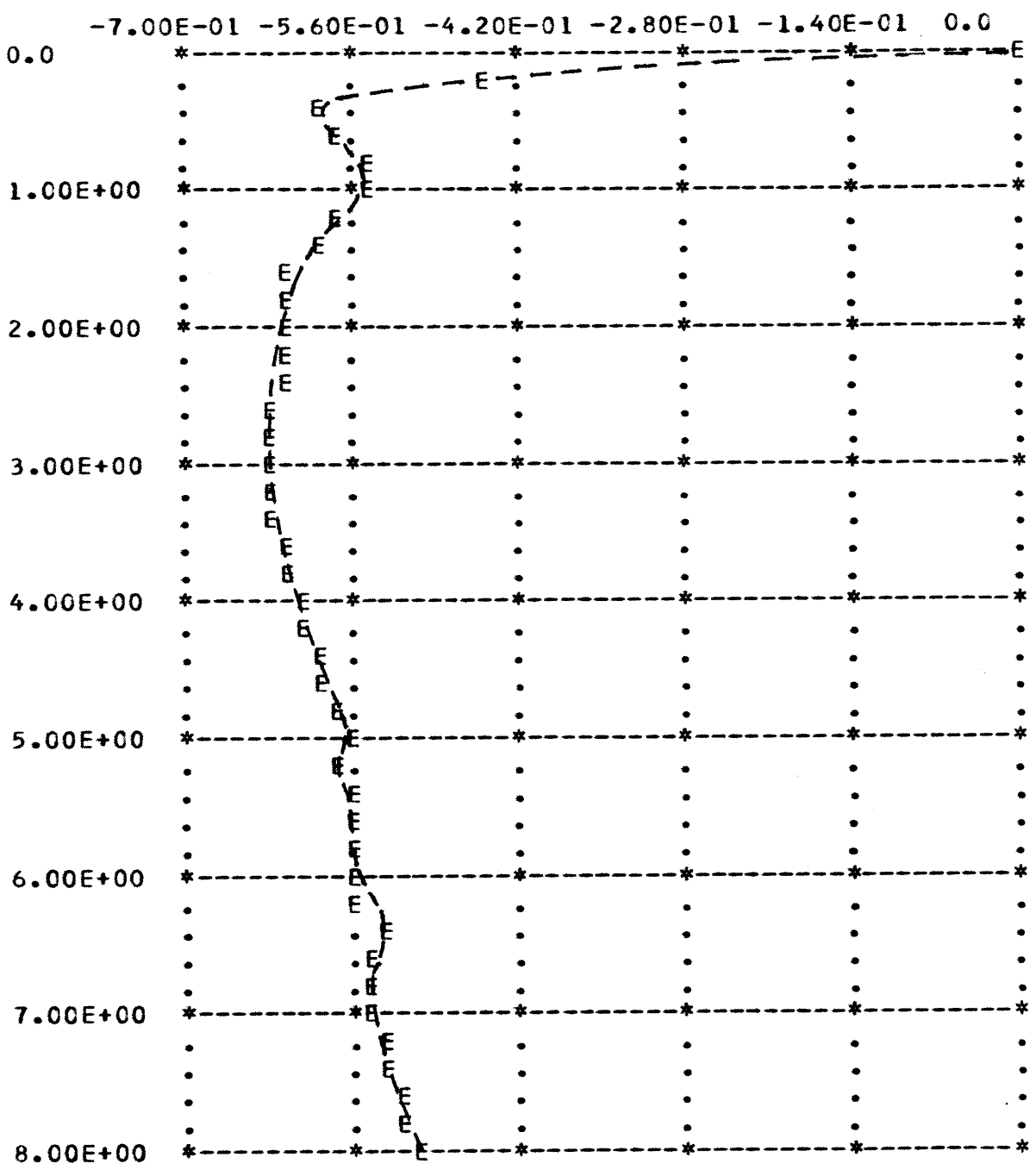

Figure D.2 (e)
KF Simulation I

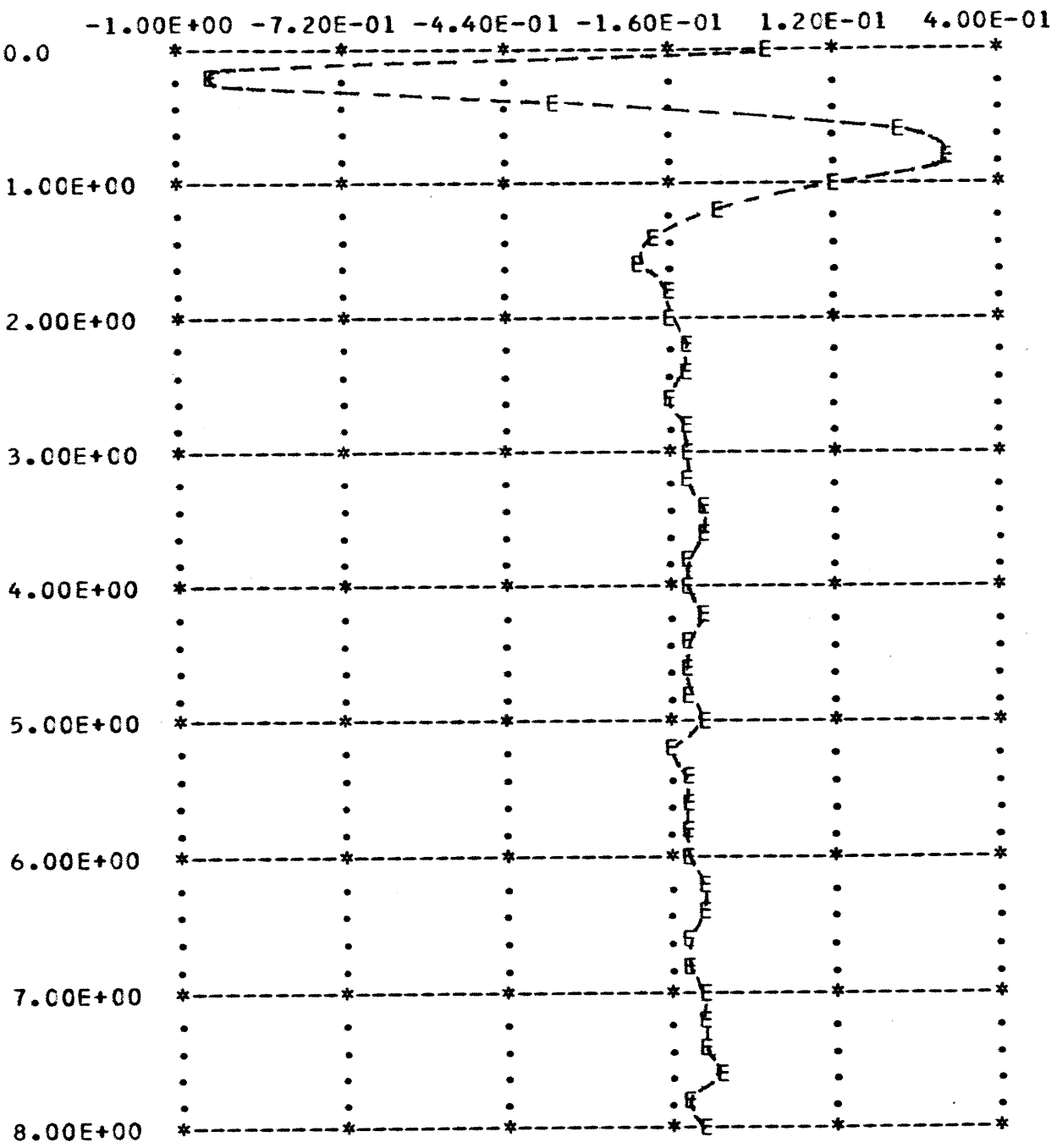

Figure D.2 (f)
KF Simulation I

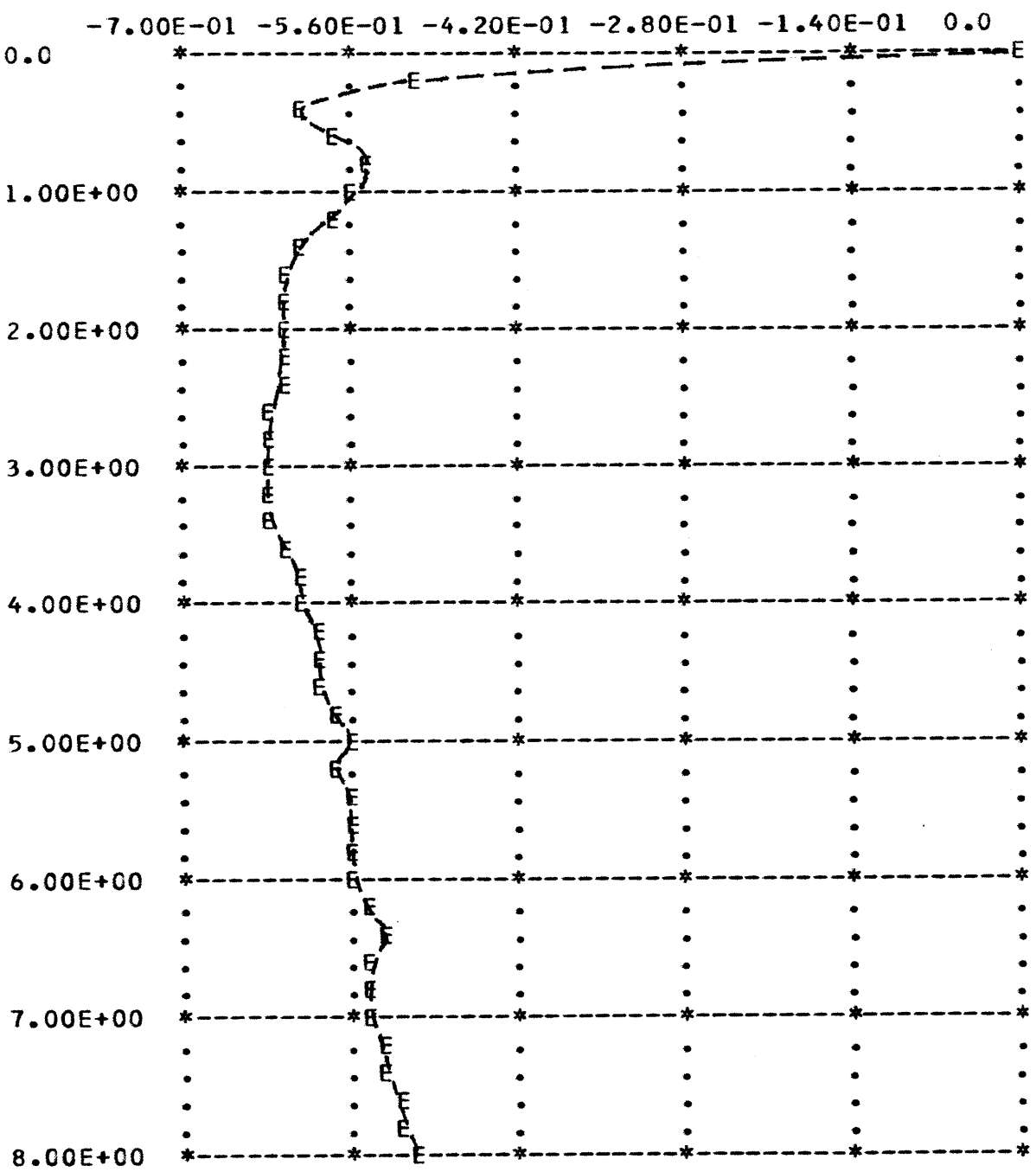

Figure D.2 (g)
K.F Simulation I

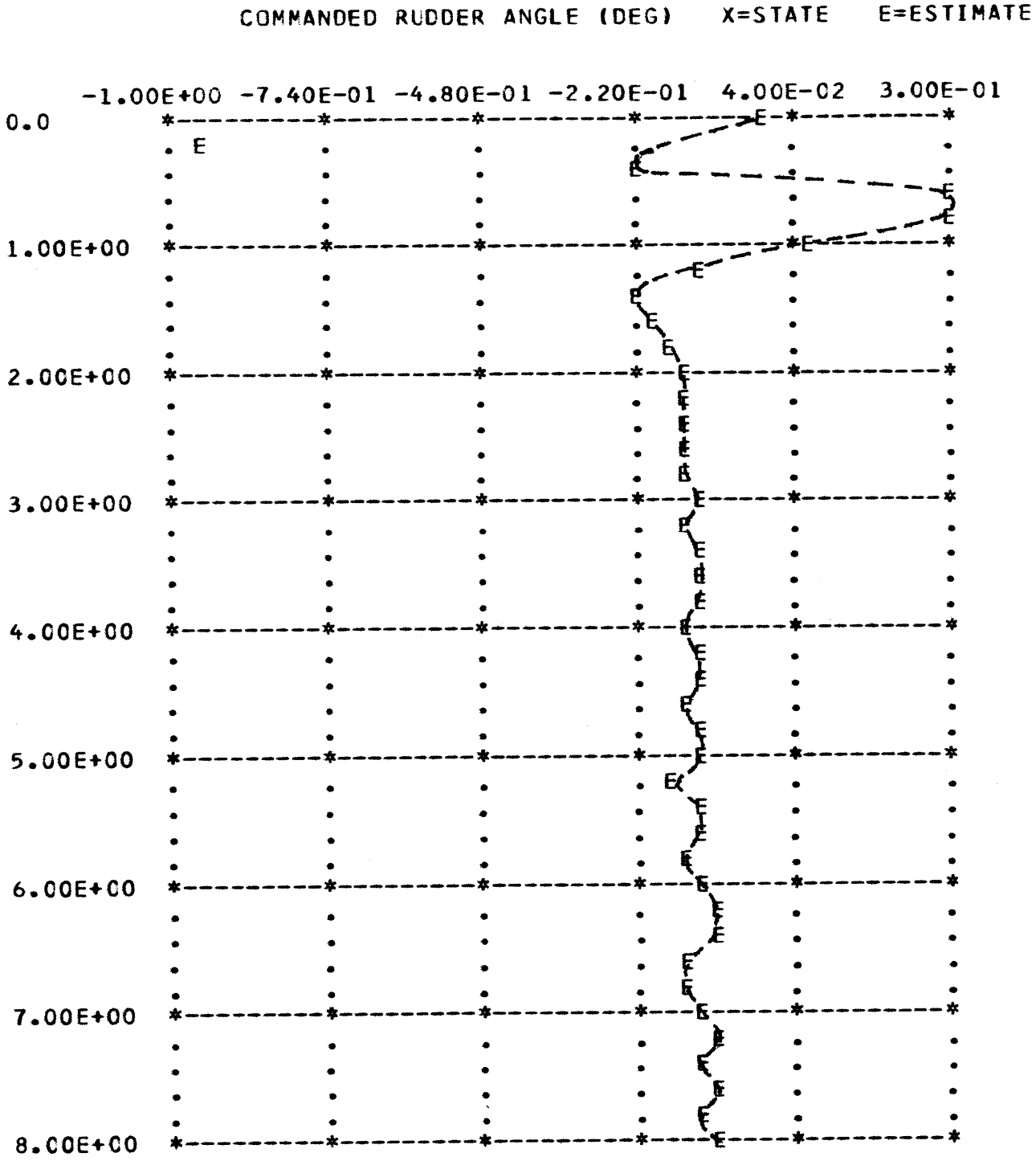

Figure D.2 (h)
KF Simulation I

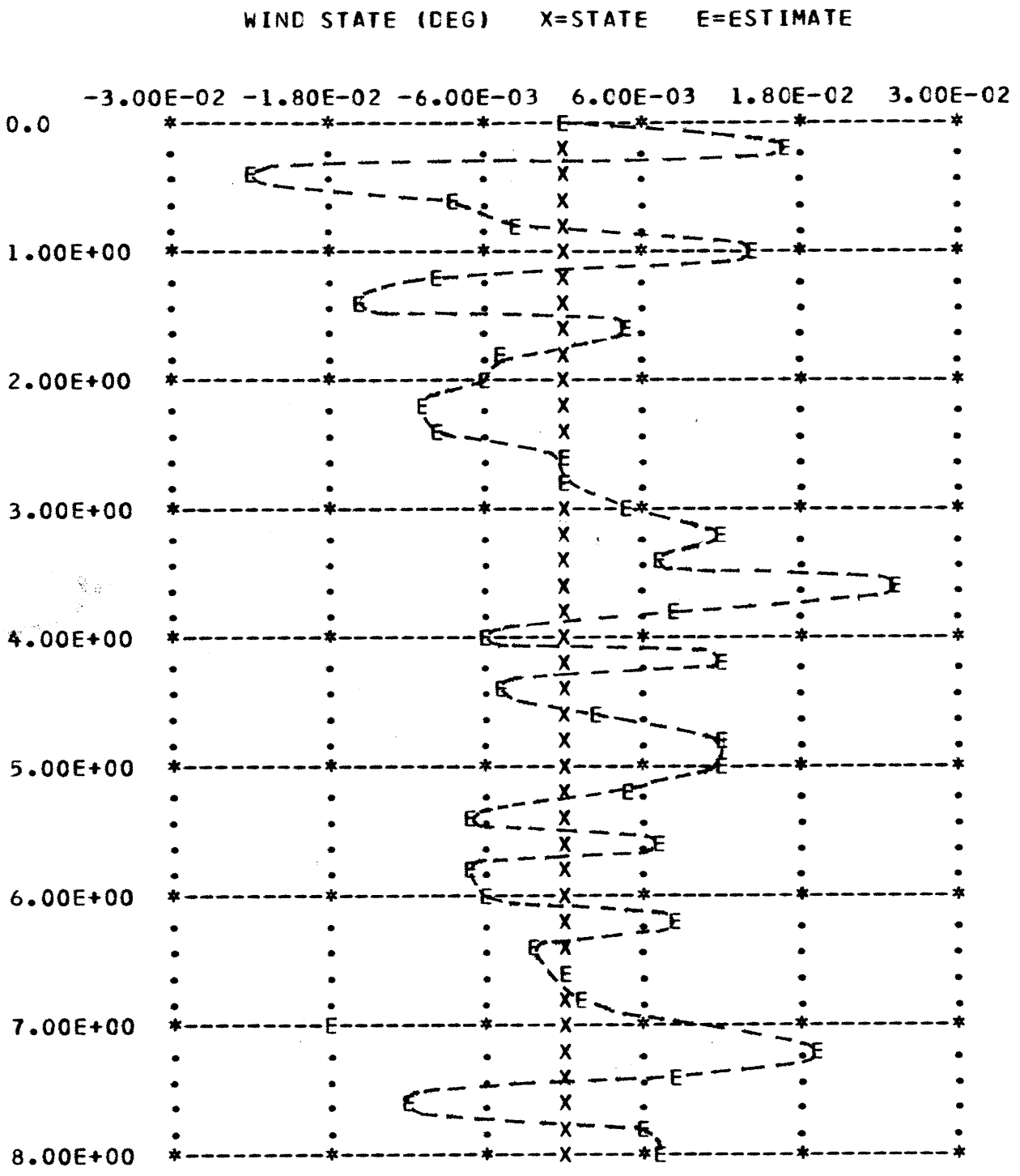

Figure D.2 (i)
KF Simulation I

Conditions for the Simulation of Figure D.3

True model: FC 19

Altitude: 40,000

Speed: Mach 1.4

Dynamic Pressure: 537 psf

Initial Conditions on the state: 45 degree bank angle (all others zero)

Initial Conditions on the filter: 45 degree bank angle

This is a matched simulation in which the filter and control gains for the true model are used. Observation noise is included, but plant noise is not included.

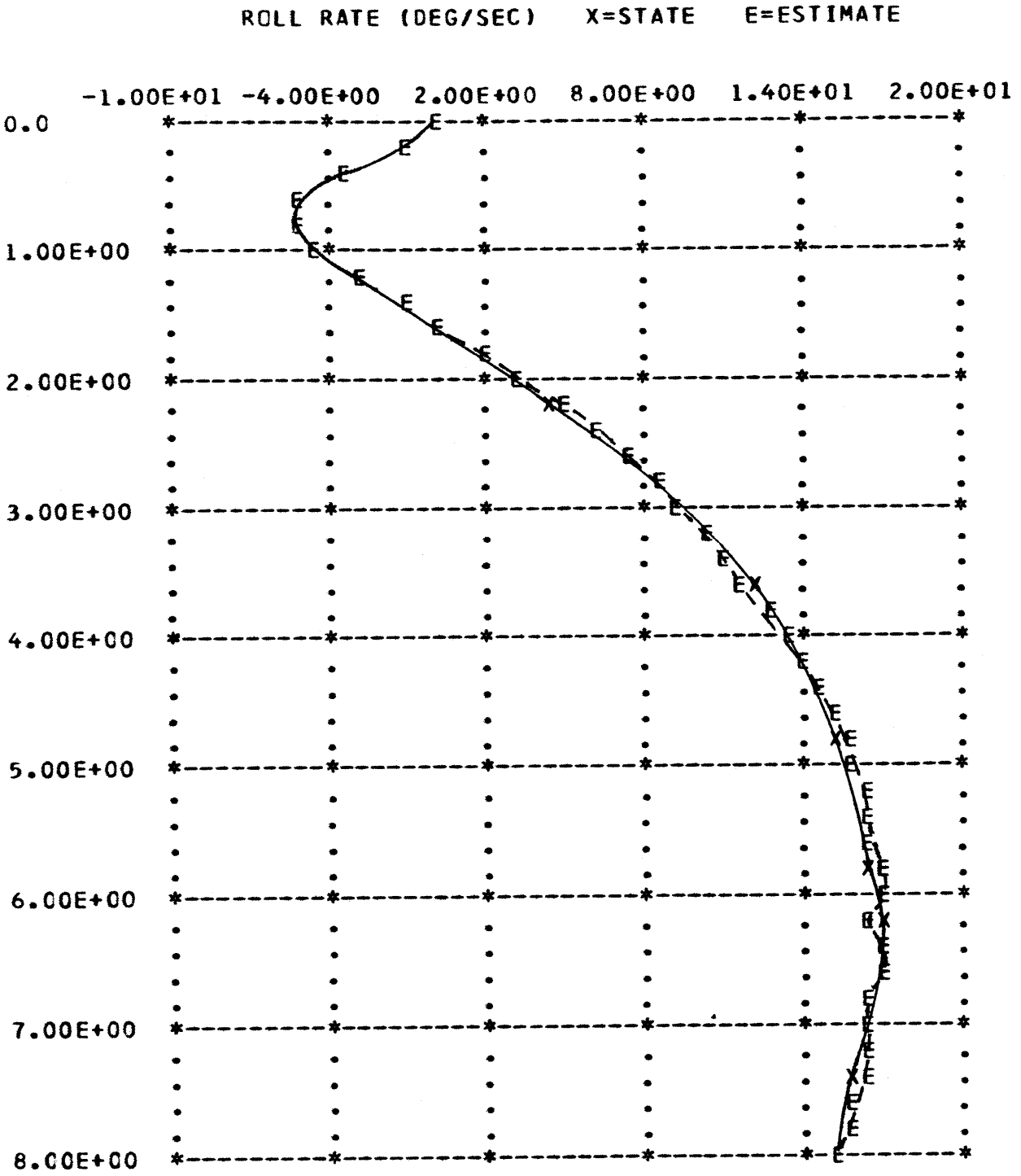

Figure D.3 (a)
KF Simulation II

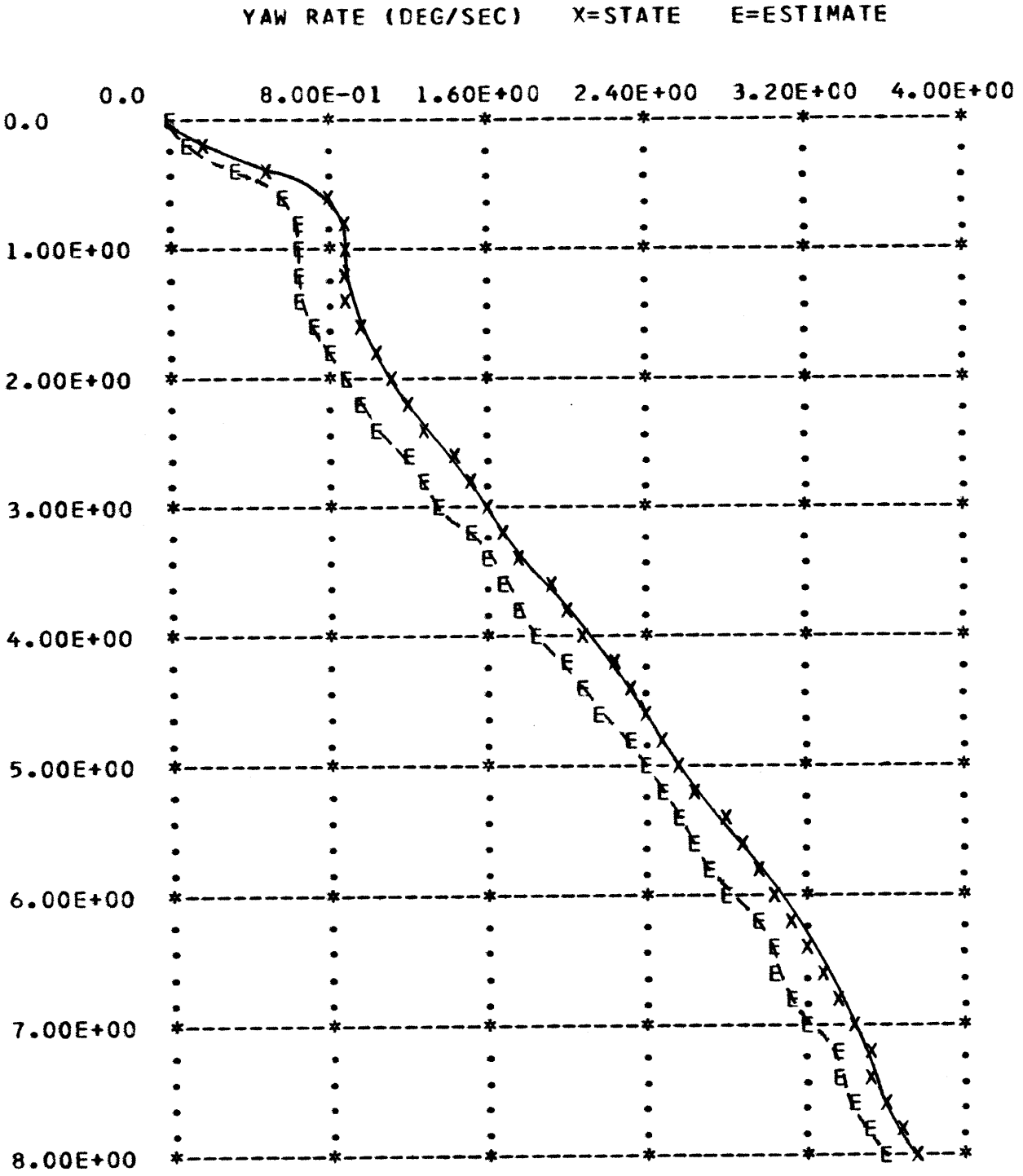

Figure D.3 (b)
KF Simulation II

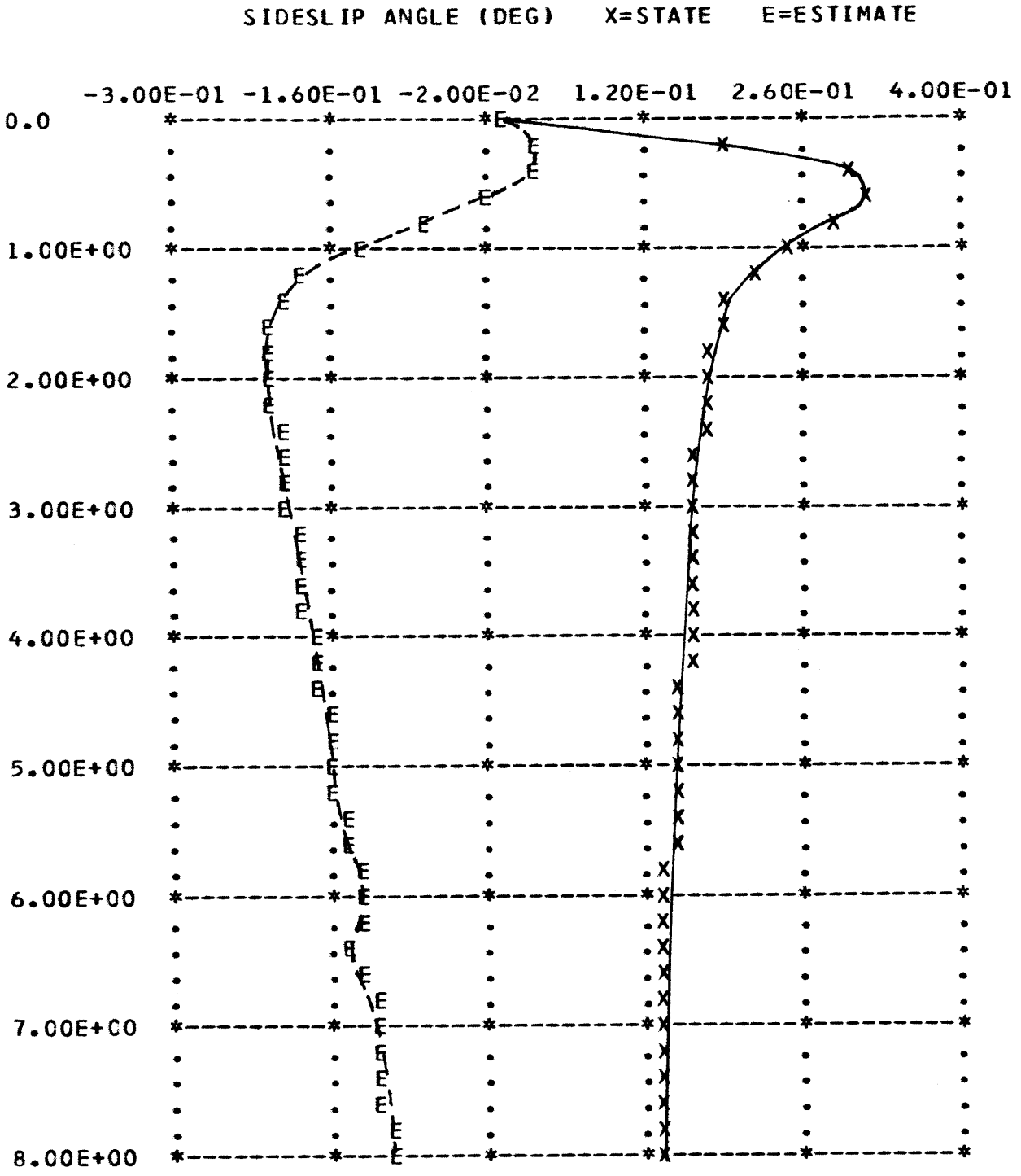

Figure D.3 (c)
KF Simulation II

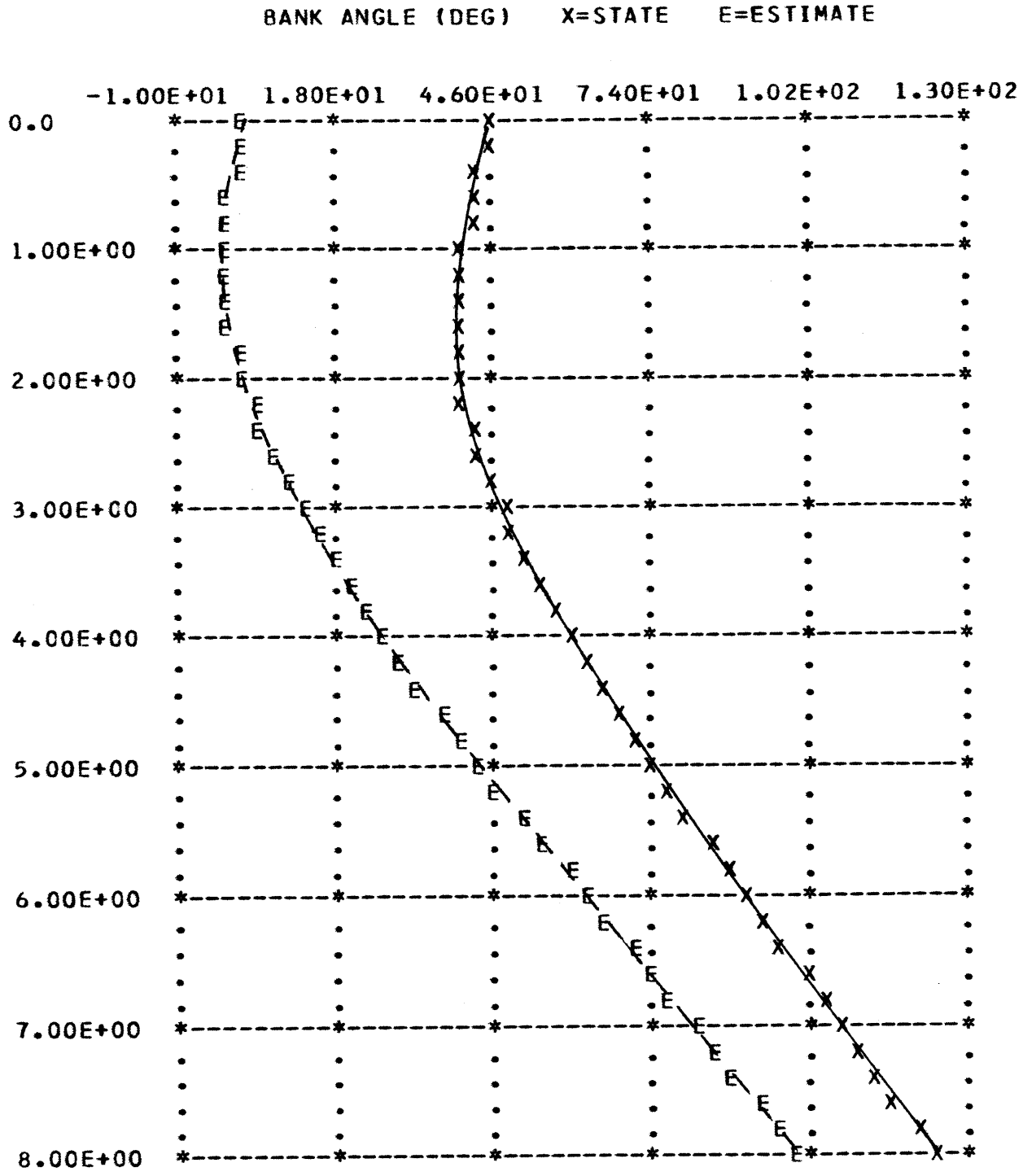

Figure D.3 (d)
KF Simulation II

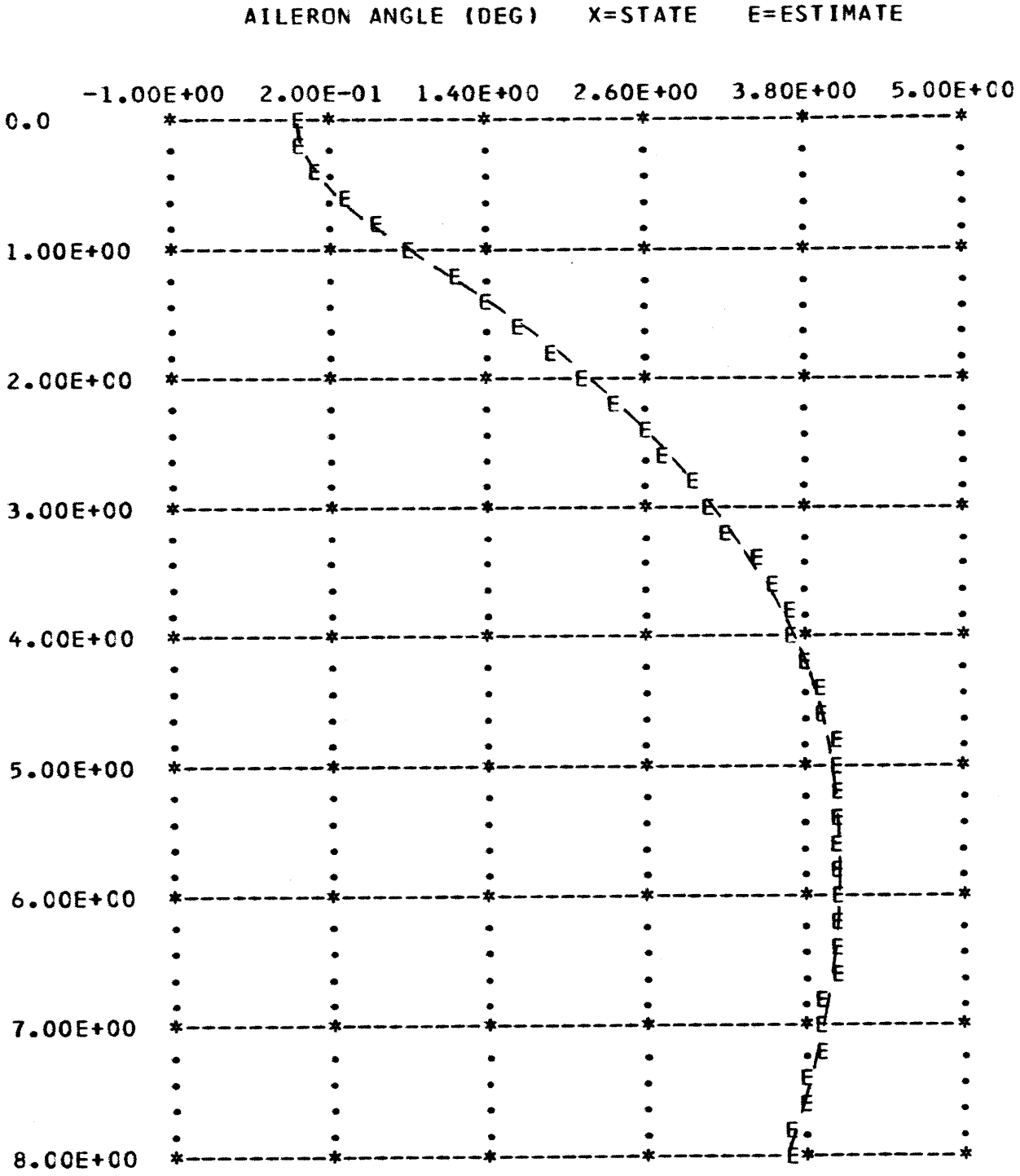

Figure D.3(e)
KF Simulation II

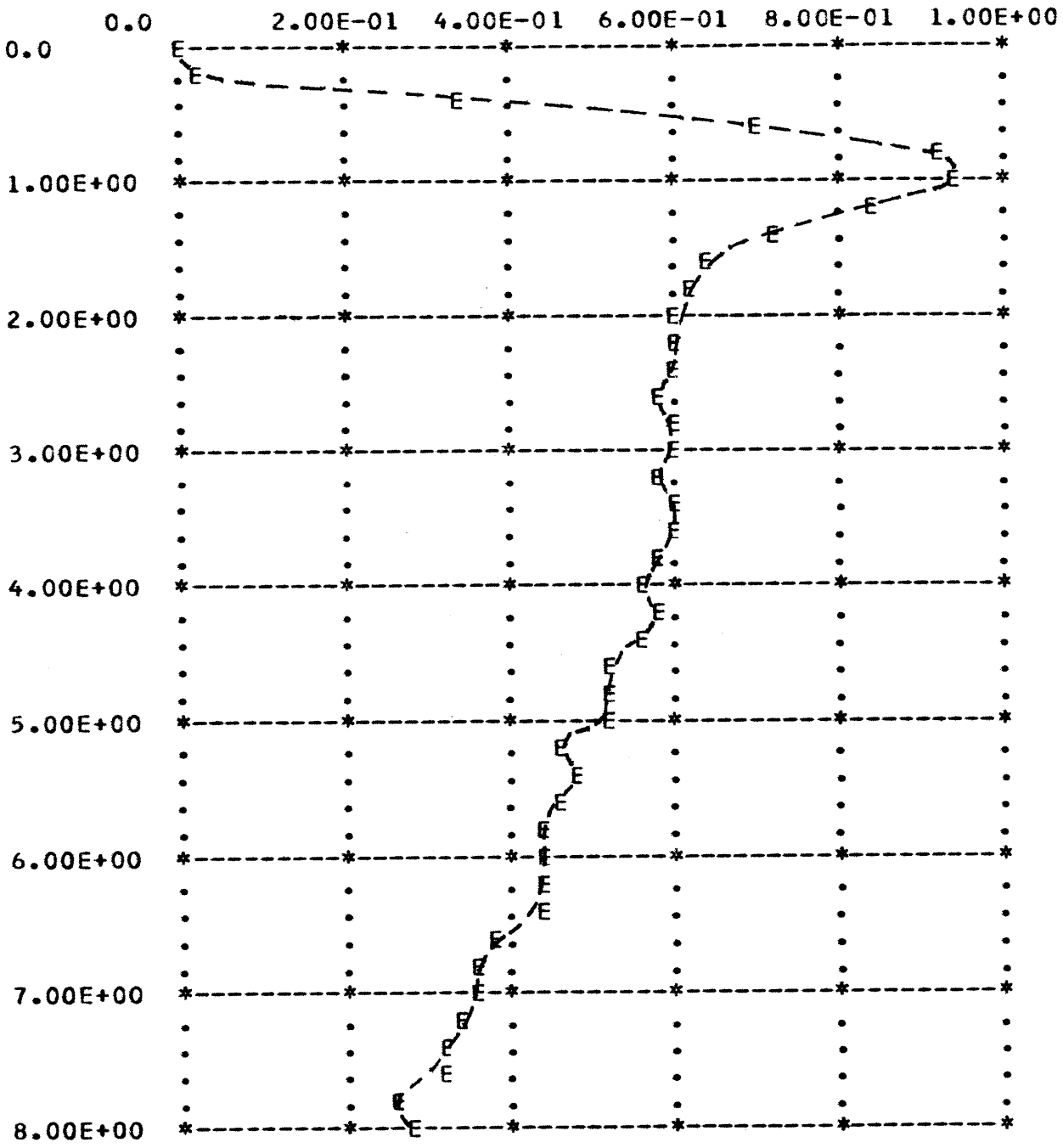

Figure D.3 (f)
KF Simulation II

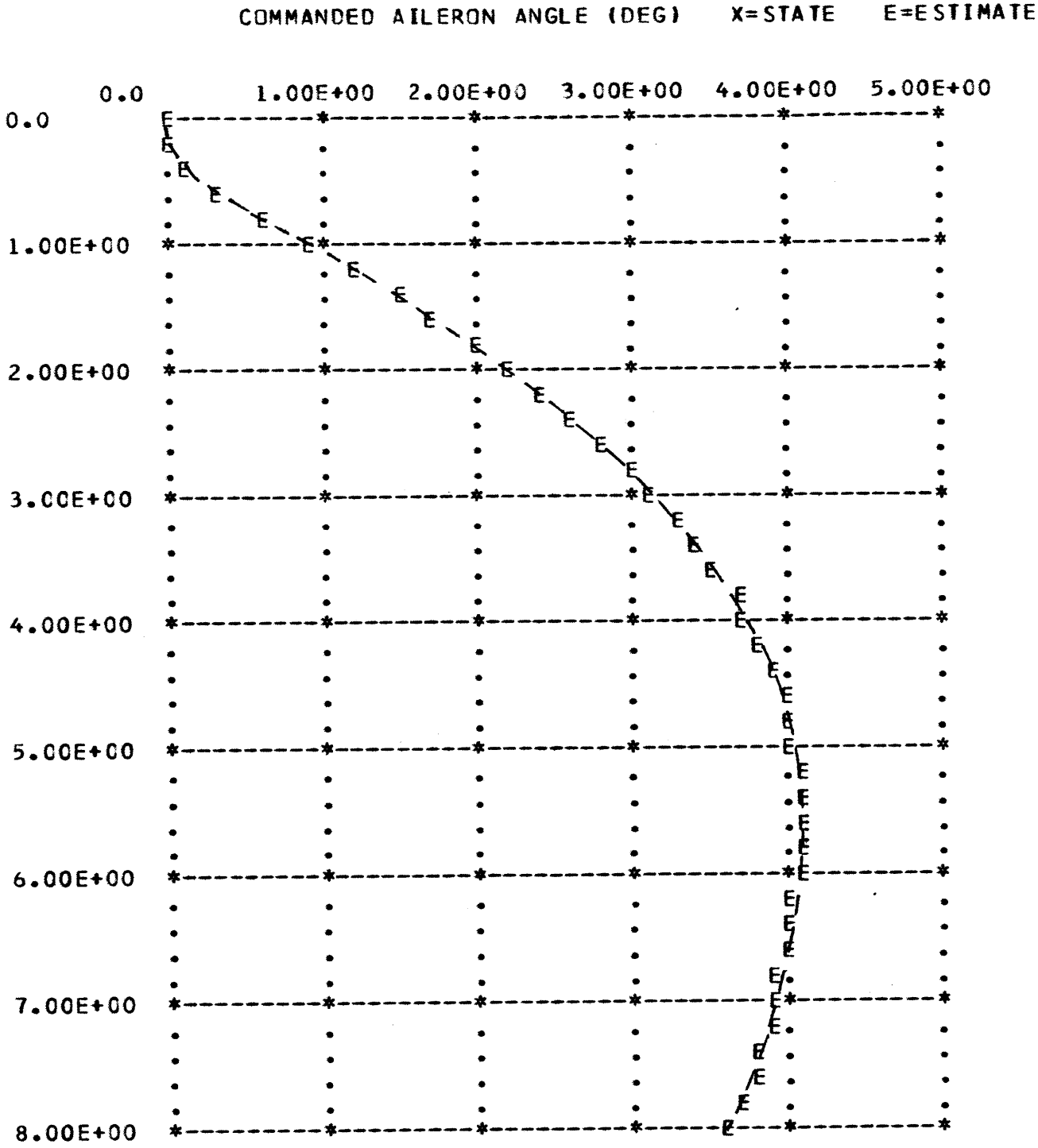

Figure D.3 (g)
KF Simulation II

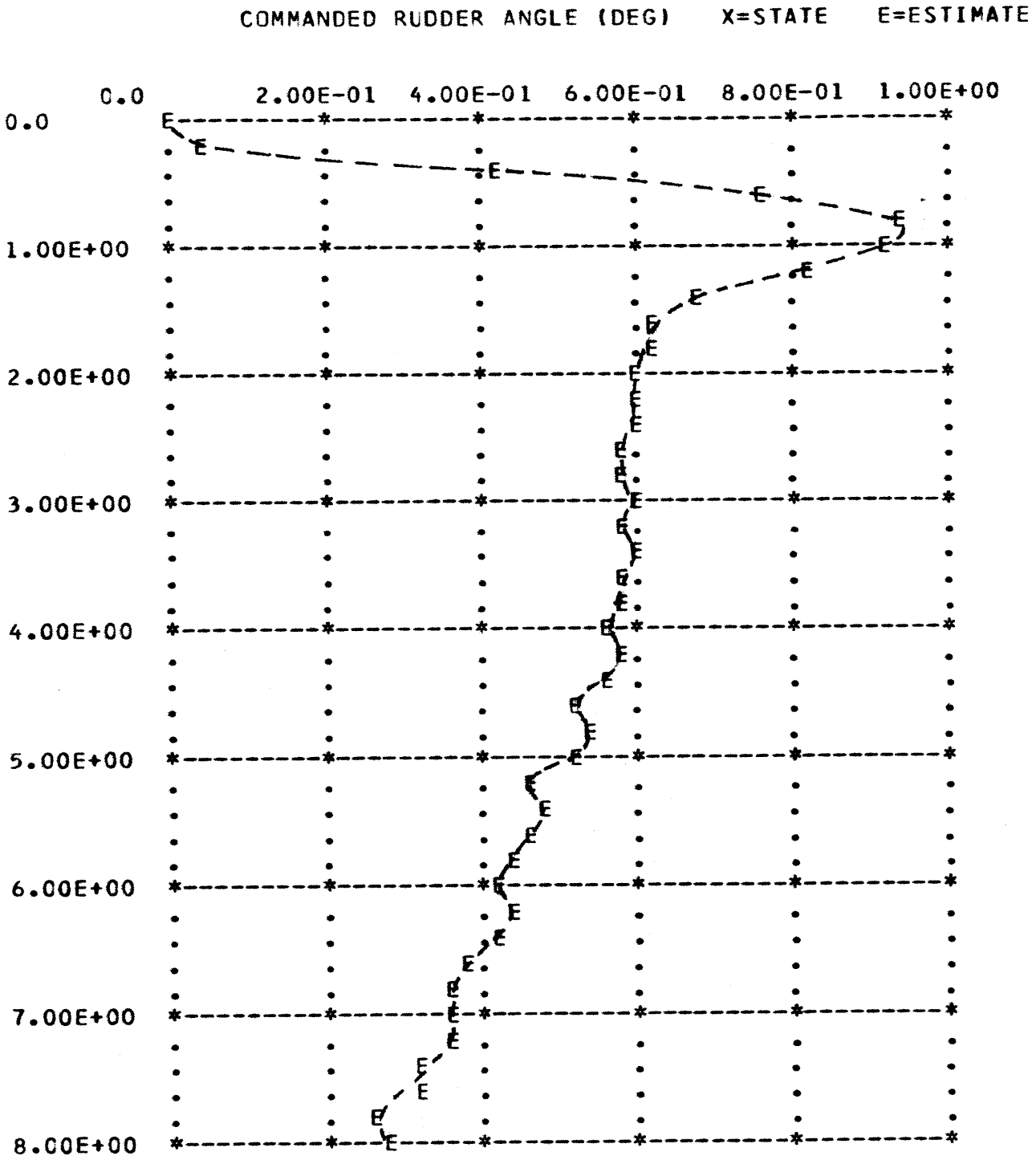

Figure D.3 (h)
KF Simulation II

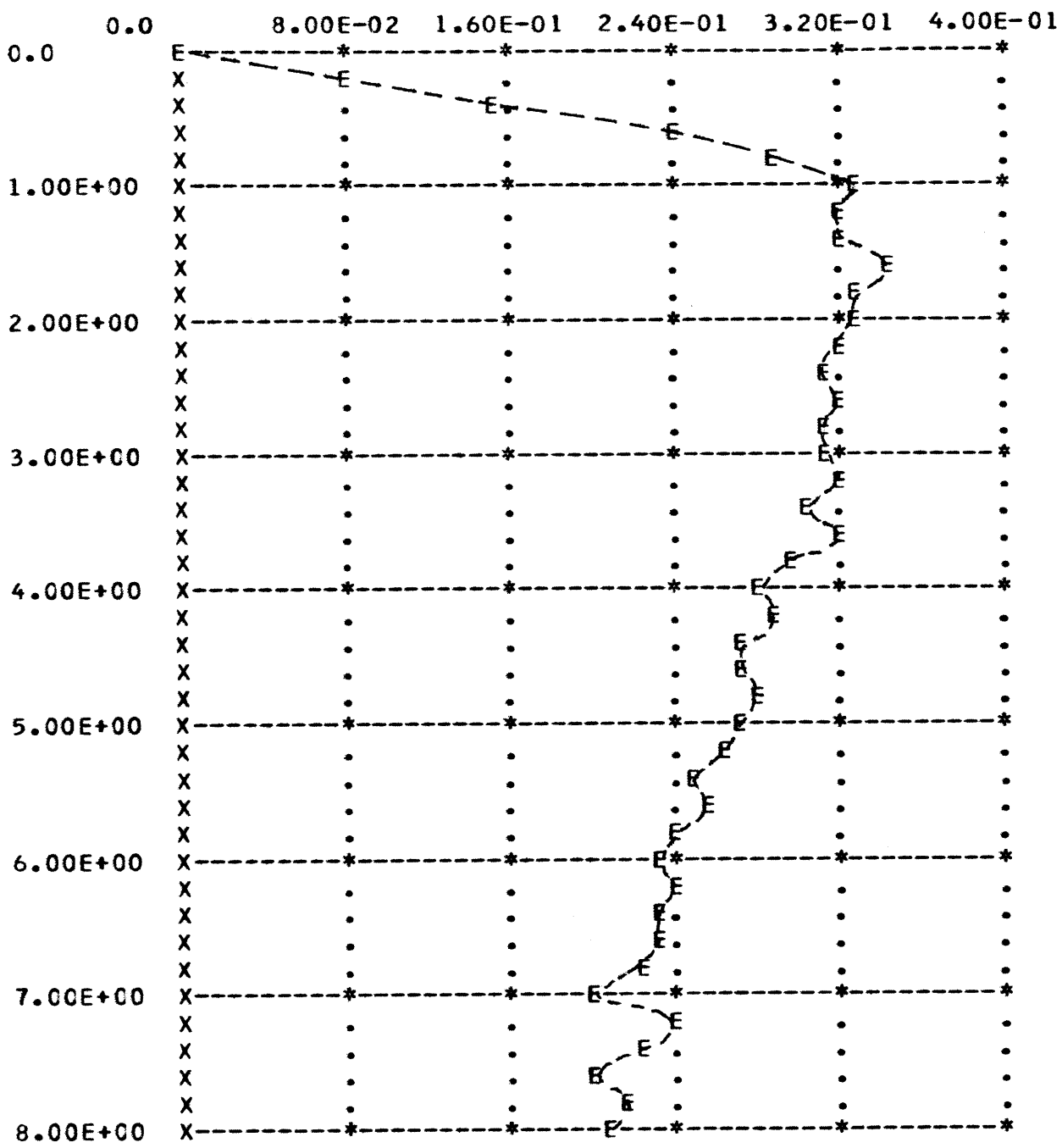

Figure D.3 (i)
KF Simulation II

Conditions for the Simulation of Figure D.4

True model: FC 19

Altitude: 40,000 feet

Speed: Mach 1.4

Dynamic pressure: 537 psf

Initial Conditions on the state: two degree sideslip angle (all others zero)

Initial Conditions on the filters: zero

Models available in MMAC: 8, 14, 18, 19 and 20

Initial probabilities: all models equal.

This simulation has the full MMAC controller turned on and the true model included in the available models. There is no noise introduced.

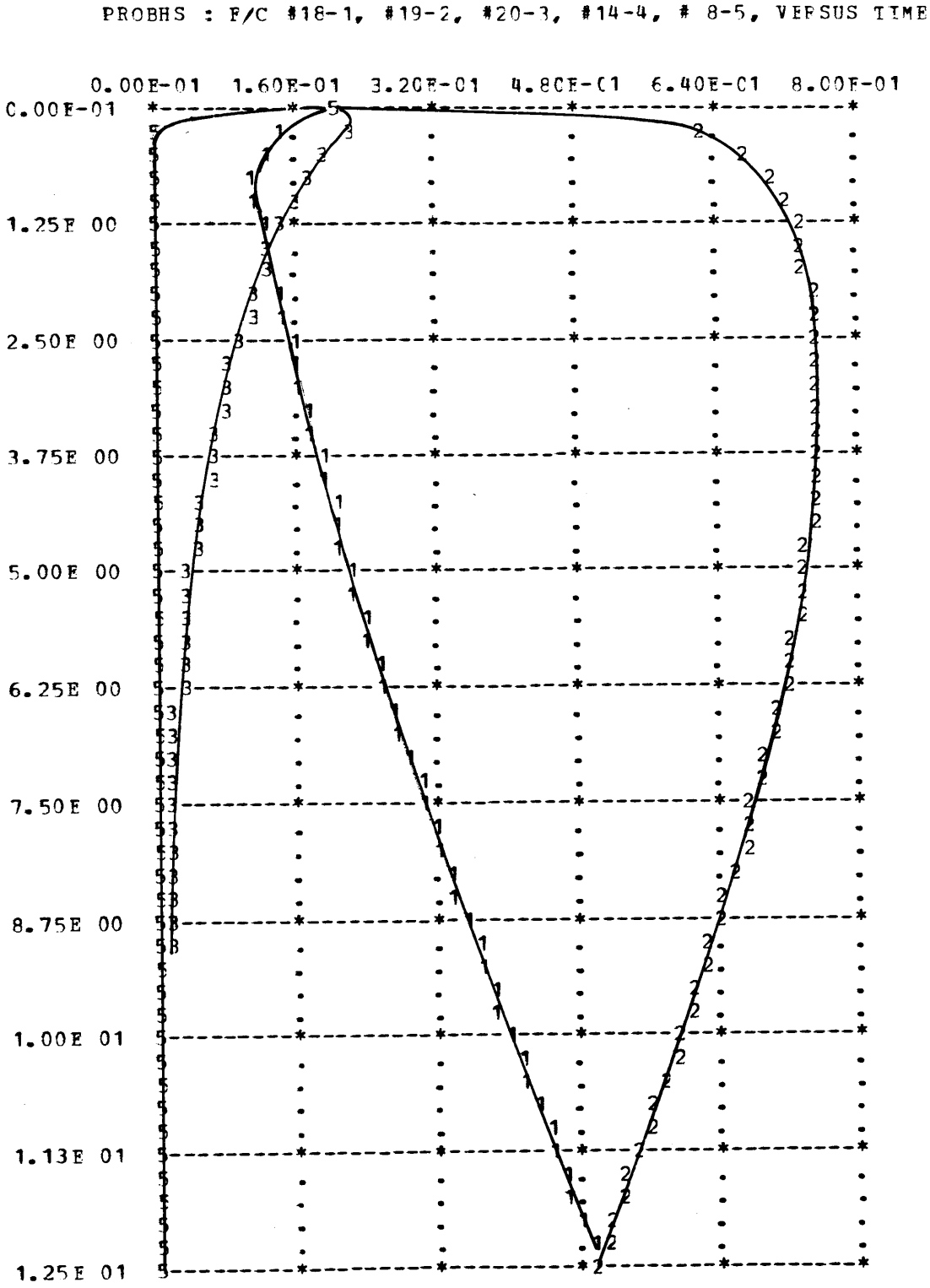

Figure D.4 (a)
MMAC Simulation
True Model Included

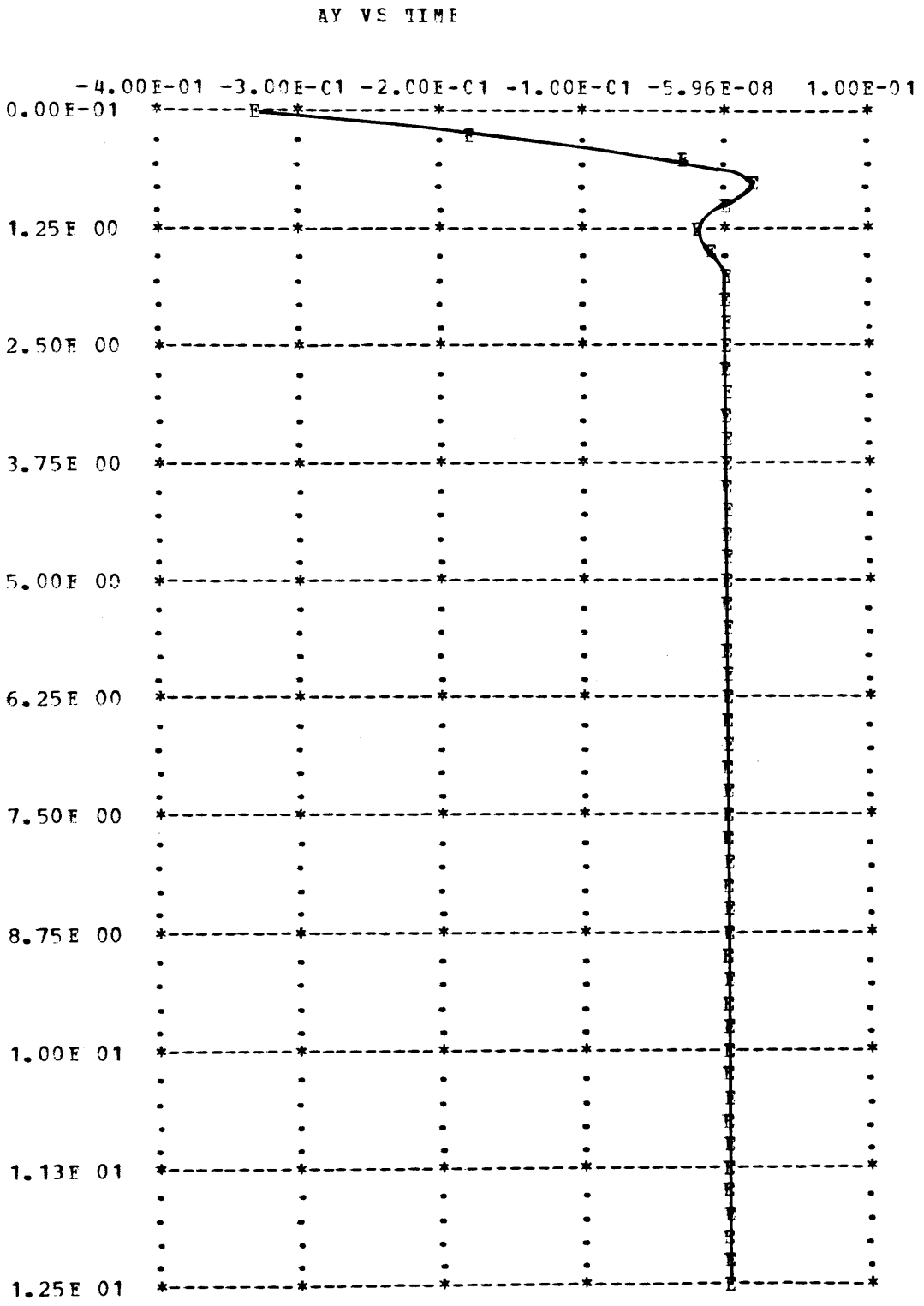

Figure D.4 (b)
MMAC Simulation
True Model Included

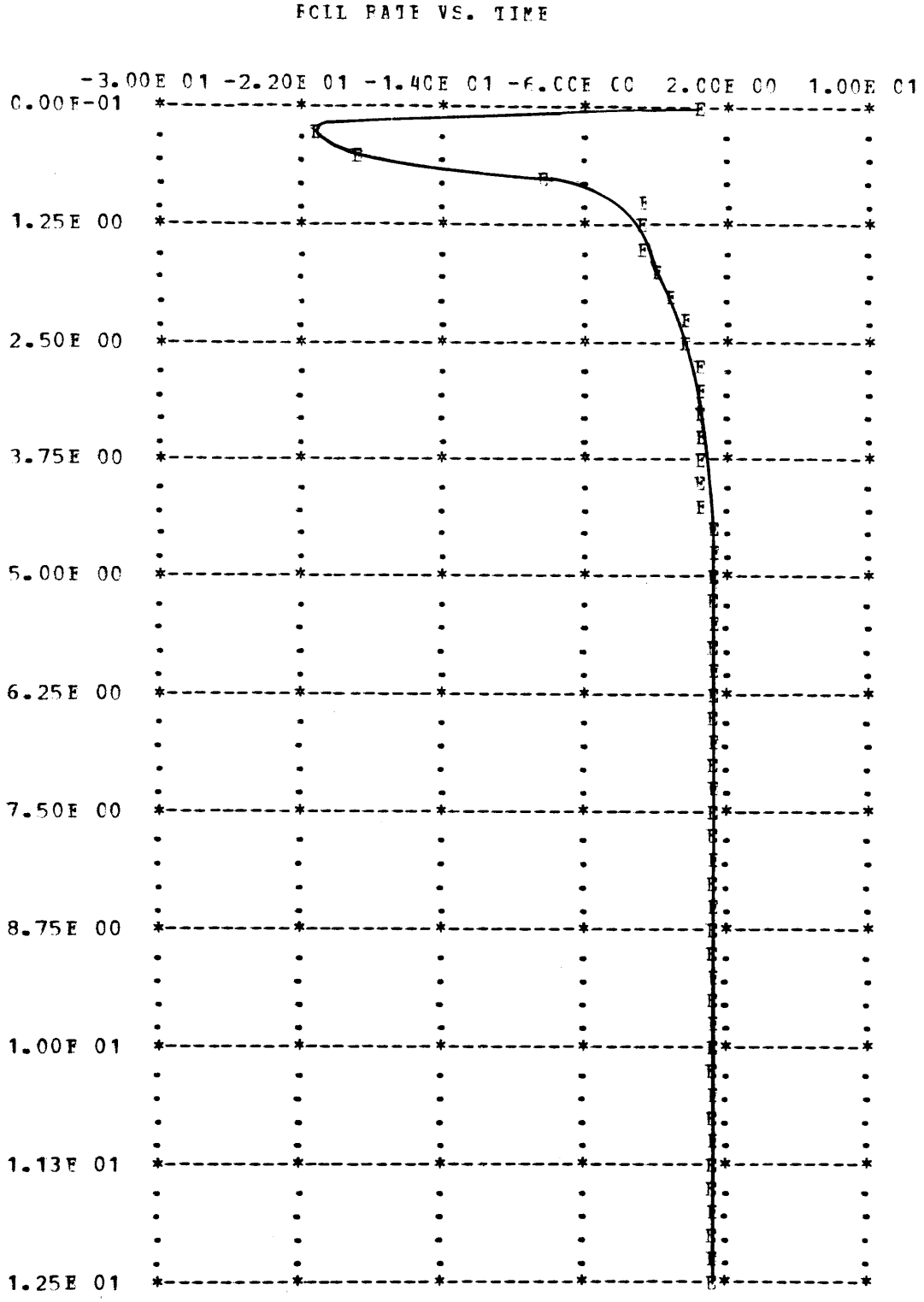

Figure D.4 (c)
MMAC Simulation
True Model Included

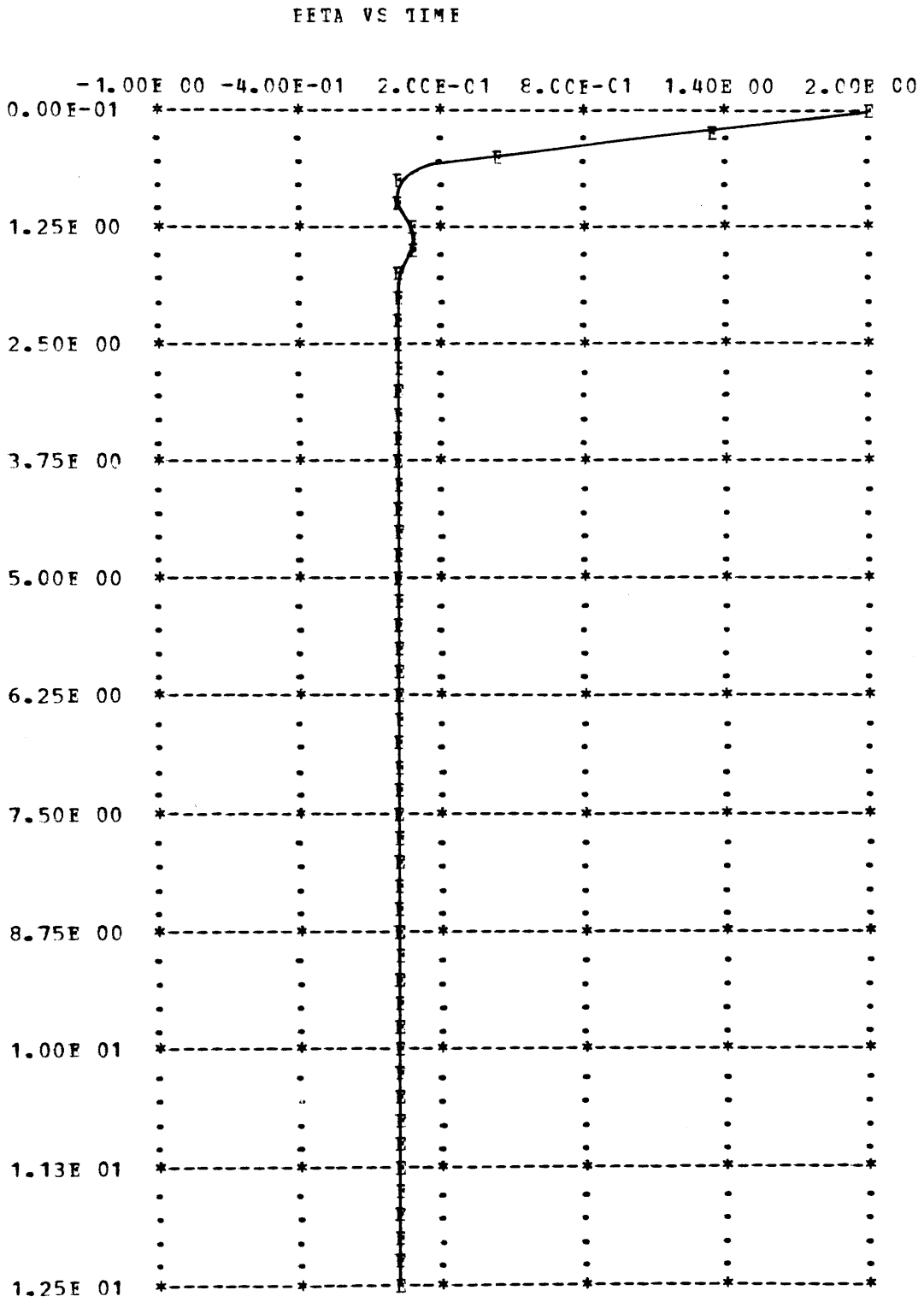

Figure D.4 (d)
MMAC Simulation
True Model Included

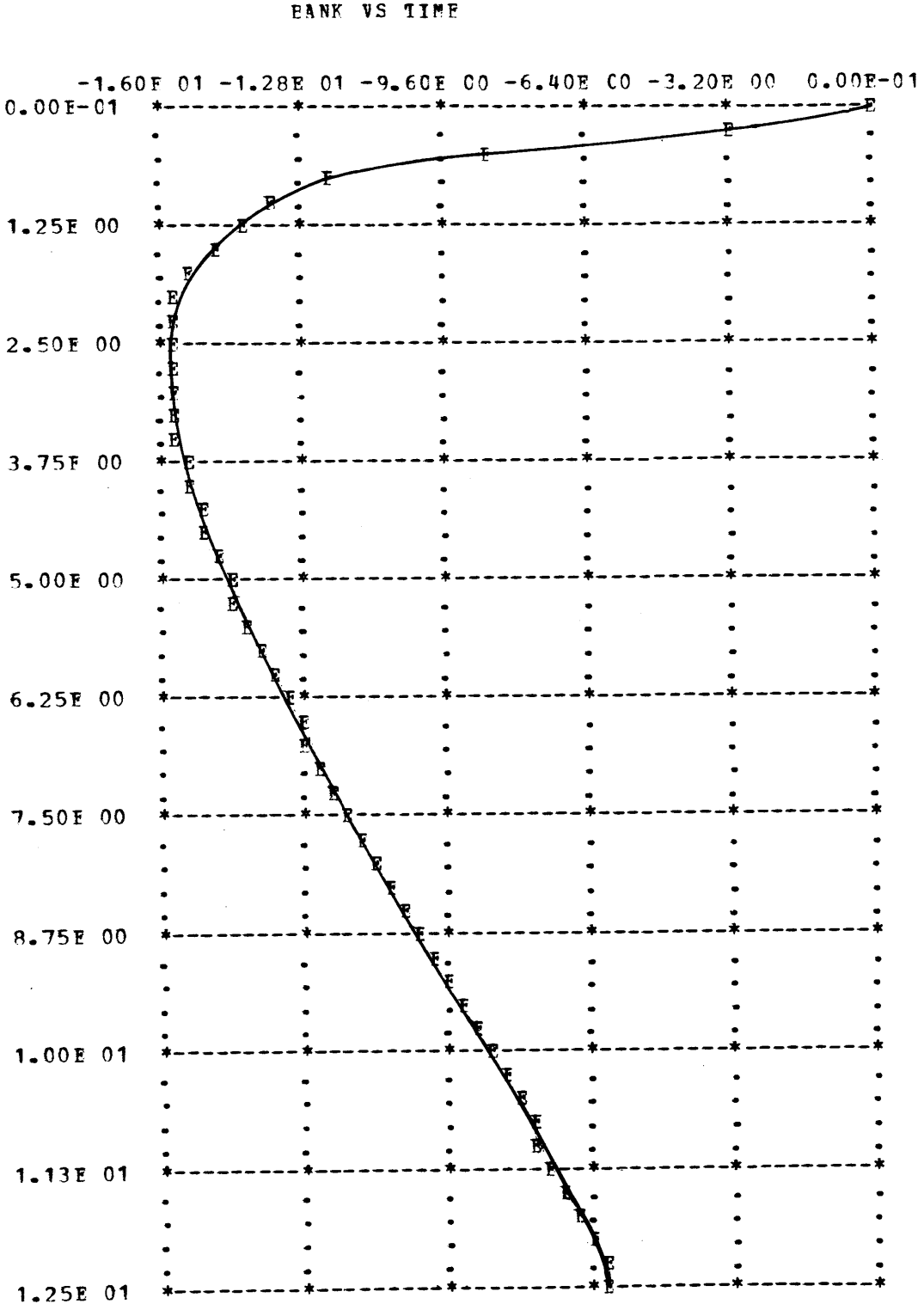

Figure D.4 (e)
MMAC Simulation
True Model Included

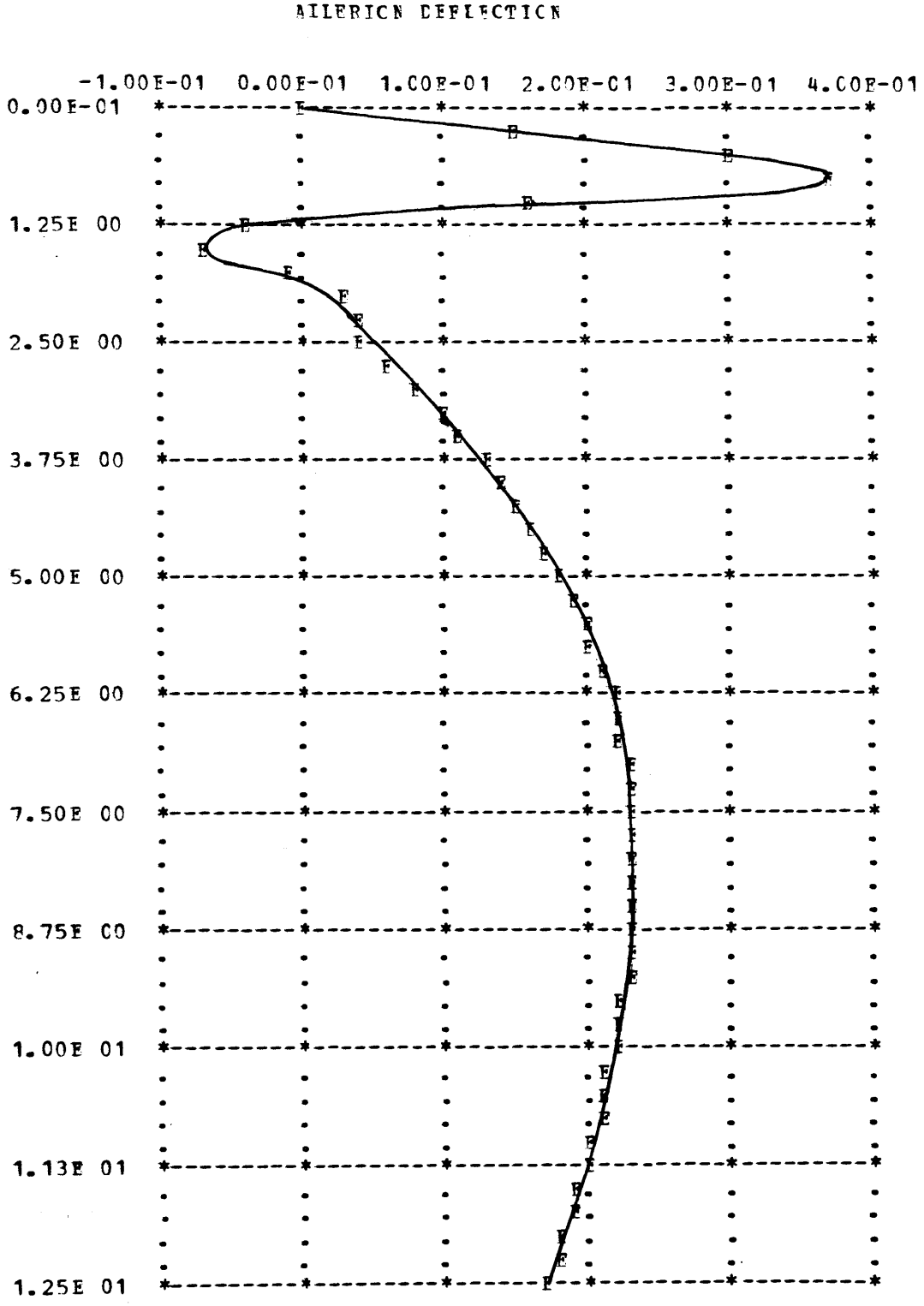

Figure D.4 (f)
MMAC Simulation
True Model Included

Conditions for the Simulation of Figure D.5

True model: FC 19

Altitude: 40,000 feet

Speed: Mach 1.4

Dynamic Pressure: 537 psf

Initial Conditions on the state: two degree sideslip angle (all others zero)

Initial Conditions on the filters: zero

Models available in MMAC: 8, 14, 18, 17 and 20

Initial probabilities: all models equal.

This simulation has the full MMAC controller turned on and the true model not included in the available models. There is no noise introduced.

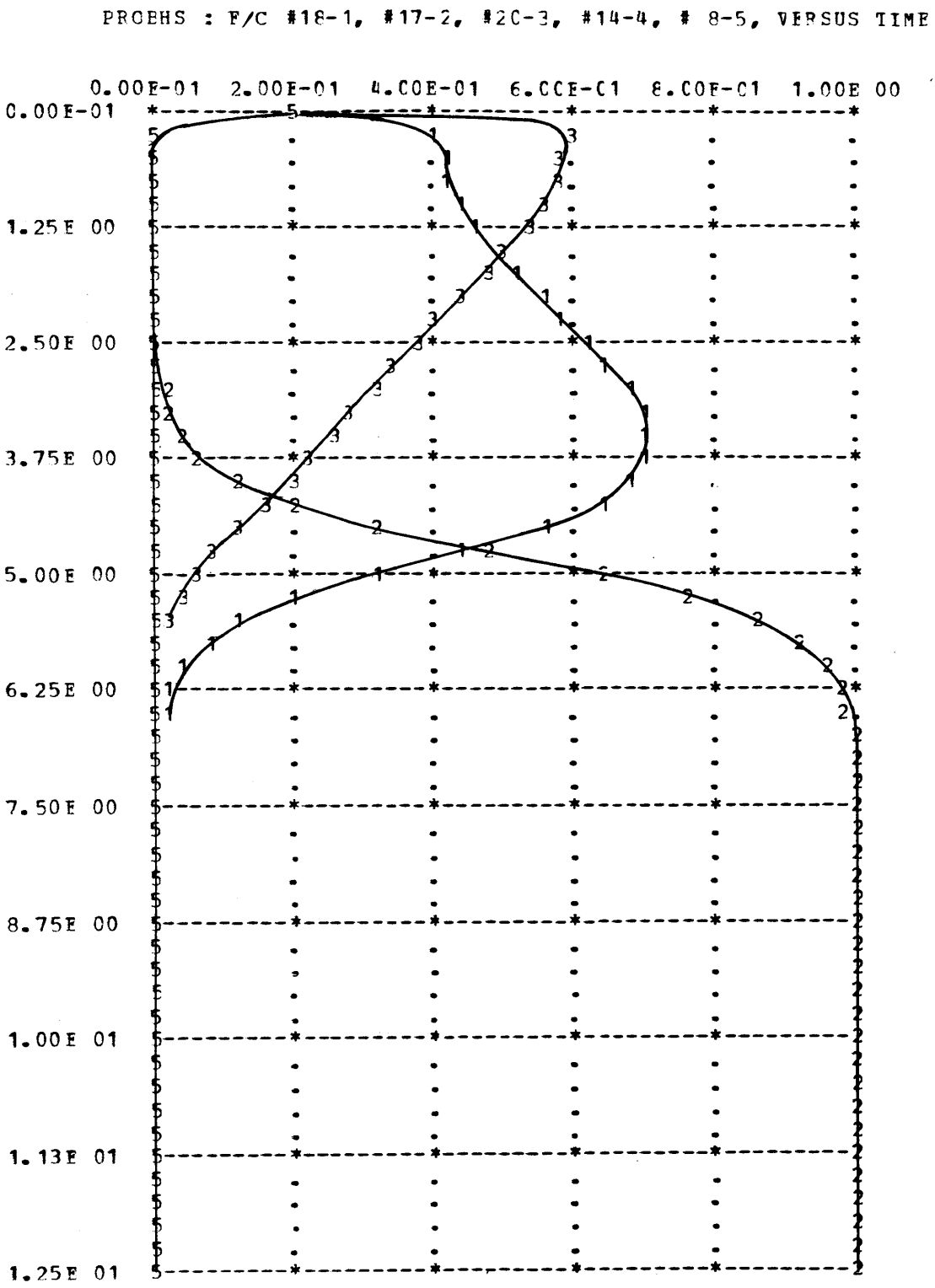

Figure D.5 (a)
MMAC Simulation
True Model Not Included

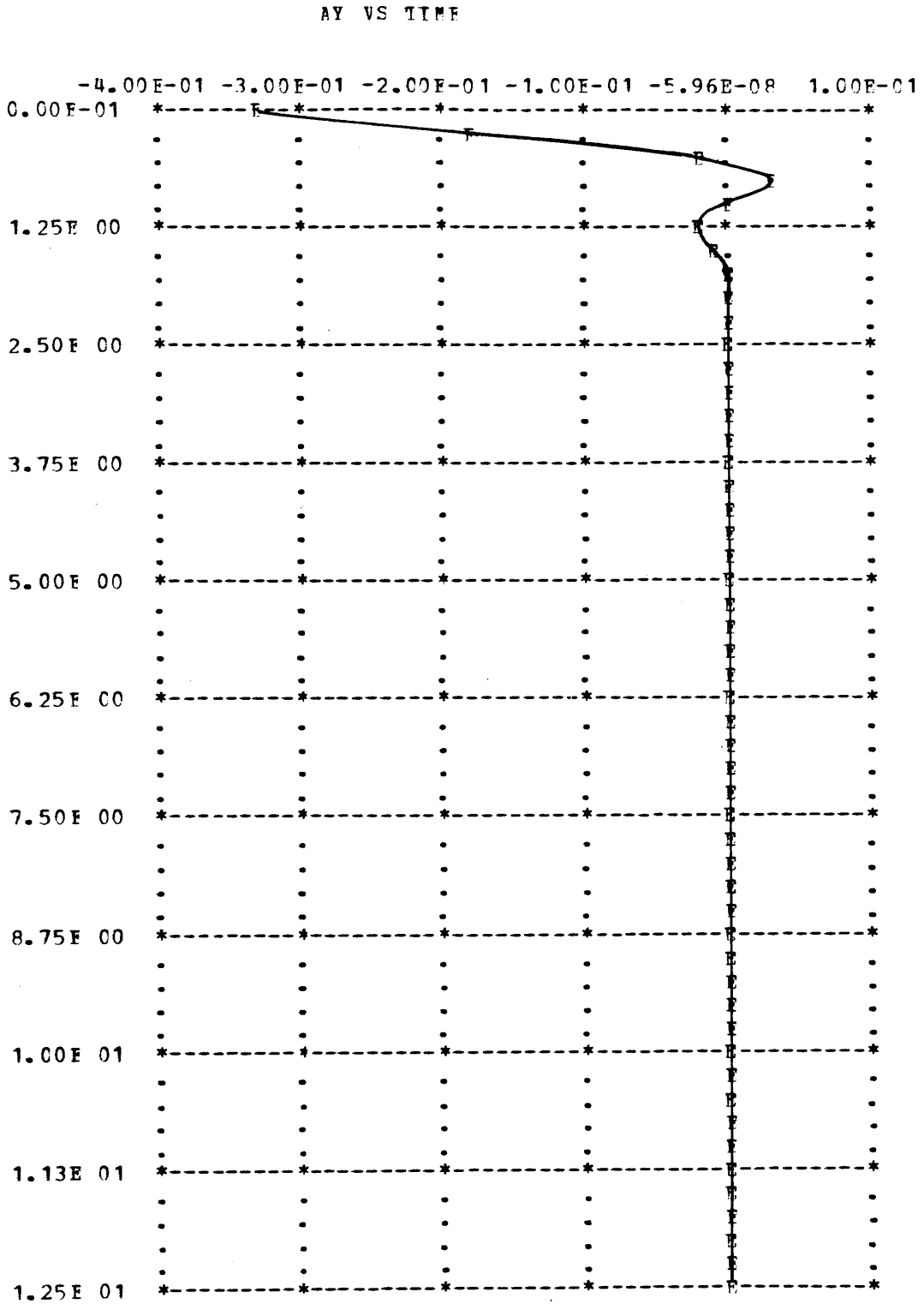

Figure D.5 (b)
MMAC Simulation
True Model Not Included

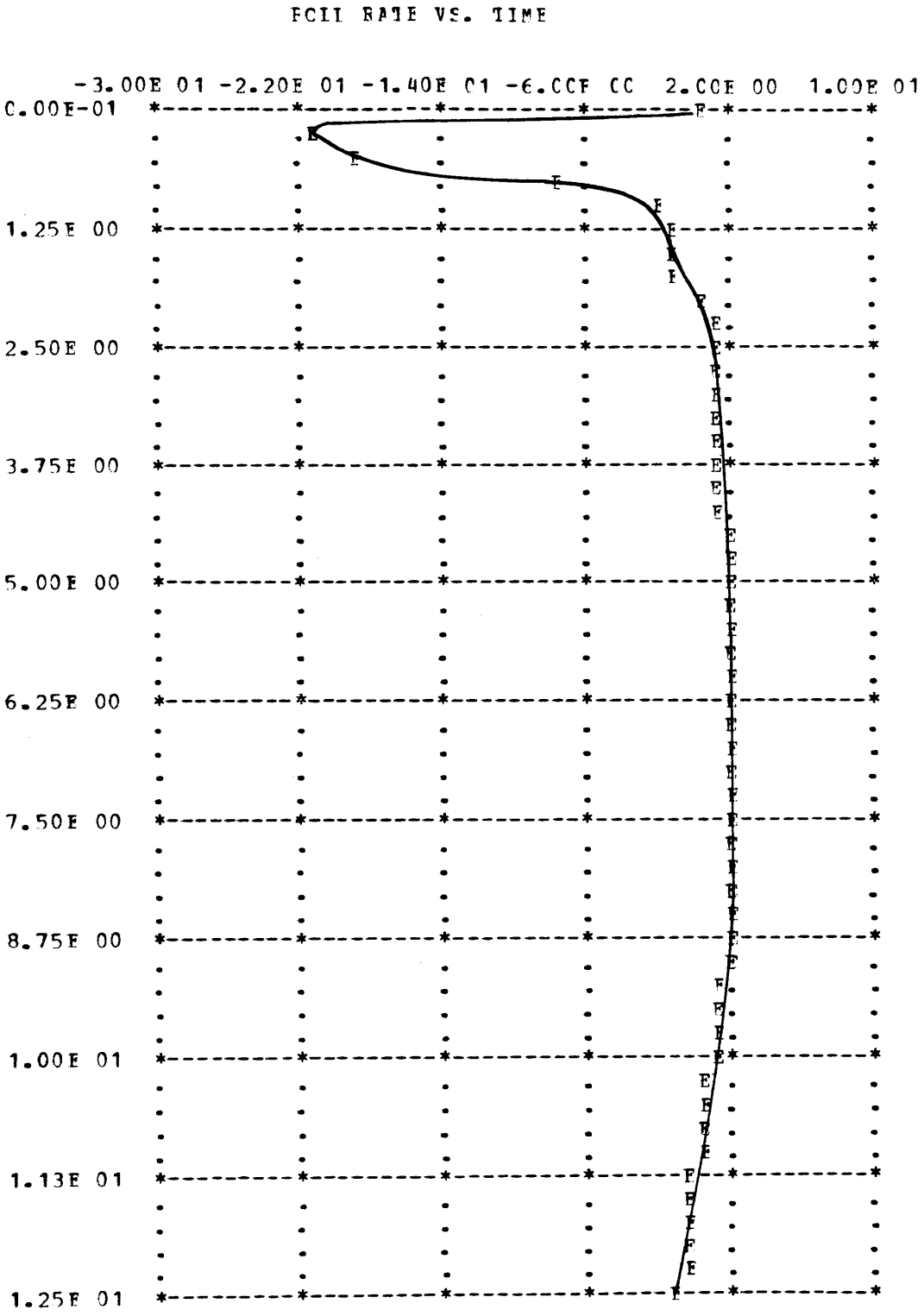

Figure D.5 (c)
MMAC Simulation
True Model Not Included

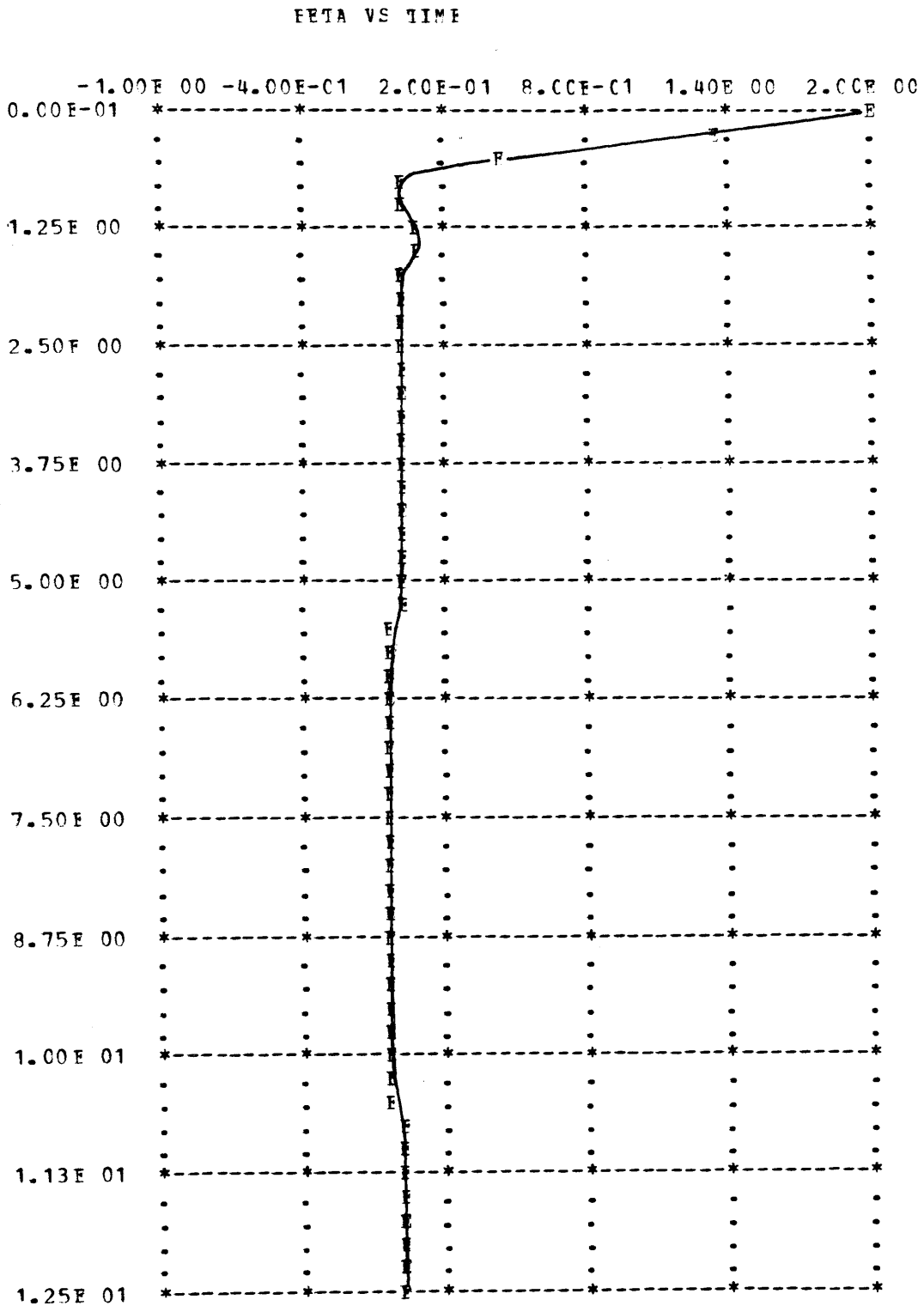

Figure D.5 (d)
MMAC Simulation
True Model Not Included

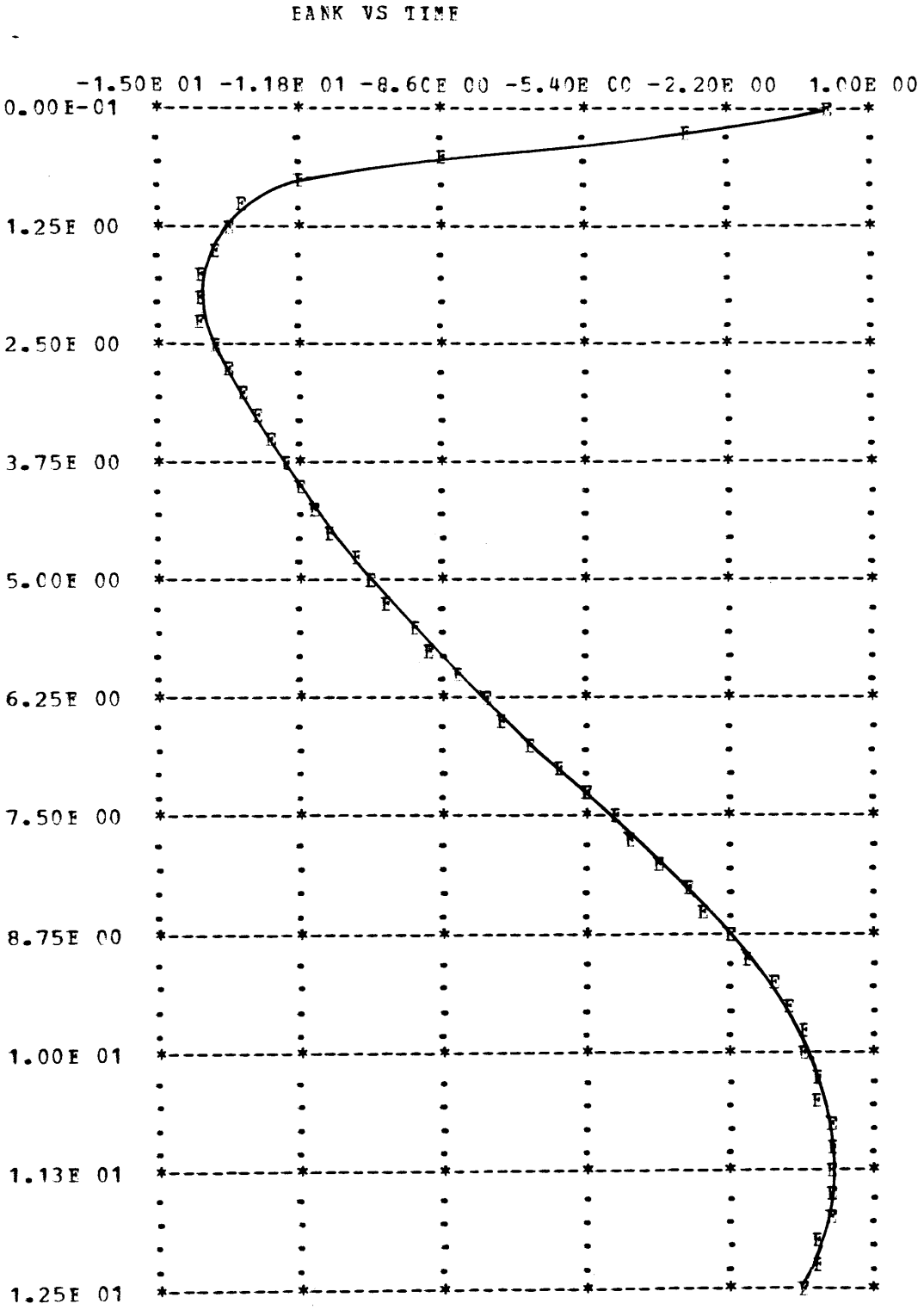

Figure D.5 (e)
MMAC Simulation
True Model Not Included

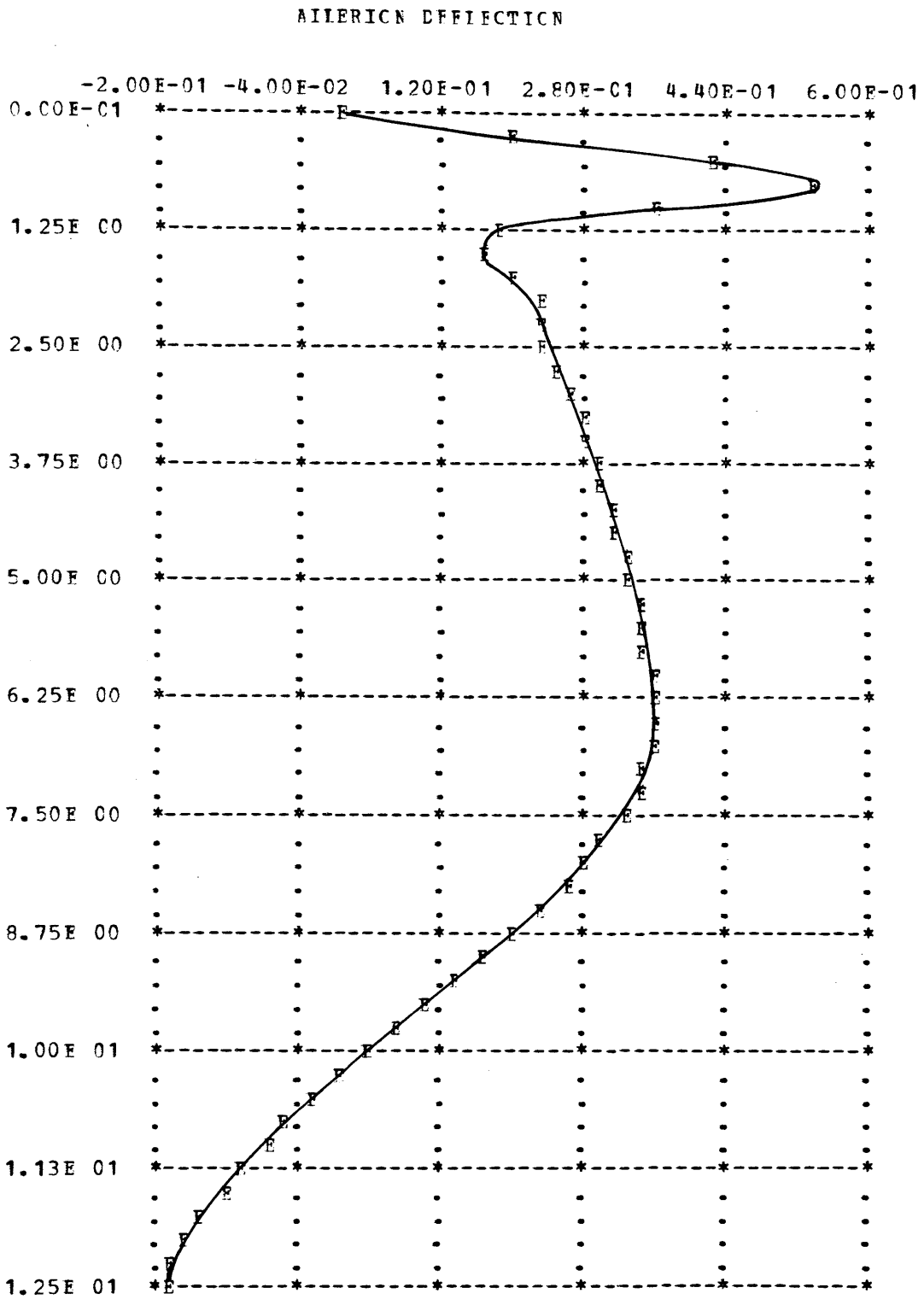

Figure D.5 (f)
MMAC Simulation
True Model Not Included

APPENDIX E

LATERAL DYNAMICS
NONLINEAR SIMULATION RESULTS

Conditions for the Simulations of Figures E.1 and E.2

True model: FC 11

Altitude: 20,000

Speed: Mach .6

Dynamic Pressure:

Initial Conditions on the state: two degree sideslip angle

Initial Conditions on the filter: zero

Figure E.1 shows the open loop response while Figure E.2 shows the response when the matched controller is used. Sensor noise is included. However, turbulence is not included.

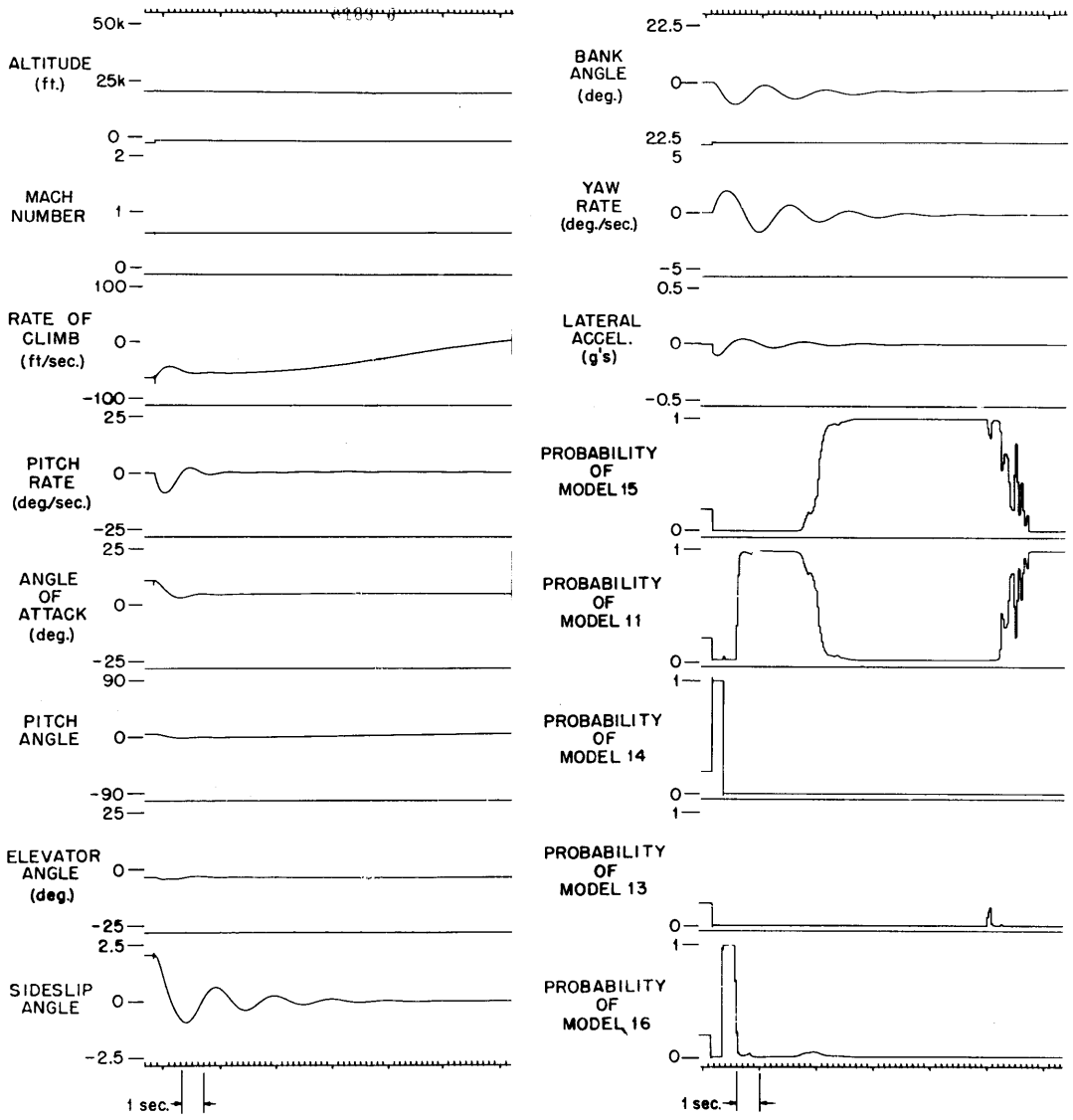

Figure E.1 Open Loop Simulation FC11

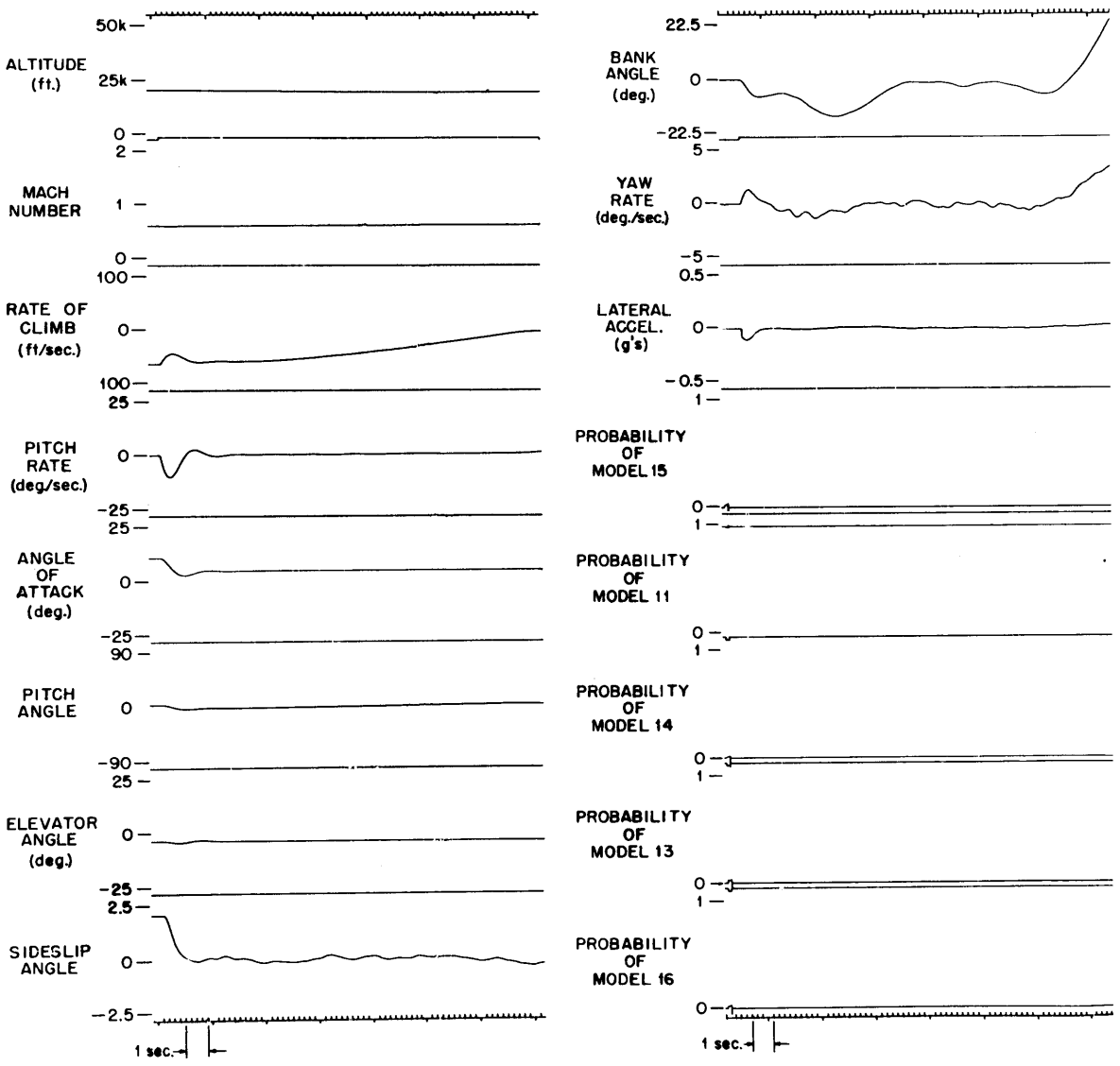

Figure E.2 Closed Loop Optimal Simulation

Conditions for the Simulations of Figures E.3, 4 and 5

True model: FC 7

Altitude: sea level

Speed: Mach .7

Dynamic Pressure: 726

Initial Conditions on the state: a two degree sideslip angle and a six degree angle of attack.

Initial conditions on the filters: zero

Models available to the controller: 5, 7, 18, 13, and 14

Initial probabilities of the models: all equal

Figure E.3 shows the open loop response, Figure E.4 shows the response with only the lateral controller operating, and Figure E.5 gives the response with the combined lateral-longitudinal controller operating. There is no turbulence, but sensor noise is included.

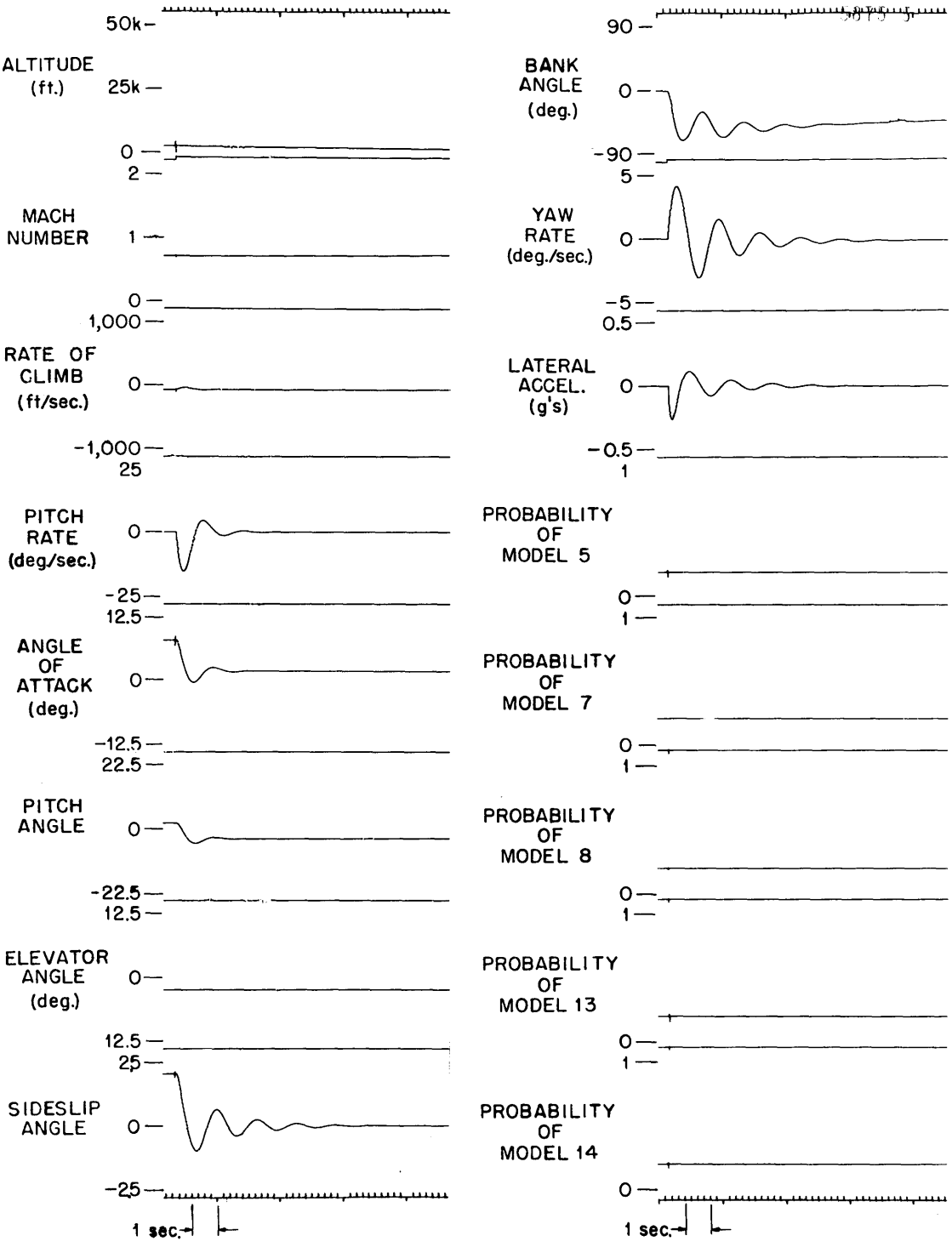

Figure E.3 Open-Loop Response II

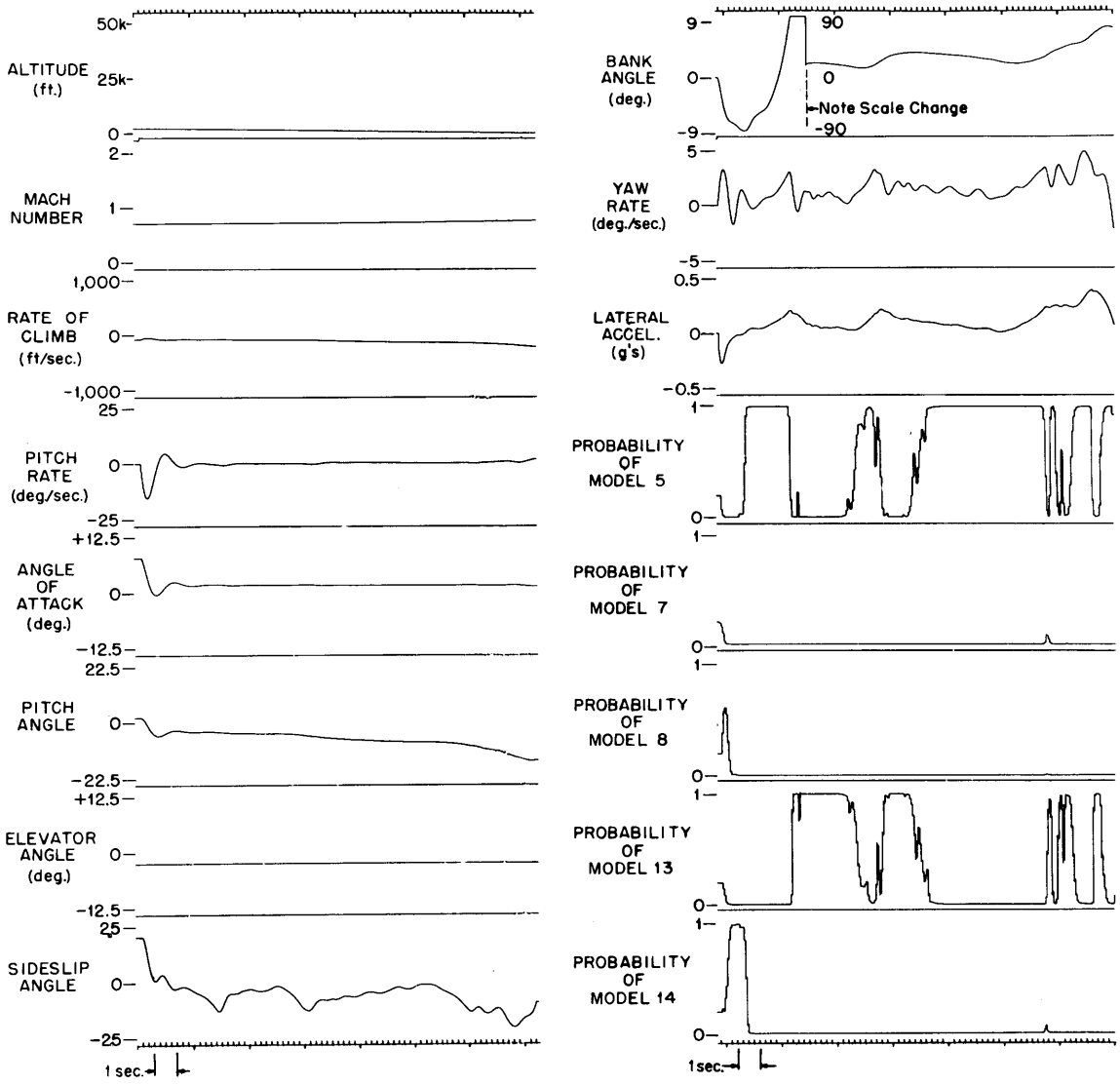

Figure E.4 MMAC Response with Lateral Controller

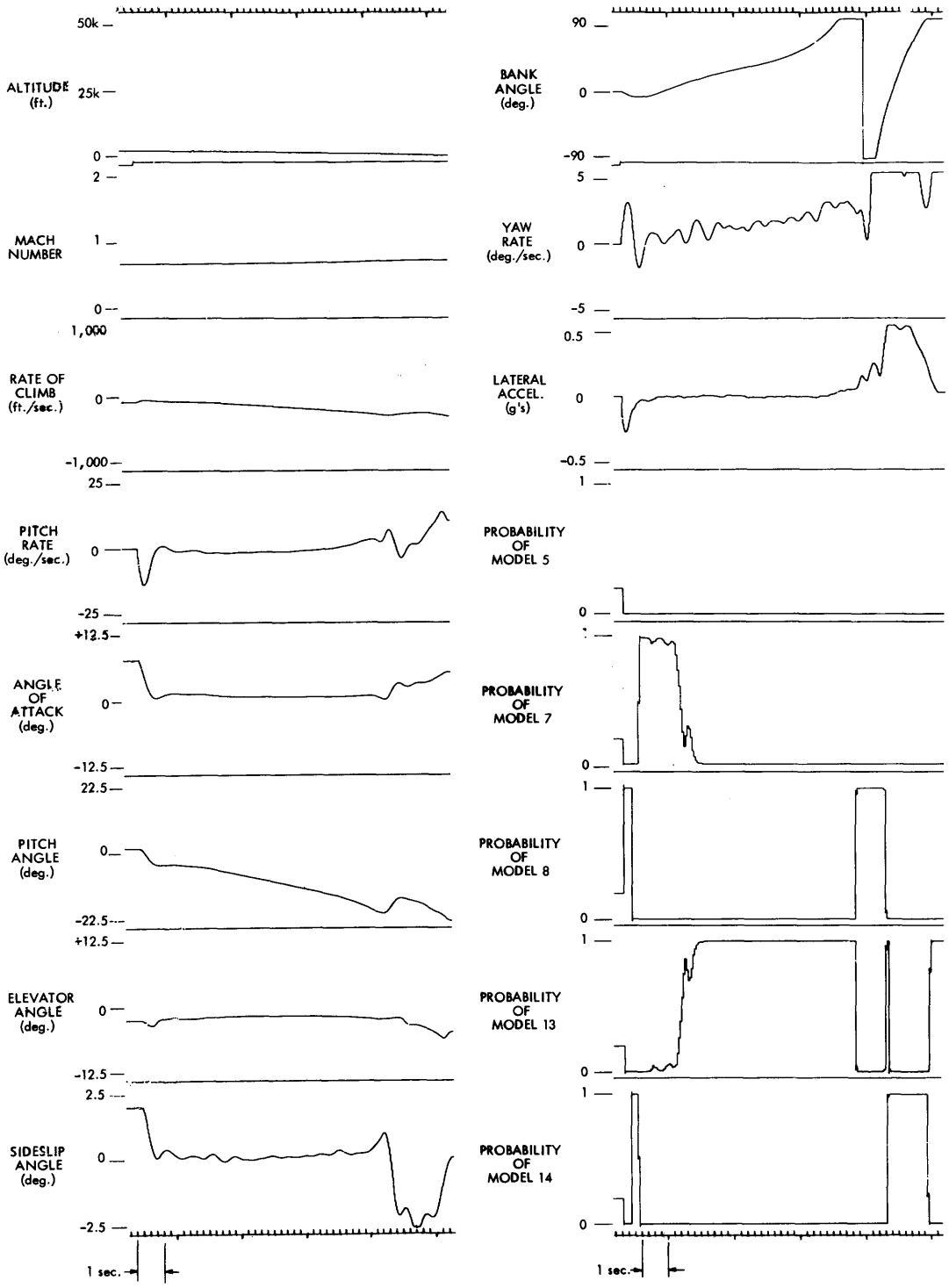

Figure E.5 MMAC Response with Combined Lateral-Longitudinal Controller

Conditions for the Simulations of Figures E.6, 7 and 8

True model: FC 7

Altitude: sea level

Speed: Mach .7

Dynamic Pressure: 726

Initial Conditions on the state: zero

Initial Conditions on the filters: zero

Models available to the controller: 5, 7, 18, 13 and 14

Initial probabilities of models: all equal

Figure E.6 shows the open loop response to moderate turbulence ($\sigma \approx 15$ deg/sec). Figure E.7 gives the response with the lateral controller operating, while Figure E.8 gives the response with the lateral-longitudinal controller included.

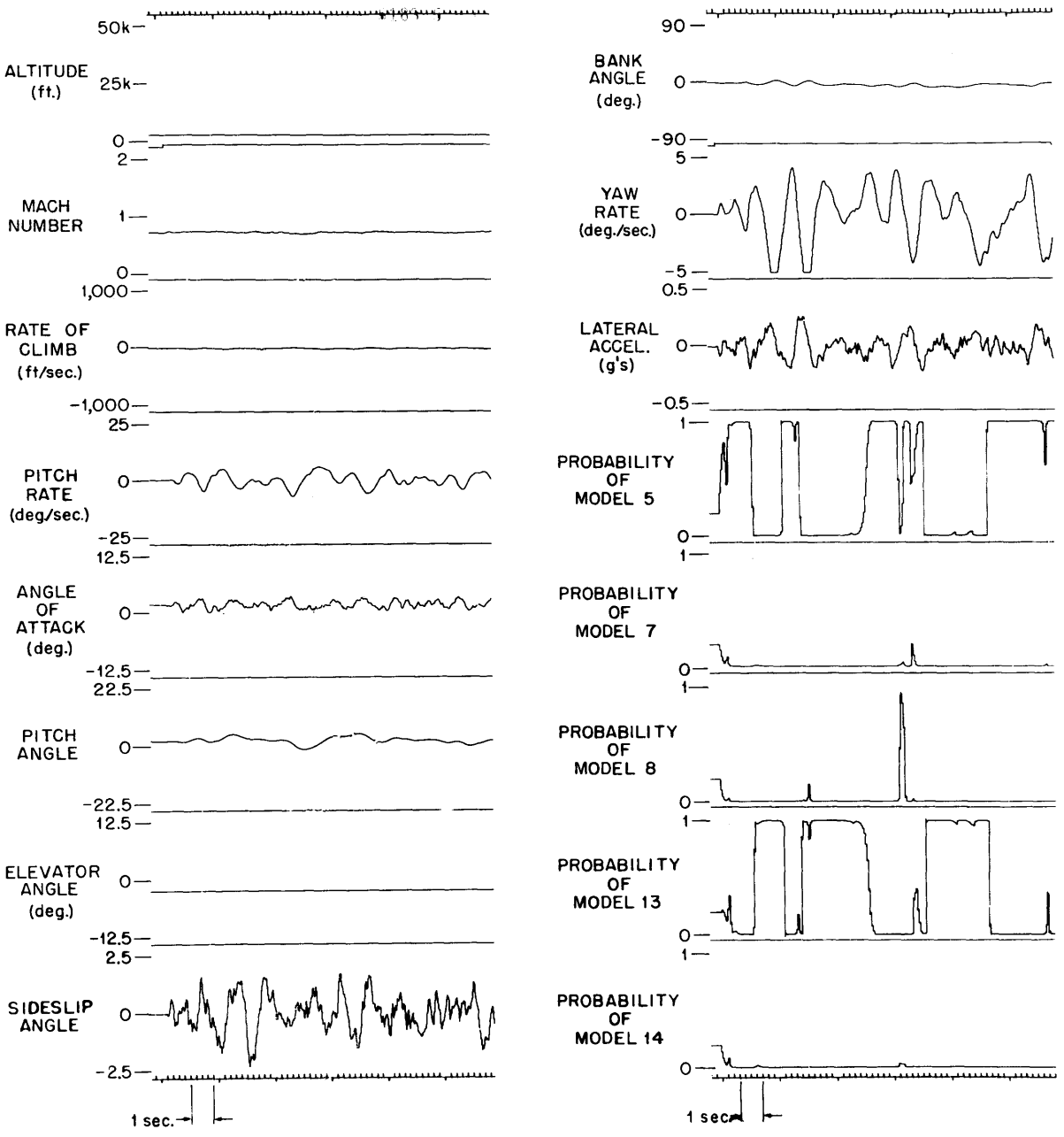

Figure E.6 Open Loop Turbulence Response

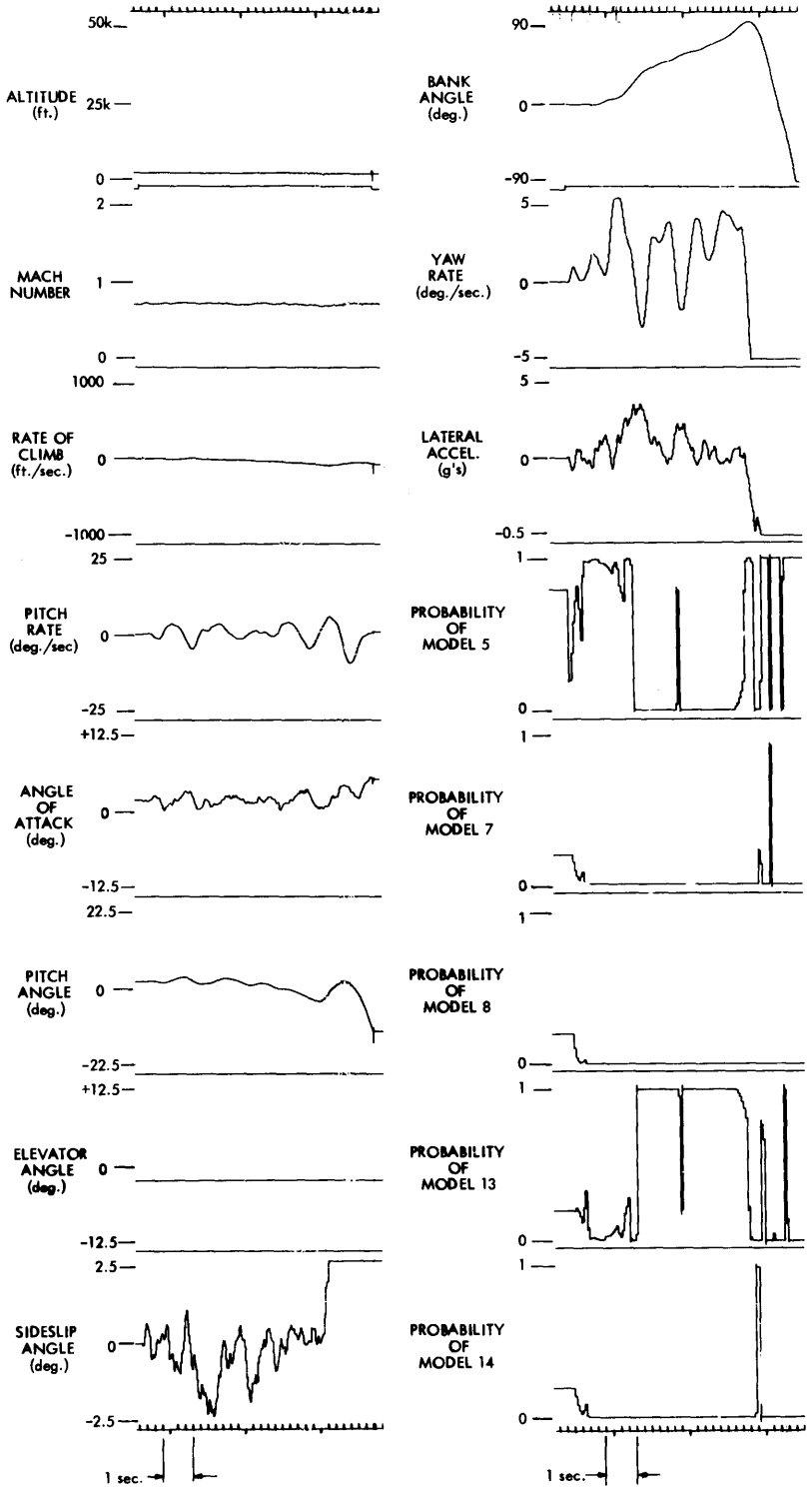

Figure E.7 Turbulence Response with Lateral Controller

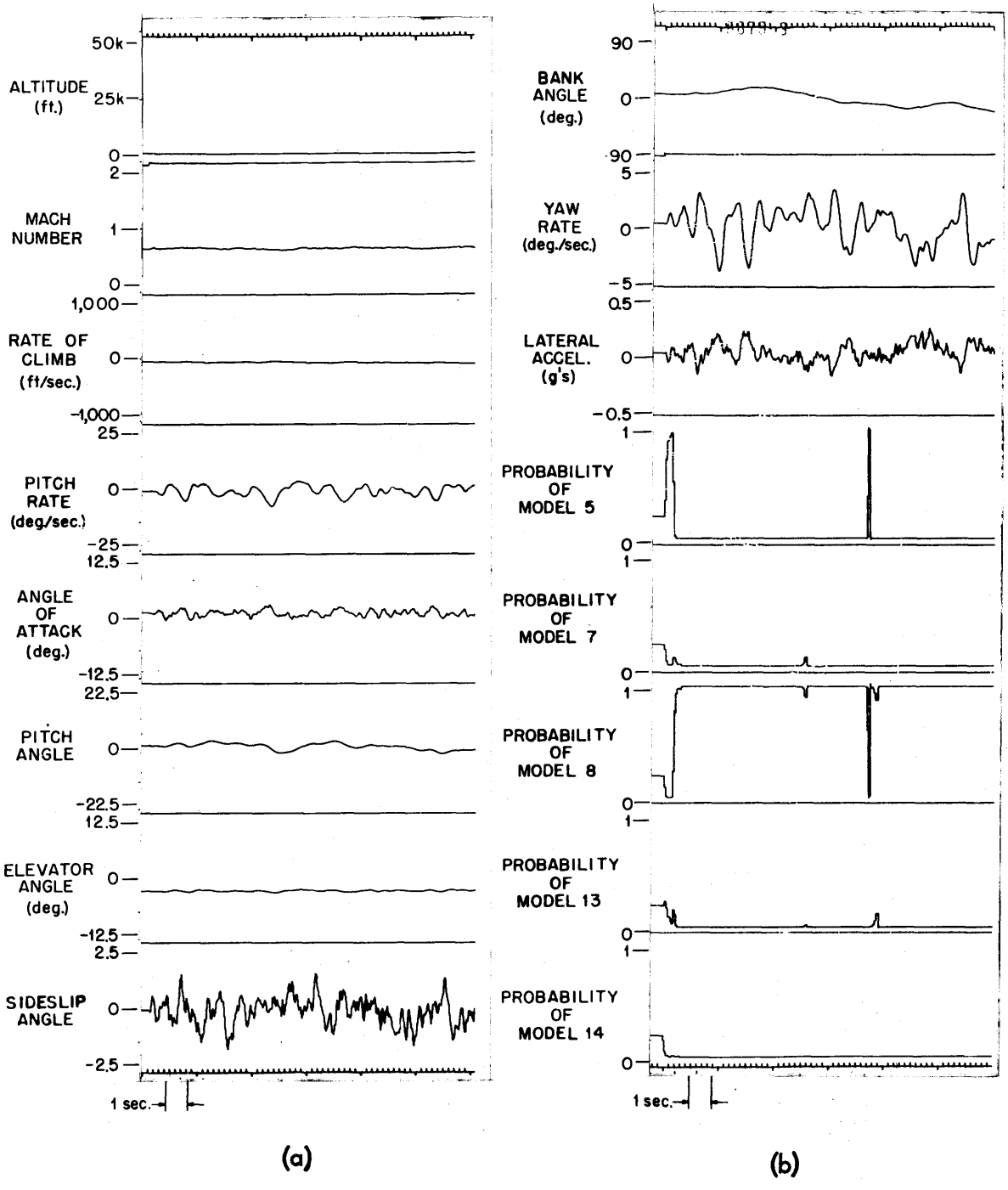

Figure E.8 Turbulence Response with Lateral-Longitudinal Controller

BIBLIOGRAPHY

1. Athans, M.: "The Role and Use of the Stochastic Linear-Quadratic-Gaussian Problem in Control System Design," IEEE Transactions on Automatic Control, Vol. AC-16, pp. 539-552, Dec. 1971.

2. Athans, M. and Falb, P.L.: Optimal Control, McGraw-Hill Book Company, New York, 1966.

3. Breza, M.J. and Bryson, A.E.: "Minimum-Variance Steady-State Filters with Eigenvalue Constraints", Fifth Symposium on Nonlinear Estimation Theory and its Applications, San Diego, California, September, 1974.

4. Deshpande, J.G.; Upadhyay, T.N. and Lainiotis, D.G.: "Adaptive Control of Linear Stochastic Systems", to appear.

5. Dunn, K.P. and Athans, M.: Linear Equations for the Continuous Time LQG Problem for the F-8 Aircraft Longitudinal Dynamics, Report ESL-IR-549, Massachusetts Institute of Technology, Electronic Systems Laboratory, April 26, 1974.

6. Dunn, K.P. and Athans, M.: The Steady State Optimal Control Gain and Closed Loop Eigenvalues for the F-8 Aircraft Longitudinal Dynamics, Report ESL-IR-550, Massachusetts Institute of Technology, Electronic Systems Laboratory, June 6, 1974.

7. Dunn, K.P. and Athans, M.: Linearized Deterministic Equations for the Discrete-Time Control Problem for F-8 Longitudinal Dynamics, Report ESL-IR-559, Massachusetts Institute of Technology, Electronic Systems Laboratory, July 12, 1974.

8. Etkin, B.: Dynamics of Atmospheric Flight, John Wiley and Sons, Inc., New York, 1972.

9. Gera, J.: Linear Equations of Motion for F-8 DFBW Airplane at Selected Flight Conditions, National Aeronautics and Space Administration, Langley Research Center, F-8 Digital Fly-By Wire Internal Document, Report No. 010-74.

10. Jazwinski, A.H.: Stochastic Processes and Filtering Theory, Academic Press, New York, 1970.

11. Kaufman H.; Alag, G,; Berry, P. and Kotob, A.: Digital Adaptive Flight Controller Development, NASA Contractor Report NASA CR-2466, National Aeronautics and Space Administration, Washington, D.C., December 1974.

12. Levis, A.H. and Athans, M.: Sampled-Dala Control of High-Speed Trains, Report ESL-R-339, Massachusetts Institute of Technology, Electronic Systems Laboratory, January 1968.

13. Magill, D.T.: "Optimal Adaptive Estimation of Sampled Stochastic Processes," IEEE Transactions on Automatic Control, Vol. AC-10, pp. 434-439, Oct. 1965.

14. Sandell, N.R. and Athans, M.: Modern Control Theory Computer Manual, Center for Advanced Engineering Study Massachusetts Institute of Technology, 1974.

15. Schweppe, F.C.: Uncertain Dynamic Systems, Prentice-Hall, Inc., Englewood Cliffs, New Jersey, 1973.

16. Stein, G. and Henke, A.H.: A Design Procedure and Handling-Quality Criteria for Laterial-Directional Flight Control Systems, Technical Report AFFDL-TR-70-152 Air Force Flight Dynamics Laboratory, Air-Force Systems Command, Wright-Patterson Air Force Base, Ohio, May 1971.

17. Upadhyay, T.N. and Lainiotis, D.G.: Joint Adaptive Plant and Measurement Control of Linear Stochastic Systems. Presented at 7th Annual Princeton Conference on Information Science and Systems, Princeton, New Jersey, March 1973.

18. Willner, D.: Observation and Control of Partially Unknown Systems, Report ESL-R-496, Massachusetts Institute of Technology Electronic Systems Laboratory, May 1973.

19. Woolley, C.T. and Evans, A.B.: Algorithms and Aerodynamic Data for the Simulation of the F8-C Digital Fly-By-Wire Aircraft, unpublished National Aeronautics and Space Administration Langley Research Center report February 5, 1975.